Università degli Studi di Ferrara

DOTTORATO DI RICERCA IN
"SCIENZE BIOMEDICHE E BIOTECNOLOGICHE"

CICLO XXIX

COORDINATORE Prof. Francesco Bernardi

Cell-based models for bone and cartilage tissue engineering: *in vitro* investigations from a biomaterialistic, cellular and molecular perspective.

Settore Scientifico Disciplinare BIO/10

Dottorando
Dott. Marco Angelozzi

Tutore
Prof. Monica Borgatti

Supervisore
Prof. Roberta Piva

Anni 2014/2016

Table of contents

Preface of the thesis

The research described in this thesis is mainly intended for the design of new strategies for bone and cartilage tissue engineering. In particular it is focused on two main points: 1) the realization of *in vitro* cell-based constructs for bone and cartilage regeneration and 2) the characterization of new molecular factors involved in the osteogenesis and chondrogenesis of human mesenchymal stem cells (hMSCs). The work is organized as described here below.

A first chapter (***Chapter 1***) is dedicated to the description of bone and cartilage tissues in healthy or pathological conditions, together with the definition of current and future therapeutic strategies, highlighting the advancements of tissue engineering approaches.

In the consecutive chapters, the experimental results obtained during my Ph.D. project are described. The research was focused on different aspects concerning bone and cartilage tissue engineering, leading to exciting outcomes which have been or will be reported in different publications in peer-reviewed journals. The main part of my work was done in the cellular and molecular biology laboratory of Prof. Roberta Piva (Department of Biomedical and Specialty Surgical Sciences, University of Ferrara), while a substantial part concerning the study of biomaterials was carried out in the laboratory of biomaterials and bioencapsulation of Prof. Claudio Nastruzzi (Department of Life Sciences and Biotechnology, University of Ferrara). Herein the work and obtained results have been divided in two main chapters, structured as follows.

Chapter 2 describes, in five sections, the realization of *in vitro* cell-based constructs realized through the employment of scaffolds or bioreactors, with the aim to stimulate cell-cell and cell-extracellular matrix (ECM) interactions. In this phase great importance has been given to ECM, which is a fundamental component in directing cell fate and differentiation. For this reason the characterization of new ECM proteins was also a final aim of the work presented in this chapter.

Chapter 3, instead, is focused on the study of new molecular factors implicated in the osteogenic or chondrogenic differentiation of hMSCs, in order to identify alternative targets to enhance

regenerative potential of cell-based approaches in tissue engineering. The work was structured in three sections, focusing in particular on the function of transcription factors and microRNAs.

Chapter 1

General overview

Bone and cartilage represent the major components in the skeleton system, ensuring structural and mechanical support and protection for soft tissues and resulting fundamental to mobility and locomotion. No less important is their involvement in other organism functions (e.g. control of calcium homeostasis, hematopoiesis, balance and equilibrium). Consequently skeletal defects often incur considerable morbidity, characterized by pain and serious invalidity. Several factors, including traumas, diseases, tumors and developmental abnormalities, could frequently irreversibly affect the skeleton good-health. In association with an increasing average population age, these disorders cause relevant disabilities in an always higher number of people with a notable impact in terms of frequency, morbidity, mortality and medical costs. Current medical strategies are mainly focused on symptomatic treatment, while tissue repair approaches frequently result in negative outcomes with the newly formation of a non-functional tissue, due to its poor similarity with native one. According to this scenario, the study of the cellular and molecular mechanisms and the development of innovative and alternative strategies play a central role in the step towards the repair of skeleton structure and functionality, possibly in a personalized medicine manner.

1. Bone and cartilage physiology

A deep comprehension of the structure, composition and function of bone and cartilage tissues is an essential step to shift towards a practical and beneficial tissue engineering approach, keeping in mind that both tissues, even if with their unique properties, share common features, providing a unique combination of rigid, yet plastic, living tissue. For instance, in the human joints cartilage, calcified cartilage and bone interact in complex ways to allow a correct function sustaining body movements. Additionally, in the endochondral ossification, one of the bone formation pathways,

cartilage tissue is firstly formed and subsequently converted into bone (*Meyer and Wiesmann, 2006; Gentili and Cancedda, 2009*). These examples let imagine how the connection between the two tissues is complex and strict, and by this point of view the study of bone become crucial to understand the cartilage physiology and *vice versa*.

1.1 Bone formation

Thanks to its stiffness and rigid nature, bone represents the main body support, providing a structure for muscle attachment and contraction, and cartilage sustains this function ensuring a flexible support (*Meyer and Wiesmann, 2006)*. Bones are formed through two different developmental processes: i) endochondral ossification (developing by the replacement of a cartilaginous model) and ii) intramembranous ossification (developing directly from progenitor mesenchymal cells). In both cases mesenchymal stem cells (MSCs) act as the progenitor cells from which osteoblasts (OBs) (actively bone extracellular matrix-producing cells) develop: MSC condensation represent the first step from which cells can go towards the intramembranous (flat bones – cranium and medial clavicles) or the endochondral (long bones – appendicular and facial bones, vertebrae and lateral clavicles) process. If in the intramembranous ossification MSCs are directly committed into osteoblasts, which are able to secrete a collagen-proteoglycan matrix that will be subsequently calcified and mineralized, in the endochondral pathway the condensed MSCs are firstly committed into chondroblasts giving rise to a cartilaginous template until chondrocytes stop dividing and start increasing drastically their volume: these hypertrophic chondrocytes produce an altered matrix able to be mineralized by calcium carbonate; in the last phases cartilage is invaded by blood vessels and chondrocytes die (formation of bone marrow), while surrounding cells differentiate into osteoblast, which start to produce bone extracellular matrix (ECM) over the degrading cartilage matrix. In formed bone mature osteoblasts which remain entrapped into the mineralized ECM become osteocytes: these cells can't be considered properly quiescent, since in their lacuna they are interconnected with other osteoblasts/osteocytes, with important role in maintaining calcium homeostasis and regulating bone remodeling. Endochondral ossification starts from the bone center (diaphysis) and spreads outward the two extremities (epiphysis) where a cartilaginous zone survives: this area, named growth plate is essential for bone growth after birth and is organized in i) a region of chondrocyte proliferation, ii) a region of mature chondrocytes and iii) a region of hypertrophic chondrocytes (directly in contact with the underlying bone) (*Gilbert, 2000*). A relevant aspect of the bone is its regenerative potential, further maintained when the growth is completed: bone constantly undergoes into tissue remodeling during life in order to respond to biomechanical

and body changes, but also to remove and replace old or microdamaged tissue, preserving bone strength and functions (*Clarke, 2008*).

1.2 Bone composition

Two "macrocomponents" constitute the bone tissue, properly the cortical and the trabecular bone. The first one is dense, solid and surrounds the marrow space, which is homed in the honeycomb-like network formed by the trabecular plates and rods. Cellular and acellular components cooperate in an elegant interplay to maintain and remodel bone structure and composition. The highly specialized ECM (acellular component) is essential for the typical rigidity and stiffness of the bone: it is composed of 50-70 % mineral phase (hydroxyapatite), 20-40 % organic matrix (collagenous or not proteins), 5-10 % water and <3% lipids. Organic phase is mainly represented by collagen type 1 (Col1a1), together with lower amounts of collagen type 3 and 5 and FACIT collagens (Fibril-Associated Collagens with Interrupted Triple Helices). FACIT collagens delineate a group of non-fibrillar collagens that function as molecular bridges, important for the organization and stability of extracellular matrices. Additionally osteoblasts secrete a series of non-collagenous proteins (e.g. osteopontin, osteocalcin, bone sialoprotein) which are involved in the regulation of matrix mineralization and other cellular activity (*Kini and Nandeesh, 2012*). Bone quality highly depends not only from the proteic composition, but also from collagen crosslinks, microarchitecture, the presence of microcrack and finally mineralization (both in terms of mineral content and organization status): all these features could vary within age, gender, site, ethnicity, health status (i.e. presence of diseases and drug therapies), affecting the good-quality of the tissue (*Boskey, 2013*).

As aforementioned the main responsible for the ECM production and deposition are osteoblasts: they derive from MSCs of the bone marrow stroma, through a differentiation process directed by the Wnt/β-catenin pathway and the transcription factor Runx2 (Runt-related transcription factor 2) (*Fakhry, 2013*). Osteoblasts, together with progenitor cells (MSCs) and osteocytes (final maturation stage of osteogenic process represented by osteoblasts entrapped in the produced bone ECM), are not the only cell population present in bone tissue. Osteoclasts can be defined as the bone-resorbing cells: they derived from mononuclear precursor cells of the monocyte-macrophage lineage and are able to break collagen fibers through the production of digestive enzymes and allow, at the same time, the release of calcium and phosphate, restoring calcium blood levels and homeostasis (*Clarke, 2008*). A sophisticated crosstalk exists between osteoblastic and osteoclastic components, essential

for the maintenance of bone homeostasis: in particular osteocytes, thanks to their extended membrane processes, act as mechanosensors piloting the balance between bone formation/resorption towards osteoblasts or osteoclasts, respectively (*Burra et al, 2010; You et al, 2008*). Secreted molecules are essential in this regulation: in particular osteoblasts and MSCs are able to produce two cytokines, M-CSF (Macrophage Colony-Stimulating Factor) and RANKL (Receptor Activator of Nuclear factor-KappaB Ligand), necessary and sufficient to sustain proliferation, survival and differentiation of osteoclast precursors, inducing bone resorption. Nevertheless osteoblastic cells can also secrete osteoprotegerin (OPG), which act as a decoy for RANK (the RANKL receptor), inhibiting osteoclast activity (*Yamashita et al, 2012; Sharaf-Eldin et al, 2016*).

1.3 Osteogenesis and mineralization process

Osteoblasts are unique cells derived from a multi-phase differentiation process where they become able to produce the specialized extracellular matrix of the bone; different maturation stages are usually recognized in this process (mesenchymal progenitors, preosteoblasts, osteoblasts, possibly osteocytes), even if the identities of the diverse stage-cells are not really understood: for instance preosteoblasts comprehend all cells transitioning from mesenchymal progenitors to mature osteoblasts, representing a highly heterogeneous population (*Long, 2012*). The differentiation of MSCs into osteoblasts requires the activation of specific transcription factors (TFs) and molecular pathways: some of these ones are well-characterized and are associated with a more defined function, but in other case a deeper understanding is crucial. TFs not only need to be present but their expression has to respect specific times in the differentiation process, defining various developmental stages of the osteoblast lineage. Sox9 is considered the main regulator of the chondrogenic differentiation of MSCs, nevertheless it is essential to define all osteochondroprogenitors: only Sox9 expressing-cells are able to give rise to functional osteoblasts. Only in a second step, when progenitors have been specified, Sox9 needs to be downregulated allowing osteoblastic commitment guided by Runx2, firstly, and Osterix (OSX), subsequently: suppression of these TFs resulted in the absence of osteoblast formation, sustaining their importance in the osteogenic differentiation process and in the bone matrix synthesis (*Long, 2012; Fakhry et al, 2013*). It is important to keep in mind that, even if Runx2 and possibly Osx are essential for osteoblastogenesis, they cooperate together with many other TFs (e.g. STAT1, NFATc1, ATF4, p53) in establishing progenitor cell fate: the role of these proteins is generally poorly understood, and evidences for both negative and positive effects have been reported, letting foresee how much is

sophisticated the molecular regulation of the osteogenic differentiation (*Kim et al, 2003; Koga et al, 2005; Xiao et al, 2005; Wang et al, 2006*). The scenario could become more labyrinthine if we think not only to TFs and we look to the action of cytokines and secreted molecules (e.g. Wnt/β-catenin pathway, BMP/TGF-β signaling, FGF signaling) or to the signals from the cell microenvironment and the relative ECM. For instance, the ECM of the niche, where MSCs reside, acts as mediator between the state/necessity of the tissue and the proper functioning of the stem cell pool, regulating the balance between stemness maintenance and differentiating cells. Moreover, it should not be forgotten the role of blood vessels and neurons in the delivery of systemic signals determining bone and, more generally, body homeostasis (*Long, 2012; Crane and Cao, 2014; Gattazzo et al, 2014; Rahman et al, 2015; Li et al, 2016b*).

If a wider comprehension of the molecular mechanisms involved in MSCs osteogenic commitment is necessary, processes governing mineralization phase remains largely unexplored and some mechanisms are still highly controversial. Nonetheless, being a hard, dense and compact tissue, bone is difficult to study both from an observational and from a molecular point of view; additionally some technical step of the analysis can alter tissue nature (e.g. chemical fixation can cause artifactual crystallization of calcium phosphate) (*Palmer et al, 2008; Boonrungsiman et al, 2012*). These issues led to the formulation of erroneous suppositions relative to the mechanism for early bone mineral formation: for example it has been assumed that mineralization could be a cell-independent phenomenon, directed by non-collagenous proteins mediating mineral nucleation from ions in solution. Providentially technical advancements allowed to highlight an active role of osteoblasts in mineralization; thus, even if mechanisms are still largely unclear, it seems assured the presence of matrix vesicles containing calcium-phosphate (CaP) deposits in mineralizing cells, confirming the existence and the importance of an intracellular phase during mineralization process. These intracellular vesicles, containing a precursor and disordered forms of amporphus CaP, mainly colocalized within mitochondria, letting suppose an active role of this organelles in the mineralization process: it has been hypothesized that intracellular calcium is condensed within phosphate inside mitochondria and subsequently transferred into intracellular vesicles in an immature form, in order to be transported and released in the extracellular environment where the maturation of apatite granules allow the formation of the bone mineralized ECM (Figure 1.1) (*Mahamid et al, 2011; Boonrungsiman et al, 2012; Kerschnitzki et al, 2016*). Furthermore, recent *in vitro* studies have elucidated mechanisms by which transiently formed clusters of calcium and phosphate ions could become orientated bone apatite via a synergistic interplay between collagen structure and nucleation inhibitors (*Nudelman et al, 2010; Dey et al, 2010; Reznikov et al, 2016*). Despite these interesting evidences, little is still known about how intracellular CaP is converted

into mature ECM-associated bone apatite and, furthermore, knowledge about the molecular and transcriptional regulation during the mineralization process is nearly inexistent. Thus a deeper comprehension of the involved pathways is fundamental, presumably leading to important clinical implication for understanding and treating pathological mineralization.

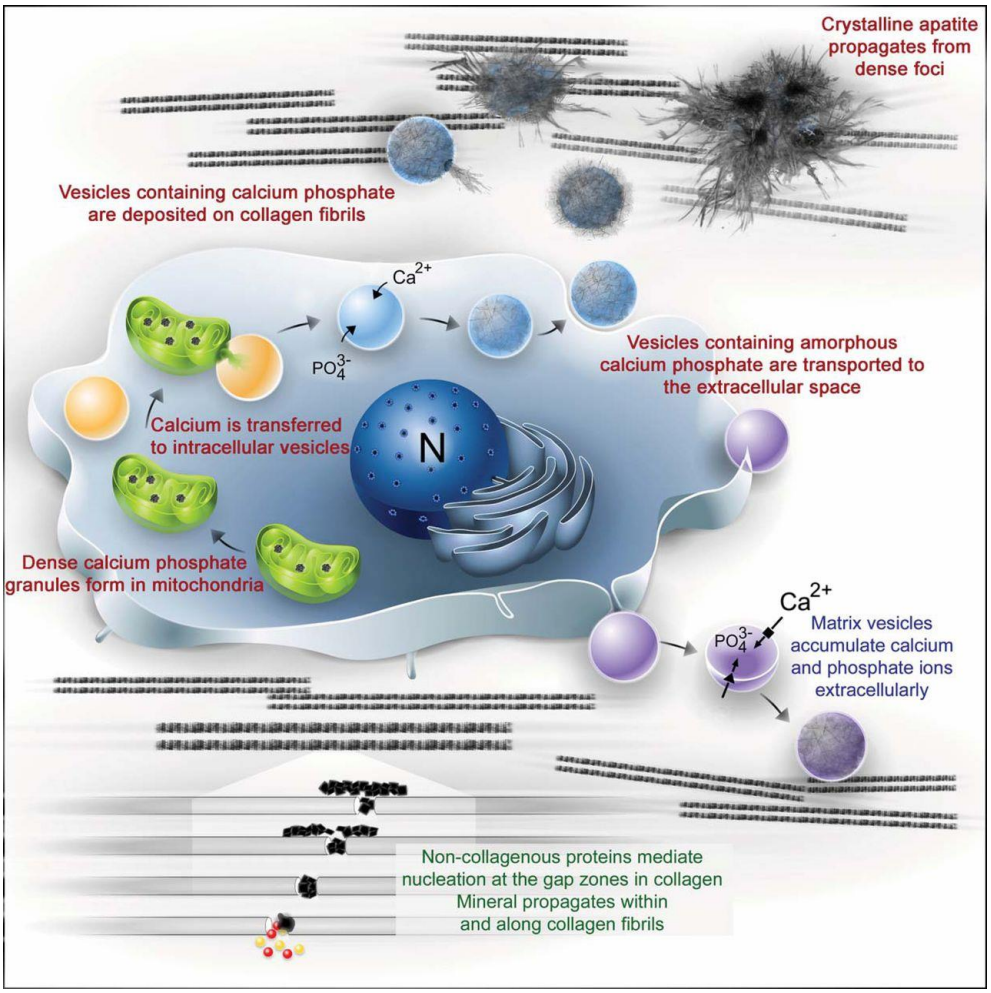

Figure 1.1: schematic representation of the mechanisms for bone mineral formation. Amorphous calcium phosphate and ionic calcium stored in mitochondria are transported via vesicles to the ECM before converting to more crystalline apatite and propagating from dense foci (upper side of the figure); alternatively matrix vesicles, which bud from the plasma membrane, accumulate calcium and phosphate ions extracellularly before associating with the collagenous ECM. Finally non-collagenous proteins associated with the gap zones in collagen mediate mineral nucleation along collagen fibrils (lower side of the figure). (*Boonrungsiman et al, 2012*)

1.4 Cartilage formation

Cartilage tissue is present in different areas of human body in three distinctive forms: fibrocartilage, elastic cartilage and hyaline cartilage; they exhibit unique and peculiar biochemical, mechanical and structural features, which are the result of the different mechanical loads to which these tissue types

are exposed during the development of the skeleton. Here the hyaline cartilage, named also as articular cartilage for its presence in body articulations, will be preferentially taken into account. This type of cartilage occurs in two biological distinct situations: i) as permanent articular cartilage and ii) as temporary template for future bone tissue. The first one is the cartilage which is conclusively present in the joints allowing smooth articulation under load-bearing conditions, while the second one underlies the endochondral ossification process, which was previously discussed (*Camarero-Espinosa et al, 2016*). As aforementioned, bone and cartilage share common progenitors cells, precisely MSCs from the limb: during development of the limbs, MSCs go through increased proliferation and condensation and subsequently are committed toward the chondrogenic lineage giving rise to a cartilage analogue. At this point cells differentiate into chondrocytes which produce large amount of collagen and hyaline ECM. Chondrocytes at the center of condensation stop proliferating and become hyperthrophic, producing growth factors which promote vascularization and ossification of the cartilage template, while chondrocytes at the extremities continue to proliferate allowing the formation of a second ossification center and the lengthen of the bones. Cartilage is not replaced by bone in two areas: i) between the diaphysis and the epiphysis, in the region called epiphyseal growth plate, which is responsible for bone growth in childhood and adolescence, and ii) at the end of the epiphysis, between the joints, where it remains during the lifetime acting as shock absorber (*Meyer and Wiesmann, 2006; Bhattacharjee et al, 2014; Camarero-Espinosa et al, 2016*). Nonetheless, during tissue maturation (also in adult age), cartilage undergoes throughout substantial changes in terms of cellular activity, ECM production, composition and structure. Furthermore continuous application of mechanical forces could heavily affect cartilage anatomy, reducing its thickness and promoting chondrocyte hypertrophy (*Luria and Chu, 2014*).

1.5 Cartilage composition

Hyaline cartilage is a predominantly acellular tissue, composed of abundant ECM where chondrocytes are dispersed (cell amount is drastically reduced from fetal to adult life when cell volume represents around 2% of the tissue): this particular feature allows the unique functionality and capability of cartilage tissue to respond to continuous mechanical stresses and soften friction/loading forces. Articular cartilage displays a zonal assembly; from outside tissue layers present this order: 1) superficial zone, with flattened chondrocytes directly in contact with the synovial fluid, 2) the mid zone, containing rounded chondrocytes at a lower cellular density in an extensive ECM, 3) the deep zone, where chondrocytes are arranged in columns separated by

collagenous fibrils, 4) the calcified cartilage, which is separated by a tidemark from the deep zone and is homed by hypertrophic chondrocytes able to calcify ECM; this layer is in close contact with subchondral bone, acting as an excellent integrating structure between cartilage and bone. As already mentioned, chondrocytes are the unique cell type found in cartilage: they are very low proliferative cells, but are responsible for the synthesis and regulation of specialized cartilage ECM, also acting as useful mechanosensors for the maintenance of biomechanical properties of this tissue. The large amount of water in the ECM (typical characteristic of the synovial fluid, too) is responsible for nutrient diffusion and also for the mechanical response induced via osmotic pressure under load. The rest of ECM is composed of collagens, proteoglycans and a small amount of non-collagenous proteins: collagen fibrils are responsible for tensile strength and their orientation and disposition change along the cartilage zones (i.e. horizontal in the superficial zone, oblique in the mid zone and perpendicular to articular surface in the deep zone). Collagen type 2 (Col2a1) is the main type of collagen in hyaline cartilage (~50% dry weight) and together with collagen type 9 forms most of the fibrils; while collagen type 11, less abundant, is present within and on the surface of fibrils: these collagens determined tissue stiffness and act as a barrier to the high pressures imparted by proteoglycans during swelling. Proteoglycans represent the main component among the non-collagenous proteins: they are composed of a core protein from which polysaccharides, mainly glycosaminoglycans (GAGs), brush; the most common cartilage-related GAGs are hyaluronan, dermatan sulfate, keratin sulfate and chondroitin, while the main proteoglycan is represented by aggrecan (Acan). Proteoglycans are responsible for the negative charges of articular ECM, generating the osmotic pressure when interacting with synovial fluid: the liquid is entrapped in the matrix causing a swelling effect that keep closely packed collagen and GAGs, providing the load-bearing capability to cartilage tissue (*Meyer and Wiesmann, 2006; Zhang et al, 2009; Sophia Fox et al, 2009; Camarero-Espinosa et al, 2016*).

1.6 Chondrogenesis

The multi-step process from which MSCs differentiate into chondrocytes is defined chondrogenesis; stages have been anticipated previously (paragraph 1.4) and can be summarized in 1) MSCs condensation, 2) proliferation and commitment into chondroprogenitors, 3) differentiation and ECM production and, potentially, 4) terminal differentiation and ossification (Figure 1.2). Cell-cell and cell-matrix interactions, together with the intervention of secret factors binding their own receptors, are essential requirements for the MSCs condensation: cells acquire a round shape and start producing a pre-cartilaginous ECM which will be fundamental in the maintenance of the

aggregate. Cell-cell adhesion molecules are indispensable for triggering chondrogenic differentiation; however their expression starts decreasing after condensation step. As differentiation proceeds, the pre-cartilaginous matrix characterized by the presence of collagen type 1 and fibronectin is replaced with one rich in collagen type 2 and aggrecan (*Chen et al, 2009; Singh and Schwarzbauer, 2012*). Transforming growth factor-β1 (TGF-β1) is one of the earliest signals intervening in the chondrogenic differentiation of MSCs, sustaining the expression of the transcription factor Sox9 and the production of the extracellular matrix. Sox9 is considered the master regulator of the chondrogenic process: it is expressed in cells undergoing condensation and it is necessary for the expression of typical ECM proteins, such as collagen type 2 or 11. Two other Sox-family TFs (i.e. Sox5 and Sox6) cooperate with Sox9 during differentiation stage to sustain MSCs chondrogenesis (*Kawakami et al, 2006; Goldring et al, 2006*). When exposed to specific signals (e.g. endochondral ossification pathway) differentiated chondrocytes could undergo towards the terminal differentiation into hypertrophic cells, characterized by the release of matrix metallopeptidases (e.g. MMP1, MMP13), able to decompose cartilage ECM, that will be replaced by a matrix composed of collagen type 1 and 10 (Col10a1), produced by the hypertrophic chondrocytes themselves and competent for mineralization. However this terminal differentiation phase should be avoided if the formation of a stable cartilage ECM is the desired goal (*Pelttari et al, 2008; Zhong et al, 2015*).

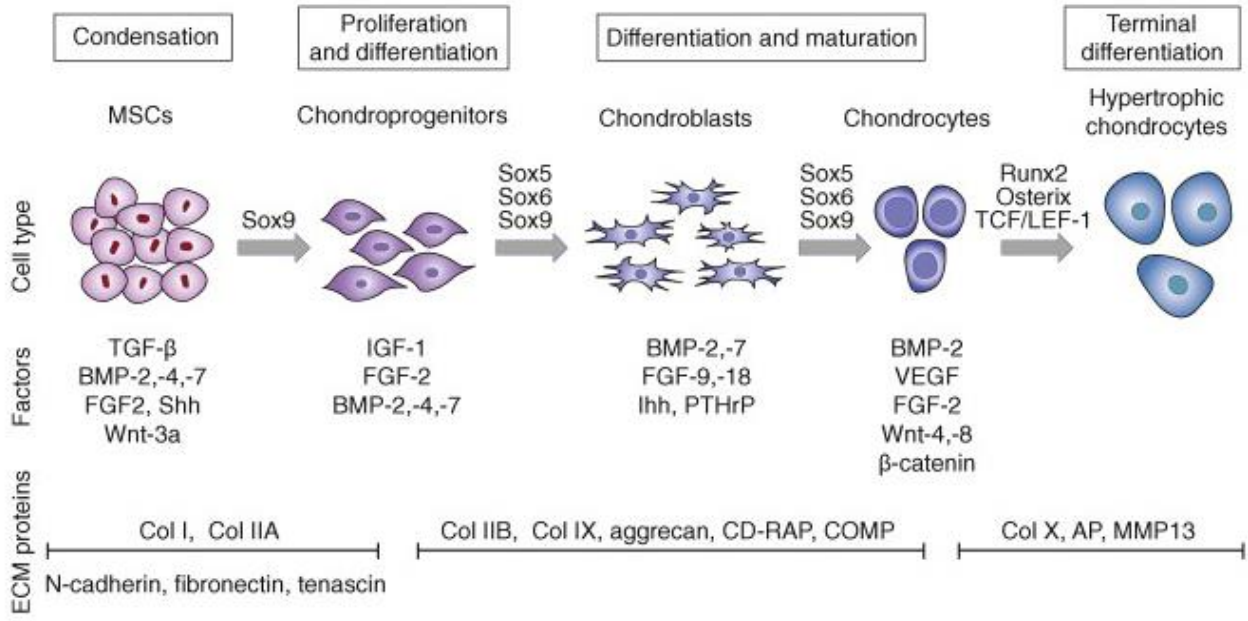

Figure 1.2: diverse stages of MSCs chondrogenic differentiation. The different stages of the chondrogenesis are outlined together with the growth factor involved and the typical expression profile specific for each step of the commintment. (*Vinatier et al, 2009*)

In light of this a better understanding of the molecular pathway and signals sustaining chondrogenic differentiation, but preventing chondrocyte hypertrophy is fundamental from a regenerative point of view. Precisely for this reason, the employment of specific growth factors (such as BMPs, FGF, IGF and in particular TGF-β), which are involved also in the regulation of bone formation and mineralization process, during *in vitro* chondrogenic procedures should be highly controlled: increasingly evidences of the controversial effects of these molecules on final cell phenotype and ECM characteristics are reported in literature, as will be discussed later (*Solorio et al, 2012; Somoza et al, 2014*).

1.7 Bone and cartilage in the "articular system"

The increasing socio-economic impact of osteochondral diseases, affecting joints' good-functionality and, thus, personal wellbeing and health, has moved the interest of tissue engineering research to identify new approaches able to ensure a complete recover of articulation performances. However it is important to underline that the anatomical and mechanical integrity of the joint depends from the correct configuration of all the elements composing it, thus, not only subchondral bone and articular cartilage, but also synovium, joint capsule, ligaments, tendons, fat pad and periarticular connective tissues: all these components collaborate to sustain bone and cartilage in responding to loading/friction forces which encumber onto articulations (*Lee and Salter, 2015*). For instance, synovium, representing the inner membrane of joint capsule, is responsible for the maintenance of synovial fluid, a viscous non-Newtonian fluid derived from plasma ultrafiltration: it contains proteins, such as the superficial zone protein (SZP), responsible for cartilage lubrication; additionally, being a non-Newtonian fluid, when pressure is applied onto cartilage, its viscosity is increased ensuring the load support (*Camarero-Espinosa et al, 2016*). Synovial fluid contains also a great amount of soluble molecules, derived from blood stream or produced by nearly-located tissues. For example, the infrapatellar fat pad secrete a series of adipokynes, particularly adiponectin, leptin and resistin: leptin seems to be implicated in cartilage inflammation, causing metabolic changes in chondrocytes and MMPs activation resulting in tissue damage and degradation; adiponectin instead has a controversial action and, even if it showed pro-inflammatory effects in some models, its role needs to be clarified (*Rainbow et al, 2012*). In this intricate and sophisticated system, an important role is covered by bone-cartilage interactions: although the articular cartilage overlies, and is in intimate contact with the underlying subchondral bone, molecular crosstalk between osteoblasts/osteocytes and chondrocytes *in vivo*, particularly in human joints, is scarcely documented. The existence of this crosstalk has been frequently discouraged due

to the hard nature of bone tissue and the separation between osteoblastic and chondroblastic cells by the calcified cartilage layer, imaging it as a real barrier; however recent evidences of increased vascularization and presence of microcracks in the interface between subchondral bone and calcified cartilage gave rise to several expectations about a real molecular interplay between osteoblasts and chondrocytes through a plethora of soluble molecules, cytokines and growth factors (*Yuan et al, 2014; Findlay and Kuliwaba, 2016*). Even though physiological communication remains still marginally described, a greater number of evidences about subchondral bone/articular cartilage molecular interaction has been reported in the osteoarthritic condition: in fact it is doubtless that osteoarthritis (OA) is a complex pathology where changes in subchondral bone are particular remarkable in early disease onset, affecting articular cartilage physiology and good-health; for this reason a deeper understanding of molecular communication between the two tissues is at the root of pathogenesis' comprehension (*Neogi, 2012; Sharma et al, 2013*). For instance it has been observed that pathological chondrocytes can induce a switch from normal osteoblastic phenotype to a sclerotic one through the mitogen activated protein kinase (MAPK) signalling pathway; from the other hand, osteoblasts from OA tissue could affect the expression of specific cartilage proteins in chondrocytes (e.g. collagen type 2, aggrecan, GAGs) (*Prasadam et al, 2010; Sanchez et al, 2005a; Sanchez et al, 2005b*). Additionally a decreased OPG/RANKL ratio has been reported in OA animal models and in human patients, favouring osteoclasts formation and activity: though osteoclasts role in OA pathogenesis is not still clear, their involvement in cartilage tissue degradation is highly plausible, also through the excessive resorption of subchondral bone (*Kwan Tat et al, 2008; Bellido et al, 2010; Upton et al, 2012*). As deducible from examples here reported, a profound knowledge of the molecular interplay connecting the different tissues present in the articular system will be fundamental to set up a real functional tissue engineering approach able to restore joint anatomy and functionality.

2. Bone and cartilage pathologies and current clinical approaches

Several bone and cartilage pathologies, characterized by a disparate etiology and disease progression, could seriously affect joint structure and stability with severe consequences for mobility and life routine. Over 150 different kinds of disorders, including rheumatoid arthritis, osteoarthritis, osteoporosis, low back pain, severe traumas and cancers, are recognized as bone and cartilage disorders, interesting millions of people worldwide: it has been estimated that an osteoporotic fracture occurs every 3 seconds with 1 in 3 women and 1 in 5 men over 50 years old,

being affected by the condition. Similarly, up to 1 in 5 women and 1 in 10 men over the age of 60 are affected by osteoarthritis. These debilitating conditions are painful for the individual, lead to the inability to work and to enjoy life fully, and are a cost to societies and countries: only in the United States about 100,000 people are unable to walk independently from bed to the bathroom because of osteoarthritis of the hip or knee. The numbers of those affected are set to rise over the next few decades, in particular in industrialized countries where the increasing numbers of elderly people is a key factor. The situation is further complicated by the lack of effective treatments, due to a superficial and trivial understanding of the mechanisms underlying these disorders together with the concomitant intervention of several biological, genetic and environmental factors influencing pathology onset and evolution (*http://www.who.int; http://www.boneandcartilage.com*). Herein the current knowledge about the most common and studied bone and cartilage diseases along with the current therapeutic approaches will be discussed.

2.1 Osteoporosis

Osteoporosis is one of the most common diseases affecting bone, characterized by the deterioration of bone mass, density and quality decreasing microarchitectural and biomechanical properties of the tissue and yielding the risk of low trauma fractures. Disease onset could be explained by two conditions: i) poor bone acquisition during youth and ii) accelerated bone loss during aging. Both environmental and genetic factors are involved in the pathology rise; hormone deficiency, poor nutrition, decreased physical activity and various pharmacological agents represent all possible causes increasing risk for osteoporosis. Additionally changes in the production of factors which modulate the response to mechanical stress to which bone is exposed during lifetime are another important element in the pathogenesis of this disease (*Raisz, 2005; Osterhoff et al, 2016*). Osteoporosis can be categorized as primary or secondary: primary one consists in the bone loss after decrease of sex hormones, aging or both; in women, where estrogen production is significantly weakened concurrently with menopause, primary osteoporosis is particularly impactful and early menopause or premenopausal estrogen deficiencies can accelerate the disease progression. Being hormones deficiency one of the first cause of illness, female population results mainly affected: it has been calculated that one in two women will go on to develop an osteoporotic fracture compared to one in four men over age 55 years. Secondary osteoporosis can occur due to chronic conditions that contribute to the acceleration of bone loss, including excess endogenous and exogenous thyroxin, malignancies, gastrointestinal diseases, hyperparathyroidism, connective tissue diseases, renal failure, medications (e.g. long term use of glucocorticoids) and alcohol and tobacco abuse

(*Downey and Siegel, 2006; Pesce et al, 2009*). It has been estimated that only in the USA osteoporosis affects around 10 million adults older than 50 years and another 34 million are at risk for it; without a competent intervention strategy the number of osteoporotic individuals is expected to increase 3-fold over the next 25 years (*Gallagher and Sai, 2010*). Since a wrong communication between osteoblasts and osteoclasts, with repercussion on bone remodeling and formation, seems to be at the basis of the pathology, bone biological research is focusing on the identification and the study of several molecules involved in these processes and potentially expendable as new pharmacological targets for the development of innovative treatments for osteoporosis.

2.2 Molecular and cellular changes in osteoporotic bone

Bone remodeling is a very dynamic process, where an optimal balance between old bone resorption and new tissue formation is essential to restore frequently occurring micro-fractures due to the daily mechanical stress to which bone is exposed. In a state of normal bone remodeling, bone formation closely matches bone resorption, in contrast with the osteoporotic condition where an accelerated osteoclastic activity dominates onto the newly ECM production by osteoblasts, leading to a net tissue loss. Nonetheless it is important to underline that decrease in bone mass could be ascribed not only to augmented osteoclast functionality, but also to defects in osteoblast formation and activity (*Martin and Seeman, 2008; Feng and McDonald, 2011*). Keeping in mind that osteoclasts origin from hematopoietic precursors and osteoblasts from MSCs, the strategically role of the bone marrow and the microvascular system, which live in intimate contact with bone tissue, is an essential factor for the maintenance of bone resorption/formation balance: stromal elements in fact address relevant signals in the decision of cell fate and thus in sustaining or blocking osteoblastogenesis and osteoclastogenesis. Additionally, as aforementioned (see paragraph 1.2), a delicate crosstalk between MSC/osteoblasts and osteoclasts exists, regulating themselves activity, through the secretion of cytokine such as M-CSF, RANKL or OPG (*Rosen and Bouxsein, 2005*). Since an estrogen-centric view of osteoporosis has dominated along these years, the alteration of these regulatory mechanisms has been particularly studied in menopausal women: in particular it has been demonstrated that estrogen deficiency is highly correlated with an increase in the RANKL/OPG ratio, supporting osteoclast differentiation and functionality. Moreover estrogens seem to stimulate production and release of TGF-β, one of the main molecule involved in bone resorption inhibition, in osteoblast differentiation and maturation and, consequently, in bone formation. These effects depend on the binding and activation of estrogen receptors (ER) α and β present on the surface of both MSCs/osteoblasts and monocytes/osteoclasts cell membranes (*Clarke*

and Khosla, 2010). Nevertheless in more recent years, the relevance of other factors in osteoporosis onset, despite the sex hormones sufficiency, has been figured out. For instance aging and inflammation are now considered essential elements in defining pathological instauration and progression: activation of T or B cells leads to the production of osteoclastogenic cytokines RANKL and TNF-α, even though T cells have shown also suppression activity on osteoclasts *in vivo*, suggesting how complex and tightly regulated is the interaction between immune and skeletal systems (Figure 1.3) (*Bozec et al, 2014; Yu and Wang, 2016*).

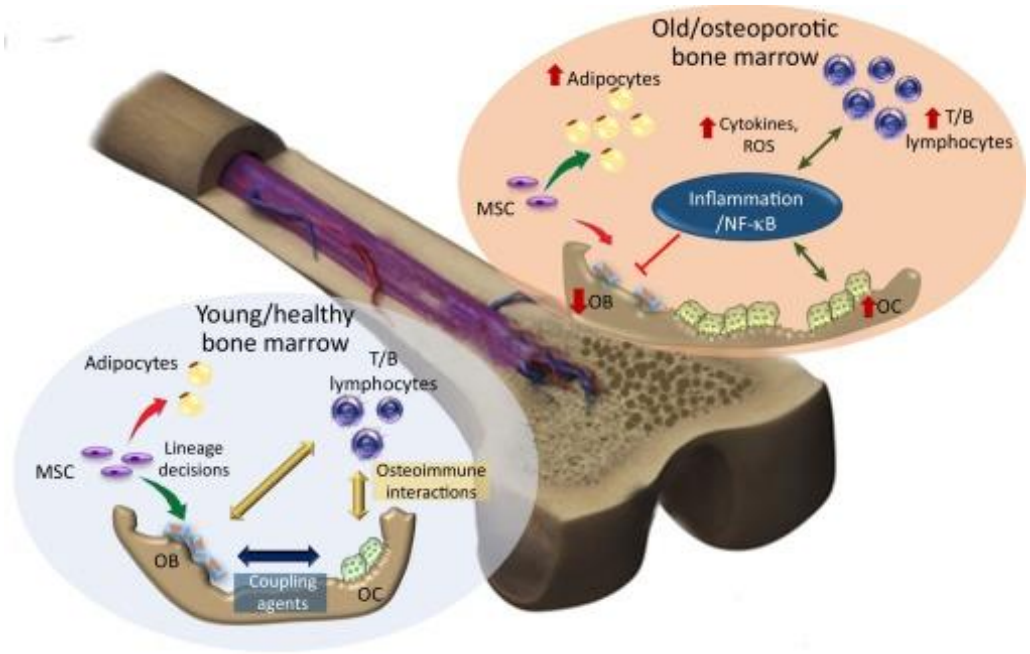

Figure 1.3: overview of microenvironmental changes in the osteoporotic bone marrow. In healthy marrow, osteoblasts and osteoclasts are balanced via coupling mechanisms (e.g. RANKL/OPG, growth factors), T/B cells reciprocally regulate bone cells through osteo-immune interactions and MSCs are more prone to differentiate towards the osteoblastic lineage rather than into adipocytes. In old/osteoporotic marrow, accumulating pro-inflammatory signals can induce a chronic inflammatory state, activating T/B cell expansion and osteoclasts, while suppressing osteoblast activities. These changes, together with a shift towards adipogenic differentiation of MSCs, can lead to osteoporotic lesions in bone matrix. (*Yu and Wang, 2016*)

Regarding aging issue, although a first phenomenon linking age maturation within osteoporosis is the decreasing estrogen production, age-related bone loss is associated with a second phenomenon, characterized by a slow, continuous decrease in bone forming activity, independent of sex hormone deficiency. Several cellular events have been related to this reduced bone formation, such as the preferential differentiation of MSCs into adipocytes, a compromised proliferative capacity of preosteoblastic cell, a reduced production of local anabolic factors (e.g. IGF-1, TGF-β) and finally

the accelerated senescence of MSCs: all these mechanism could be related to an increased oxidative stress in bone tissue. Even though this slow decrease in bone matrix formation is still underestimated, it could result into thinning of the bone trabeculae, increased trabecular separation and decreased cortical thickness, contributing to the deterioration of bone microarchitecture and strength associated with fractures (*Marie, 2010; Chen et al, 2013*).

2.3 Current therapies for osteoporosis

Since the ultimate goal of osteoporosis therapies is to restore bone mass and density and to inhibit excessive resorption, and being sex hormone deficiency one of the main cause in disease etiology, current pharmacological treatments are based on the use of antiresorptive drugs, such as estrogens (hormone replacement therapy – HRP), selective estrogen receptor modulators (SERMs), bisphosphonates and calcitonin. All these treatments are able to reduce osteoclastogenesis and osteoclast resorptive activity; nonetheless, to date, a decrease of only 30-40% in the risk of non-vertebral fractures has been reported: this partially failure is related to the long-term adverse effects of these drugs on osteoblast and new bone formation (e.g. osteonecrosis of the jaw), limiting bone mass increasing and tissue restoration (*Downey and Siegel, 2006; Gallagher and Sai, 2010; Kawai et al, 2012*). For this reason osteoporosis treatment is shifting towards the employment of anabolic drugs: presently the only one approved is a recombinant form of the parathyroide hormone (PTH), which, even though is consistent in increasing bone mineral density (BMD) and reducing fracture risk, reaches a plateau effect after 2 year treatment, omitting its potential carcinogenicity (*Yu and Wang, 2016*). Surgical approach is especially requested when fractures occur; however, due also to poor bone quality, technical issues and problems with surgical fixation make particularly tricky this type of treatment (*Pesce et al, 2009*). Consequently the improvement of pharmacological treatments preventing osteoporotic changes in bone tissue is highly desirable; nonetheless there is still a need to develop efficient and safe drugs promoting bone strengthening and formation. One promising option could be to target molecules involved in Wnt/β-catenin pathway, since its relevant implication in MSCs fate commitment, bone mass maintenance, mechanical stress response or age-related bone loss (*Yu and Wang, 2016*). For instance Yadav et al showed how the deletion of the low-density lipoprotein receptor–related protein 5 (LRP-5), a main receptor in Wnt/β-catenin signaling, reduces bone mass in a mechanism dependent from gut-secreted serotonin: if confirmed, these finding could pave the way to new therapeutic strategies based on serotonin antagonists (*Yadav et al, 2008*). Conversely the loss sclerostin (SCL), an inhibitor of the Wnt/β-catenin pathway produced by osteocytes, results in increased bone mass and a sclerostin antibody treatment has

resulted in positive effects on bone formation and strength in a rat model of postmenopausal osteoporosis (*Li et al, 2009b*). Additionally activation of canonical Wnt signaling, through glycogen synthase kinase 3 (GSK3) inhibitors, has shown to promote bone formation and to prevent bone loss in aged or ovariectomized osteopenic mice, confirming the notable role of this molecular pathway in bone balance and maintenance (*Kulkarni et al, 2006*).

2.4 Osteoarthritis

Osteoarthritis is the most common degenerative disease of the joints, mainly affecting knee, hips and hands. It represents the primary cause of medical consultation after cardiovascular disorder, affecting 10-20 % of worldwide population with the incidence estimated to increase due to escalating life expectancy. Osteoarthritis encases a variety of multifactorial and heterogeneous pathological conditions where the articular cartilage degeneration appears as the main feature in a really more complex and buried situation involving the whole articular environment. Thus, different clinical phenotypes could be identified including posttraumatic, metabolic, age-related or genetic ones; common characteristics are represented by articular cartilage degradation, inflammation of the synovial membrane and sclerosis of subchondral bone within formation of osteophytes (*Thysen et al, 2015; Vinatier et al, 2016; Xie et al, 2016*). To homogenize the profile of the disease on the basis of recent advancements in the comprehension of the pathophysiology, the OsteoArthritis Research Society International (OARSI) has revised the definition of osteoarthritis as "a disorder involving movable joints characterized by cell stress and extracellular matrix degradation, initiated by micro- and macro-injury that activates maladaptive repair responses including pro-inflammatory pathways of innate immunity. The disease manifests first as a molecular derangement (abnormal joint tissue metabolism) followed by anatomic, and/or physiologic derangements (characterized by cartilage degradation, bone remodeling, osteophyte formation, joint inflammation and loss of normal joint function) that can culminate inillness". OARSI group also proposed a pathology classification based on histological features of OA progression, where increasing grade indicates a more biologically aggressive disease and OA depth advancement (see Table 1.1) (*Pritzker et al, 2006*). Additionally osteoarthritis could be classified as primary or secondary: if primary (or idiopathic) OA is associated with aging and articular components consume during lifetime, secondary one is instead strictly correlated to a specific cause, such as traumas, malformation, metabolic or endocrine disorders (*Michael et al, 2010*). Even though progresses have been made in disease comprehension, the complexity of the biological processes, sustaining pathological

condition, remain a notable impediment in obtaining a definitive categorization and therapy for osteoarthritis.

Table 1.1: Osteoarthritis Cartilage Histopathology Assessment (OARSI) System (*Pritzker et al, 2006*)

Grade	Key feature	Associated criteria
0	Surface intact, cartilage morphology intact	*Matrix*: normal architecture *Cells*: intact, appropriate orientation
1	Surface intact	*Matrix*: superficial zone intact, oedema and/or superficial fibrillation (abrasion), focal superficial matrix condensation *Cells*: death, proliferation (clusters), hypertrophy, superficial zone
2	Surface discontinuity	*Matrix*: as above plus discontinuity at superficial zone (deep fibrillation), cationic stain matrix depletion (Safranin O or Toluidine Blue) upper 1/3 of cartilage, focal perichondronal increased stain (mid zone), disorientation of chondron columns *Cells*: death, proliferation (clusters), hypertrophy
3	Vertical fissures (clefts)	*Matrix*: as above plus vertical fissures into mid zone, branched fissures, cationic stain depletion (Safranin O or Toluidine Blue) into lower 2/3 of cartilage (deep zone), new collagen formation (polarized light microscopy, Picro Sirius Red stain) *Cells*: death, regeneration (clusters), hypertrophy, cartilage domains adjacent to fissures
4	Erosion	Cartilage matrix loss: delamination of superficial layer, mid layer cyst formation Excavation: matrix loss superficial layer and mid zone
5	Denudation	Sclerotic bone or reparative tissue including fibrocartilage within denuded surface. Microfracture with repair limited to bone surface
6	Deformation	Bone remodelling (more than osteophyte formation only). Includes: microfracture with fibrocartilaginous and osseous repair extending above the previous surface

2.5 Molecular and cellular changes in osteoarthritic joint

Even though it is indisputable that ageing is one of the major causes associated with osteoarthritis, it is important to not confuse an aged joint with an osteoarthritic one; it is more like ageing acts as a cofactor together with the other OA risk determinants. Rather mounting evidences directly correlate osteoarthritis within low-grade systemic and local inflammation: a plethora of inflammatory mediators are unleashed acutely in the joint after injury, but perturbation of many of these molecules and pathways persists beyond the acute post-injury phase, being also evident in

idiopathic OA (*Li et al, 2013; Loeser et al, 2016*). Although cartilage tissue has been mainly studied in OA pathogenesis, it is necessary to keep in mind that it is a disease of the entire joint, and increasing evidences are highlighting the role of subchondral bone and synovium in the release of the inflammatory factors which are at the basis of OA onset (*Berenbaum, 2013; Thysen et al, 2016; Punzi et al, 2016*). Most of these mediators are cytokines and chemokines produced by macrophages in response to injury or infection, such as interleukin 1 (IL-1), IL-6, IL-8, IL-17, reactive oxygen species (ROS): these molecules increase the catabolic activity of chondrocytes with the consequent release of aggrecanases or MMPs responsible for cartilage matrix destruction. However it is important to underline that a balance mechanism exists, where ECM degradation liberates bound-to-matrix growth factors (e.g. BMPs, TFG-β, IGF) previously produced by chondrocytes: these molecules serve to stimulate matrix production and to inhibit proteolytic enzymes. In OA cartilage this mechanism seems to be insufficient and defective and in idiopathic osteoarthritis it could be related to a minor cellular response due to ageing (*Loeser, 2006; Sokolove and Lepus, 2013*). Earliest changes in osteoarthritic cartilage are represented by the loss of negatively charged GAGs associated with an increasing swelling effect and high water content in the matrix; cartilage matrix degradation occurs initially in the superficial zone of the cartilage but later extends to deeper zones as OA progresses. Marked phenotypical changes can be observed also in chondrocytes, where, after the initial disruption of the pericellular matrix (by a process not completely understood), an initial syntethic activity of proteoglycans could be noticed as an attempt to repair; then, appearance of clonal cluster of chondrocytes and apoptotic manifestations (e.g. presence of cell-membrane 'ghosts', nuclei fragmentation) characterize an advanced OA. Macroscopically, cell and matrix degeneration are associated with the appearance of surface fibrillations characterized by microscopic cracks in the superficial zone, which, as the disease progresses, lead firstly to the exfoliation of fragments of cartilage and fissures extending into the deeper cartilage layers, and then to complete delamination and exposure of the underlying zones of calcified cartilage and subchondral bone (Figure 1.4). An interesting aspect of osteoarthritis condition is the instauration of a cyclic-like mechanism, since cartilage destruction gives rise to breakdown products, such as damage-associated molecular patterns (DAMPs) and alarmins, which in turn induce inflammation on the adjacent synovial tissues and subchondral bone within the new release of pro-inflammatory cytokines increasing the catabolic state of chondrocytes (*Goldring and Goldring, 2016*). In this situation the importance of the crosstalk between the different articular tissues appears always more critical for the maintenance of a physiological and functional joint. An increasing number of studies are evidencing the impact of the subchondral bone changes in osteoarthritic articulation: increased cortical plate thickness and alterations of trabecular bone mass

and architecture are two of the main features of OA bone, with an extent related to disease progression.

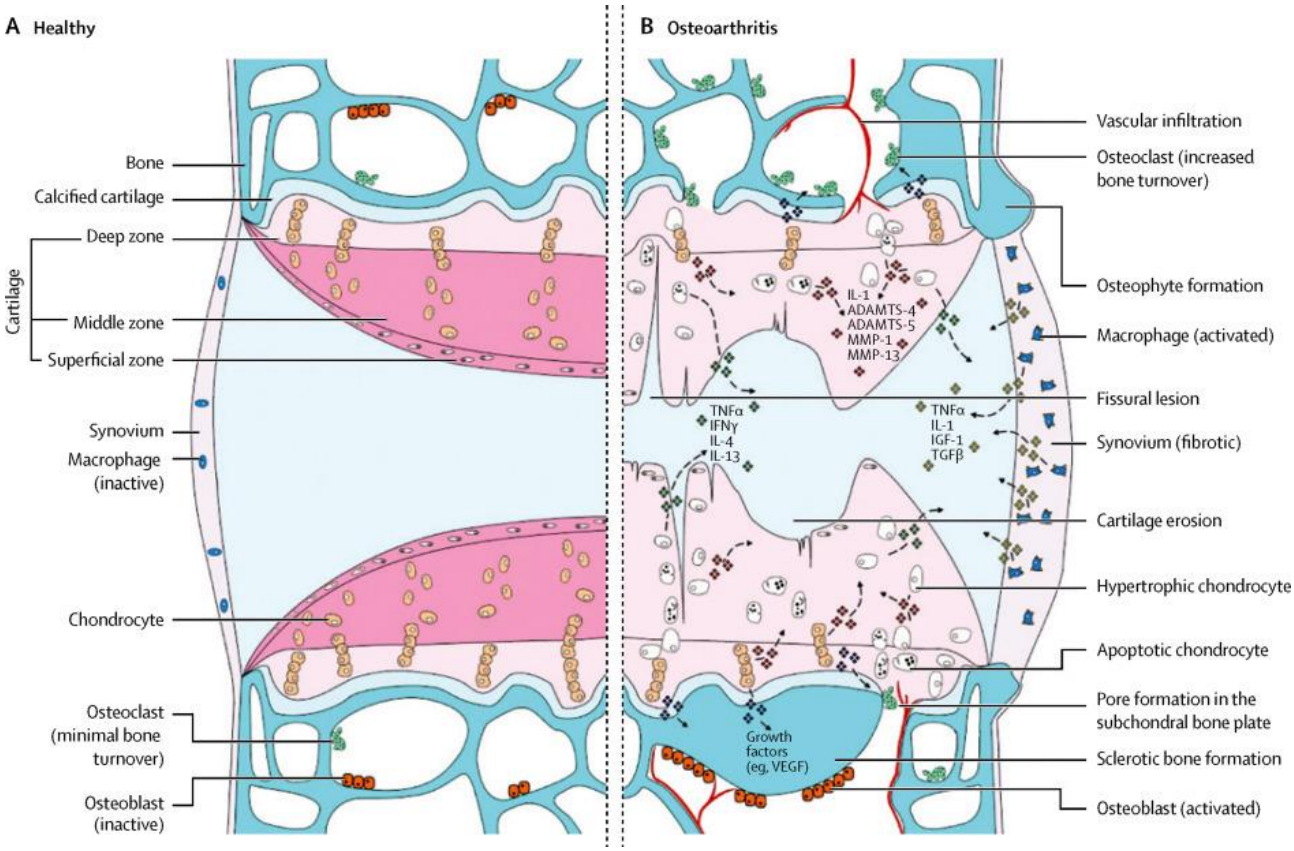

Figure 1.4: Structural changes and signaling patwhays implicated in the pathogenic condition of the osteoarthritic joint. (*Glyn-Jones et al, 2015*)

Additionally bone turnover defects, modification in the mineral content, development of bone cysts and bony outgrowths (known as osteophytes) at joint margins affect the ability of the bone to deform under load increasing the risk of structural damages and cartilage fibrillation (*Henrotin et al, 2012; Goldring and Goldring, 2016*). However the significance of the subchondral bone is not only in the structural feature of the joint, but also in the molecular crosstalk which exists between osteoblasts and chondrocytes, as aforementioned. Even though mediators of this interplay has not been identified yet, *ex vivo* and *in vitro* studies have demonstrated how subchondral bone and osteoblasts participate in the maintenance of chondrocytes viability and phenotype; furthermore OA osteoblasts, showing a gene expression profile different from normal cells, sustain the expression of MMP1 and MMP13 in co-cultured chondrocytes together with the reduction of typical chondrogenic markers such as Sox9, Acan and collagen type 2 (*Sharma et al, 2013*).

2.6 Current therapies for osteoarthritis

Current OA treatments are only symptomatic and not etiologic, allowing, at best, pain relief but failing to prevent cartilage damage and destruction of other joint tissues. The lack of an effective therapy able to stop disease progression or to restore articulation functionality is due to the complex biological and cellular condition present in OA joint, as previously described. Since inflammation has been established as one of the major component in osteoarthritis, current pharmacological therapies are based mainly on anti-inflammatory drugs, such as non-steroidal anti-inflammatory molecules, cyclooxygenase-2 (COX-2) selective agents or intra-articular injection of corticosteroids or hyaluronic acid; when disease progress towards a more severe stage the use of opioids analgesics is also considered to reduce patient pain, even though consistent adverse effect are usually reported (e.g. nausea, sleepiness, headache) (*Michael et al, 2010; Zhang et al, 2016a*). In the perspective of multi-tissue pathology, new treatments targeting subchondral bone have been supposed and their use is under experimentation. For instance, antiresorptive drugs, such as bisphosphonates, have been considered since their beneficial and protective effects on bone and cartilage tissue in animal models of OA, although a direct outcome in chondrocytes functionality was not observed. Risedronate, a bisphosphonate drug, have showed only scarce positive benefits in patients enrolled in phase III clinical study, nevertheless these results encourage for the possible development of multiple-target therapeutic approach (*Goldring and Goldring, 2016*). Pharmaceutical treatment could be considerably improved by physical therapy: moderate exercise and appropriate weight loss can adjust the imbalanced mechanical stress, lessen joint pain and may delay the progression of OA (*Christensen et al, 2005; Brakke et al, 2012*). For severe cases surgical option is also taken into account, when conservative therapy results ineffective: arthroscopic irrigation and debridement are employed to reduce pain but are not beneficial for long-term recovery, while drilling and microfracture techniques aim at penetrating the subchondral plate to induce bone marrow stromal cells for spontaneous repair, but the repaired tissue is inferior and consists of less durable fibrocartilage. However total joint replacement (arthroplasty) is considered the best surgical procedure for advanced OA, reducing pain and restoring joint functionality; unfortunately, this strategy is not recommended for young patients, since artificial implants have limited lifespan (10-15 years) and long-terms benefits are controversial (*Zhang et al, 2016a*). Alternatively a regenerative cell-therapy is possible: autologous chondrocytes implantation (ACI) is widely used in clinical practice and more than 15000 patients have received this treatment worldwide. The procedure encases three main steps: 1) the collection of a small mass of healthy cartilage tissue (~150–300 mg) during an arthroscopic biopsy procedure, 2) chondrocytes isolation and culture *in vitro* to acquire a consistent number of cells to re-implant and 3) re-implantation of chondrocytes

into the damaged area of the articular cartilage in a second open-knee procedure. More recently improvement has been achieved through the *in vitro* culture of chondrocytes onto/into three-dimensional scaffolds, ensuring long-term cell maintenance and reducing surgical time; this variant has been called matrix-induced autologous chondrocytes implantation (MACI). Even though considerable clinical improvements have been reported after ACI/MACI treatment, some crucial issues still remain, such as chondrocytes dedifferentiation or apoptosis during *in vitro* culture or after re-implantation, risk of infection associated with multiple surgical interventions and possible donor site morbidity (*Kon et al, 2012; Zhang et al, 2016a*). These unresolved questions are directly related to a high number of implant failures or to the reconstruction of a non-functional fibrocartilage and for this reason, as will be discussed later, research is searching for alternative cell sources like MSCs or for the development of new approaches, ensuring the success of the procedure.

2.7 Other osteochondral defects

If up to here major osteochondral degenerative lesions have been described, also focal lesions could occur: they are mainly caused by physical macro- and micro-trauma or diseases, such as osteochondritis dissecans or osteonecrosis. A briefly description of these defects will be presented out below, although it is important to underline that, due also to the low reparative ability of cartilage, the progression of a focal lesion towards a degenerative one is highly possible (*Gadjanski and Vunjak-Novakovic, 2015*).

Osteochondritis dissecans

Osteochondritis dissecans (OCD) consists in an idiopathic lesion of the subchondral bone which begins to separate from its surrounding region with the involvement of the above articular cartilage. The disease affects mainly knee, ankle and elbow in children and young adults and its etiology is still poorly understood: different causes have been proposed, from the lack of vascular supply to continuous traumas, from genetic factors to, more recently, vitamin D deficiency. OCD origins in a stable form, but as disease progresses, an unstable type together with mechanical symptoms arises (*Zanon et al, 2014; Nepple et al, 2016*). OCD treatment is mainly based on conservative options (e.g. cessation of sport activity, temporary immobilization) which are intended for favoring the healing of the injured bone interface and minimizing cartilage damage. This kind of therapy is particularly effective in young patients, but, where an unstable OCD arose or conservative treatment failed, surgical procedures are recommended (e.g. drilling, fixation, debridement, osteochondral

autograft transplant). However optimal treatment strategies for OCD remain to be defined, and a deeper comprehension of cellular and molecular changes occurring in joints together with the improvement of diagnostic procedures will be helpful to ameliorate patients life routine (*Winthrop et al, 2015; Nepple et al, 2016*).

Osteonecrosis

Osteonecrosis (ON) is a rare osteochondral disease mainly affecting knee or hip with considerable pain. It could be grouped in three categories: 1) spontaneous or primary, with higher prevalence in patients over 55 years of age, 2) secondary, largely observed in young patients and associated with a number of risk factors, and 3) post-arthroscopic surgery (*Karim et al, 2015*). Even though the etiology is not really clear, osteonecrosis has been associated with a deficiency in blood supply causing the subsequent necrosis of bone tissue and osteochondral defect, and this hypothesis is partially confirmed by studies evidencing the presence of insufficiency fractures and low mineral density in osteonecrotic bone with accumulation of blood fluid in bone marrow space (*Yamamoto et al, 2000; Fondi and Franchi, 2007*). Treatment depends from symptoms, staging and size of the defect; in particular small and medium lesions (< 5 cm squared) tend to regress after pharmacological treatment, while non-regressing and larger lesions require surgical procedure, such as prosthetic arthroplasty (*Karim et al, 2015*). Among tested drugs, bisphosphonates are largely employed, and, even if beneficial effects in delaying subchondral collapse and surgical treatment were reported, a recent work from Jureus and collegues indicate this therapeutic option as effective for initial stage of osteonecrosis (*Jureus et al, 2013*). Furthermore it is important to underline how a chronic exposure to bisphosphonates has been correlated to a particular form of osteonecrosis in the jaw of treated patients, namely medication-related osteonecrosis of the jaw (MRONJ): pathogenesis of this kind of ON is not still fully elucidated, but it seems to be correlated to an event caused by bisphosphonates in the oral cavity, and particularly in jaw bone, such as an altered resorption, tissue inflammation or compromised angiogenesis (*Rosella et al, 2016*). Thus, an alternative therapy for the treatment of osteonecrosis, and osteoporosis too, is fundamental and the comprehension of the mechanism leading to tissue unbalance will help to find new molecular targets.

Trauma-derived defects

Post-traumatic lesions mainly affect young people performing sport activity, leading to different degree of immobility and pain. During these traumas, shear forces cause the separation of the articular cartilage from the underlying calcified layers; depending on the involvement of the subchondral bone, defects can be categorized as chondral or osteochondral. In chondral defects the

lack of vascularization in the damaged cartilage impedes the natural healing of the tissue, while in osteochondral lesions some spontaneous repair by progenitor cells residing in bone marrow is achieved, even if usually the newly formed tissue does not cover the entire defect and present fibrocartilagineous characteristics. Treatment options for post-traumatic defects could be surgical or not, depending on the entity of the trauma; in any case total joint replacement using artificial prostheses, even if represents a good choice for reducing pain and restoring tissue functionality, is not recommended for young patients, as aforementioned, and ACI/MACI procedures should be optioned. Finally it is important to delimit and restore as soon as possible the damage, in order to avoid the possible progression toward a degenerative disease, such as osteoarthritis (*Martin et al, 2005; Yan et al, 2015*).

3. Bone and cartilage tissue engineering

In the last decades tissue engineering (TE) has emerged as an effective option for human tissue or organ repair, restoration and replacement. Initial efforts have focused on skin equivalents for treating burns, but notable advancements in biomaterial sciences, cellular and molecular biology and delivery systems have allowed the engineering of a large variety of tissues: extraordinary results have been obtained from tissue engineered bone, blood vessels, liver, muscle, and even nerve conduits. In Table 1.2 some of the successful products from tissue engineering, already approved by Food and Drug Administration (FDA) and employed in regenerative medicine approaches, have been listed. However it is important to underline that the regulation about the clinical use and commercialization of tissue-engineered derived products need for a clarification and implementation, since it remains still ambiguous the homogeneous treatment of these hybrid devices, made of biomaterials, cells and bioactive factors (all or some of these components) (*Nature Biotechnology supplement, 2000; Mao and Mooney, 2015*). Definitely, in order to ensure the maximum levels in terms of safety and functional performances, an impeccable and highly controlled interplay between the three fundamental units composing the implantable product should be reached. For this reason *in vitro* and *in vivo* researches are examining the specific properties of single biomaterials, cells and signaling molecules in a widely available choices, trying to obtain a construct with the best mechanical and biological characteristics, able not only to regenerate tissue anatomy and functionality but with the intent of a real integration between implant and native tissue (Figure 1.5).

Table 1.2: FDA-approved products for tissue engineering and regenerative medicine (*Mao and Mooney, 2015*)

Product name	Biological agent	Clinical application
laViv	Autologous fibroblasts	Improving nasolabial fold appearance
Carticel	Autologous chondrocytes	Cartilage defects from acute or repetitive trauma
Apligraf, GINTUIT	Allogeneic cultured keratinocytes and fibroblasts in bovine collagen	Topical mucogingival conditions, leg and diabetic foot ulcers
Cord blood	Hematopoietic stem and progenitor cells	Hematopoietic and immunological reconstitution after myeloablative treatment
Dermagraft	Allogenic fibroblasts	Diabetic foot ulcer
Celution	Cell extraction	Transfer of autologous adipose stem cells
GEM 125	PDGF-BB, tricalcium phosphate	Periodontal defects
Regranex	PDGF-BB	Lower extremity diabetic ulcers
Infuse, Infuse bone graft, Inductos	BMP-2	Tibia fracture and nonunion, and lower spine fusion
Osteogenic protein-1	BMP-7	Tibia nonunion

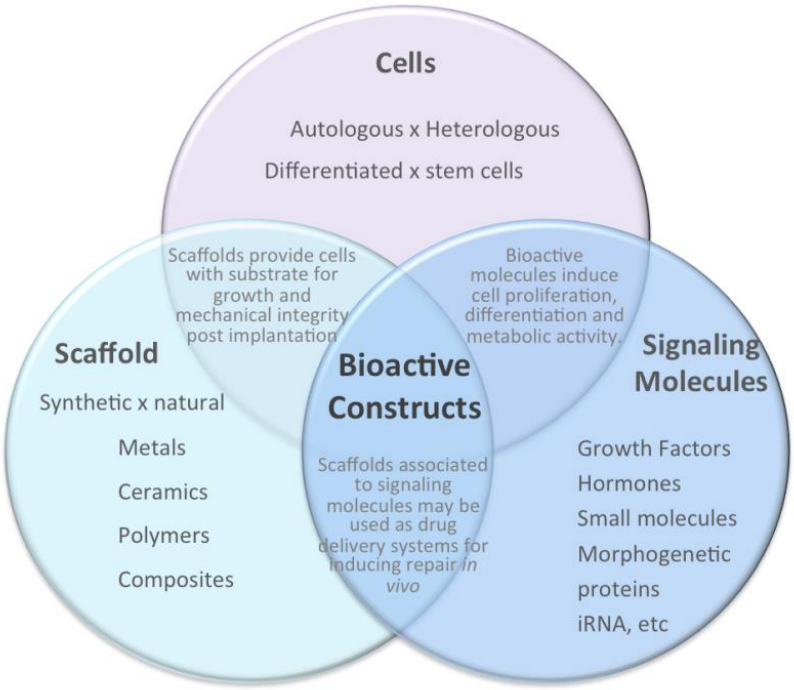

Figure 1.5: Schematic representation of a typical tissue engineering approach based on the combination of cells, scaffolds and bioactive molecules. A wide number of possibilities and combination is possible to obtain the optimal construct for tissue regeneration and integration. (*Lott Carvalho et al, 2013*)

Regarding bone and cartilage tissue engineering and the repair of osteochondral defects, biomaterials, usually representing the core of the construct, should closely resemble the double nature of the osteochondral unit, presenting a precise composition and an accurate texture reproducing both strength and compactness and elasticity of the bone/cartilage system. From a cellular point of view, not only the choice of the cell type (e.g. precursor *versus* mature cells) is relevant, but also a controlled culture condition results notably impactful on cell phenotype and, consequently, on the final outcome of the implant (*Naveena et al, 2012; Nukavarapu and Dorcemus, 2013*). In light of this, the employment of the appropriate growth factors and cytokines able to direct cell fate and a correct ECM formation is a crucial point: since osteochondral tissue is composed by different tissue layers, the right combination of biological molecules, capable to lead to the restoration of the unique properties of each layer, should be hit. In order to ensure a controlled release/exposure to these biological mediators, finely tuned delivery systems should be developed. Finally the manageability and the quality standardization of the tissue-engineered product represent an essential requisite to facilitate the implantation success (*Martin et al, 2006*). In this section the current and future strategies related to the field of bone and cartilage TE will be discussed, focusing the attention on the different components and the technical issues leading to the obtainment of an optimal tissue-engineered construct.

3.1 Cells

Cells remain a critical component in a successful tissue engineering approach, even though several cell-free strategies have been developed. A wide variety of cell sources are theoretically available for the employment in TE constructs, but several considerations should be kept in mind, such as the ideal type of cell which could produce an ECM as similar as the native tissue, the number of obtainable cells or, even more important, a definite characterization of cell phenotype and an accurate control of their fate (*Howard et al, 2013*). One of the best options surely relies on the use of autologous cells, directly isolated from the patient and expanded for a limited time *in vitro* before their re-implantation *in vivo*: one of the main advantages of this approach is the escape from the immune system response, but, unfortunately, this opportunity is not always possible. Firstly, it could induce a second damage site during cell collection, together with a high risk for infection and site inflammation, and, secondly, some patients could not benefit from autologous cells, such as elderly people or subjects with systemic or advanced-stage disorders: for this reason the employment of allogeneic or xenogeneic cells has been also proposed (*Heath, 2000*). Another important aspect about the type of cells is the choice of the maturation state, that is mature or stem

cells: if the first ones are safer and generally well-characterized, the second ones have the possibility for great proliferation and multi-differentiation, maintaining a self-renewing stem cell population. Among stem cells, great interest is emerging for adult and extra-embryonic tissue-derived stem cells, which are free from ethical issues and can be more easily collected (in particular the second group) (*Cancedda et al, 2003; Polak and Bishop, 2006*). Surely, the microenvironment in which cells are cultured *in vitro* or implanted *in vivo* is an essential element: mechanical, chemical and biological cues should be supplied to cells to ensure their regenerative potential and proper differentiation, suggesting the employment of an appropriate scaffold and specific bioactive molecules in combination (*Barthes et al, 2014*). A last consideration that should be done is the final role of the implanted cells; indeed they could act as the proper effector of the tissue regeneration, or alternatively they could only prime the repair process performed by the host cells.

3.1.1 Cells for bone and cartilage tissue engineering

Here below a description of the cells already used or potentially employable for bone and cartilage TE strategies will be reported, emphasizing the critical aspects just discussed above.

Mature cells: osteoblasts and chondrocytes

Osteoblasts can be isolated from adult bone tissue and periosteum through enzymatically or mechanical procedures; isolated cells reach the confluence in 3-6 weeks, maintaining the expression of typical osteogenic lineage protein, such as collagen type 1, osteocalcin (OC) or alkaline phosphatase (ALP). Furthermore, if cultured in presence of typical chemical inducers (β-glycerophosphate, ascorbic acid and dexamethasone), they are able to produce typical mineralization nodules, consisting in calcium-phosphate crystals embedded in the extracellular matrix, resembling typical bone ECM. It has been reported that the use of differentiated osteoblasts enhanced the rate and extent of bone tissue regeneration; nonetheless some issues are associated with the use of these cells since they have relatively short lifespans and need to be continually replaced: maintenance of the cell population depends also from the bone turnover rate and use of therapeutic agents, such as estrogens, could increase OBs lifetime, through anti-apoptotic effects and sustaining their proliferation and differentiation (*Jayakumar and Di Silvio, 2010; Rupani et al, 2012*).

Harvesting and enzymatic isolation of mature chondrocytes from articular cartilage have been performed for long considering their application in ACI procedures. However, since it is not

possible to obtain large amount of cells, chondrocytes need to be expanded in vitro and this step represent a significant issue: indeed monolayered chondrocytes go throughout a de-differentiation process, where, concurrently with the increasing culture passages, they begin to lose their phenotypical characteristics, moving from their typical rounded shape to a fibroblastic-like spindle shape morphology and lowering the production of cartilage markers such as Sox9, Col2a1, aggrecan or GAGs, in favor of collagen type 1 expression (*Schnabel et al, 2002; Ma et al, 2013*). These phenotypical changes consistently affect the clinical outcomes of chondrocytes implantation, leading to the development of alternative culture strategies: in particular three-dimensional (3D) cell culture systems have been proposed in order to maintain chondrocytes phenotype or induce their re-differentiation. Both scaffold-based and scaffold-free approach have been reported: the first one is mainly based on the employment of hydrogels and polymeric scaffolds in which cells are entrapped, re-assuming their rounded morphology and the production of chondrocytic proteins; as aforementioned these material-based devices has been largely applied in the advancement of ACI procedures, the MACI technique (matrix-induced autologous chondrocyte implantation). Scaffold-free approaches (that will be discussed in the paragraph 3.1.2), instead, are mainly based on high-density cell cultures, such as pellet or micromass (*Homicz et al, 2003; Dehne et al, 2010; Caron et al, 2012*). Additionally the employment of chondrogenic growth factors or cells from other sources has been proposed: for example, chondrocytes from nasal septum or auricular cartilage have been shown the ability to produce an ECM closely similar to articular cartilage with good mechanical properties (*Pleeumekers et al, 2014*).

Even though limitations associated with these mature cells (i.e. donor site morbidity and limited matrix production following cell expansion) will reduce their clinical use in favor of stem cell-based application, primary osteoblasts and chondrocytes still represent optimal cellular models for *in vitro* studies and the obtainment of a deeper understanding of the molecular mechanisms underlying osteo- and chondrogenesis.

Mesenchymal stem cells

Mesenchymal stem cells represent a wide class of progenitor cells which can be found in the stroma of different tissues, both adult and extra-embryonic ones. MSCs were originally isolated from bone marrow, but over the years cells with very similar characteristics were discovered in adipose tissue, peripheral blood, dental pulp, periodontal ligament, umbilical cord (Wharton's jelly or cord blood), amniotic fluid and other several tissues. These cells share common characteristics, which are fundamental for their identification as MSCs: 1) the self-renewal and proliferative ability, together with the colony-forming capacity; 2) the expression of typical surface markers, such as CD29,

CD44, CD90, CD105 and CD73, and the absence of hematopoietic and epithelial surface proteins, such as CD31, CD34, CD45, CD11 or CD19; 3) the multipotency, demonstrated by the ability to undergo toward osteogenic, chondrogenic and adipogenic differentiation (*Marion and Mao, 2006; Lindner et al, 2010*). Nevertheless, more recently, the different *in vivo* regenerative potential of MSCs isolated from diverse sources has been reported, suggesting that native microenvironment could highly influence the biology of these cells, which, beyond their common features, preserve a biological memory affecting clinical outcomes (*Sacchetti et al, 2016*). However, thanks to their multipotent ability, MSCs have emerged as a promising cell source both for bone and cartilage tissue engineering: indeed, in favorable microenvironment and under appropriate stimulation MSCs can differentiate towards both the osteogenic and the chondrogenic lineages. *In vitro* differentiation is obtained by the exposure to specific molecules, in particular β-glycerophosphate, ascorbic acid and dexamethasone for osteogenic induction and TGF-β, dexamethasone, ascorbic acid, insulin, selenious acid, transferrin and sodium pyruvate for chondrogenesis, which occurs only in 3D cell culture systems. Nonetheless, these established protocols frequently lead to controversial results in terms of cell functionality and phenotype, suggesting that further investigations on the role of these molecules during MSCs osteogenesis and/or chondrogenesis and the research of alternative stimulating factors which could ensure a precise control on cell behavior are essential to obtain safe, standardized and functional clinical expectations (*Gimble et al, 2008*). Even though a better characterization of the molecular mechanisms guiding MSCs regenerative potential is required, several clinical trials based on MSCs employment are already registered in the database of US National Institutes of Health: up to June 2015, 44 ongoing studies were reported (*Squillaro et al, 2016*). It is important to underline that the beneficial effects of MSCs depend not only from their regenerative potential, but also from their immune-modulatory and homing abilities: for example a clinical trial with co-transplanted MSCs for the treatment of steroid-refractory graft-versus-host disease (GVHD) is currently in progress (*Yagi et al, 2010*). This property could be exploited also for bone and cartilage diseases with inflammatory basis, such as osteoarthritis or post-traumatic lesions. One of the main issues in the use of MSCs is occurring cell senescence during *in vitro* expansion after several culture passages (*Campisi et al, 2007*): in order to overcome these limitation and enhance the clinical potential of MSCs, a charming combination with biomaterials and growth factors or cell engineering techniques could be applied, as will be discussed in the next sections.

Induced pluripotent stem cells

Induced pluripotent stem cells (iPSCs) represent a population of pluripotent cells with self-renewal ability, like embryonic stem cells (ESCs), but without the unfavorable ethical issues associated with

these cells. The first generation of iPSCs was reported in 2006 by Takahashi and Yamanaka, by the transduction of mouse fibroblasts with four reprogramming factors (c-Myc, Klf4, Oct3/4 and Sox2) which could reprogram the nuclei of somatic cells into pluripotent ones. From that moment several works have reported the potency of iPSCs to differentiate into numerous different somatic cells, including osteochondroprogenitors, osteoblasts and chondrocytes, making these pluripotent cells an optimal candidate for bone and cartilage tissue engineering (*Tsumaki et al, 2014*). One of the main advantages from iPSCs technique is the possible utilization of autologous cells reprogramming easily-obtainable cells from patient, such as fibroblasts; however studies in which iPSCs are derived from an individual donor, differentiated, and transplanted back into that donor needs still to be performed (*Phillips et al, 2014*). Furthermore different differentiation protocols have been proposed, each one presenting advantages and limitation, and, thus, leading to variable outcomes in terms of amount of differentiated cells and quality of produced ECM. Finally a deeper characterization of the biology of these cells and the effective proof of their ability to generate bona fide bone and cartilage are highly needed (*Tsumaki et al, 2014*): these aspects, together with the high risk to induce tumor formation, are moving the research to develop optimal protocols for ensuring a controlled differentiation of iPSCs towards mesenchymal progenitors and osteogenic/chondrogenic lineage before their transplantation. Although iPSCs have shown to be a promising cell source for tissue engineering approach, their clinical employment seems to be still distant.

3.1.2 Three-dimensional cell culture systems

Since cells naturally reside in a three-dimensional microenvironment which provides physical structure, but also biological and mechanical stimuli, the need to develop *in vitro* 3D culture system have emerged to study several biological processes, including cell differentiation and tissue regeneration mechanisms. Regarding tissue engineering approaches, the fact to maintain cells in a 3D condition, closer to *in vivo* situation, ensures the preservation of their phenotypical characteristics and, thus, their regenerative potential. The beneficial effects of these three-dimensional arrangements mainly depend from their ability to reproduce typical cell-cell and cell-matrix interactions (*Kleinman et al, 2003; Haycock, 2011; Edmondson et al, 2014*). However the main drawback of current 3D culture systems is the lack of transport mechanisms for nutrients and oxygen into the inner part of the cell construct, which is continuously exposed to the risk for necrosis: in order to overcome this issue, miniaturization of the culture devices or the development of vascular systems have arisen as optimal solutions. From the other side the restricted nutrition and

oxygenation actually better mimic the microenvironment of *in vivo* tissue to a certain extent (*Edmondson et al, 2014; Knight and Przyborski, 2015*). A wide variety of techniques currently exist to culture cells in 3D condition: they could be categorized in scaffold-based and scaffold-free approaches (Figure 1.6). Scaffold-based strategies consist in culturing cells into/onto devices composed of biomaterials: the choice of the most appropriate material depends on its biological, structural and mechanical properties, which should be adequate for the final purpose of the construct. (*Fitzgerald et al, 2015*).

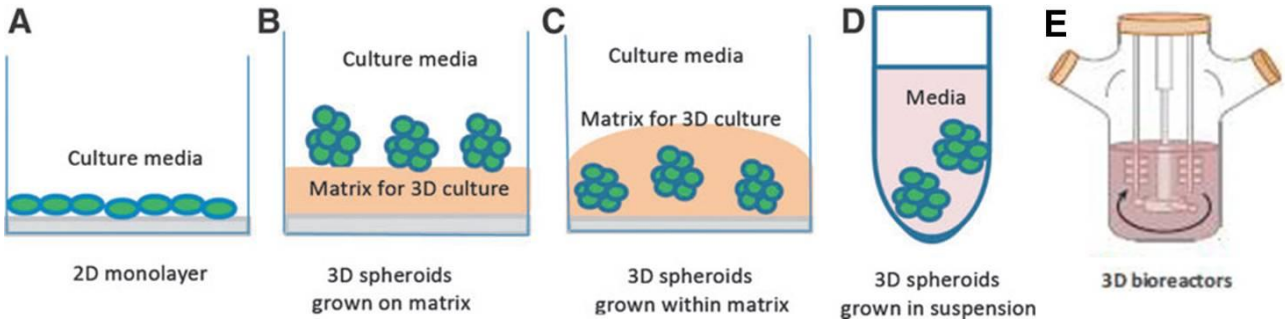

Figure 1.6: Schematic diagrams of the traditional two-dimensional (2D) monolayer cell culture (A) and typical three-dimensional (3D) cell culture systems: cell aggregates grown onto matrix (B), cells embedded within biomaterial-derived matrix (C), scaffold-free cell spheroids in suspension (D) and culture in bioreactor system (E). (*Edmondson et al, 2014*)

Although scaffolds remain largely employed and have shown great utility in the development of 3D culture systems, they present some issues mainly associated with the presence of an exogenous structure which could highly influence cellular and metabolic responses, altering the natural cell behavior. Scaffold could also release degradation products which could further affect biological reactions and, additionally, the arbitrary cell distribution inside the architectural arrangement of the scaffold could not facilitate cell-to-cell contacts, which is a key aspect of *in vivo* tissues (*Ozbolat, 2015; Cheng and Changyong, 2015*). For these reason also scaffold-free approaches have been proposed: they are based on the self-aggregating ability of the cells, which are then triggered to deposit ECM which acts as a natural cell scaffold (*Achilli et al, 2012*). Biomaterials and derived scaffolds will be deeply discussed in the next section (paragraph 3.2), while herein some of the scaffold-free strategies will be described. However it is important to underline that if for cartilage this kind of 3D cultures have found a wide employ (probably also for their ability to recapitulate the initial condensation phase in MSCs chondrogenesis), the production of bone-like structures remain anchored to the use of stiff and consistent biomaterials.

Cell spheroids

Cell spheroids represent a simple strategy to obtain 3D scaffold-free cultures, since they are produced by the employment of culture substrates which impede plastic-attachment, supporting cell self-aggregation. Several techniques have been reported for the spheroid formation, such as hanging drop, pellet culture, micro-molding, microfluidic or rotating wall vessel (*Fitzgerald et al, 2015; Ozbolat, 2015*). Spheroids technique is largely employed in MSCs chondrogenesis and chondrocyte re-differentiation, resembling the condensation step which is essential for a proper chondrogenic differentiation and cartilage-like ECM production (*Lee et al, 2011; Ghone and Graysone, 2012; DuRaine et al, 2015*). Cell spheroids of autologous chondrocytes, namely Chondrosphere®, are currently in a phase III clinical trial for the treatment of cartilage defects in knee joint (*https://clinicaltrials.gov/ct2/show/NCT01222559*). However cell spheroids have been proposed also for bone tissue formation: for example Scotti and colleagues in 2010 showed how it is possible to employ MSCs pellet cultures to recapitulate endochondral ossification pathway through an osteogenic stimulation after occurred chondrogenesis; the group demonstrated also the bone tissue formation *in vivo* when hypertrophic spheroids were implanted subcutaneously in nude mice (*Scotti et al, 2010*). Additionally some groups demonstrated also the possibility to directly differentiate MSCs spheroids towards the osteoblastic lineage with increasing expression of osteogenic markers and typical bone ECM proteins. However these work, rather than showing an enhanced osteogenesis in 3D cell aggregates, reported an increased maintenance of cell osteogenic potential, which could be successively exploited *in vivo* for bone regeneration (*Yamaguchi et al, 2014; Murphy et al, 2016*).

Cell sheets

In cell sheets technology cells are growth as a contiguous sheet with their natural ECM; these sheets are then collected without breaking them, maintaining their naturally formed networks intact, without the use of proteolytic enzyme treatment or the use of instruments to detach them from the culture surface. Cell sheets formation is generally established on thermo-responsive culture dishes, which enables reversible cell adhesion to and detachment from the dish surface by controllable hydrophobicity of the surface: cell sheet can be collected simply by reducing culture temperature lower than 32 °C and directly implanted in the host damaged tissue (*Yang et al, 2005; Elloumi-Hannachi et al, 2009*). Even though this kind of implant are more suitable for tissue with high cell density and a relatively minor presence of ECM (e.g. heart or liver), cell sheet technology has been proposed also in bone and cartilage TE applications. For example in a recent work by Itokazu and coauthors, chondrogenic cell sheets composed of MSCs derived from human bone marrow (hBM-

MSCs) cultured in presence of FGF-2 were designed for the repair of osteochondral defects in a rat model (*Itokazu et al, 2016*). Similarly Pirraco and colleagues produced cell sheets of rat BM-MSCs that were implanted subcutaneously in nude mice, demonstrating the formation of new mineralized and vascularized bone-like tissue. However a mechanical and structural characterization of the newly-derived tissues needs to be performed to establish the effective clinical potential of this technology in bone and cartilage repair strategies: for example, regarding bone TE, it has been hypothesized that cell sheet approach could be more appropriate for flat bones, such as in cranial defects, where lower mechanical properties are required (*Pirraco et al, 2011*). An interesting aspect of cell sheet technology is the possibility to create a multilayered construct by the superimposition of several sheets: this opportunity could be speculated for the reproduction of typical multilayered structure of the osteochondral tissue (*Mitani et al, 2009*).

Bioreactors

Bioreactors can be defined as devices that use mechanical means to influence biological processes in closely monitored and tightly controlled dynamic environment: in particular bioreactors provide mechanical cues and ensure a more homogenous delivery of nutrients and oxygen, stimulating cell aggregation and the ECM production (*Plunkett and O'Brien, 2011*). Although bioreactors can be employed to enhance the properties of scaffold-free constructs, they have been also explored for sustaining biological processes in scaffold-based devices. Different kinds of bioreactors are available, which can be grouped in spinner flasks, rotating wall vessels, perfusion bioreactors and compression systems (*El Haj and Cartmell, 2010; Plunkett and O'Brien, 2011*). Mechanical stimulation together with sustained ECM synthesis and enhanced construct maturation favored the increasing use of bioreactors for the production of bone and cartilage cell-based devices. Several works in the last years have demonstrated the feasibility of culturing mesenchymal precursors, chondrocytes or osteoblasts in different types of bioreactor in combination with scaffolds or through scaffold-free approach, in order to obtain chondrogenic/osteogenic construct with regenerative potential *in vivo* (*Furukawa et al, 2008; Rath et al, 2012; Kang et al, 2014; Li et al, 2016a*).

3.1.3 Cell engineering and gene therapy

Gene therapy consists in the delivery of DNA or RNA into cells or tissues: in tissue engineering approaches this technique could be used to enhance the regenerative potential of transplanted cells or for the direct treatment of the damaged tissue. Indeed gene therapy can be performed both *in vivo* and *ex vivo*: in the first case genetic materials is directly injected into the host tissue through the

employment of delivery system, while the second option involves the genetic modification of autologous or allogenic cells that are successively implanted in the damaged site. *In vivo* gene therapy is simpler and minimizes the risk of infection since only one procedure is required, however it may elicit inflammatory response and, furthermore, the proper delivery to the targeted cells is not frequently specifically achieved, resulting in low expression levels of the transgene. From the other side *ex vivo* gene therapy ensures a prolonged transgene expression, but it may increase the risk for host morbidity and infection (in particular in the case of autologous cells) and it has not yet been established if the implanted cells could persist for a period of time sufficient to heal the defect. Both viral and non-viral (i.e. based on the employment of transfection reagent, such as liposomes) strategies have been proposed: viral vectors guarantee an enhanced efficiency, but are more expensive and are associated with elevated immunogenicity (*Hu, 2014; Nayerossadat et al, 2016*). Different studies have reported the direct injection of viral vectors in injured tissue for the delivery of pro-osteogenic (e.g. BMP-2, BMP-6, BMP-9, VEGF) or pro-chondrogenic (e.g. TGF-β1, Sox9, IGF-1, FGF-2) factors in order to increase the formation or reduce the degeneration of bone or cartilage tissues, respectively (*Kimelman Bleich et al, 2012; Cucchiarini et al, 2015*). Alternatively to the direct injection of viral vectors, the employment of gene activated matrices (GAMs) has been suggested: they consist in biomaterial-based devices containing the genetic material that should be delivered in the host tissue, allowing a slow and controlled release to the surrounding cells (*Raisin et al, 2016*). For the *ex-vivo* strategy the use of MSCs results particularly attractive, since their homing ability to reach the injury site could be exploited. Even in this case, the engineering of these cells with different pro-chondrogenic or pro-osteogenic factors, both through viral vectors or transfection reagents, have been reported in literature (*Longo et al, 2012; Balmayor and van Griensven, 2015*). An interesting alternative approach is the engineering of cells with antisense oligonucleotides which, instead of directly enhance the regenerative potential, target and induce the down-regulation of other cellular factors or microRNAs (miRNAs) negatively involved in the regenerative process (*Lee and Roth, 2003*; *Beavers et al, 2015*). Finally it is important to underline that a great strengthening to gene therapy strategy will come from the optimization of delivery systems, which should ensure an increased efficiency in transgene conveyance together with a tunable and controlled release for a sustained persistence of the therapy (*Jo and Tabata, 2015; Cucchiarini, 2016*).

3.2 Biomaterials

Biomaterials should promote tissue regeneration acting as a carrier for cells and therapeutic agents, but also providing structural and mechanical properties to the damaged tissue; additionally an ideal biomaterial should provide a micro-architectural framework reminding native extracellular matrix and should degrade at comparable rate to growth of new tissue at the site of implantation (*Lee et al, 2014*). Over the years, several biomaterials have been explored: natural ones enhance biological interactions with loaded cells and host tissue, but result in a mechanical inferiority, while synthetic ones ensure a higher control on the mechanical, chemical and structural properties of the scaffold at the expense of its biocompatibility (*Bernhard and Vunjak-Novakovic, 2016*). However in order to maintain the useful features of different kind of biomaterials, the development of composite scaffold is always more frequent: these heterogeneous devices could result really convenient for the restoration of the osteochondral environment, which is natively composed by ECM of different biological and mechanical nature (*Nooeaid et al, 2015*). It should be underlined that not only the type of material is relevant in the scaffold production, but also processing techniques and macro- and micro-architectural design appear impactful in the success of implantation procedures (*Lu et al, 2013*).

3.2.1 Materials for osteochondral scaffolds

Current biomaterials for bone and cartilage TE can be grouped in 5 classes: natural polymers, synthetic polymers, metals, inorganic materials and ECM-derived matrices. Each of these categories includes a wide variety of materials which present unique and peculiar characteristics. The main features of the different groups and the application of the most studied biomaterials will be reported below.

Natural polymers

Natural polymers can be extracted from animal or plant sources and thanks to their flexibility can be arranged into versatile scaffold type, such as fibers, sponges or gels, allowing the adaptation of their shape to required form. Among main employed polymers in bone and cartilage TE field, it is possible to include alginate, agarose, collagen, hyaluronic acid, chitosan and silk. Some of these materials (e.g. alginate, agarose, silk) are unrecognizable to human enzymes, favoring a slow degradation rate and providing more time to initiate and support tissue regeneration; others (e.g. collagen and hyaluronan) retain specific molecular domains, resembling native ECM, which sustain

cell attachment and proliferation and trigger their regenerative potential, together with the integration in the implantation site (*Bernhard and Vunjak-Novakovic, 2016*). Also polymers, which do not contain molecular cues, could be functionalized with specific signals to guide cell behavior; for example alginate hydrogels have been frequently modified with bioactive peptides to increase cell adhesion ability: RGD sequence (Arginine-Glycine-Aspartic acid), which is abundant in adhesion molecules, and KHIFSDDSSE peptide, mimicking the binding domain of the neural cell adhesion molecule (N-CAM), have been largely employed with positive outcomes (*Hersel et al, 2003; Dalheim et al, 2015*). On the contrary collagen, being one of the main components of bone and cartilage ECM, maintain the native typical signals, guaranteeing not only cell adhesion, but also stimulating the synthesis and assembly of new ECM: thus, collagen scaffolds are already employed in MACI procedure to sustain the maintenance of chondrocytes phenotype and the production of new functional tissue (*Nixon et al, 2015*). Alginate and agarose hydrogels, instead, find preferentially employment in micro-encapsulation procedures: this practice allows the immobilization of cells or bioactive agents inside hydrogel devices, which exhibit a semi-permeable membrane ensuring the diffusion of small molecules, such as oxygen and nutrients (essential for cell viability and functionality), or the controlled release of the entrapped biological mediators. Additionally the membrane acts as an immune-isolating barrier protecting encapsulate cells from host immune system, with really impactful repercussion in heterologous cell transplantation (*Murua et al, 2008; Nafea et al, 2011*). Micro-encapsulation procedures have been widely employed in cartilage and bone tissue engineering, both for the immobilization and transfer of potentially regenerative cells (from precursors to mature chondrocytes/osteoblasts) and for the delivery of biological molecules. For instance in a recent work Gonzalez-Fernandez et al. developed gene-activated alginate hydrogels, where MSCs were co-encapsulated with expression vectors for TGF-β3 and BMP2 complexed with nano-hydroxyapatite particles: authors demonstrated how the different combination of co-encapsulation could increase the expression of GAGs or typical collagenous proteins for cartilage or bone ECM repair (*Gonzalez-Fernandez et al, 2016*). Although natural polymers showed advantageous biological properties supporting osteoblastic/chondroblastic phenotype, their ability to stimulate *in vivo* regeneration and integration is yet to be determined; finally a major issue is represented by their low mechanical features, which instead represent an important component of osteochondral tissues physiology (*Bernhard and Vunjak-Novakovic, 2016*).

Synthetic polymers

Due to their hydrophobic surface, synthetic polymers offer a reduced biological activity and interaction, which is counterbalanced by the possibility to be submitted to a wide range of

chemistries and processing options allowing a more ideal control over the micro-architectural and mechanical properties of the resulting scaffold. In addition the laboratory fabrication of synthetic polymers can be scaled up to industrial-scale manufacturing processing, which is a requirement to meet potential clinical demands (*Nooeaid et al, 2012*; *Bernhard and Vunjak-Novakovic, 2016*). This class of biomaterials includes a variety of polyesters, such as polyglycolic acid (PGA), polylactic acid (PLA), poly lactic-co-glycolic acid (PLGA) or polycaprolactone (PLC), polycarbonates, polyanhydrides and polyphosphazenes: PGA and PLA have gained particular interest thanks to their high biodegradability and being already employed in clinic for sutures (*Asti and Gioglio, 2014*). As for natural polymers, also synthetic ones could be functionalized to increase their biological properties: Zouani et al. developed polyethylene terephthatalate (PET) films, where surfaces were grafted with different BMPs and/or adhesion peptides, demonstrating an effective increase in expression of osteogenic markers and production of extracellular matrix by pre-osteoblast like MC3T3-E1 cells (*Zouani et al, 2010*). More recently, Lee and colleagues demonstrated the pro-chondrogenic effects of PGLA scaffolds functionalized with MSCs and PD98059, an inhibitor of extracellular singal-regulated kinases (ERKs) and chondrocytes hypertrophy: *in vivo* implantation of these scaffolds resulted in the restoration of an osteochondral defect in a rabbit model, without the appearance of hypertrophic cartilage areas, which remains one of the main issue in cartilage reparative approaches (*Lee et al, 2014*). As demonstrated by this interesting work, and many others, these synthetic polymers, thanks to their tunable biodegradable properties, could be exploited also for the development of drug delivery systems with high controlled release (*Gavasane and Pawar, 2014*). Although positive results have been widely reported employing systems based on synthetic polymers, the degree of regeneration achieved thus far has not been convincing enough to justify clinical translation and, probably, a further advancement is necessary to recreate an environment more similar to native tissue (*Bernhard and Vunjak-Novakovic, 2016*).

Metals

Rigidity and stiffness of metallic materials are particularly interesting features in bone tissue engineering approaches; thus, they are frequently used as implanting materials in dental and orthopedic surgery to replace damaged bone or to provide support for healing bones (*Alvarez and Nakajima, 2009*). Among the most employed metals, titanium and tantalum have shown, over the years, good qualities in terms of biocompatibility, mechanical strength and bone growth induction. Even though tantalum porosity has been identified an essential characteristic for obtaining an optimal cell proliferation and ECM production, the main disadvantage of metallic biomaterials remains their lack of biological recognition signals: for this reason surface coating and modification

(e.g. with bioactive ions) have emerged as an attractive strategy to increase bioactivity of these scaffolds maintaining their mechanical properties. For instance calcium-phosphate coating has been largely employed to increase osteoconductivity of metallic scaffolds, exhibiting an increased interaction with osteoblastic cells and a rapid and more effective biomineralization. Another substantial limitation of metallic devices is their low/absent biodegradability, which remains a crucial point in the biocompatibility definition (*Alvarez and Nakajima, 2009; Nooeaid et al, 2012*). In this context the use of biodegradable metals, such as magnesium- or iron-based alloys, has been optioned: *in vivo* positive outcomes on bone formation after porous magnesium scaffold implantation have already been reported, together with an accompanied degradation of the material (*Witte et al, 2007*). However a further optimization of this new class of metallic biomaterials is highly required to meet clinical requirements, such as controllable degradation rate, prolonged mechanical stability and excellent biocompatibility: for example the possible release of toxic corrosion-derived products and ionic leaching remain two major issues in the use of these scaffolds (*Li et al, 2014*).

Inorganic materials

The role in promoting biomineralization is well-known for some type of ceramics, such as calcium-phosphate, hydroxyapatite (HA) or β-tricalcium phosphate (TCP), and bioactive glasses (e.g. Bioglass®). The osteoconductive and osteoinductive properties of these materials have been widely demonstrated both *in vitro* and *in vivo*, showing also a good ability to bind native bone and, thus, high integration degree (*Nooeaid et al, 2012; Baino et al, 2015*). Another remarkable feature of this kind of materials is the tunable control on their degradation rate dependent from the scaffold porosity; anyway increasing pore dimensions heavily affect the mechanical properties of these bioceramics and bioglasses (*Gariboldi and Best, 2015*). For this reason a combined approach with polymeric materials could be attempted, where a synergistic effect is expected from bone-favoring properties of these inorganic materials and adaptable structural characteristics of polymers. For example Bretcanu et al. fabricated porous composites by using Bioglass® as a porous inorganic matrix and by coating it with the polymer poly(3-hydroxybutyrate) (P3HB): the polymer acted as glue holding the inorganic particles together when the scaffold struts started to fail, increasing the compressive strength twice respect to the bare Bioglass® scaffolds (*Bretcanu et al, 2009*). This kind of composite devices have found occupation also in clinical practice: for instance HA/polyethylene porous composites, marketed under the commercial name “Hapex”, are currently employed for the repair of orbital floor fractures (*Tanner, 2010*).

ECM-derived materials

In the last years there was an increasing interest in creating biological scaffolds directly derived from tissue and organs decellularization and composed of extracellular matrix. This event is ascribable to the need for generating devices able to reproduce a 3D microenvironment more similar to native tissue, since, up to now, other biomaterials failed in this crucial challenge. Additionally increasing evidences showed how ECM is an active component of the tissue, interacting with cells and determining their fate; from the other side, cells continuously react to microenvironment changes, also inducing modification in the surrounding matrix (*Gattazzo et al, 2014*). This intricate interplay, governed by a plethora of adhesion and secreted signals, is highly difficult to reproduce *in vitro* and in scaffold arrangement. For this reason ECM-derived biomaterials arose as an optimal option in supporting and encouraging specific tissue formation, through the retention of unique growth factors, topographic characteristics and microenvironmental cues which could direct regenerative cell fate (*Zhang et al, 2016b*). The employment in clinic of some of these decellularized matrices has been already approved by FDA, such as for Alloderm® from dermis tissue, Synergraft® from porcine heart valves and porcine urinary bladder matrix (UBM) (*Chen et al, 2015*). The decellularization process is essential in the production of these biomaterials since it reduces antigenicity and the risk for disease transmission, inflammation and host immune response, particularly in the case of xenogeneic and allogeneic donor tissues (*Crapo et al, 2011*). Even though each tissue possesses its own typical structure and composition, the mechanism guiding cell differentiation and formation of new tissue seems to be more generic, allowing the use of ECM scaffold derived from a different tissue respect to the target one with a great extent of success and making possible the employment of xenogeneic and allogeneic ECM, too (*Benders et al, 2013*). All these beneficial aspects have encouraged the use of ECM-derived biomaterials also in the field of bone and cartilage TE. For example Chen and coauthors showed how ECM-based scaffolds derived from porcine menisci were able to sustain *in vitro* chondrogenesis of hBM-MSCs and induce new tissue formation without immunogenicity after implantation in rat (*Chen et al, 2015*). In a more intriguing work by Aulino et al., the authors proposed an acellular scaffold derived from skeletal muscle (MAS) as a multipotent biomaterial able to induce the regeneration of different tissues of the musculo-skeletal system, including bone and cartilage: indeed they demonstrated the presence of regenerating myofibers together with mineralized bone ECM and cartilaginous tissue in the site of MAS implant in a mouse model of musculo-skeletal damage, precisely between the skeletal muscle and the adjacent bone in the anterior tibia or in the mandible (*Aulino et al, 2015*). The positioning of the implant, but also the size of defect could be crucial point in an effective functionality of these scaffolds obtained from extracellular matrix, as hypothesized by Turner et

colleagues in a similar work, studying the effect of small intestinal submucosa ECM-derived scaffold (SIS-ECM) in a dog model of musculo-skeletal injury: indeed even though a functional restoration of muscle tissue was not obtained, authors observed the generation of new bone and cartilage tissue with good qualities (e.g. bone vascularization) when SIS-ECM was implanted in close apposition to bone (*Turner et al, 2012*). These data indicate how, not only implanted ECM-scaffold could influence the behavior of resident cells, but also the host microenvironment is decisive for the successful tissue repair. As could be noted in these examples and from the literature, the decellularization and employment of ECM from soft connective tissues is quite successful, while the obtainment of ECM-derived scaffolds from compact tissues like bone or cartilage remains still technical problematic, and only in the last years positive outcomes have been reported (*Chen et al, 2015*). For example in a recent work Cunniffe and coauthors described the employment of ECM derived from hypertrophic cartilage to induce endochondral ossification of hBM-MSCs *in vivo*, observing *de novo* mineral accumulation and vascularization (*Cunniffe et al, 2015*). Although great results have been obtained with different kind of ECM-derived scaffolds, a more profound knowledge of the effect of the source and preparation method on the biological activity of the biomaterial and, thus, of the mechanisms guiding ECM-based scaffold/host microenvironment interplay in tissue regeneration will be fundamental to deeply understand the clinical potential of these biological materials.

3.2.2 Geometry and design of the scaffold

Architectural and structural properties of bone and cartilage devices represent a critical point in a successful TE approach; let consider how porosity could influence cell infiltration, tissue ingrowth and neovascularization, but at the same time could affect mechanical strength of the scaffold. Pore size and distribution, accessibility and tortuosity, but also the entire shape and geometry of the device should be considered in the design of the most suitable scaffold (*Izadifar et al, 2012; Gariboldi and Best, 2015*). In an elegant work Tseng and colleagues showed how changes in scaffold shape and architecture could directly influence MSCs behavior, through the realization of thermo-responsive devices composed of shape memory polymers (SMPs): the heat-triggered transition from strain-aligned scaffold, where cells were aligned along the fiber direction, to random-fiber oriented form induced cytoskeleton rearrangement, leading to the loose of this preferential cell disposition (*Tseng et al, 2013*). Also curvature degree of the scaffold has been recognized has an important element in cell-cell interactions and, consequently, in tissue regeneration; in particular positive outcomes in terms of biological response have been reported for

concave surfaces: for example it has been observed that *in vitro* mineralization occurs inside the cavities created on the surface of calcium phosphate ceramics and not on the planar surfaces (*Zadpoor, 2015*). Regarding micro-architectural properties, the presence of both macro and micropores are important in scaffold-dependent biological response, since macropores promote cell migration and micropores promote cell–cell interaction and mass transport, improving tissue formation especially *in vivo*. Thus, it has been evidenced how chondrogenesis may vary with pore size: small pore sizes might help maintain chondrocyte phenotypes, while larger pore sizes increase the extension of ECM. Furthermore pore interconnectivity can influence the ability of a scaffold to support cell viability and differentiation as well as the quality of formed tissue: interconnected structures with open pores are more capable of facilitating homogeneous cell seeding and better nutrient dispersion throughout the construct, ensuring a homogeneous chondrogenesis/osteogenesis with cartilage/bone like-tissue formation in the whole scaffold volume (*Izadifar et al, 2012*).

3.2.3 Multiphasic scaffolds

Multilayered scaffolds are highly promising in bone and cartilage tissue engineering, in particular in the repair of osteochondral defects: they are, indeed, designed to imitate the multiple nature and characteristics of the osteochondral system, presenting a hierarchical structure from articular cartilage to subchondral bone throughout calcified cartilage layer (*Marrella et al, 2016*). Biphasic and triphasic scaffolds are constructs presenting two or three, respectively, different architectures or materials: indeed, also only one material could be used to produce different layers with significant variations in physical properties. Gradient scaffolds have been instead elaborated to respond to an increasing attention toward the cartilage-bone interface, ensuring continuity between the distinct layers of the device. Furthermore, in order to recreate an internal microenvironment as close as possible to the osteochondral native one, a specific combination of progenitor/mature cells and growth factors and cytokines could be included in each layer of these multiphasic scaffolds (*Yousefi et al, 2014*). Different technical approach can be considered in the fabrication of these constructs. One option consists in producing bone and cartilage phases separately, culturing them with osteogenic or chondrogenic cells and medium, respectively, and finally assembling the two layers; however this technique results in the poor integration and the potential separation of the two components. Alternatively interdiffusion is also possible: it provides the penetration of the cartilage-mimicking layer into the superficial zone of the bony one. Even though better integration was reported, the interface between the two layers was highly different from the cartilage-bone one in the osteochondral unit. In this context gradient scaffolds have emerged, since, through the

reproduction of structural, mechanical and biological native gradient, eliminate the need to integrate distinct layers and circumvent the challenge of fabricating a physiologically relevant or very thin calcified cartilage scaffold that must be pre-integrated with the bone and cartilage sections (*Yousefi et al, 2014; Boushell et al, 2016*). For instance Di Luca and colleagues recently developed a construct presenting a gradient in pore shape and fiber alignment, demonstrating a pro-chondrogenic effect of square pores on hMSCs, with an increasing expression of osteogenic markers and ALP activity as pores progressively moved toward a rhomboidal conformation (*Di Luca et al, 2016*). Gradients of growth factors could be also incorporated in these precisely arranged scaffolds, to enhance the ability of each layer to sustain the proper cell differentiation and specific ECM production together with a better integration among the different architectures of the newly formed tissue (*Boushell et al, 2016*). Even though multiphasic and gradient scaffolds are in an initial stage of development and trials, they represent the future of osteochondral tissue engineering, allowing a unique combination of structural, mechanical and biological elements. It is undoubted that the most appropriate formulation must be found before remarkable clinical outcomes will be observed, and in these circumstances a great support will be given from the advancement in the field of computational analysis and bioprinting techniques (*An et al, 2015; Boccaccio et al, 2016; Liu et al, 2016*).

3.3 Bioactive molecules and signaling pathways

Signaling molecules play a fundamental role in modulating cell-to-cell signaling, cell fate and activities with significant repercussion in the proper formation and maturation of bone and cartilage tissues. Several growth factors, transcription factors and miRNAs involved in tissue development and homeostasis have been considered for application in tissue engineering approaches, both for the obtainment of a superior control of cell fate in *in vitro* 3D constructs and for sustaining tissue regeneration and implant integration *in vivo* (*Kwon et al, 2016; Lopez-Ruiz et al, 2016*). Here below the main investigated molecular pathways with a potential role in bone and cartilage TE will be considered.

TGF-β/BMP signaling

The TGF-β superfamily includes a wide class of molecules, among which the main ones are transforming growth factors beta (TGF-βs) and bone morphogenetic proteins (BMPs). Their signaling is initiated by the binding to type II receptors which engages and phosphorylates type I receptor, resulting in the subsequent phosphorylation and activation of Smad proteins which

translocate in the nucleus to turn on target genes expression. The triggering of this pathway could result in a large variety of cellular responses, since the final gene activation depends from the TGF-β, BMP and receptor isoforms involved, which are finely regulated to switch on the proper gene expression signature. For example seven types of receptor I exist: TGF-β can bind activin receptor-like kinase 5 (ALK5) and together with type II receptor TβRII activate Smad2/3 complex, or alternatively in some cell types it has been demonstrated the binding to ALK1, which together with TβRII induce the activation of Smad1/5/8 complex. Instead BMPs activate Smad1/5/8 binding ALK2, ALK3 or ALK6, which act together with the type II receptors BMPRII, ActRII and ActRIIB, while the BMP-mediated activation of ALK4 or ALK7 in collaboration with ActRII and ActRIIB induce Smad2/3 phosphorylation. Additionally through a still unclear mechanism TGF-β can activate Smad1/5/8 through the BMP-dependent receptors ALK2, ALK3 and ALK6. After phosphorylation Smad2/3 and Smad1/5/8, named also receptor Smads (R-Smads), form a complex with the common partner Smad4 (Co-Smad), which mediates the nucleus translocation with the binding to regulatory elements in target genes (*Huang and Chen, 2012*). TGF-β-activated Smad2/3 has been shown to stimulate Sox9 expression, which subsequently induce the production of typical cartilage-related proteins such as Col2a1 and aggrecan. Smad2/3 has also a protective effect on cartilage inhibiting the expression of hypertrophic markers, such as collagen type 10, ALP, MMP13, osteopontin, osteocalcin and vascular endothelial growth factor (VEGF): this inhibitory signal is fundamental to preserve chondrocytes from phenotypic changes that characterize osteoarthrtitic or ageing conditions (*Yang et al, 2001; Furumatsu et al, 2005*; *van der Kraan and van den Berg, 2012*). Conversely Smad1/5/8 sustains terminal differentiation and hypertrophic condition of chondrocytes and osteoblasts differentiation and maturation through the activation of Runx2, which is associated with the expression of the proteins mentioned above (*Hellingman et al, 2011*). This complex and antithetical mechanism only partially could explain the controversial role of TGF-β in cartilage homeostasis and its involvement in osteoarthritis development. Indeed, even if TGF-β is widely employed in classical chondrogenic differentiation protocols, several research groups have demonstrated that many shadows are still present on its implication in cartilage and bone physiopathology (*Baugé et al, 2013*). For example *in vitro* studies regarding chondrocytes and MSCs have demonstrated that an initial positive effect of TGF-β exposure on ECM synthesis and chondrogenic phenotype of the cells is subsequently counteracted by a switch in sustaining hypertrophic changes and terminal differentiation with the production of collagen type 10, collagen type 1 and MMPs (*Pelttari et al, 2006; Narcisi et al, 2012a*). Also *in vivo* studies reported negative long-term effects of TGF-β inducing osteoarthritic changes in subchondral bone and articular cartilage (*Zhen et al, 2013; Bush and Beier, 2013*). These evidences do not lower the importance of

TGF-β pathway in sustaining bone and cartilage homeostasis, rather they sustain the attention which should be pay to control molecular levels and exposure time to TGF-β during the different maturation stage of chondrogenesis/osteogenesis and the influence of other microenvironmental parameters on controversial TGF-β effects (*Blaney Davidson et al, 2007; Wang et al, 2014*).

Wnt signaling

Wnt (Wingless/Integrated-type) family proteins are widely expressed in skeletal tissues, suggesting the relevance of this signaling pathway in the development and homeostasis of bone and cartilage. Wnt family comprises 19 secreted glycoproteins able to bind the Frizzled (FZD) family receptors on the plasma membrane to initiate several distinct cascades classified as either canonical or non-canonical, depending on whether β-catenin is involved. In the canonical pathway, Wnts bind to Frizzled receptors and the low-density lipoprotein receptor-related protein 5 or 6 (LRP5/6) leading to stabilization of β-catenin, inhibiting its phosphorylation by GSK3 and its consequent degradation: β-catenin can translocate to nucleus to activate the transcription of target genes. The amplitude of the signaling is fine-tuned by negative feedback mechanisms, involving different Wnts antagonists such as secreted frizzled related proteins (sFRPs), Wnt inhibitory factors (Wifs), Dickkopf (Dkk) factors and sclerostin (*Mariani et al, 2014; Hojo et al, 2015*). Multiple roles of Wnt pathway have been reported in literature, both in the maintenance of mature articular cartilage and in the hypertrophic maturation towards endochondral ossification (*Usami et al, 2016*). Furthermore the essential activation of Wnt signaling has been reported for osteoblast commitment of precursor cells, positively regulating the expression of typical osteogenic proteins, like osterix, osteocalcin and collagen type 1 (*Yavropoulou and Yovos, 2007; Saidak et al, 2015*).

FGF signaling

Fibroblastic growth factors (FGFs) consist of a family of 22 proteins involved in skeletal development: mutations in FGF receptors (FGFR) result in abnormalities of the skeletal tissues, such as chondrodysplasia or craniosynostosis (*Kwon et al, 2016*). It has been demonstrated that FGF signaling stimulates osteoblast commitment of MSCs, and inhibits osteocyte differentiation: in particular FGF-2, through MAPK pathway, induce the phosphorylation and activation of Runx2, regulating the formation of bone-cells (*Hayrapetyan et al, 2015*). Furthermore FGF signaling has been shown to be determinant *in vivo* in the regulation of bone density and cortical thickness by mature osteoblasts (*Valverde-Franco et al, 2004; Xiao et al, 2004*). FGF pathway is relevant not only for osteogenesis and bone homeostasis, but also in the chondrogenic counterpart: FGF-2 is one of the main growth factors employed in cartilage tissue engineering, even though its role in

chondrogenesis remains still poorly clear. Furthermore FGFR3 is implicated in chondrocyte proliferation and differentiation, while other members of the FGF family, such as FGF-9, 10 and 18, are expressed in the later stage of chondrogenesis (*Kwon et al, 2016*).

IGF signaling

The insulin-like growth factor (IGF) exists in two isoforms, namely IGF-1 and IGF-2, which act through the binding to a family of tyrosine kinase receptors, primarily IGF-1R, and the activation of the phosphoinositide 3-kinase (PI3K)/ serine/threonine-protein kinase AKT pathway (*Denduluri et al, 2015*). Implication of IGF-1 and IGF-2 have been reported both for bone and cartilage tissues. IGF-1 is one of the major factors regulating MSCs chondrogenesis, increasing cell proliferation and the expression of specific markers (e.g. collagen type 2 and Sox9) in pellet culture: IGF-1 action seems to be independent, but some evidences showed an enhanced positive effect on chondrogenesis in combination with TGF-β/BMP signaling (*Longobardi et al, 2005*). Furthermore IGF signaling results also involved in the maintenance and survival of differentiated articular chondrocytes; however the ability of chondrocytes to respond to IGF stimulation appears altered during ageing or OA condition (*Loeser et al, 2000; Oh and Chun, 2003*). From the other side IGF pathway have been demonstrated to sustain osteoblasts differentiation and bone matrix synthesis: in particular IGF-1 has been correlated to longitudinal bone growth and the maintenance of bone mass (*Hayrapetyan et al, 2015*).

MicroRNAs

MicroRNAs play a crucial role in the regulation of cellular function, proliferation and differentiation, through the post-transcriptional control of gene expression, with relevant repercussion in tissue development and homeostasis, also in bone and cartilage (*Hong and Reddi, 2012; Lian et al, 2013*). Nonetheless, being miRNA research relatively young and due to the enormous number of possible target genes, only a small subset has been effectively implicated in cartilage and/or bone biology. miRNA expression profiling studies have evidenced how miRNAs are tissue-specific and developmental-stage-specific, sustaining the existence of a miRNA signature. For instance, it has been observed that miR-196a, miR-196b, miR-433 and miR-202, together with other several miRNAs, are preferentially expressed in chondrocytes from growth plate that in osteoblasts from calvaria in mice (*Kobayashi et al, 2008*), while other groups of miRNAs have been found up- or down-regulated during different stages of articular cartilage development in rats (*Sun et al, 2011*). Similar studies have been performed also during *in vitro* osteogenesis/chondrogenesis of MSCs to identify microRNAs able to enhance or affect cell

differentiation and their regenerative potential: for example, miR-145 has been recognized as an inhibitor of MSCs chondrogenesis, negatively affecting Sox9 expression (*Yang et al, 2011a*), while the miR-23a/27a/24-2 cluster has been determined as a negative regulator of Runx2 and osteoblast differentiation (*Hassan et al, 2010*). However, it should be highlighted that the set of miRNAs associated with osteogenic and/or chondrogenic differentiation of MSCs diverge between analyses performed by different research groups: this discordance could be associated with the heterogeneous nature of the MSCs and various methods used for cell culture and differentiation induction (*Hong and Reddi, 2012*). Although these controversial data, increasing or inhibiting the expression of miRNAs positively or negatively correlated, respectively, with bone and cartilage tissue formation could be a successful strategy for tissue engineering. A further interesting aspect is the possibility to employ miRNA-based approach in tissue engineering, not only to enhance the regenerative potential of implanted cells, but also to increase their resistance to apoptotic and inflammatory signals present in the damaged tissue, or to modulate the host immune response against the graft (*Sen, 2014*).

Chapter 2

Bio-inspired constructs for bone and cartilage TE

The main aim of the work reported in this chapter is the realization and characterization of *in vitro* new cell-based constructs intended for bone and cartilage tissue engineering. Particular attention has been given to the optimization of the experimental conditions for achieving a cellular microenvironment as close as possible the *in vivo* microenvironment, where cells are in strict contact with other cells and specialized extracellular matrix. The production of 3D *in vitro* culture systems with specific biological cues able to maintain cell phenotype and functionality is an essential feature for the success of a tissue engineering strategy.

In this context the first two sections (***Sections 1 and 2***) of this chapter described the production of microfibrous alginate-based scaffolds functionalized with ECM-derived materials for the re-differentiation of de-differentiated chondrocytes: the employment of these composite devices ensure good structural and morphological characteristics enhancing the biological performances of the scaffolds, in terms of sustaining cell viability, functionality and ECM production.

Although scaffolds maintain a central role in tissue engineering approaches, biomaterials and their degradation products represent an exogenous component which could influence molecular and metabolic responses of the cells, modifying their natural behavior. For this reason the development of scaffold-free approaches is highly considerable, even though particularly challenging, especially if we think to the fact that several cell types live together in continuous communication to control tissue homeostasis, as occurs in bone. ***Section 3*** describes the realization of a 3D scaffold-free bone-mimicking construct through the co-culture of osteoblasts and osteoclasts in a rotating bioreactor, sustaining cell-cell interaction and specific ECM production.

Being ECM an essential actor in cellular microenvironment able to influence cell behavior and functionality, the study of its components is a relevant aspect to obtain a proper control on

differentiation and regenerative properties of the cells. This intent is at the basis of the work reported in ***Section 4***, where a new role in the early phases of hMSCs osteogenic differentiation is hypothesized for collagen type 15 (ColXV). The detection and characterization of these novel ECM molecules is of high interest in tissue engineering, allowing the development of new construct able to better sustain cell differentiation and tissue regeneration.

The relevance of the experimental evidences reported in this chapter will be discussed in ***Section 5***, emphasizing the intriguing aspects for bone and cartilage tissue engineering.

Chapter 2 – section 1

Production of ECM-alginate microfibers

Outline of the work

The production of a scaffold with the optimal properties is at the basis of a successful tissue engineering approach: structural, morphological and biological characteristics may highly influence the performances of the device both *in vitro* and *in vivo*. The work presented in this chapter is based on this assumption and is intended to the realization of composite microfibrous scaffolds for bone and cartilage tissue engineering, made of alginate and biomaterials derived from extracellular matrix, such as gelatin or decellularized urinary bladder matrix (UBM). These "bio-inspired devices" aim to take advantage from the structural tunable properties of the alginate, on the one hand, and from the ability to interact with cellular component of the ECM-based materials, on the other. In order to obtain a strict control on the architecture, dimensions and morphological features of the microfibers, a microfluidic approach was applied, monitoring how changes in production parameters could affect scaffold characteristics. Finally, to evaluate the biological properties of the obtained microfibers, they were used for the encapsulation of SaOS-2 cell line and the biomineralization ability of these cells was tested, demonstrating how alginate functionalization with ECM-based materials can enhance this phenomenon: the mineralization-promoting effect strictly depends on the hydrogels structural, compositional and morphological features derived from the interaction between the above mentioned two components.

Introduction

Despite the high level of innate repair capability, the physiological bone healing does not always occur, especially in large-scale traumatic bone injury (*Petite et al, 2000*). Autografts and allografts represent current strategies for bone repair, but they are associated to limitations, such as donor-site

morbidity and in the case of autograft and the risk of disease transmission by allograft (*Ng, 2012*). In an attempt to overcame these limitations, tissue engineering approaches has been proposed in recent years, involving the use of natural and synthetic scaffolds, appropriate growth factors and cells, and, more recently, the use of stem cells (*Fini et al, 2002; Ilan and Ladd, 2003; Leach et al, 2006*). Using tissue engineering techniques, it is possible to design new scaffolds and tissue grafts aiming to decrease the disadvantages of traditional grafts and improve graft osteogenicity and osteoinductivity. For instance, recently published papers have demonstrated the efficacy of approaches based on the employment of 3D bone scaffolds, combining appropriate scaffold and cells (*Hutmacher, 2000; Karageorgiou and Kaplan, 2005*). Moreover, these scaffolds could in principle satisfy the different types of fractures and the wide variety of bone disorders. In this scenario, an appealing strategy is the development of scaffold new geometries or new combinations of biomaterials with different physicochemical characteristics. Unfortunately, the success of fracture healing or the restoration of the bone mineral density and mechanical characteristics of the new regenerated bone tissue depend on the tissue ability to maintain over time the properties acquired through the modulation of specific molecular factors which are only in part known (*Dimitriou et al, 2005*). This tissue ability is also a peculiar characteristic of the patient, so it is difficult to design 3D constructs able to fit in all patient situations. Therefore, bone regenerative engineering focuses on new strategies based on the balanced combination of stem cells, biomaterials, and osteomodulation molecules, offering solutions to ensure and maintain bone healing in various situations (i.e. pathologies) (*Dawson and Oreffo, 2008*). In this context, it will be extremely interesting to identify possible 3D biofabrication protocols able to successfully induce osteogenic differentiation, since there is a need to find new methods of scaffold fabrication or improving the existing methods. In particular, different technologies have been indeed proposed to produce polymeric fibers as 3D materials, including melt spinning (*Lee et al, 2005*), wet spinning (*Chevalier et al, 2008*) and electrospinning (*Leong et al, 2003*). Many of these approaches, however, have limitations on the control of the morphology, dimension, or direction of alignment of obtained fibers and, more importantly on the preservation of cell viability, in case of uses as biomaterials. When hydrogels and cells pass through conventional nozzles they are indeed subjected to high shear forces causing cytotoxic effects. Microfluidic methods have found applications in many areas such as analitycal chemistry, clinical analysis, molecular biology, and drug formulations and delivery (*Whitesides, 2006; Tripathi et al, 2013*). Microfluidics has had such a large amount of success since there are many benefits resulting from the miniaturization of devices and offers precise high throughput applications for the production of novel functional materials. Concerning the production of fibrous materials, the shear stress developed in microfluidic

channel is significantly reduced during fiber production due to the envelop of a laminar core by a sheath flow. Furthermore, microfluidics, due to small channel dimensions and efficient mixing, allows a precise control of the dimensional and morphological characteristics of the produced microfibers, providing new routes for in situ fabrication of fibrous scaffold (*Su et al, 2009*). However, to the best of our knowledge, no reports are present in the literature describing the use of microfluidic devices for the production of polymeric microfibers for bone tissue engineering. With respect to the polymer we have selected for microfiber production, it is important to underline that alginate is structurally similar to one of the major components of the ECM in human tissue, glycosaminoglycan. For this reason, alginate is widely used as component of scaffolds for tissue engineering applications, but in spite of the excellent properties offered by this natural polymer, many reports have demonstrated that two or three polymers in combination, are able to impart new properties to the scaffold, which in turn might facilitate cell adhesion, viability, proliferation, and differentiation (*Xu et al, 2004; Navarro et al, 2004; Kong et al, 2006*). In the present study, we propose a composite biomaterial in which alginate is combined with gelatin, or urinary bladder matrix, yielding transparent fiber-reinforced hydrogels. Alginates lack indeed the bioactivity and constructive host tissue response characteristics of ECM-derived scaffolds, therefore, combining alginates with gelatin or UBM offers the advantages of both types of biomaterials. For instance, alginate, in presence of multivalent cations, produces a mechanically resistant scaffold which can be handled easily in comparison with gelatin scaffold, while gelatin, being a hydrolysed form of collagen retains informational signals, such as the Arg–Gly–Asp sequence, facilitates cell attachment and differentiation. The idea of combining a polysaccharidic polymer with gelatin-UBM based materials in a microfibrous device was valided by embedding in the produced microfibers SaOS-2 osteoblastic-like cells that were employed as model cells to investigate the ability of the scaffold constructs to support cell adhesion, viability, proliferation, and 3D colonization, as well as osteogenic differentiation.

Materials and methods

Materials and equipment

Delrin 100 BK 602 acetal resin was purchased from Du Pont de Nemours Italiana S.r.l., Milan, Italy. Sylgard 184 silicone elastomer kit was obtained from Dow Corning Corporation, Midland, MI, USA. Dulbecco's Modified Eagle Medium (DMEM) high glucose, fetal calf serum (FCS), streptomycin and penicillin were purchased from Gibco, BRL, Milan, Italy. Agarose, $BaCl_2$, $CaCl_2$,

$SrCl_2$, Polyethylene glycol (PEG) 600, LR White embedding kit were obtained from Sigma Aldrich, St. Louis, MO, USA. Sodium alginate IE-1105 (viscosity, 20.0–40.0 cP; pH, 6.0–8.0, C 1/4 1%, H_2O) was obtained from Inotech Biosystem International, Switzerland. Gelatin 200 Bloom Type A was purchased from Rousselot International. Micromachining tool Micro miller MF 70 with a 0.8 mm HSS drill bit Cat. N. NO 28 852 (Proxxon, Föhren, Germany) and DREMEL 200 (purchased from Robert Bosch S.p.a., Milan, Italy) were employed.

Precision tips #T1 (30 gauge-ID size 0.15 mm), #T2 (27 gauge-ID size 0.20 mm), #T4 (18 gauge-ID size 0.84 mm), #T5 (16 gauge-ID size 1.19 mm), #T6 (15 gauge-ID size 1.37 mm) were purchased from Nordson EFD (USA&Canada). Plastic fluorinated ethylene-propylene (FEP) (#T3) with 1/16" OD, 0.75 mm ID, Upchurch Scientific tubes were obtained from VWR International S.r.l., Milan, Italy. Tube H-PTFE (#T7) 4.0/2.2 mm (OD/ID), catalog Timmer 2001 was purchased from Timmer-Pneumatik GmbH. Silicon tube (#T8) was 7.0/4.1 mm (OD/ID); stainless steel tube (#T9) was 6.4/4.5 mm (OD/ID) and glass tube (#T10) was 7.5/4.7 mm (OD/ID). 2.5 and 5.0 mL syringes and 21 gauge hypodermic needles were purchased from Pic Solution, Como, Italy. Syringe pump KDS Model 100 Series was purchased from Kd Scientific Holliston, MA, USA.

Microchip fabrication

The general procedure for the preparation of microfluidic chips by the "shrinking" approach is elsewhere reported (*Focaroli et al, 2014*). Briefly, according to the design of the channel structures, the production of the template was initially performed. To this aim, a 50 × 50 × 8 mm plate (made of Delrin 100 BK 602 acetal resin) was micromachined to produce squared interlinking microfluidic channels (0.8 × 0.8 mm). Masters were later produced by a replica molding technique, employing an aqueous dispersion of agarose. Finally, the masters were slowly peeled away from the templates, leaving the micropatterns imprinted on the agarose dispersion with a high fidelity of replication. Master shrinking was accomplished by immersing the masters in PEG 600. After 24 h, the shrink masters were removed from the shrinking liquids and allowed to further shrink in air for additional 2 days. A replica molding approach was also used to produce replicas: prepolymer mixtures were poured onto the agarose masters and, after consolidation, polydimethylsiloxane (PDMS) microstructures comprising interlinking channels were obtained. The addition of ports was accomplished by minor modifications of the procedures described elsewhere (*Mazzitelli et al, 2009; Das et al, 2009; Capretto et al, 2010*). Finally, the open microfluidic channels were sealed using a slab of partially cured master polymer to give irreversible sealing at RT.

Microfiber production by microfluidic procedure

Alginate microfibers were produced by a microfluidic procedure with a syringe-pump letting flow the sodium alginate solution into the microfluidic chip and after in a gelling solution constituted of a 6 mM water solution of $BaCl_2$, $CaCl_2$ or $SrCl_2$. The sodium alginate solution was composed by alginate IE-1105 2.0% w/v. A 2.5 mL syringe containing the alginate solution was connected by a Teflon microtube (700 μm internal diameter) to microchip MC1 and the terminal part of the microchip outlet tube was perpendicularly immersed in the gelling solution where the Na-alginate flow stream was gelled to produce the final Ba-, Ca- or Sr-alginate consolidated microfibers, namely Ba-A*f*, Ca-A*f* and Sr-A*f*. The identification code, material and dimensions of the outlet tube employed for alginate microfiber preparation are reported in Table 2.1.1.

Table 2.1.1: identification code, material and dimensions of the outlet tube employed for alginate microfiber preparation.

ID code	Tube internal diameter (mm)	Material thickness (mm)	Tube external diameter (mm)	Material
#T1	0.150	0.080	0.310	Stainless steel
#T2	0.200	0.110	0.420	Stainless steel
#T3	0.700	0.430	1.560	PTFE
#T4	0.840	0.215	1.270	Stainless steel
#T5	1.190	0.100	1.390	Polyethylene
#T6	1.370	0.140	1.650	Stainless steel
#T7	2.200	0.900	4.000	Polyethylene
#T8	4.100	1.450	7.000	Silicone
#T9	4.500	0.950	6.400	Stainless steel
#T10	4.700	1.400	7.500	Glass

UBM isolation and purification

UBM has been isolated and purified following the below reported procedure (*Birk and Silver, 1984; Ray et al, 2001*). Briefly, porcine urinary bladders were harvested from pigs, immediately following euthanasia. The connective tissue excess and the residual urine were removed. By mechanical treatment, the tunica serosa, tunica muscularis externa, tunica submucosa, and majority of the tunica muscularis mucosa were removed; thereafter, urothelial cells of the tunica mucosa were detached from the luminal surface by incubating the tissue in saline solution. The resulting tissue, which was composed of the basement membrane of the urothelial cells plus lamina propria, is termed "urinary bladder matrix", shortly UBM. The obtained UBM sheets were then treated by a solution containing 0.1% (v/v) peracetic acid (Sigma), 4.0% (v/v) ethanol (Sigma), and 95.9% (v/v) sterile water for 2 h. Peracetic acid residues were then removed with washes with phosphate-buffered saline (pH 7.4) and sterile water. The decellularized UBM were then lyophilized and milled to obtain a particulate form using a Wiley Mini Mill (Thomas Scientific, Swedesboro, NJ, U.S.A.).

Cell line and culture conditions

Osteosarcoma SaOS-2 cell line, used for the production of composite alginate microfibers were maintained in DMEM high glucose with 10% FCS, supplemented with 50 units per mL penicillin and 50 mg/mL streptomycin, under 5.0% CO_2.

Preparation of composite microfibers

Composite alginate microfibers (containing cells, extracellular matrix components or both) were produced using the two inlets and a single straight channel MC2 or micromixing (snake type) channel MC3 chips, following the below reported procedure. A sodium alginate solution (2.0%, w/v) containing SaOS-2 cells and sodium alginate solution (2.0%, w/v) containing the extracellular matrix components (i.e. gelatin or UBM) were delivered via the two inlets of the microchips MC2 or MC3 at a total flow rate of 1.5 mL/min. The two alginate solutions contained different amounts of either extracellular matrix components (2.25% w/v gelatin and 0.50% w/v UBM) or SaOS-2 cell suspension (1.0-3.0 × 10^6 cells/mL). The output from the chip outlet was transferred via a #T3 outlet tube into a 6 mM $BaCl_2$ where the alginate stream was gelled to produce the final alginate/gelatin and alginate/UBM microfibers, namely Ba-AG*f* and Ba-AUBM*f* respectively.

Geometrical and morphological analysis of microfibers

The dimension and morphology of microfibers were evaluated using optical stereomicroscopy. Quantitative analyses were obtained using the photomicrograph analysis software EclipseNet version 1.16.5. The mean diameter of the microfibers (± SD) was obtained by taking 9 measurements along the (10 mm) length of the samples at equal intervals, in triplicate. Additional evaluation of gelatin and UBM distribution in alginate composite microfibers was performed by Coomassie Brilliant Blue staining: microfibers were incubated with staining solution (0.1% Coomassie Brilliant Blue R-250, 50% methanol and 10% glacial acetic acid) at room temperature for 1 hour and then washed in the destaining solution (40% methanol and 10% glacial acetic acid) at room temperature overnight. Gelatin and UBM distribution in stained microfibers was evaluated by optical stereomicroscopy.

Assays for cell viability and proliferation

The viability of the cells was analyzed by double staining with propidium iodide (PI) and calcein-acetoxymethyl ester (calcein-AM) assay (Sigma- Aldrich Chemical Co.) according to the manufacturer's instructions. For Calcein-AM and propidium iodide analysis, the cells were visualized under a fluorescence microscope (Nikon, Optiphot-2, Nikon corporation, Japan) using the filter blocks for fluorescein and propidium. Dead cells were stained in red, whereas viable ones appeared in green. Calcein-AM and PI images were merged using ImageJ (open source NIH image processing software). The proliferation rate of SaOS-2 cells in alginate fibers was determined by using the alamarBlue^{TM} assay (Invitrogen Corporation, Carlsbad, CA). The test is based on the metabolic activity of proliferating cells that results in a chemical reduction of alamarBlue, previously added to the *in vitro* cultured cells. Briefly, after different length of time, a medium containing 5.0% alamarBlue was added to the transfected cells, at 37°C and 5.0% CO_2. After 4 hours of incubation, 200 µL samples of culture medium were withdrawn, centrifuged, and subsequently placed on 96-well plates. The visible light absorption of collected samples was determined at 570 and 620 nm by a Microplate Absorbance Reader (Sunrise, Tecan, Austria). Final values were calculated as the difference in absorbance units between the reduced and oxidized forms of alamarBlue.

Real-Time Video Microscopy

For time-lapse phase contrast imaging, Ba-A*f* containing SaOS-2 cells were monitored using the BioStation IM microscope equipped with a thermostatic chamber (Nikon Instruments Inc). Images were acquired every 4 hours for a period of 72 hours and analyzed with BioStation software.

Hystological sections

Ba-A*f* containing SaOS-2 cells were fixed with paraformaldehyde 4% in phosphate-buffered saline (PBS) for 30 min, dehydrated through an ethanol gradient and embedded in LR White Resin. The resin was allowed to polymerize for 72 h at 60 °C and subsequently solid specimens were collected. 5 μm sections were obtained with a glass blade and stained with toluidine blue, mounted in glycerol and observed using a Leitz microscope.

Evaluation of biomineralization potential

For the analysis of osteogenic differentiation, both free SaOS-2 (growing as monolayer) and alginate microfiber containing cells were incubated in osteogenic medium (DMEM high glucose supplemented with 10% FCS, 10 mM β-glicerophospate, 100 μM ascorbic acid and 10^{-7} M dexamethasone) up to 14 days. For Alizarin Red-S (ARS) staining, free SaOS-2 (growing as monolayer) and cells embedded in microfibers were fixed and then stained with 40 mM Alizarin Red-S solution (pH 4.2) at room temperature for 10 min. Samples were then rinsed five times with distilled water and washed three times in PBS on an orbital shaker at 40 rpm for 5 min each to reduce nonspecific binding. The stained matrices were microphotographed by an optical microscope (Nikon, Optiphot-2; Nikon Corporation, Tokyo, Japan).

Real-time polymerase chain reaction (qRT-PCR)

Prior real-time polymerase chain reaction (PCR) analysis, Ba–A*f*, Ba-AG*f* and Ba-AUBM*f* were dissolved after incubation at 37°C in a 50 mM ethylenediaminetetraacetic acid disodium salt (EDTA) solution (pH 7.00) for 10 min in order to obtain free cells. Total RNA was extracted using the RNeasy Mini Kit (Qiagen, Hilden, Germany), according to the manufacturer's instruction. Total RNA was used for reverse-transcription and stored at −80°C. Briefly, cDNA was synthesized from

total RNA (500 ng) in a 20 µl reaction volume using the TaqMan High Capacity cDNA Reverse Transcription kit (Applied Biosystems) as previously described (*Lambertini et al, 2012*). For quantification of Col1A1 and Runx2 the appropriate TaqMan probes were purchased from Applied Biosystems followed by detection with the CFX96TM PCR detection system (Bio-Rad, Hercules, CA). Glyceraldehyde 3-phosphate dehydrogenase (GAPDH) reference gene was used for normalization. All reactions were performed in triplicate and the experiments were repeated at least three times. The method used for the analysis of relative gene expression data was the 2-ΔΔCt. This method is a convenient way to analyze the relative changes in gene expression from real-time quantitative PCR experiments.

Results and discussion

Preparation of microfluidic chips for microfibers production

The experimental procedures required for the preparation of complete microfluidic chips, including ports and connecting tubing, is generally expensive and require specific facilities and equipment. In order to provide an alternative to the high cost standard procedures for the preparation of microfluidic chips, in the current paper we propose a low cost approach, for the production of microchips specifically designed for the controlled production of cell embedding biocompatible microfibers. In Figure 2.1.1 are schematized the steps involved in the production of the microfluidic chips, namely: 1. template preparation; 2. master production and shrinking; 3. replica formation by resin pouring and curing; 4. port assembly; and 5. microchip sealing. As a preliminary step, the design and drawing of three chips with different channel configurations were performed by a freeware program (Blender 2.69). The templates were obtained using micromilling, which represents a very convenient approach when compared to other microfabrication methods such as photolithography. As material for template production ready to use commercially available Delrin plates, were employed. The masters, intended as the positive replica of the templates, present relief structures on their surface, therefore, masters were obtained by pouring an agarose solution on top of the templates, followed by subsequent agarose gelling and progressive shrinkage, resulting in a substantial reduction of channel width and depth. The duplication of the information (shape, morphology, and structure) presented on the surface of the agarose masters was then obtained by PDMS. Once the replicas were cured, the connection and interfacing (i.e. porting) were performed using two simple methods for PDMS masters. The port assembly was performed following, with some modification, the “reservoir approach”; the connections, produced with inexpensive

commonly available materials in the laboratory, were robust and allowed an easy and resistant system to interface the microfluidic chips with the fluidic equipment. Interfacing of the PDMS devices was performed using a "wall plug inspired approach" (*Capretto et al, 2010*). In this case, hypodermic needles were inserted in the FEP tubes, deeper than the interface between tube and hole in order to leverage the wall plug effect. This method gives tight junctions between the FEP tubes and microchip inlet/outlet, allowing the chip to work at high pressures and avoiding the problems described above. Connection with pumps was achieved using "custom made" luer lock adapters (*Mazzitelli et al, 2009*).

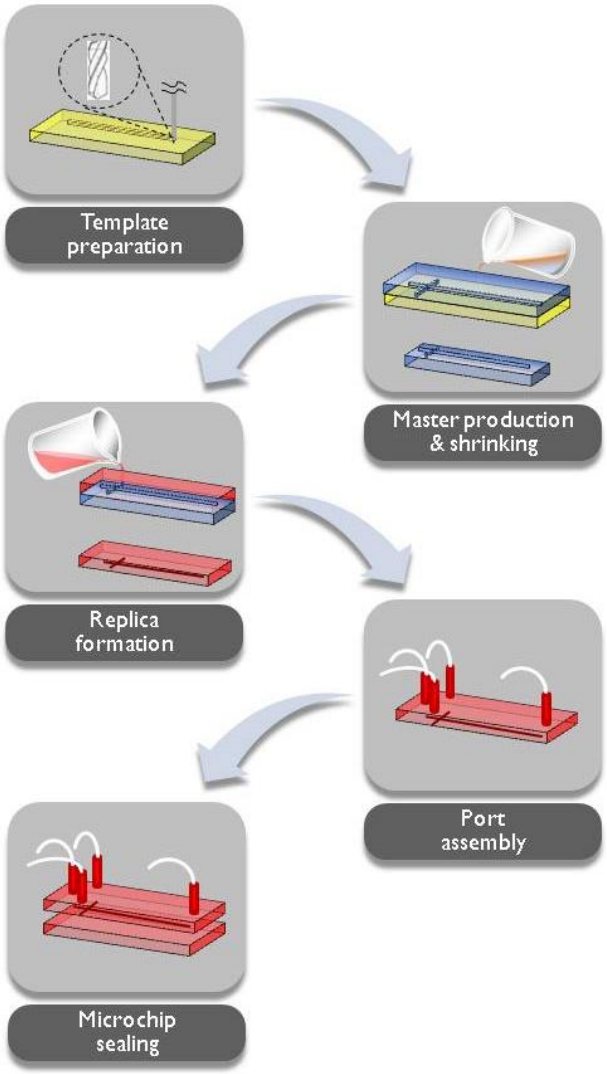

Figure 2.1.1: general scheme depicting the major steps of the "hydrogel shrinking approach" employed for the production of the low cost microfluidic chips.

As the final step, microchannel sealing was carried out, employing an irreversible sealing method by simply placing them onto a slab of partially cured PDMS. Following the above describe

procedure, three different microfluidic chips were prepared (see scheme reported in Figure 2.1.2A), namely: single inlet and a straight channel microchip (MC1); two inlets and a straight channel microchip (MC2) and two inlets and micromixing (snake type) channel microchip (MC3).

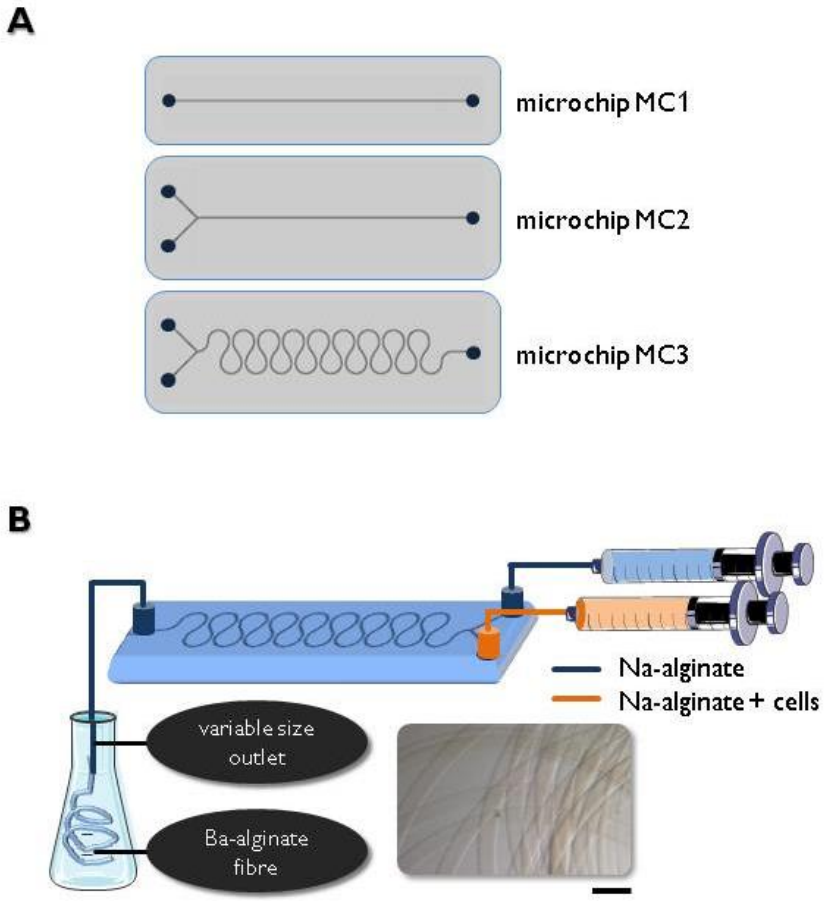

Figure 2.1.2: (A) Microfluidic chips employed for the production of alginate microfibers. One inlet straight channel microchip (MC1); two inlets straight channel microchip (MC2) and two inlets snake micromixing chip (MC3). (B) Microfluidic set-up for producing the alginate microfibers together with a microphotograph showing an example of microfiber. Bar corresponds to 1.2 mm.

Production of alginate microfibers by microfluidics

Alginate microfibers were produced by a microfluidic procedure in order to precisely control the dimensional and morphological characteristics and assure the reproducibility of the obtained microfibers. Indeed, the control of dimensional characteristics is essential for the possible implantation of tissue engineering scaffolds and the dimensional homogeneity of microfibers is crucial in controlling the rate of exchange of nutrient and bio-regulatory products (such as hormones and growth factors) in and out the tissue engineering device. The polymer used was sodium alginate IE-1105, which is currently the most widely used biomaterial for cell embedding

due to its ability to allowing cell adhesion, spread, migration and interaction with other cells. In order to evaluate the robustness of the strategy and the produced microchip, the microfibers were initially prepared by MC1 and following the general procedure schematized in Figure 2.1.2B. The preparation was based on the use of a syringe-pump that allowed regulating the flow of the sodium alginate solution through the microfluidic chip at appropriate flow rates. The gelation of alginate was accomplished by a gelling solution containing the same molar amount (6 mM) of the following divalent cation containing salts: barium chloride, calcium chloride and strontium chloride. For obtaining the gelation of sodium alginate solution, the terminal part of the microchip outlet tube was perpendicularly immersed (by 10 mm) into the gelling solution where the polymer flow stream was gelled to produce the final ionically crosslinked alginate consolidated microfibers. In order to understand the operational parameters which could affect the characteristics of alginate microfibers, different experimental settings were investigated. The internal diameter of the outlet tube (reported in Table 2.1.1) was analyzed with respect to the dimension of the obtained microfibers, showing that microfibers with a diameter spanning from 0.130 (using #T1) to 2.700 mm (using #T10) can be conveniently produced without effects on microfibers morphology. As expected, the internal diameter of the outlet tube influenced the dimension of the microfibers, as appreciable from the microphotographs reported in Figure 2.1.3, showing constant diameter through the entire microfiber length. Notably, we observed that in the case of outlet tubes with an internal diameter greater than 2 mm (#T7-#T10), the diameter of the obtained microfibers was significantly lower than the inner diameter of the tubes. This finding was attributed by the phenomenon called die swell or Barus effect, common when polymer solutions flow out of cylindrical channels. For highly elastic, non-Newtonian fluids such as polymer solutions and melts, flowing out of cylindrical channels, the thickness of the polymer jet may be several times greater (at high pumping rates) or smaller (at low pumping rates) than the channel dimension (*Malkin et al, 1976*).

Figure 2.1.3: effect of the microchip outlet tube on the dimensions and morphology of the obtained microfibers. The identification codes, dimensions and material of the outlet tubes are reported in Table 1. Bar corresponds to 500 µm.

The pumping rate effect on microfiber dimension was also considered, since the dimensional properties of microfibers are expected to be influenced by the balance between the rate of the alginate flow and the outlet tube dimension. Data reported in Figure 2.1.4 and Table 2.1.2 confirmed that an increase of microfiber diameter was observed when pumping rate was set from low to high levels (related to outlet tubes #T3, #T4, #T7, #T8 and #T9); for instance, in case of #T3 the microfiber diameter varied from 611.3 (at 0.50 mL/min) to 688.6 (at 1.50 mL/min). The correlation between the pumping rate and the microfibers diameter was attributed, as previously discussed, by the Barus effect.

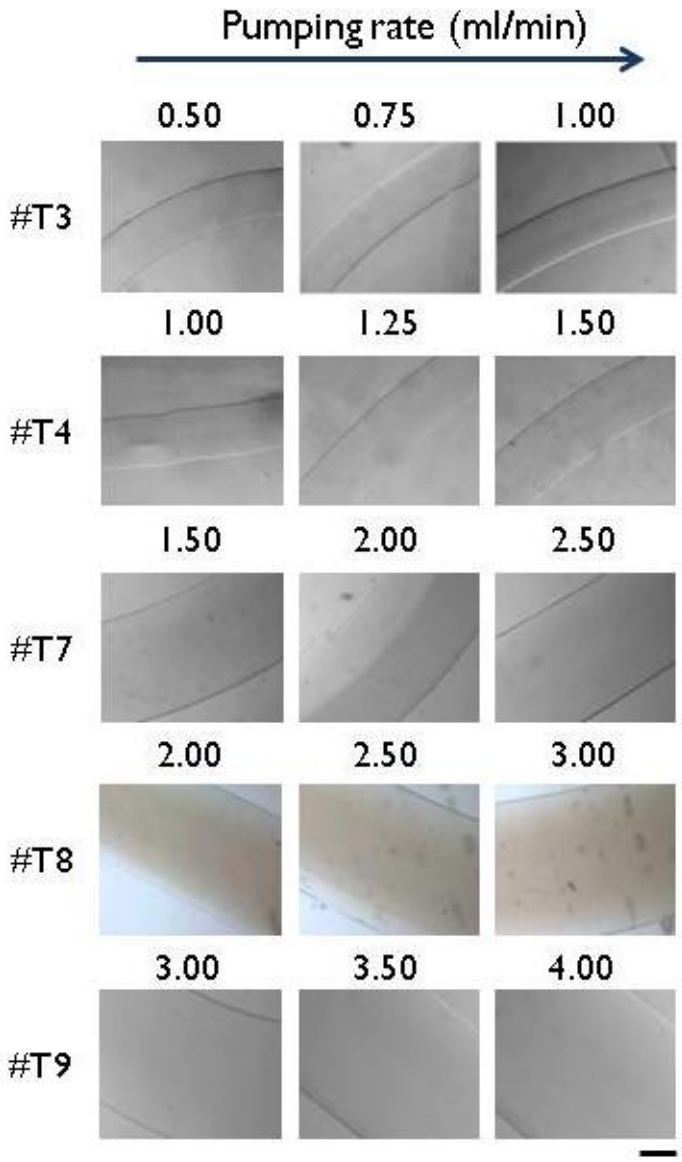

Figure 2.1.4: Effect of pumping rate (indicated in figure) and outlet tube (internal diameter) on the dimensions and morphology of the obtained microfibers. The identification codes, dimensions and material of the outlet tubes are reported in Table 1. Bar corresponds to 500 µm.

Table 2.1.2: effect of pumping rate and microfluidic chip outlet tube on the dimension of alginate microfibers.

ID code	**#T3**	**#T4**	**#T7**	**#T8**	**#T9**
Pumping rate (mL/min)	**Diameter[a] (µm)**	**Diameter [a] (µm)**	**Diameter [a] (µm)**	**Diameter [a] (µm)**	**Diameter [a] (µm)**
0.50	611.3±6.2	bcpr	bcpr	bcpr	bcpr
0.75	646.2±2.2	800.3±10.1	bcpr	bcpr	bcpr
1.00	655.3±3.4	812.7±5.1	bcpr	bcpr	bcpr
1.25	644.3±3.6	845.1±12.9	bcpr	bcpr	bcpr
1.50	688.6±5.4	888,8±7.9	1551.16±10.8	1706.3±15.9	bcpr
2.00		885.4±8.6	1677.9±8.1	1767.4±18.1	bcpr
2.50			1643.5±14	1994.1±49.5	bcpr
3.00				1945.3±16.7	2005.6±7.1
3.50					2376.5±3.8
4.00					2490.4±7.2

a: the mean diameter of the microfibers (± SD) was obtained by taking 9 measurements along the (10 mm) length of the samples at equal intervals, in triplicate.
bcpr: below critical pumping rate

Since microfibers were designed for cell encapsulation and considering that the size of cells or cell clusters usually exceeds one hundred microns, microfibers with diameter ~ 600 µm were desirable. On one hand, if the diameter of the microfibers is too small, the number of partially protruding cells/cells clusters could proportionally increase, together with the probability of inflammatory responses after *in vivo* transplantation (*de Vos et al, 2006*). On the other hand, microfibers thicker than 600 µm could impair the exchange of nutrients and metabolites products of embedded cells. In this respect, tubes #T3 and #T4 were selected for further investigations. Figure 2.1.5 shows more in detail the effect of pumping rate on microfibers dimension. Interestingly, the experiment denoted that if the pumping rate is set at low values (typically in the range 0.1-0.5 mL/min) the resulting microfibers are heavily affected by morphological defects. As shown in Figure 2.1.5B, pumping rates lower than a "critical pumping rate" (0.2 mL/min for #T3 and 0.5 mL/min for #T4) resulted in the formation of large blobs (arrowed in the microphotographs).

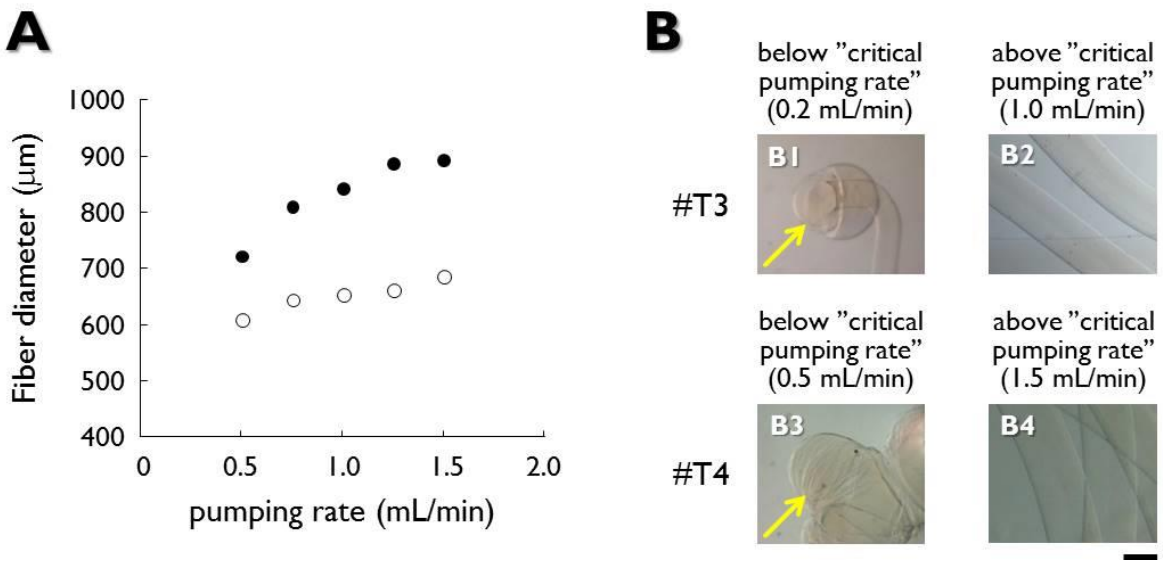

Figure 2.1.5: effect of pumping rate and outlet tube on the dimensions (A) and morphology (B) of the obtained microfibers. The microfibers were prepared with outlet tubes #T3 (open circles) and #T4 (filled circles). The identification codes, dimensions and material of the outlet tubes are reported in Table 1. Pictures reported in panels B1 and B3 show the effect of pumping rates lower than the "critical pumping rate" resulting in the formation of large blobs (arrowed). Bar corresponds to 500 μm.

It is well known that sodium alginate water dispersions can be conveniently gelled by a ionotropic gel formation, through the typical egg box structure (*Kuo and Ma, 2001*). In this respect different divalent cations (i.e. Ba^{2+}, Ca^{2+}, Sr^{2+}) were employed in order to evaluate the effect of the gelling conditions on microfiber characteristics and, as later discussed, on the embedded cells. In particular, 6 mM $BaCl_2$, $CaCl_2$, or $SrCl_2$ solutions were employed to gelify the microfluidic produced microfibers. As reported in Table 2.1.3 and in Figure 2.1.6A and B, the pumping rate influenced the dimension of all the microfibers, irrespectively of the employed gelling ion. The diameter of the obtained microfibers increased when pumping rates was set from low to high levels. As expected, the ion employed for the preparation of gelling solution, had an effect on the microfibers size. Ba-A*f* presented indeed the smaller diameters, our finding is well in agreement with many papers describing the high affinity of alginate for barium ions (*Ouwerx et al, 1998*) that causes the shrinkage of the gels formed in the presence of barium ions, resulting in compact and stiff gels. Conversely, gelling solution with strontium ions resulted in Sr-A*f* with the largest diameter and a soft aspect. This result is well in agreement with recent reports showing that Sr^{2+} cation has a smaller surface charge density with respect to Ba^{2+} and Ca^{2+} ions, resulting in weaker physical crosslinks of alginate and hence lower modulus hydrogels (*Kaklamania et al, 2014*). Finally, Ca-A*f* had intermediate dimensional values between Ba-A*f* and Sr-A*f*.

Table 2.1.3: effect of *in vitro* aging on the dimension of alginate microfibers gelled with different ions.

	$BaCl_2$	$CaCl_2$	$SrCl_2$
Time (days)	**Diameter (µm)**	**Diameter (µm)**	**Diameter (µm)**
0	785.9±10.1	836.5±12.1	885.0±22.9
7	826.6±28.9	923.7±23.2	991.4±25.2
14	878.8±10.7	922.0±8.2	1067.2±29.0
21	894.9±23.4	970.9±14.9	985.4±14.9
28	900.8±30.4	978.6±13.4	1096.6±28.6

*Microfibers were produced with a gelling solution containing 6 mM ions

The effect of gelling time on microfibers size was also considered in the case of Ba-A*f*. The results reported in Fig. 2.1.6C show that microfibers incubated in 6 mM $BaCl_2$ solution for different length of time (1-30 min), progressively decrease their dimension from about 790 µm, immediately after the preparation down to about 720 µm after 30 min incubation. Indeed, a longer incubation in the gelling solution gives the possibility for more ions to crosslink the alginate leading to a thinner consolidated alginate microfiber. In spite of this finding, is to be considered that in experiments concerning the production of microfibers embedding cells, the gelling time was limited to 5 min. This choice was made in order to prevent possible, even if controversial, cytotoxic effects of barium ions on the embedded cells (*Zimmermann et al, 2005*). Finally, the effect of microfiber aging in cell culture condition, on the handling and dimension of microfibers was studied at 37°C up to 28 days. Figure 2.1.6D shows that Ba-A*f*, Ca-A*f* and Sr-A*f* display a common behavior. For all the tested ions, microfibers display an initial, up to 15 days, rapid swelling with a progressive increase of their diameter; thereafter (from 15 to 28 days) the swelling effect appear to be less pronounced, without large modifications of the microfiber size. The swelling was attributed to two concomitant effects; on one side, the loss of divalent ions from the hydrogels by ion exchange with monovalent ions in the surrounding culture media (*Lee et al, 2000*); on the other by the osmotic effect due to the imbalance of barium ions inside and outside from the microfiber. Irrespectively of the variation in dimension, it is important to underline that microfibers remained intact and well manageable, providing the structural integrity necessary for *in vitro* or *in vivo* applications.

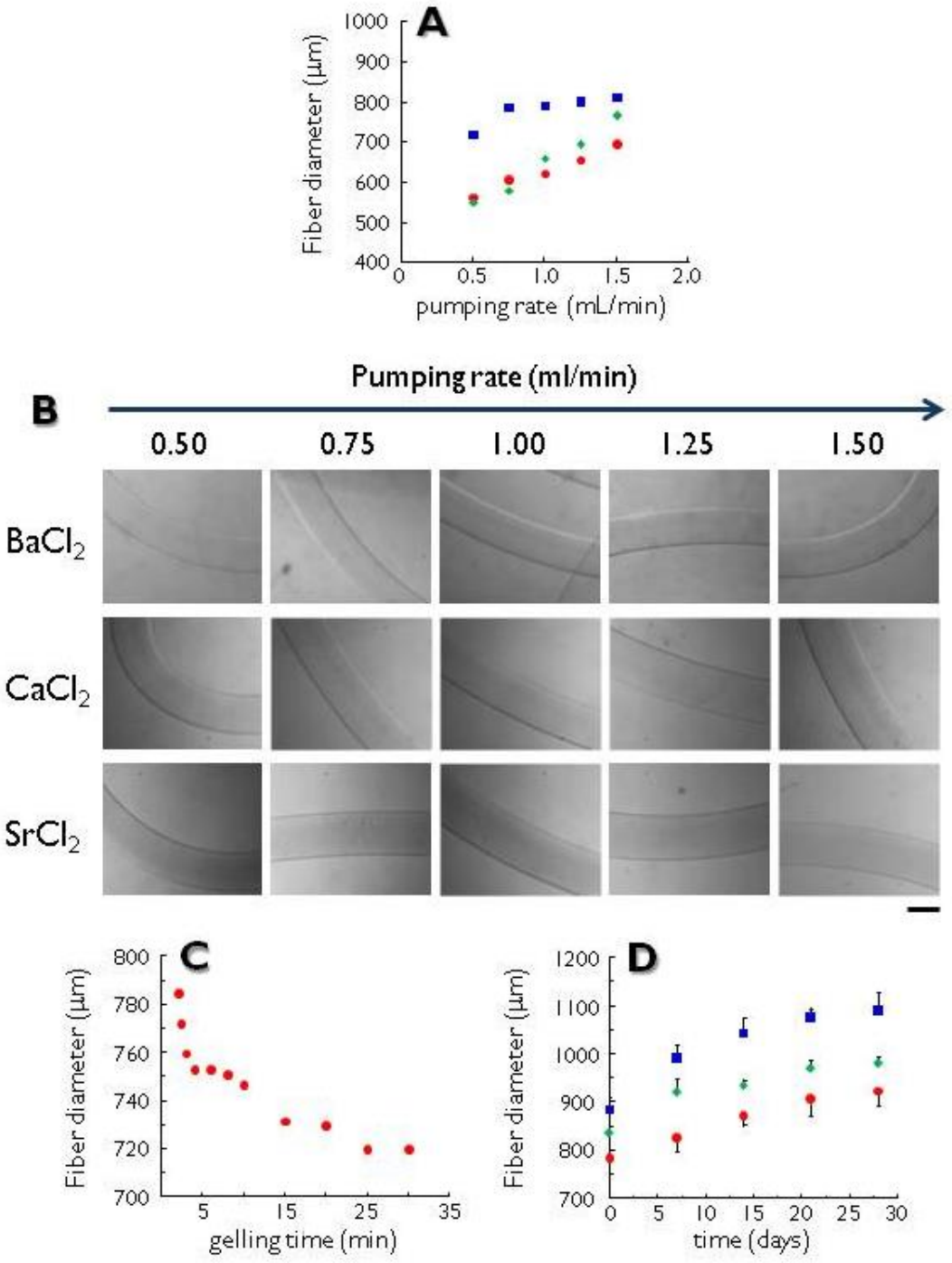

Figure 2.1.6: effect of gelling ions, pumping rate (A, B), gelling time (C) and *in vitro* aging (D) on the dimensions and morphology of microfibers. Aging experiments (panel D) were performed placing the microfibers in cell culture medium (DMEM high glucose), thereafter measuring microfiber diameters immediately after the production and after 7, 14, 21 and 28 days. The microfibers were prepared with 6 mM $BaCl_2$ (circles), $CaCl_2$ (diamonds) or $SrCl_2$ (squares) solutions, using the outlet tube #T3. Bar corresponds to 500 µm.

Alginate microfibers for cell embedding

Taking advantage from the above described experiments and conclusions, microfibers for cell embedding were produced using the following, well established experimental set up: (a) 2%, w/v alginate solution, (b) Ba^{2+} as gelling ion at 6 mM, (c) pumping rate at 1.50 mL/min and (d) the outlet tube #T3. Initially, microchip MC2 (two inlets and a straight channel) was tested for the production of cell embedding alginate microfibers. We shift to MC2 in consideration of the following reasons. Firstly, a chip with two inlets gives the possibility to produce microfibers containing desired amounts of cells in an adjustable manner by varying ‘‘on demand’’ the content of the cells within the microfibers, adjusting the flow rates of the two independent pumps, delivering either plain alginate or alginate containing cells, through the two independent feeding channels. Secondly, the mixing of plain alginate and alginate containing cells within the microchip allows overcoming a well-known phenomenon related to the sedimentation of cells. In classical biological experiments, the most straight-forward solution to keep cells in suspension is to shake large volumes. This approach is not very compatible with the syringe/syringe pump used to inject small amounts of liquid in confined geometries, such as microfluidic systems (*Baret, 2009*). Unfortunately, as clearly appreciable from the optical stereo photomicrographs reported in Figure 2.1.7A, the use of a straight channel microchip resulted in a segregated distribution of cells along the microfibers. For instance, all cells were embedded along only one side of the microfiber, corresponding to the inlet position from which they were injected. This result was assigned to the fact that the dispersion of particulate matter, in laminar fluid flow conditions, typical of microfluidic devices, is only scarcely affected by passive molecular diffusion. The use of particulate elements (such as cells), that are characterized by low diffusion coefficients, together with the high viscosity of the carrier flow (alginate solution), resulted in a poor dispersion of the particulate phase (segregation), within the microfiber structure. Therefore, in order to possibly overcome this issue, a microchip design that produces transverse transport inside the microfluidic device was considered, for an effective dispersion of the particulate phase. The design of microchip MC3 provided a snake type micromixing channel allowing a homogeneous mixing of alginate and cells (see Figure 2.1.7B). Therefore the following embedding experiments with cells were performed by MC3.

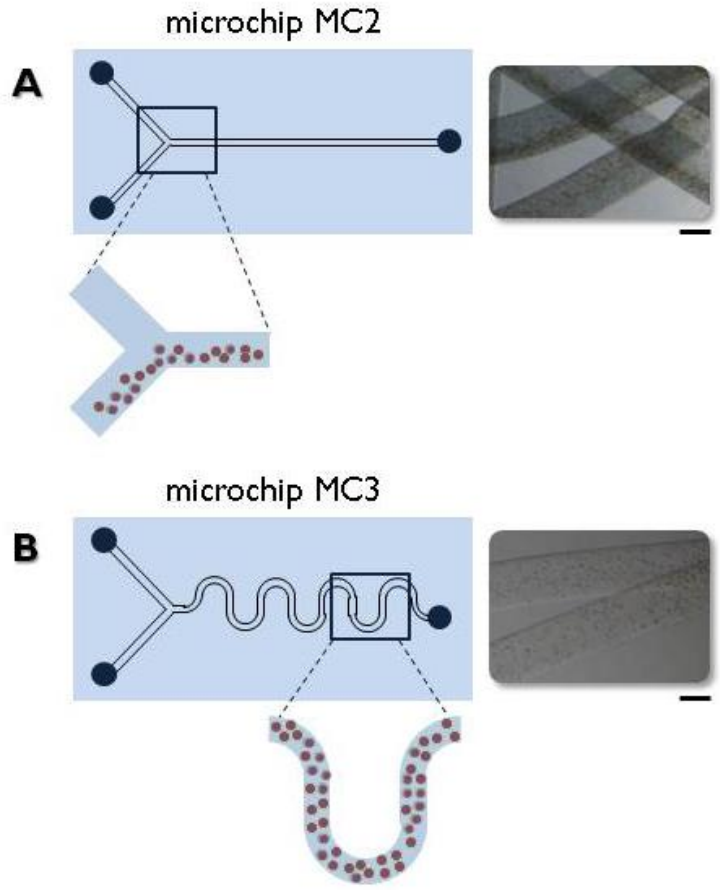

Figure 2.1.7: representation of the microfluidic chips MC2 and MC3 used for the production of cell embedding microfibers. The schemes respectively show the cells segregation within the chip channel (A) or the homogeneous cells distribution (B). Optical stereo photomicrographs show alginate microfibers containing SaOS-2 cells. Microfibers were produced by two independent syringe pumps, one pumping alginate solution (Pump #1), the other pumping alginate solution containing cells (1 x 106 cells/mL) (Pump #2). Microfibers were prepared with a total flow rate of 1.50 mL/min and a Pump #1/Pump #2 rate ratio of 0.25. Bar corresponds to 500 µm.

By employing MC3 chip an homogeneous distribution of cells was accomplished as displayed in the microphotographs reported in Figure 2.1.8 (A, C, E). Since embedding protocols involving cell/scaffold interactions may have considerable effects on cells viability, the effect of embedding on SaOS-2 cells (a human osteosarcoma cell line which maintains the cellular features of osteoblasts) was investigated. The viability test performed by double staining with calcein-AM and PI demonstrated that SaOS-2 cells maintain an elevate (> 95%) viability as demonstrated by the fluorescence microphotographs reported in Figure 2.1.8 (B, D, F) that shows the viability of SaOS-2 cells encapsulated in Ba-A*f* after 1, 7 and 14 days, respectively.

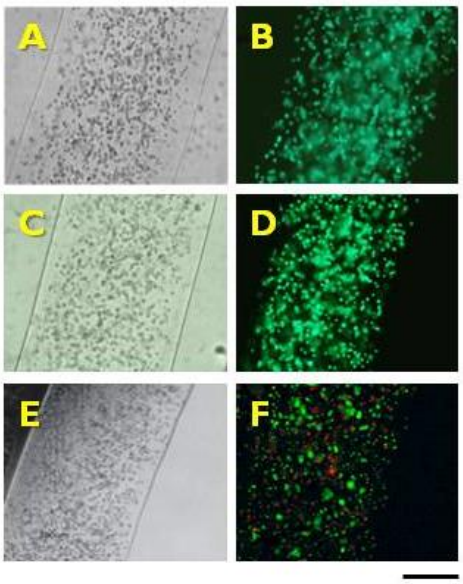

Figure 2.1.8: Optical (A, C, E) and fluorescence (B, D, F) microphotographs of Ba-A*f* containing SaOS-2 cells. Fluorescence images were taken after double staining with Calcein-AM and PI, at day 1 (B), 7 (D) and 14 (F). Bar corresponds to 250 μm.

One of the major aims of tissue engineering for hard tissues is the development of new biomaterials able to maintain high viability for the seeded/entrapped cells as well as to promote and support the bone mineralization process. In this respect, as schematized in Figure 2.1.9 the viability and mineralization activity of SaOS-2 cells embedded in alginate microfibers was determined and compared to that of cells growing as monolayer. Both cells in monolayer and in microfiber were cultured up to 14 days in DMEM high glucose (control) or osteogenic conditions (culture medium containing β-glycerophosphate, ascorbic acid and dexamethasone). The effect of the embedding in alginate gel microfibers was also investigated in microfibers consolidated by different gelling solutions (i. e 6 mM $BaCl_2$, $CaCl_2$ and $SrCl_2$) respectively resulting in Ba-A*f*, Ca-A*f* and Sr-A*f* and thereafter *in vitro* cultured in DMEM high glucose (control condition) as well as in osteogenic medium.

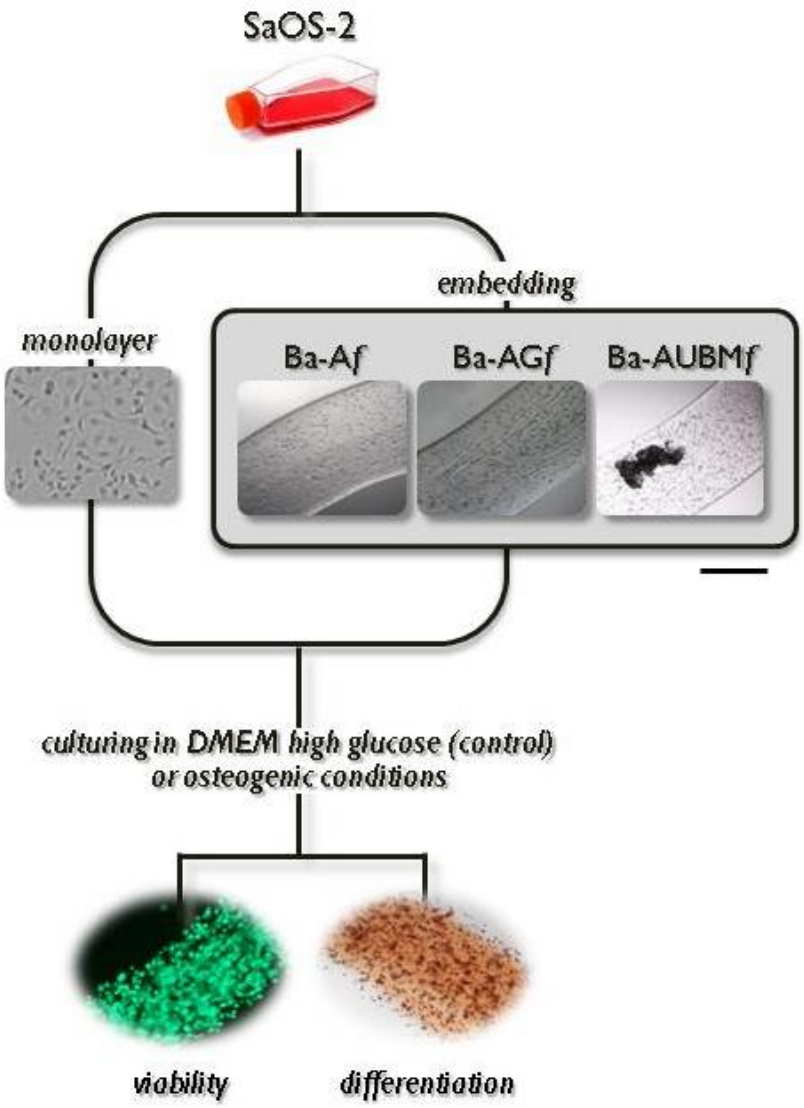

Figure 2.1.9: schematic representation of the experimental strategy used to assess the biomineralization potential of SaOS-2 cells embedded in microfibers. SaOS-2 cells were grown as monolayer or embedded in plain or composite microfibers (Ba-A*f*, Ba-AG*f* and Ba-AUBM*f*) and thereafter tested for viability and osteogenic differentiation, after 7 and 14 days of culturing in DMEM high glucose (control) or osteogenic conditions. Bar corresponds to 80 µm (monolayer) and 500 µm (microfibers).

Cells were assayed both by alamarBlue (Figure 2.1.10, upper panel) and viability double staining with calcein-AM/propidium iodide (Figure 2.1.10, lower panel). AlamarBlue test results suggested that in each gelling and culture media conditions the embedded SaOS-2 cells display a slight increase in proliferation as indicated by the increment of the percentage of alamarBlue reduction from day 1 to day 14. To confirm the results obtained by the proliferation assay, the viability double staining was also performed after 14 days of cell culture. In Figure 2.1.10 the fluorescence

photomicrographs indicated that SaOS-2 cells were highly viable in all tested conditions, as proved by the extremely low number of cells red stained.

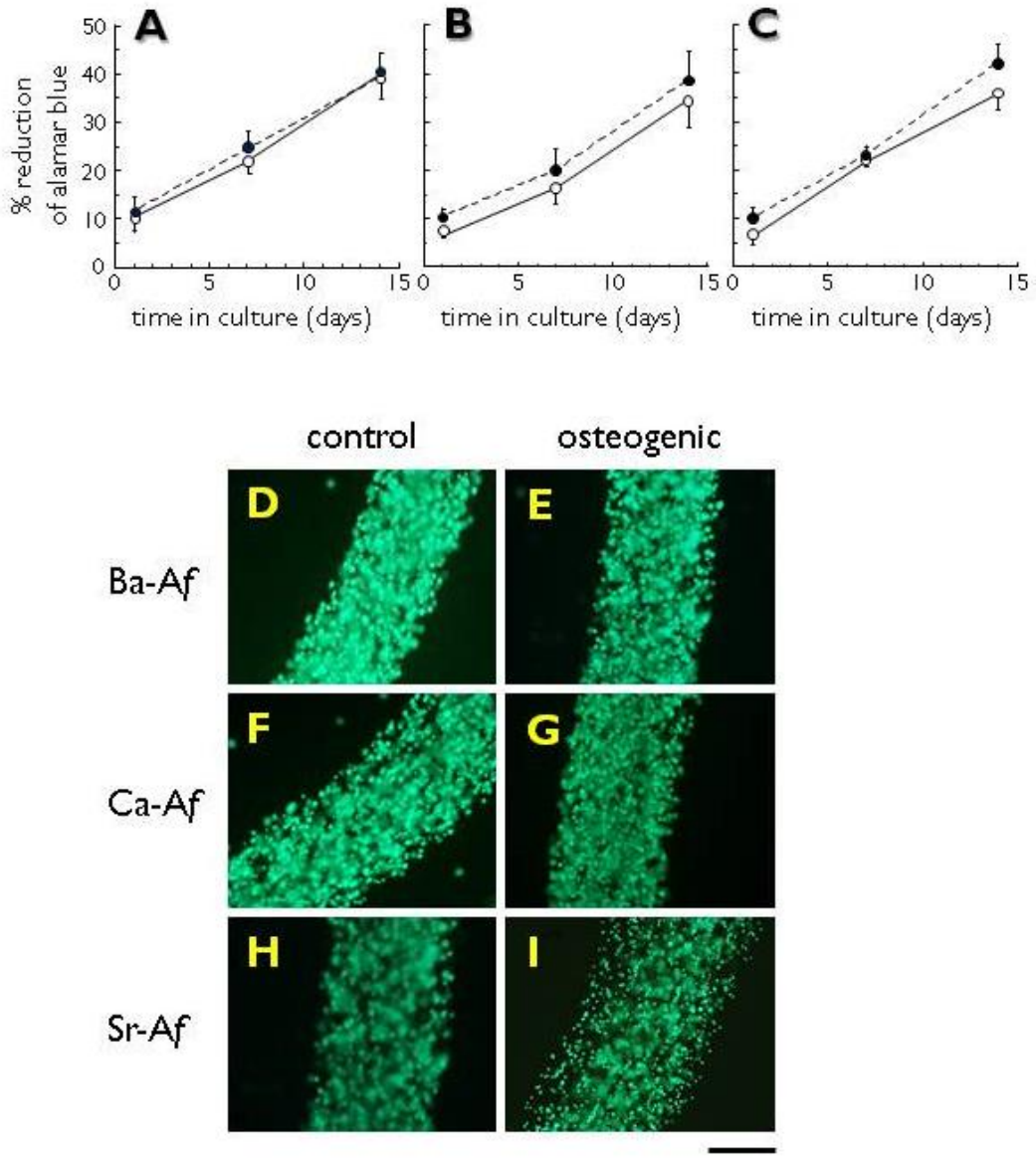

Figure 2.1.10: effect of culture conditions on the proliferation (A-C) and viability (D-I) of SaOS-2 cells embedded in Ba-A*f* (A), Ca-A*f* (B) and Sr-A*f* (C). Cells were maintained in DMEM high glucose (control, open circles) or in osteogenic conditions (osteogenic, filled circles). Proliferation data represent the percentage of alamar blue reduction ± SD (n=3). Fluorescence microphotographs were taken after calcein-AM/PI double staining, at day 14. Bar corresponds to 500 µm.

In order to obtain information on the morphology of SaOS-2 cells and subcellular structures, a histochemical analysis was performed. Microfibers were maintained in osteogenic conditions and in order to examine the cell behavior in a 3D culture environment. In this respect, it is to be noted that many of the popular methods for the preparation of histological samples for cells in alginate

hydrogels, often lead to distortions of the scaffold shape, resulting in poor image quality and misinterpretation of the cellular morphology. Therefore, an improved method for embedding and sectioning of alginate based microdevices was employed. In Figure 2.1.11 are reported microphotographs showing cells after 7 and 14 days of *in vitro* culturing; photographs were taken after embedding the microfibers in LR White Resin and cutting specimens into thin sections. Histological analysis demonstrated that SaOS-2 cells were evenly distributed within the alginate microfibers, with some cells remaining as single entities together with the presence of cellular aggregates in form of spheroidal structures, typically formed by few tens of cells. SaOS-2 maintained a uniform dimensions without any appreciable enlargement of the cellular volume. Nuclei and cytoplasms of the embedded cells appear to be unmodified with respect to control cells grown on cell culture plasticware. Notably, SaOS-2 cells embedded in alginate presented a spherical shape since alginate does not promote cell attachment because mammalian cells do not possess receptors for this polymer.

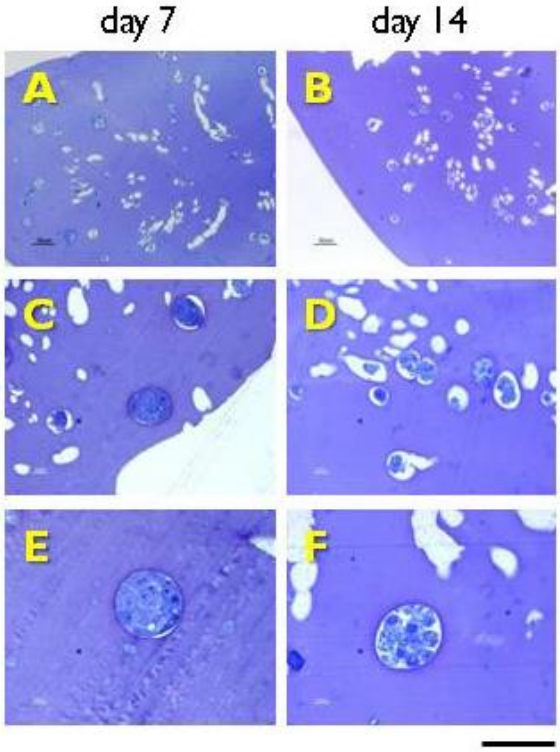

Figure 2.1.11: histological analysis of SaOS-2 cells embedded in Ba-A*f* after 7 (A, C, E) and 14 (B, D, F) days of culture in osteogenic conditions. Photographs were taken after toluidine blue staining. Bar corresponds to 150, 300, 450 µm in panels A-B, C-D and E-F, respectively.

It is known that rapidly proliferating cells (i. e. fibroblasts or tumor cell lines) when encapsulated in alginate, often migrate from the inner part of the scaffold to the periphery and finally escape from

the device, preferring to adhere and grown on the surface of the plastic used for *in vitro* culturing (*Pokrywczynska et al, 2008*). In order to asses if SaOS-2 cells would remain stably embedded in alginate or escape from it, a compact cell incubator and monitoring system for live cell imaging, was employed. Figure 2.1.12 shows consecutive microphotographs of cells, taken at 1, 4, 8, 12, 24, 72 hours. The results obtained revealed that cell migration phenomena were not detectable, cells maintained indeed their position within the alginate microfibers for the entire period observed.

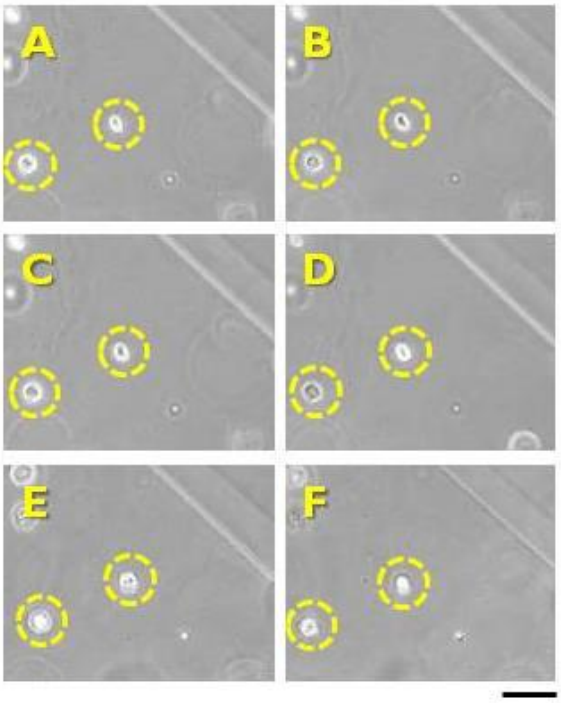

Figure 2.1.12: time-lapse live cell imaging of SaOS-2 embedded in Ba-A*f*. Images were acquired after 1 (A), 4 (B), 8 (C), 12 (D), 24 (E) and 72 (F) hours from the preparation of microfibers. Cell positions are circle-dotted in yellow. Bar corresponds to 40 µm.

Hydrogel forming polymers supporting/enhancing biomineralization are among the most promising classes of biomaterials for bone repair, or their regeneration (*Petite et al, 2000; Ilan and Ladd, 2003; Dimitriou et al, 2005; Lee et al, 2005; Dawson et al, 2008; Chevalier et al, 2008; Ng, 2012*). Biomineralization is the general phenomenon by which mineral forms in living organisms. The process is complex and presents species-specific features and the nature of the physiological/pathologic state, localization in the body and the type of biomaterials eventually employed greatly influence the process. As initial experiment, the differentiation of SaOS-2 cells embedded in microfibers cross-linked with $BaCl_2$, $CaCl_2$ and $SrCl_2$ was determined after 7 or 14 days of cell culture in DMEM high glucose (control) or osteogenic conditions. The deposition of calcium phosphate, taken as an indication for osteogenic differentiation, was evidenced by ARS

staining, a colorimetric assay that identifies mineral deposition as red stained areas. From the results of this experiment, summarized in Figure 2.1.13, the following conclusions could be withdrawn:

a) Cells cultured as monolayer in DMEM high glucose do not present any sign of calcium phosphates depositions whereas monolayer in osteogenic conditions present only after 14 days a clear evidence of Alizarin red stained areas.

b) Microfibers in osteogenic conditions display, starting from day 7, strong presence of mineral deposits evidenced by ARS. Notably, the entire volume of the microfiber is stained in red, in addition particulate aggregates of mineral deposition are also well evident inside the microfibers.

c) Interestingly, also the microfibers maintained in standard (i. e. without inducers) display, even if in lower extent the presence of positive for small nodular aggregates.

d) Microfibers cross-linked with Sr^{2+} ions and, to a lower extend with Ba^{2+} ions, appear to be more effective in influencing the differentiation ability of the embedded SaOS-2 cells. At day 14 Ba-A*f* and Sr-A*f* are indeed extremely stained by Alizarin showing a massive deposition of calcium phosphate precipitates.

Taking together the experimental evidences indicate that the 3D environment could enhance the biomineralization potential.

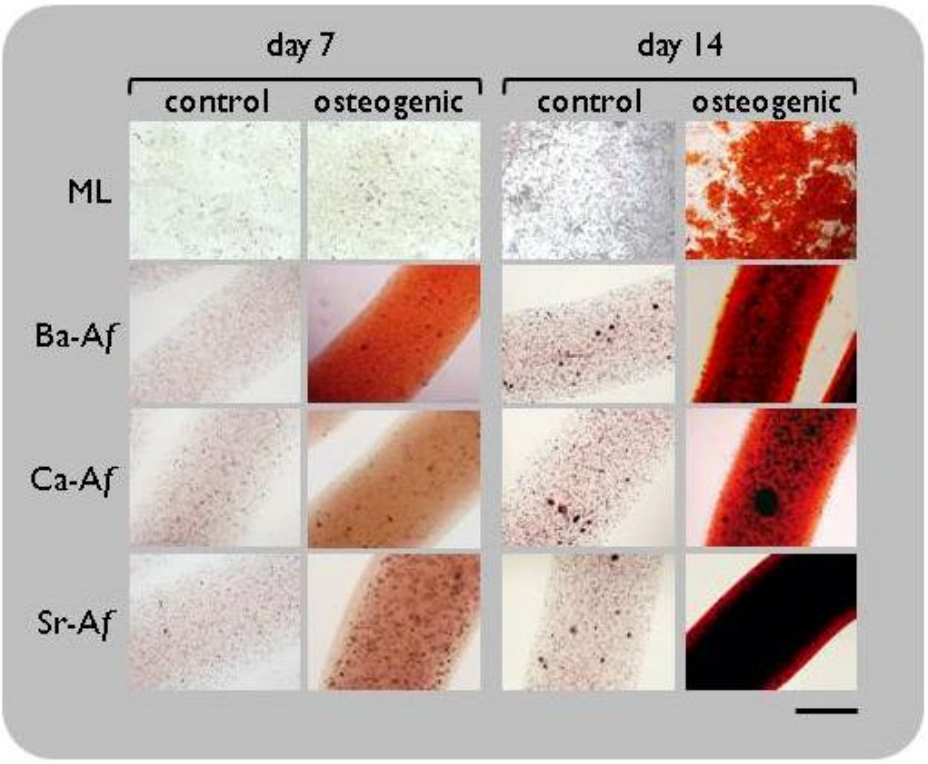

Figure 2.1.13: Alizarin red-S staining of SaOS-2 cells cultured as monolayer (ML) or embedded in Ba-A*f*, Ca-A*f* and Sr-A*f*. Staining was performed after 7 or 14 days of cell culture in DMEM high glucose (control) or osteogenic conditions. Bar corresponds to 500 µm.

Composite alginate microfibers for cell embedding

It should be considered that alginate-based hydrogels are different from the cellular microenvironment normally present in human tissues. Therefore we tested the possibility to produce composite alginate microfibers containing different constituents promoting cell adhesion and differentiation. In an attempt to reconstitute the cell environment maintaining the biocompatibility properties of alginate we produced microfibers employing mixtures alginate/gelatin (Ba-AG*f*) or alginate/UMB (Ba-AUBM*f*). The composite Ba-AG*f* and Ba-AUBM*f* were produced by MC3 and outlet tube #T3 pumping from one inlet plane alginate solution and from the other the extracellular matrix components in form of solution, in case of gelatin (2.25% w/v) or suspension in case of UBM flakes (0.50% w/v). The dimensions of the composite fibers were almost identical to that obtained for Ba-A*f* (constituted of plain alginate), being 675 and 692 µm for Ba-AG*f* and Ba-AUBM*f*, respectively. In order to evaluate the distribution of gelatin and UBM within the microfiber volume a colorimetric method for protein revelation was used, based on Coomassie Brilliant Blue staining. As evident from stereo microphotographs reported in Figure 2.1.14A, B, the use of snake micromixer chip allowed to obtain an extremely regular distribution of gelatin throughout the microfibers, as proved by the homogeneous Coomassie staining. Similar results were obtained also for UBM flakes that being solid and lamellar in shape represented a difficult material to be evenly distributed. Figure 2.1.14C, D clearly demonstrated that UBM flakes were well dispersed on the entire fiber length.

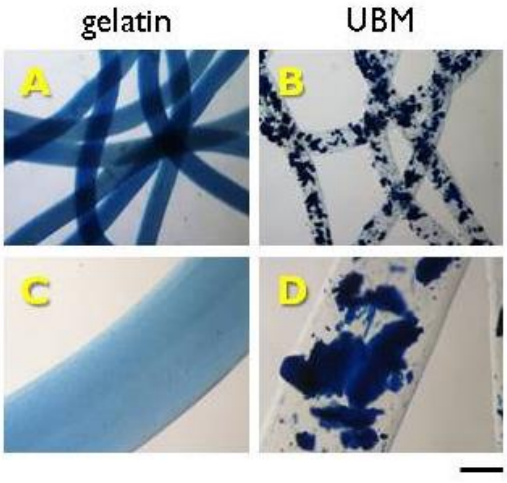

Figure 2.1.14: stereo microphotographs of Ba-AG*f* (A, C) and Ba-AUBM*f* (B, D) after Coomassie Brilliant Blue staining. Bar corresponds to 1.4 mm and 280 µm in panels A, B and C, D, respectively.

Analogously to the experiment preformed for plain alginate fibers, the viability of SaOS-2 cells in composite microfibers was determined by live/dead cell double staining. The fluorescent microphotographs were recorded after the live/dead test performed 14 days after incubation of microfibers in basal or in osteogenic condition. As shown in Figure 2.1.15, after 14 days of culture, SaOS-2 cells maintain an elevate viability (> 95%), both in DMEM high glucose as well as in osteogenic condition.

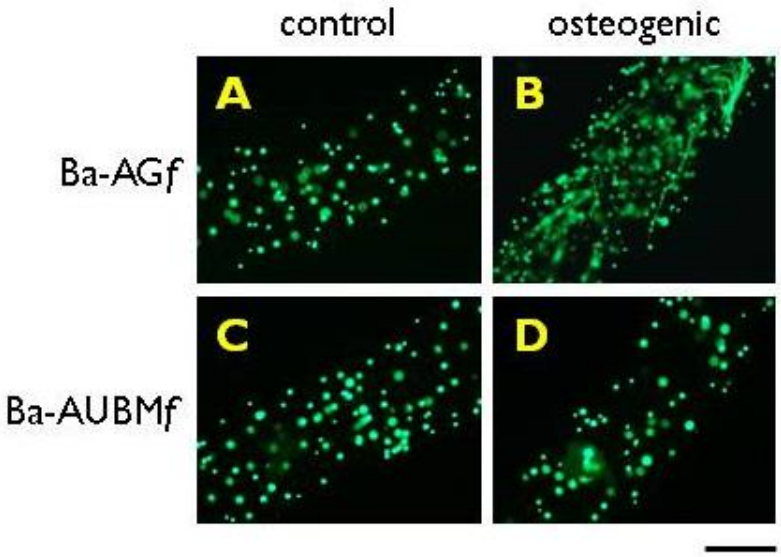

Figure 2.1.15: viability test performed on composite microfibers with double staining calcein-AM/PI, after 14 days of culture. The test was performed on Ba-AG*f* and Ba-AUBM*f* cultured in DMEM high glucose (control) or osteogenic conditions. Bar corresponds to 500 µm.

Composite microfibers were also tested for their effect on differentiation of SaOS-2 cells and biomineralization. The Alizarin Red Staining was performed after 7 and 14 days from the preparation of the microfibers that were maintained in DMEM high glucose (control) or in osteogenic medium. Photomicrographs in Figure 2.1.16 demonstrate that SaOS-2 cells embedded in Ba-AG*f* and in Ba-AUBM*f* began to produce mineralized matrix since day 7 and progress up to day 14. Notably, SaOS-2 cells grown in standard 2D condition typically display signs of differentiation not earlier than day 12-14. In particular the deposition of mineral matrix appears to be co-localized with UBM particles, which surface is strongly positive to the Alizarin Red-S staining.

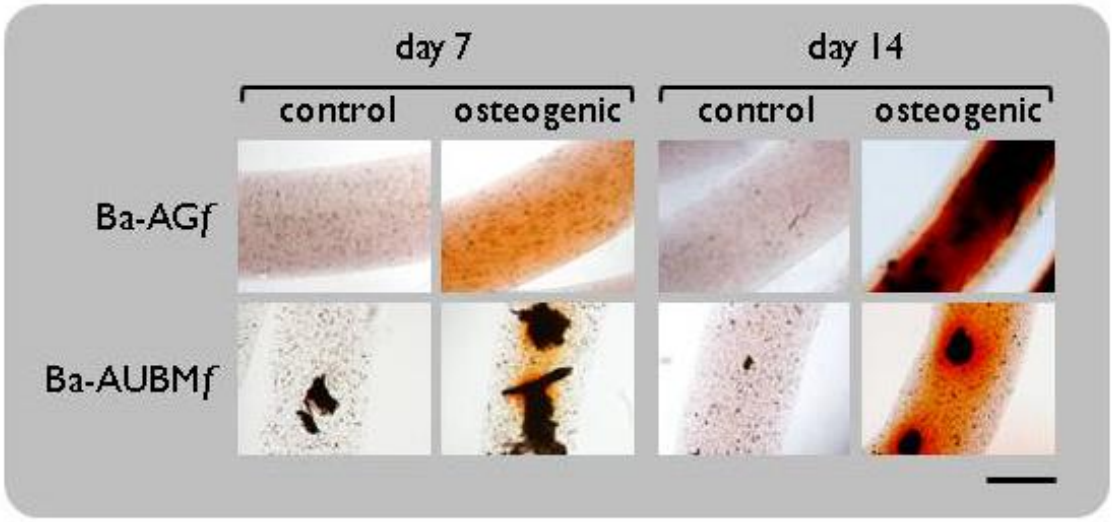

Figure 2.1.16: Alizarin red-S staining of SaOS-2 cells embedded in Ba-AG*f* and Ba-AUBM*f*. Staining was performed after 7 or 14 days of cell culture in DMEM high glucose (control) or osteogenic conditions. Bar corresponds to 500 µm.

Finally, in order to confirm at molecular level the differentiation of SaOS-2 cells, a qRT-PCR analysis was performed. For PCR analysis, SaOS-2 cells were firstly recovered from the microfibers by dissolving them with EDTA, and later total RNA was extracted. After 14 days of culture in DMEM high glucose or osteogenic conditions the following specific osteoblastic genes were analyzed for expression level both for microfibers and monolayer: Col1A1 and Runx2. The results of the experiment reported in Figure 2.1.17 can be summarized as follows:

a) As expected, cells growing as monolayer in DMEM display low levels of expression for both analyzed genes. After induction, by osteogenic conditions the levels raised considerably (3-5 fold increase).

b) The levels of Col1A1 and Runx2, in the case of cells cultured in DMEM in microfibers are much higher than those determined for cells growing as monolayer (3-6 fold increase). Notably such levels are almost identical to those expressed by monolayers in osteogenic conditions.

c) The gene expression level of osteogenic markers for cells growing in microfibers are similar, with slightly higher levels for cells in microfibers maintained in osteogenic than in DMEM conditions. Particularly, cells in Ba-AUBM*f* displayed higher expression levels for both Col1A1 and Runx2.

The obtained data suggest that the 3D and molecular conditions offered by the composite microfibers enhanced the expression of the analyzed osteogenic markers, even in absence of osteogenic inducers.

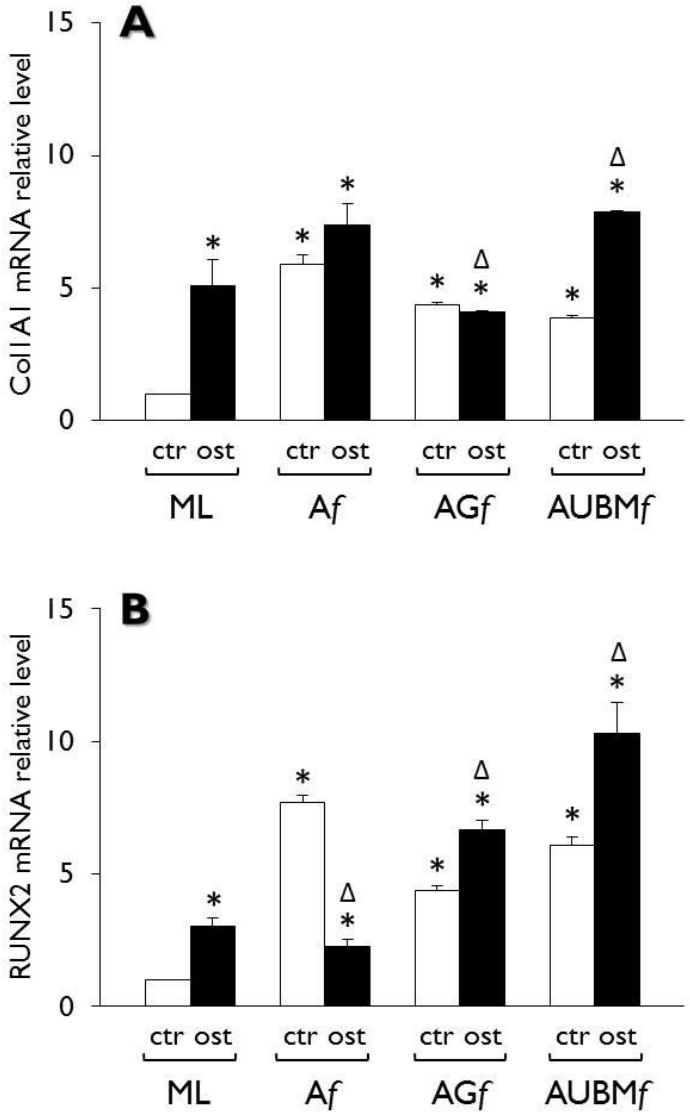

Figure 2.1.17: gene expression analysis of SaOS-2 cells cultured as monolayer (ML) or embedded in Ba-A*f*, Ba-AG*f* and Ba-AUBM*f*. The mRNA levels for Col1A1 (A) and Runx2 (B) were determined by qRT-PCR analysis after 14 days of cell culture in DMEM high glucose (ctr) or osteogenic conditions (ost). Results were calculated using 2-ΔΔCt method. mRNA expression data are presented as percentage variation respect to GAPDH expression level. Statistical analysis was performed for each condition versus cells cultured as monolayer in DMEM high glucose (*) or in osteogenic conditions versus relative control for each microfiber condition (Δ). p-values ≤ 0.05 were considered significant.

Conclusions

The main purpose of the present study has been the investigation of composite microfibers produced with the combined use of alginate and ECM derived components for cell embedding and biomineralization potential. This paper described the production of alginate microfibers, with highly controlled morphological and dimensional properties, by a microfluidic procedure employing a two

inlets, snake micromixing chip, represent an important experimental set up for the preparation of novel hybrid biomaterial scaffold intended for cell embedding and tissue engineering applications. The microfluidic procedure allowed a precise control of the dimensional and morphological characteristics of the microfibers, favourable influencing the viability and function of the embedded cells. Notably, the use of a two inlets micromixing chip resulted in an even distribution of cells and other constituents within the entire volume of the microfiber. We were able to demonstrate that the combined utilization of alginate (representing the main component of the device) and ECM constituents (in form of gelatine solution or UBM particles) resulted in a synergistic activity of both materials, positively influencing the viability and functions of the embedded cells.

In this respect, the engineered microfibers represent a smart scaffold offering: a) the mechanical and material properties of alginates, which can be in turn varied through different gelling conditions such as diverse divalent cations and b) the bioactive function given by the presence of gelatin and UBM, improving the viability and differentiation ability of the embedded SaOS-2 cells.

The bimodal nature of the microfibers provided the ideal environment for the deposition of biomineralized particles as proved by the intense mineralization evidenced in relatively short culture time (i. e. 7 days). In conclusion, the engineered microfiber concept here presented could be used to improve both the cell survival and function in devices fabricated for tissue engineering and cell transplantation purposes.

Chapter 2 – section 2

Encapsulation of de-differentiated chondrocytes

Outline of the work

Since articular cartilage lesions do not heal spontaneously, they represent a therapeutic challenge in orthopedic care and tissue engineering approaches have emerged as a promising alternative, thanks to the use of biomaterials able to support cartilage regeneration. In this context, the composite microfibers, described in the previous chapter, herein were engineered with de-differentiated chondrocytes, to test their effectiveness into modulating the behavior and re-differentiation of encapsulated cells. A complete re-differentiation at the single cell level without cell aggregate formation was obtained, associated with significative expression of chondrogenic markers and high cellular secretory activity of pericellular dense ECM material and collagen fibers. Notably, no sign of collagen type 10 deposition was observed, indicating the inhibition towards the undesired hypertrophic maturation. Moreover, the composite microfibers appeared resistant to freezing allowing to recover highly viable and functional cells also after thawing. As a whole, these data suggest that de-differentiated chondrocytes regain a functional chondrocyte phenotype in a 3D microenvironment created by a mixture of alginate and gelatin or UBM. With this approach we demonstrated for the first time that the presence of UBM is beneficial for chondrocytes activity, contributes to the formation of a microenvironment around individual cells mimicking the *in vivo* situation, and meets the need for proposing new cartilage tissue engineering platforms.

Introduction

The main component of the articular cartilage is represented by a highly specialized extracellular matrix (ECM) where a relative small number of cells are dispersed. This ECM is mainly composed by collagen type 2 and proteoglycans, which determine cartilage-typical mechanical characteristics such as tensile strength coupled with flexibility and resistance to compressive loading (*Muir, 1995*).

Damage and subsequent degeneration of this peculiar ECM lead to the loss of cartilage functionality, associated with pain condition and reduced mobility in the patients. Chondrocytes, which are entrapped in the ECM, do not manage to grow out of the dense matrix hindering self-healing and the deposition of neo-cartilaginous matrix. This stimulates a growing interest in the development of different cartilage engineering reparative strategies based on the combination of scaffold, cells and biomolecules aiming at generating a functional ECM (*Poole et al, 2001; Chang et al, 2005; Moutos and Guilak, 2008; Liao et al, 2014*). Cell-based tissue engineering approaches for cartilage repair and regeneration are focused on ideal cell source, on controlling differentiation using soluble chemical factors and mechanical stimulation, and on developing adequate biomaterial scaffolds. Chondrocytes, being the cellular components of the mature and functional cartilage, are the most obvious choice and have been extensively studied for cartilage repair and used in clinics in an autologous setting. However, progress in their utility in tissue engineering is limited by their instability in monolayer culture which on the one hand is needed to expand the cells, but on the other causes dedifferentiation with loss of differentiated phenotype. Other limitations include the rareness of the donor tissue and difficulties of exercising precise control over the cells' differentiation potential in a complex 3D setting. For the restoration and maintenance of the chondrocytic phenotype, 3D environments consisting of natural or synthetic scaffold with a favorable milieu for chondrogenesis represented by supplementation of chondrogenic inducers (i.e. TGF-β) are routinely adopted. Hydrogels, particularly alginate, resulted successful in chondrocyte re-differentiation (*Guo et al, 1989; Häuselmann et al, 1996; Caron et al, 2012*). Alginate forms biocompatible, biodegradable and shape-adaptable hydrogels which can be employed as cell carriers allowing bidirectional exchange of nutrient, oxygen and cell waste products, but protecting the delivered cells from the host immune system (*Penolazzi et al, 2010; Mazzitelli et al, 2013; Bidarra et al, 2014*). Concerning chondrocytes, alginate supports the retention of their typical rounded morphology and the phenotype maintenance, sustaining the cartilage matrix-forming ability of these cells (*Guo et al, 1989; Bonaventure et al, 1994; Häuselmann et al, 1996*). However, the alginate scaffolds are far from being the typical biological microenvironment, which instead provides a variety of signals through the ECM, where chondrocytes reside. The lack of these biological signals affects the interaction between the entrapped/seeded cells and the biomaterial, and compromises the onset of molecular signaling that guides the effective integration of the implanted construct with the surrounding host tissue (*Lee and Mooney, 2001*). Regarding this issue, the present study aims to improve a microfibrous alginate scaffold combining it with UBM, a natural decellularized matrix, or gelatin to obtain embedded cells with a differentiated and stable chondrocyte phenotype. These natural materials maintain original ECM collagenous network and

water-bound GAGs that are crucial in supporting cell viability, proliferation, adhesion, migration and differentiation (*Badylak et al, 2009; Gómez-Guillén et al, 2011; Santoro et al, 2014*). In particular, among decellularized materials which have received regulatory approval for use in human patients and are commercialized for therapeutic applications, one of the most representative is indeed UBM (Urinary bladder matrix; ACell) (*Gilbert et al, 2012*). It has been demonstrated that the presence and integrity of basement membrane complex in processed UBM promotes inductive tissue remodeling (*Brown and Badylak, 2014*), but little is known about UBM as material supporting chondrocyte activity. Recently, UBM was successfully used for articular cartilage regeneration in a canine model demonstrating the efficacy to treat dogs with chronic osteoarthritis of the hip joint (*Rose et al, 2009*). Therefore, in order to create a 3D scaffold potential suitable for a fiber-based tissue such as cartilage, composite hydrogel scaffolds were here produced in form of microfibers, by a previously described microfluidic approach (see Section 1; *Angelozzi et al, 2015*). Human advanced dedifferentiated nasal chondrocytes from monolayer passage P6 were employed to restore or maintain the chondrocyte phenotype after embedding into the microfibers. It has been demonstrated that variations of material composite and culture conditions often lead to significantly different outcomes on chondrocyte phenotypes. The debate on the methods that can precisely control the microenvironment in a culture system and, as a consequence, the fate and function of the embedded cells is widely open. In this regard, we were interested to investigate the potential of our composite microfibers i. in controlling chondrocyte differentiation for proper cartilage matrix reconstruction, and ii. in affecting the microenvironment around individual mature chondrocytes which, as well known, are surrounded by their own matrix and do not form cell-to-cell contacts *in vivo*. In order to avoid undesired off target effects, the intrinsic properties of the microfibrous scaffolds and the endogenous potential of cells were investigated without adding exogenous chondrogenic inducers. Finally, in order to set up, in the future, a bank of "microfibrous scaffolds embedded chondrocytes", which would allow the frozen samples to be delivered instantaneously to the operating theatre, the properties of thawed chondrocytes embedded into the microfibers, after freezing procedure, have been investigated.

Materials and methods

Chondrocyte Cultures

Cartilage fragments from nasal septum were obtained from 15 donors between 25-60 years old, which underwent septoplasty surgery procedures after informed consent and approval of the Ethics

Committee of the University of Ferrara and S. Anna Hospital. Briefly, cartilage fragments were minced into small pieces and rapidly incubated with type VIII Collagenase (Sigma-Aldrich Chemical Co., St. Louis, MO) at 37°C for 16 h (*do Amaral et al, 2012*). Cells were harvested by centrifugation and plated (p0) in 25 cm^2 tissue culture flasks or 8-well culture slides in standard medium (50% DMEM high-glucose/50% DMEM F-12/ 10% FCS) (Euroclone S.p.A., Milan, Italy) supplemented with antibiotics (penicillin 100 mg/mL and streptomycin 10 mg/mL), at 37°C in a humidified atmosphere of 5% CO_2. After 7 days, the culture medium was removed and then changed twice a week. At 70–80% confluence, cells were scraped off by 0.05% EDTA (Gibco, Grand Island, NE), washed, plated and allowed to proliferate in standard conditions (50% DMEM high-glucose/ 50% DMEM F-12/ 10% FCS) in order to induce chondrocyte de-differentiation (until p6). De-differentiated chondrocytes at different culture passages were scraped off counted by hemocytometric analysis, assayed for viability, and thereafter used for molecular analysis or for encapsulation procedures.

UBM isolation and purification

Porcine urinary bladders were harvested from pigs, immediately following euthanasia. The connective tissue excess and the residual urine were removed. By mechanical treatment, the tunica serosa, tunica muscularis externa, tunica submucosa, and majority of the tunica muscularis mucosa were removed; thereafter, urothelial cells of the tunica mucosa were detached from the luminal surface by incubating the tissue in saline solution. The resulting tissue, which was composed of the basement membrane of the urothelial cells plus lamina propria, is termed UBM. The obtained UBM sheets were then treated by a solution containing 0.1% (v/v) peracetic acid (Sigma), 4.0% (v/v) ethanol (Sigma), and 95.9% (v/v) sterile water for 2 h. Peracetic acid residues were then removed with washes with PBS (pH 7.4) and sterile water. The decellularized UBM were then lyophilized and milled to obtain a particulate form using a Wiley Mini Mill (Thomas Scientific, Swedesboro, NJ, U.S.A.).

Microfibers' production and encapsulation procedure

Composite alginate microfibers (containing cells, extracellular matrix components or both) were produced using a two inlets snake micromixing chip. Briefly a sodium alginate solution (2.0%, w/v), without cells for empty microfibers production and containing de-differentiated chondrocytes

(2 x 10^6 cells/mL) for encapsulation procedure, and sodium alginate solution (2.0%, w/v) containing different amounts of extracellular matrix components (i.e. gelatin or UBM) were delivered via the two inlets of the microchips at a total flow rate from 0.5 to 1.5 mL/min for empty microfibers and of 1.5 mL/min during cell encapsulation. The output from the chip outlet was transferred via a 700 µm (internal diameter) outlet tube into a 6 mM $BaCl_2$ where the alginate stream was gelled to produce the final alginate, alginate/gelatin and alginate/UBM microfibers, namely A*f*, AG*f* and AUBM*f* respectively. After the extrusion, cells-containing microfibers were washed three times with saline and cultured in standard chondrocyte medium at 37 °C in a humidified atmosphere of 5% CO_2 for 7 or 14 days.

Geometrical and morphological analysis of microfibers

The dimension and morphology of microfibers were evaluated using optical stereomicroscopy. Quantitative analyses were obtained using the photomicrograph analysis software EclipseNet version 1.16.5. The mean diameter of the microfibers (± SD) was obtained by taking 9 measurements along the (10 mm) length of the samples at equal intervals, in triplicate. Additionally the distribution of different amount of gelatin (1.125, 2.25 and 4.5% w/v) and UBM (0.1, 0.5 and 1% w/v) in composite microfibers was evaluated by Coomassie Brilliant Blue staining: microfibers were incubated with staining solution (0.1% Coomassie Brilliant Blue R-250, 50% methanol and 10% glacial acetic acid) at room temperature for 1 h and then washed in the destaining solution (40% methanol and 10% glacial acetic acid) at room temperature overnight. Gelatin and UBM distribution in stained microfibers was evaluated by optical stereomicroscopy.

Micromass culture system

Dedifferentiated chondrocytes were harvested from monolayer culture and resuspended in standard medium at 2x10^7 cells/mL. Droplets (10 µl) were carefully placed in each well interior of a 12-well plate. Cells were allowed to adhere at 37 °C for 3 h, followed by the addition of standard medium supplemented with 10% FCS. After 24 h, the cell droplets coalesced and became spherical. Medium was changed every 3 days and micromasses were harvested on days 7 and 14.

Viability analysis of encapsulated cells

Viability of embedded cells was assessed after 7 and 14 days from encapsulation procedure. Cell survival was evaluated by Calcein-AM/PI staining (Cellstain double staining kit, Sigma Aldrich) according to the manufacturer's instructions. Cells were visualized under a fluorescence microscope (Nikon, Optiphot-2; Nikon Corporation, Tokyo, Japan) using the filter block for fluorescein: dead cells stained red, while viable ones appeared green.

Cell recovery from microfibers

Encapsulated chondrocytes were retrieved from microfibrous scaffolds after 7 and 14 days of culture. Microfibers were incubated at 37 °C in a 100 mM EDTA solution (pH 7.0) for 10 min to dissolve the Ba-alginate based constructs and obtain the free cells. Recovered cells were employed for successive analyses.

GAG and DNA quantification

De-differentiated chondrocytes before encapsulation procedure or recovered chondrocytes from microfibers or micromasses were lysed with 50 µl of RIPA buffer. Total sulfated GAG content was determined in RIPA samples from day 7 and day 14 cultures by using 1,9-dimethylmethylene blue (DMMB), as previously described (*Caron et al, 2012*). A standard curve of chondroitin sulfate in PBS-EDTA was included to determine the GAG concentration in the samples. 100 µl of diluted RIPA sample (5 µl RIPA sample and 95 µl PBS-EDTA) or standard (95 µl standard and 5 µl RIPA) was added to 200 µl of DMMB solution and the extinctions were determined spectrophotometrically at 595 nm. GAG content was determined using the generated standard curve corrected for DNA content and expressed as µg GAG/ng DNA. DNA content in the same RIPA samples was determined using SYBR® Green I Nucleic Acid stain (Invitrogen). A serially diluted standard curve of genomic control DNA (DNA Ladder G571A, Promega) in Tris-EDTA (TE) buffer was included to quantify DNA concentration in the samples. Before measurement, RIPA samples were diluted in TE buffer (1 µl RIPA sample and 99 µl TE buffer) and standard were prepared (99 µl standard in TE and 1 µl RIPA buffer). SYBR® Green was diluted 10000 times in TE buffer and 100 µl of this solution was added to 100 µl of the above prepared samples or standards. Fluorescence was determined in standard 96 wells plates in a SpectraFluor Plus reader (Tecan): excitation 485 nm and emission 535 nm. DNA concentration was determined using the

standard curve.

Gene expression analysis

Total RNA was extracted from de-differentiated chondrocytes before encapsulation procedure, encapsulated chondrocytes cultured in alginate-based scaffolds or the same cells maintained in micromass by using the RNeasy Mini Kit (Qiagen, Hilden, Germany), according to the manufacturer's instruction. Total RNA was used for reverse-transcription and stored at −80°C. Briefly, cDNA was synthesized from total RNA (500 ng) in a 20 μl reaction volume using the TaqMan High-Capacity cDNA Reverse Transcription kit (Applied Biosystems) as previously described (*Lolli et al, 2014*). Gene expression analyses by qRT-PCR were performed for Col1A1, Col2A1, Acan and Col10A1 mRNA levels, through the use of Taqman probes (Life Technologies, Carlsbad, CA). The CFX96^{TM} PCR detection system (Bio-Rad, Hercules, CA) was used and results were calculated using the $2^{-\Delta Ct}$ method using GAPDH as reference gene for normalization.

Alcian Blue Staining

Glycosaminoglycans content was assessed by Alcian Blue staining in monolayered cells. Cells were rinsed with PBS and fixed in 10% formaldehyde in PBS for 10 min. Cultures were then stained with Alcian Blue pH 2 (1% in 3% acetic acid) (Sigma-Aldrich Chemical Co., St. Louis, MO) 30 min at 37°C. Subsequently cells were washed with water and observed using a Leitz microscope. The presence of GAG deposits appeared as blue staining areas.

Immunocytochemistry

Immunocytochemistry analysis was performed on freshly, de-differentiated and recovered chondrocytes employing the ImmPRESS (Vectorlabs, Burlingame, CA) or 4plus AP universal (Biocare Medical, Concord, CA) detection kits. Cells grown in chamber slides were fixed in cold 100% methanol and permeabilized with 0.2% (v/v) Triton X-100 (Sigma-Aldrich Chemical Co., St. Louis, MO) in Tris-buffered saline (TBS). Cells were treated with 3% H_2O_2 in TBS, and incubated in 2% normal horse serum (Vectorlabs, Burlingame, CA) for 15 min at RT. After the incubation in blocking serum, the different primary antibodies were added and incubated at 4°C overnight: polyclonal antibodies for Col1A1 (rabbit anti-human, 1:200 dilution, Santa Cruz Biotechnology,

CA), Col2A1 (mouse anti-human, 1:200 dilution, Abcam, Cambridge, UK), aggrecan (mouse anti-human, 1:200 dilution, Santa Cruz Biotechnology, CA), Sox9 (rabbit anti-human, Santa Cruz Biotechnology, CA). Cells were then incubated in Vecstain ABC (Vectorlabs, Burlingame, CA) or Universal AP detection (Biocare Medical, Concord, CA) reagents for 30 min and stained, respectively, with DAB solution (Vectorlabs, Burlingame, CA) or Vulcan Fast Red chromogen kit (Biocare Medical, Concord, CA). After washing, cells were mounted in glycerol/TBS 9:1 and observed using a Leitz microscope. Quantitative image analysis of immunostained cells was obtained by a computerized video-camera– based image-analysis system (with NIH, USA ImageJ software, public domain available at: http://rsb.info.nih.gov/nih-image/) under brightfield microscopy. Briefly images were grabbed with single stain, without carrying out nuclear counterstaining with hematoxylin and unaltered TIFF images were digitized and converted to black and white picture to evaluate the distribution of relative gray values (i.e. number of pixels in the image as a function of gray value 0-256), which reflected chromogen stain intensity. Images were then segmented using a consistent arbitrary threshold 50% to avoid a floor or ceiling effect, and binarized (black versus white); total black pixels per field were counted and average values were calculated for each sample. Three replicate samples and at least four fields per replicate were subjected to densitometric analysis. We performed the quantification of pixels per 100 cells and not per area in order to take into account the different cell morphology and confluence.

Transmission electronic microscope (TEM) analysis and toluidine staining

Cell-containing microfibers were fixed in glutaraldehyde 2.5% buffered solution and osmium tetroxide 2% buffered solution and dehydrated through an ethanol gradient; samples were araldite embedded (ACM Fluka Sigma-Aldrich Co., St. Louis, MO) and the ultra-thin sections of a selected area were contrasted with uranyl acetate lead citrate and observed at transmission electron microscopy (TEM; ZEISS EM 910 electron microscope; Zeiss, Oberkochen, Germany). For toluidine staining 5 μm sections from the same specimens were obtained with a glass blade. Sections were stained with toluidine blue, mounted in glycerol and observed using a Leitz microscope.

Microfibers cryopreservation

Cryopreservation of A*f*, AG*f* and AUBM*f* embedded chondrocytes was performed by adapting a previously published protocol (*Pravdyuk et al 2013*). Microfibers embedded cells were directly freezed in standard culture medium with 10% FCS and supplemented with 10% of dimethyl

sulfoxide (DMSO). The samples were cryopreserved at -20 °C for 30 min, maintained at -80 °C for 24 h and then immersed in liquid nitrogen, where they were kept until the thawing day. Cryovials within microfibers were thawed in a warm water bath (37 °C) and, when ice was totally melted, microfibers were washed twice with culture medium and subsequently cultured in standard conditions prior to performing morphological, viability and immunocytochemical analysis.

Statistical analysis

All cell-related experiments were repeated with chondrocytes derived from 5 different donors and performed in triplicate for each donor. Data are presented as means ± SEM. The normal distribution of data was verified using the Kolmogorov-Smirnov test. In case of single comparison, statistical significance was determined by paired Student's t-test for normally distributed data and Wilcoxon matched-pairs signed-ranks test for non-normally distributed data. In case of multiple comparisons, statistical significance was analysed by one-way analysis of variance (ANOVA) and Bonferroni post hoc test if the values followed a normal distribution, or by Kruskal–Wallis analysis (nonparametric one-way ANOVA) and Dunn's post hoc test if the values were not normally distributed. For all statistical analysis, differences were considered statistically significant for p-values ≤ 0.05.

Results and discussion

Production and characterization of composite microfibers

Alginate (A*f*), alginate plus gelatin (AG*f*) and alginate plus UBM (AUBM*f*) microfibers were produced by a microfluidic procedure throughout a chip (MC3) consisting in two inlets, a snake micromixing channel and an outlet tube (#T3) with 700 µm internal diameter (Figure 2.2.1A), as described in Materials and Methods section. Photomicrographs of microfibers obtained with different flow rates (from 0.5 mL/min to 1.5 mL/min) and following dimensional analysis demonstrated that the microfluidic procedure allowed a strict control on microfibers' morphology and diameters (Figure 2.2.1B and C). Indeed microfibers presented a highly smooth surface and a uniform shape with constant diameters' dimensions. Concerning the effect of the flow rate on scaffolds' size, as we expected, higher pumping rates positively correlated with increased microfiber diameters: this behaviour can be attributed to the Barus effect (*Malkin et al, 1976*). Moreover photomicrographs and dimensional analysis demonstrated that the addition of gelatin or

UBM to alginate solution didn't affect microfiber morphology and surface and caused only a slight shift towards broader diameters.

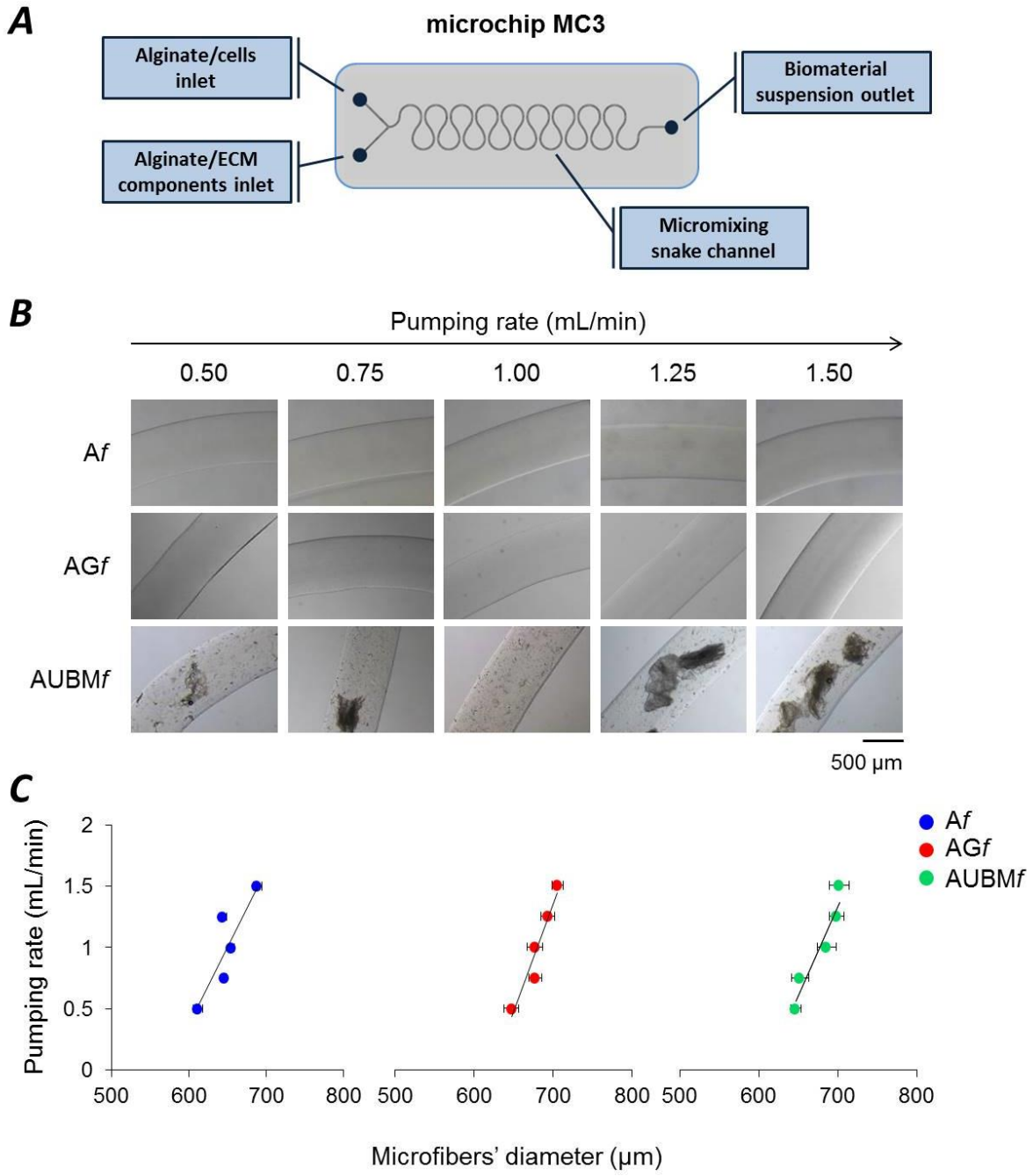

Figure 2.2.1: production and dimensional and morphological analysis of composite microfibers. (A) Schematic representation of the microchip (MC3) employed for composite microfibers' preparation. The chip presents two inlets where the alginate suspension (2%) containing cells or gelatin (2.25% w/v) or UBM (0.5% w/v) were delivered through the micomixing snake geometry channel and a 700 µm outlet tube (#T3) into a 6 mM $BaCl_2$ solution, to obtain alginate (A*f*), alginate plus gelatin (AG*f*) or alginate plus UBM (AUBM*f*) microfibers. (B) Photomicrographs of A*f*, AG*f* and AUBM*f* obtained with different pumping rates (from 0.5 to 1.5 mL/min). Bar corresponds to 500 µm. (C) Dimensional analysis of diameters of microfibers showed in B.

The maintenance of the good structural and morphological properties of the microfibers was probably due also to the optimal and even distribution of gelatin and UBM, as shown by Coomassie Blue Brilliant staining (Figure 2.2.2). Indeed, as evaluable by photomicrographs, the MC3 channel geometry allowed a homogeneous disposition of ECM-derived components along the whole microfiber, also when the amount of gelatin or UBM was reduced or, conversely, increased.

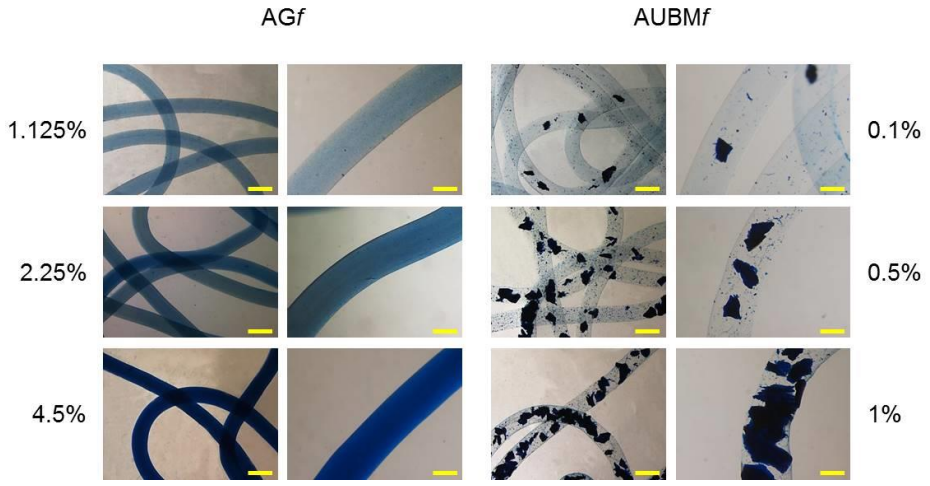

Figure 2.2.2: effect of gelatin and UBM concentration on composite microfibers. Different amounts of gelatin (1.125%, 2.25% and 4.5% w/v) or UBM (0.1%, 0.5% and 1% w/v) were resuspended in alginate solution 2% (w/v) to obtain, respectively, AG*f* or AUBM*f* with diverse concentration of ECM-components, which were subsequently stained with Coomassie Blue Brilliant. Bar corresponds to 1 mm in lower magnification photomicrographs and to 400 µm in higher magnification images.

Chondrocytes expansion and evaluation of de-differentiation process

Chondrocytes from 5 different donors were subcultured up to passages P6 and selected for setting up the encapsulation procedure, as reported in "Material and Methods" and schematized in Fig. 2.2.3. We used nasal chondrocytes in order to have an adequate amount of healthy cartilage tissue, available for experimental planning. Most of the research on cell-based regenerative medicine is promoting the use of cells from ethical and non-invasive procedures such as the recovery of tissue surgical waste. In this regard nasal septum, easily harvested from surgical procedures with minimal morbidity, represents an ideal source. Surgical specimens of nasal septum present good mechanical integrity and structural stability that possibly remain in the memory of the chondrocytes when cultured in a favorable environment. The comparison with articular chondrocytes demonstrated that nasal chondrocytes were able to sustain the production of a cartilage matrix with adequate functional and biomechanical characteristics both *in vitro* and *in vivo* (*do Amaral et al, 2012; Pleumeekers et al, 2014*). As expected (*Caron et al, 2012*), during the de-differentiation process

chondrocytes undergo a substantial change in cell morphology, from rounded to fibroblast-like shape, and a dramatic decrease of GAG content in ECM composition (as demonstrated by Alcian Blue staining). The cartilaginous phenotype was progressively lost over several passages in culture as confirmed by a decrease of typical chondrogenic markers including Col2A1, Acan, Sox9 and an increase of Col1A1 (Figure 2.2.3).

De-differentiated chondrocytes in composite microfibers

De-differentiated chondrocytes were collected at a concentration of 2 x 10^6 cells/ml in the three different biomaterial solutions composed of i) alginate 2% (A); ii) alginate 2% plus gelatin 2.25% (AG) or iii) alginate 2% plus UBM 0.5% (AUBM). The different cells/biomaterial combinations were used to produce microfibers (A*f*, AG*f* and AUBM*f*) with encapsulated cells by letting flow the cell suspension in a $BaCl_2$ gelling bath with a pumping rate of 1.5 mL/min in order to obtain scaffolds with diameters between 650-750 µm, according to previous dimensional analysis. Encapsulated cells were maintained in culture medium without adding chondrogenic inducers up to 14 days, and analyzed for their viability and morphology at different time of culture. In this condition, de-differentiated chondrocytes returned to a rounded shape, which continues to be maintained over time resembling freshly isolated chondrocyte phenotype, as demonstrated by double staining with Calcein-AM/propidium iodide (Figure 2.2.3). Green fluorescence was highly detectable in living cells, while no red fluorescent dead cells were observed up to 14 days of culture in standard medium condition. These data validated the encapsulation procedure that didn't compromise cell viability.

Next, we investigated how the UBM affects chondrocyte activity, in terms of proteoglycan formation defined by toluidine blue metachromasia of matrix. As shown in Figure 2.2.4, it has been possible to appreciate that already after only 7 days the embedded de-differentiated chondrocytes reverted to a rounded shape in all different matrices. The current biomimetic 3D culture system appears to prevent cell-to-cell contacts, facilitating the onset of a context similar to the environment of mature chondrocytes in cartilage. The presence of metachromatic areas with secretory vesicles in a well-defined pericellular space at day 7 and 14 of culture was evident, indicating the effective release and deposition of cartilage-like ECM. Therefore, all three composite microfibers allow the onset of a microenvironment around individual chondrocytes supporting cell maturation. Even if this kind of analysis doesn't allow the volumetric quantification of pericellular metacromasia, however our data indicate that the presence of UBM doesn't prevent chondrocyte-like cells activity.

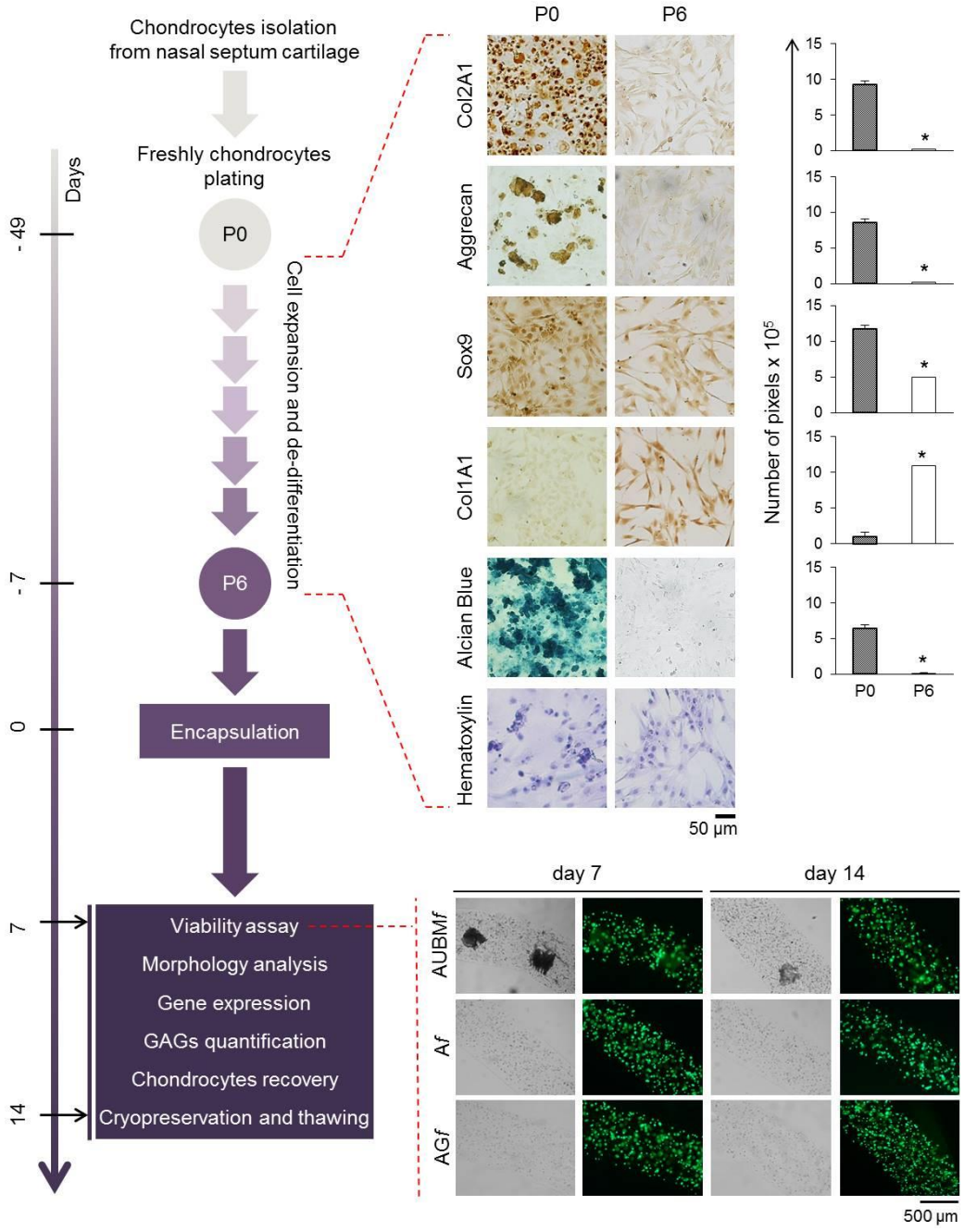

Figure 2.2.3: a schematic representation of the experimental approach. Human chondrocytes were isolated from nasal septum biopsy, expanded and de-differentiated up to the sixth culture passage (P6). Cells were then collected, embedded in composite microfibers, maintained in culture up to 7 or 14 days and then subjected to the indicated analysis. De-differentiation process from passage 0 (P0) to passage 6 (P6) has been monitored: protein expression of cartilage-related genes (Col2A1, Aggrecan, Sox9) and Col1A1 was investigated by immunocytochemical analysis. Alcian Blue staining for GAG detection is also reported. Cell morphology was evaluated by hematoxylin staining. Representative optical photomicrographs are reported. Pictures of at least four random fields of three replicates were captured for densitometric analysis using ImageJ software. Data are presented as means of pixels per one hundred cells ± SEM. (*$P \leq 0.05$). Cell viability of A*f*, AG*f* and AUBM*f* embedded chondrocytes has also been included. Optical and fluorescence photomicrographs after double staining with Calcein-AM/PI at day 7 and 14 of culture in basal medium are reported. The green fluorescence indicates the presence of calcein-labelled live cells, while PI-labelled dead cells are revealed by red fluorescence. Merged photomicrographs are reported.

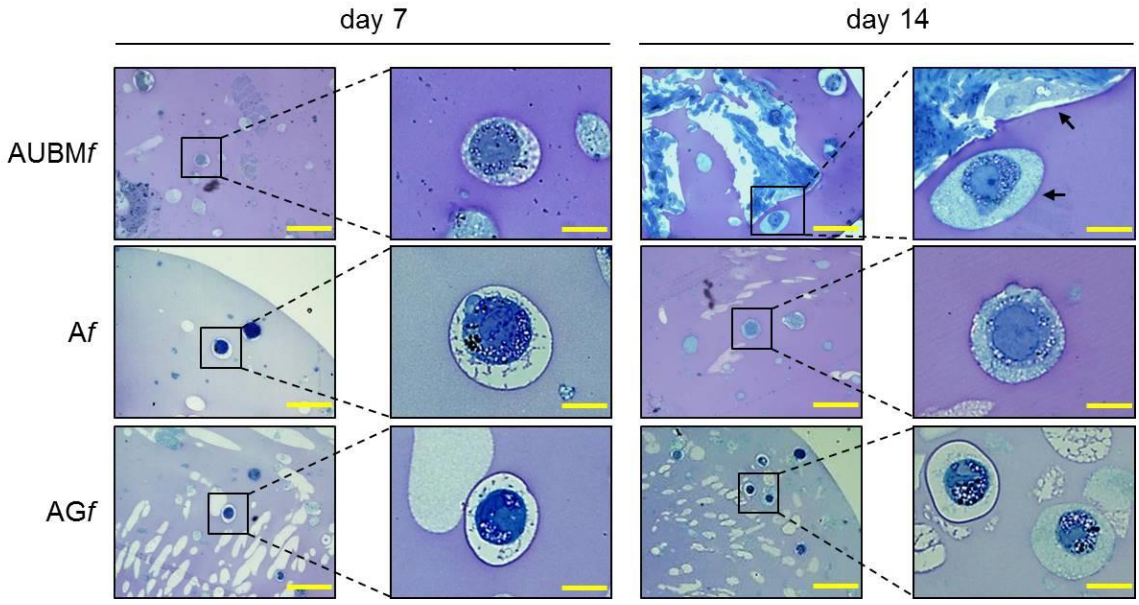

Figure 2.2.4: presence of secretory vescicles and metachromatic areas. AUBM*f*, A*f*, and AG*f* embedded chondrocytes at day 7 and 14 of culture were stained with Toluidine blue. Representative photomicrographs showed the presence of extracellular matrix deposition in the pericellular space of the single cells (as clearly evidenced in the higher magnification images) and the presence of metachromatic area (pink). Black arrows: single or UBM-attached chondrocyte. Bar corresponds to 25 μm for lower magnification photomicrographs and to 10 μm for higher magnification ones.

It is important to underline that cells used in these experiments are at high passages and are typically described as irreversibly de-differentiated chondrocytes. They are not recommended for transplantation since they become apoptotic, inhibit key signaling proteins in the MAPK pathway, produce matrix degrading enzymes, losing, as a whole, their chondrogenic potential definitively (*Dell'Accio et al, 2001; Schulze-Tanzil et al, 2004*). The possibility to utilize cells at higher culture passages with results comparable to lower passages cells allows to have a large amount of cells for clinical application satisfying surgical requests and overcoming the issue of relative small and insufficient donor samples (*Melero-Martin and Al-Rubeai, 2007*).

Chondrogenic properties of chondrocytes in composite microfibers

TEM ultrastructural analysis of the A*f*, AG*f* and AUBM*f* embedded chondrocytes at day 14 revealed a high cellular secretory activity. As shown in Figure 2.2.5, the presence of secretory vesicles containing extracellular matrix dense materials, and collagen fibers with their typical banding pattern is clearly appreciable. The released materials accumulated and assembled in a sparse matrix in the surrounding lacuna, resembling the biological microenvironment of

chondrocytes. These preliminary evidences confirmed the deposition of a cartilage-like extracellular matrix in this area, as hypothesized after the toluidine blue staining (see Figure 2.2.4). Interestingly, AUBM*f* showed the presence of cells able to interact with each other and with UBM flakes (characterized by typical collagen fibers) located in the closed areas.

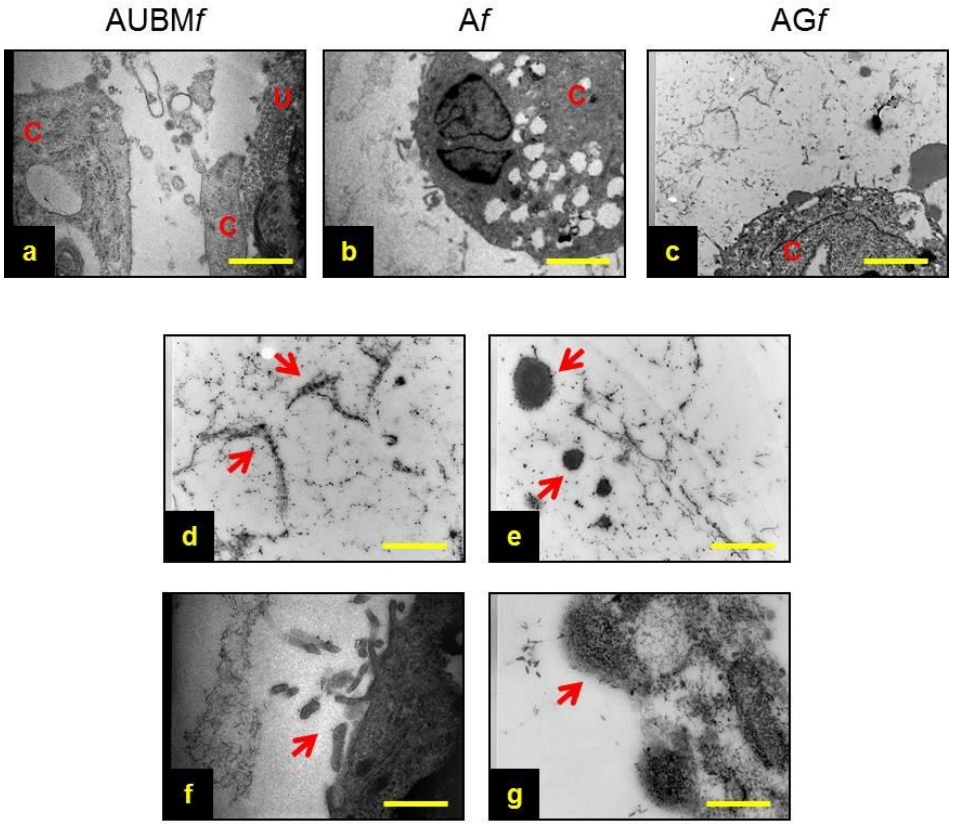

Figure 2.2.5: chondrogenic properties of chondrocytes in microfibrous scaffolds: TEM ultrastructural analysis of AUBM*f*, A*f*, and AG*f* embedded chondrocytes at day 14 of culture. Lower magnification photomicrographs showed the typical ultrastructure of an embedded chondrocyte in AUBM*f* (a), A*f* (b), and AG*f* (c). In the images at higher magnification red arrows indicated the presence of ECM dense material and collagen fibers with their typical banding pattern in the pericellular space (d,e) and evidenced the ECM-containing vesicles release from embedded chondrocytes (f,g). Bar corresponds to 2.6 μm in a-c, 1 μm in d-f and 0.4 μm in g. C = cell; U = UBM.

In order to analyze the recovery of the chondrogenic differentiation, the expression of ECM components was evaluated in the de-differentiated chondrocytes after embedding in the microfibers. For this purpose, chondrocytes were harvested from microfibers at day 7 and 14 of culture, and subjected to qRT-PCR and GAG analysis. As shown in Figure 2.2.6A, the main cartilage-specific ECM component, collagen type 2, and the major proteoglycan in cartilage, aggrecan, were highly expressed in chondrocytes from AUBM*f*, A*f*, and AG*f* compared to chondrocytes cultured in standard micromass (MM). Micromass culture system has been chosen instead of pellet culture

since it may be maintained in culture medium also without adding TGF-β supplementation. Col2A1 and Col1A1 expression levels were compared calculating the differential index (the ratio between the two collagen types). As shown in Figure 2.2.6C, Col2A1/Col1A1differential index was significantly increased (from 20 to 120 times) in all microfibrous scaffolds compared to micromass culture, showing a significative expression of Col2A1. This also shows that the small amount of TGF-β inside the added FCS is not sufficient to support chondrogenesis in standard conditions of micromass which requires exogenously added chondrogenic inducers. Conversely, microenvironments created by microfibers allowed the activity of chondrocytes also with very low dose of TGF-β. This evidence represents an important added value considering the recently reported controversial action of TGF-β. Among several identified growth and differentiation factors up to now that are able to stimulate cartilage development and maintain chondrocyte phenotype, the most widely chondrogenic inducer is considered this cytokine that, effectively, is commonly utilized to induce *in vitro* chondrogenesis. Despite many well described advantages, the use of traditional exogenous differentiating agents is beginning to be questioned for their undesired off target effects and controversial outcomes. Recently it has been demonstrated that the presence of TGF-β during chondrocyte proliferation may be detrimental for the re-differentiation process and may promote the rapid and undesirable differentiation into fibroblast like cells (*Mueller et al, 2010; Narcisi et al, 2012b*). The negative effect of this cytokine in wound repair of cartilage has been observed in several experimental models suggesting the hypothesis that the inhibition of TGF-β may induce cartilage repair (*Blaney et al, 2007; Khaghani et al, 2012*). Therefore, our experimental conditions allow testing not only the endogenous potency of the cells, but also the intrinsic properties of alginate based biomaterials in view of their possible combined use *in vivo*.

Moreover, we here demonstrated that the expression of Col10A1, which encodes the collagen type 10 alpha 1 chain traditionally associated with chondrocyte hypertrophy, resulted undetectable both at 7 and 14 days (Figure 2.2.6C). This suggested that microfiber environment is suitable to prevent undesired hypertrophic maturation which can widely affect the successful outcome of the graft transplantation. Hypertrophy represents, in fact, one of the major drawbacks in autologous chondrocytes implantation and also in MSCs-based strategies (*Melero-Martin and Al-Rubeai, 2007; Blaney et al, 2007; Mueller et al, 2010; Khaghani et al, 2012; Narcisi et al, 2012b; Niethammer et al, 2014*).

GAG quantification performed as total GAG content normalized to DNA content (Figure 2.2.6B), confirmed that AUBM*f*, A*f*, and AG*f* embedded chondrocytes highly regain their chondrogenic capacity at comparable levels. This kind of analysis validated all three microfibers as favorable

environment to redifferentiate de-differentiated chondrocytes, in particular demonstrating for the first time that the presence of UBM may be beneficial for chondrocytes activity. This last sentence was supported by the next step aimd at investigating the effectiveness of these three different microenvironments in maintaining the acquired properties of the cells. This kind of information is essential in view of the use of microfibers *in vivo*. For this purpose, re-differentiated chondrocytes were recovered from the microfibers and grown up to 7 days as monolayered culture in standard medium without adding chondrogenic inducers. Interestingly, even if plated in unfavorable conditions, the cells maintained a round morphology, a low adhesion ability, and generated micro-aggregates, demonstrating a behavior comparable to freshly isolated chondrocytes (Figure 2.2.7). Alcian blue staining showed the presence of GAG, and immunocytochemical analysis confirmed the presence of Col2A1 in all experimental groups up to 7 days. The presence of UBM was particularly effective in promoting the maintenance of chondrogenic phenotype as evidenced by a larger number of Col2A1 positive spontaneous microaggregates that persisted over 7 days.

As a whole, these data validated the intrinsic potency of microfibers in mantaining chondrogenic activity of the re-differentiated chondrocytes once released from the confined 3D microenvironment of the scaffolds.

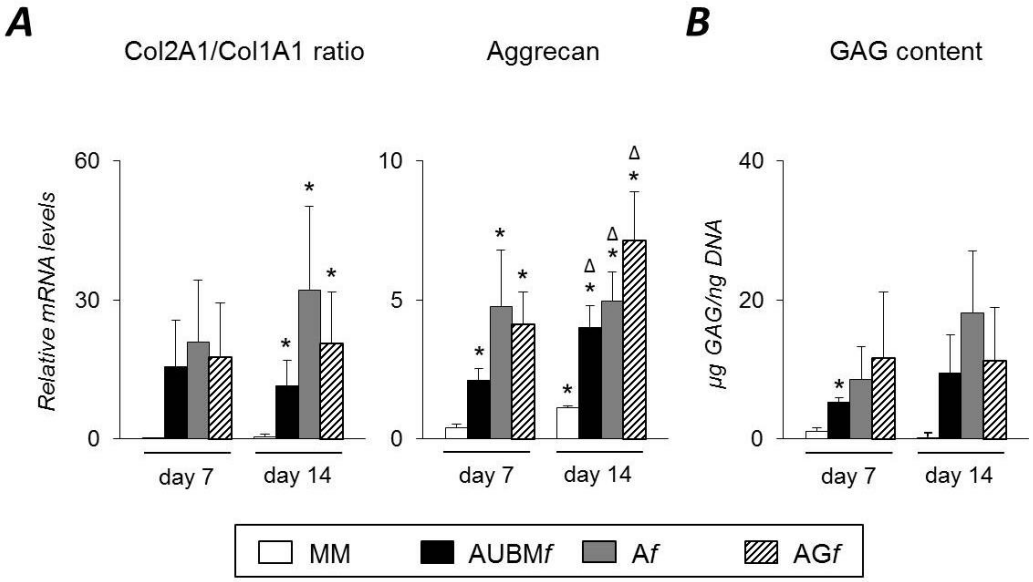

C

	Condition	Col2A1/Col1A1 ratio	Aggrecan	Col10A1	GAG content *(µg GAG/ng DNA)*
	ML	0.01 ± 0.01	0.22 ± 0.07	ND	ND
day 7	MM	0.17 ± 0.12	0.41 ± 0.11	ND	1.15 ± 0.51
day 7	AUBM*f*	15.58 ± 10.02	2.09 ± 0.42	ND	5.26 ± 0.62
day 7	A*f*	20.97 ± 13.31	4.77 ± 2.02	ND	8.53 ± 4.80
day 7	AG*f*	17.64 ± 11.71	4.12 ± 1.15	ND	11.73 ± 9.41
day 14	MM	0.52 ± 0.49	1.12 ± 0.07	ND	0.09 ± 0.06
day 14	AUBM*f*	11.51 ± 5.37	4.01 ± 0.79	ND	9.47 ± 5.45
day 14	A*f*	31.99 ± 18.14	4.94 ± 1.06	ND	18.11 ± 8.95
day 14	AG*f*	20.69 ± 11.03	7.15 ± 1.74	ND	11.28 ± 7.67

* ND = not detectable

Figure 2.2.6: chondrogenic properties of chondrocytes in microfibrous scaffolds: evaluation of cartilage markers expression of AUBM*f*, A*f*, and AG*f* embedded chondrocytes. AUBM*f*, A*f*, and AG*f* embedded chondrocytes or chondrocyte micromasses (MM) cultured for 7 or 14 days were compared for chondrogenic capacity by analysing the expression of cartilage markers. (A) The expression of Col2A1, Col1A1 and aggrecan was evaluated by qRT-PCR. Col2A1/Col1A1 ratio is reported. Data are presented as means ± SEM of three independent experiments, using the 2-ΔCt method as percentage vs GAPDH expression levels. Statistical analysis was performed all conditions vs micromass of day 7 (*$p<0.05$) or vs micromass of day 14 (Δ$p<0.05$). (B) Biochemical evaluation of the GAG content by DMMB staining on cellular lysates from AUBM*f*, A*f*, and AG*f* embedded chondrocytes or chondrocyte micromasses (MM) at day 7 or 14 of culture. Values are reported as µg GAG/ng DNA. Statistical analysis was performed all conditions vs micromass of day 7 (*$p<0.05$) or vs micromass of day 14 (Δ$p<0.05$). (C) Quantification of Col2A1/Col1A1 ratio, aggrecan and Col10A1 expression, and GAG content for each experimental condition are reported. Values obtained from de-differentiated chondrocytes before the encapsulation procedure (ML) are also reported. Data are presented as means ± SEM of three independent experiments. ND = not detectable.

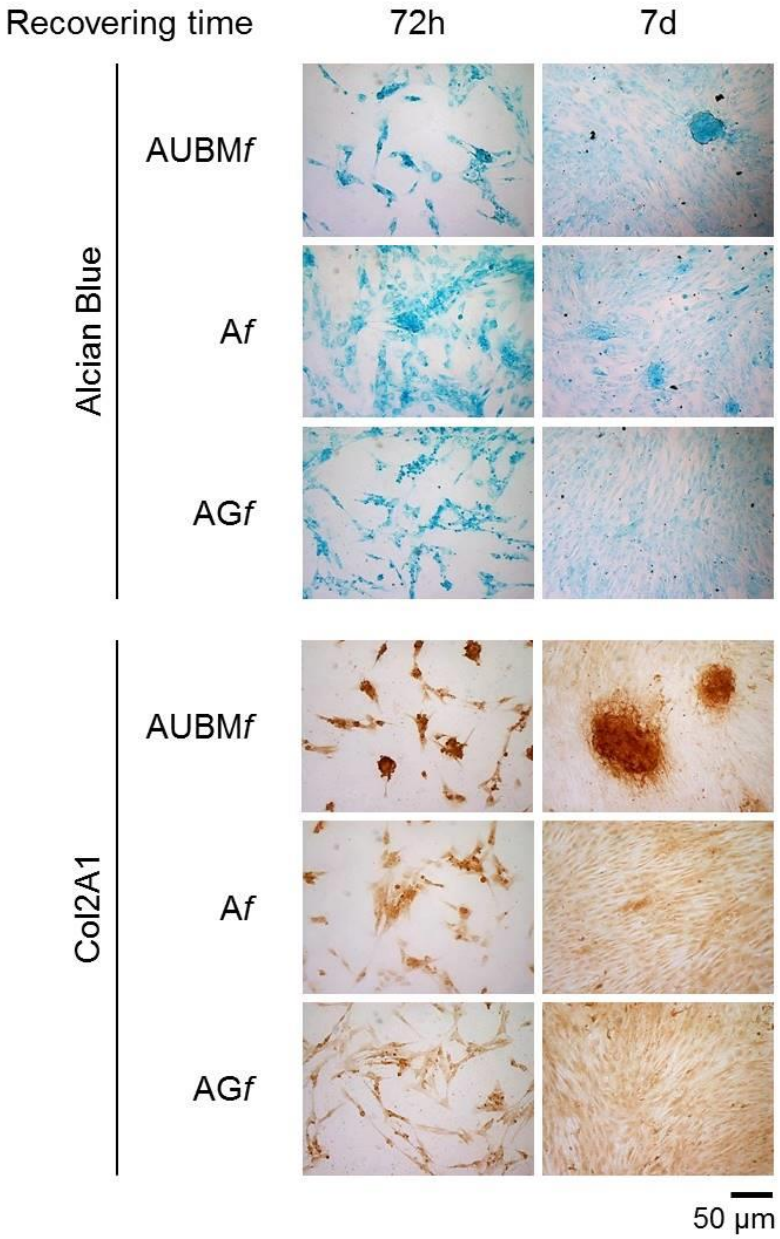

Figure 2.2.7: properties of AUBM*f*, A*f*, and AG*f* – recovered chondrocytes. Chondrocytes were recovered from microfibers after 14 days of culture, and then subjected to immunocytochemical analysis and Alcian Blue staining after growing in monolayer for 72 h or 7 days. Optical photomicrographs of Alcian Blue and Col2A1 positivity indicate the maintenance of acquired chondrogenic properties.

Cryopreservation of Af, AGf and AUBMf embedded chondrocytes.

In order to explore the possibility to set up a bank of "microfibrous scaffolds embedded chondrocytes" for further *in vitro* and *in vivo* manipulations, we performed a preliminary assessment of the properties of thawed A*f*, AG*f* and AUBM*f* embedded chondrocytes after freezing procedure. The chondrocytes were frozen directly within microfibrous scaffolds in complete culture

medium supplemented with 10% DMSO, stored at −196°C in liquid nitrogen, thawed and assessed for cellular viability and chondrogenic properties. Similarly to the freshly A*f*, AG*f* and AUBM*f* embedded chondrocytes, thawed samples maintained a high cell viability and a round shaped cell morphology (Figure 2.2.8). To investigate the functionality and the phenotype maintenance after thawing, cells were then recovered from microfibers and cultured for 24 hours under the same conditions described in Figure 2.2.7. Also in this case, despite the unfavorable conditions represented by monolayer culture, thawed samples preserved GAG production and Col2A1 expression as shown by Alcian Blue staining and immunocytochemical analysis (Figure 2.2.8). Therefore, the composite microfibers appear resistant to freezing and allow us to recover highly viable and functional cells also after thawing. Consequently, composite biomaterials such as those here developed may be proposed as tool for *in vitro* re-differentiation process and recovering of an effective and functional chondrocyte population potentially able to produce a neo-cartilage tissue *in vivo*. This evidence is also important in view of a future chondrocyte bank that would be of great help as a permanent source of cartilage cells.

4. Conclusions

The aim of this study was to develop 3D chondrogenic constructs engineerized with re-differentiated chondrocytes embedded into alginate hydrogels combined with ECM-derived biomaterials without chondrogenic growth factors supplementation such as TGF-β for possible treatment of cartilage defects.

We demonstrated the effectiveness of alginate-based composite scaffolds produced in form of microfibers by a microfluidic approach i. in supporting chondrogenic process of advanced de-differentiated chondrocytes from monolayer passage P6 and ii. in maintaining chondrogenic properties of the re-differentiated chondrocytes once released from the confined 3D microenvironments of the scaffolds. The 3D microenvironments created by alginate together with the components of gelatin or ECM derived from urinary bladder (UBM) are able to exert their effect in the presence of very low amount of TGF-β.

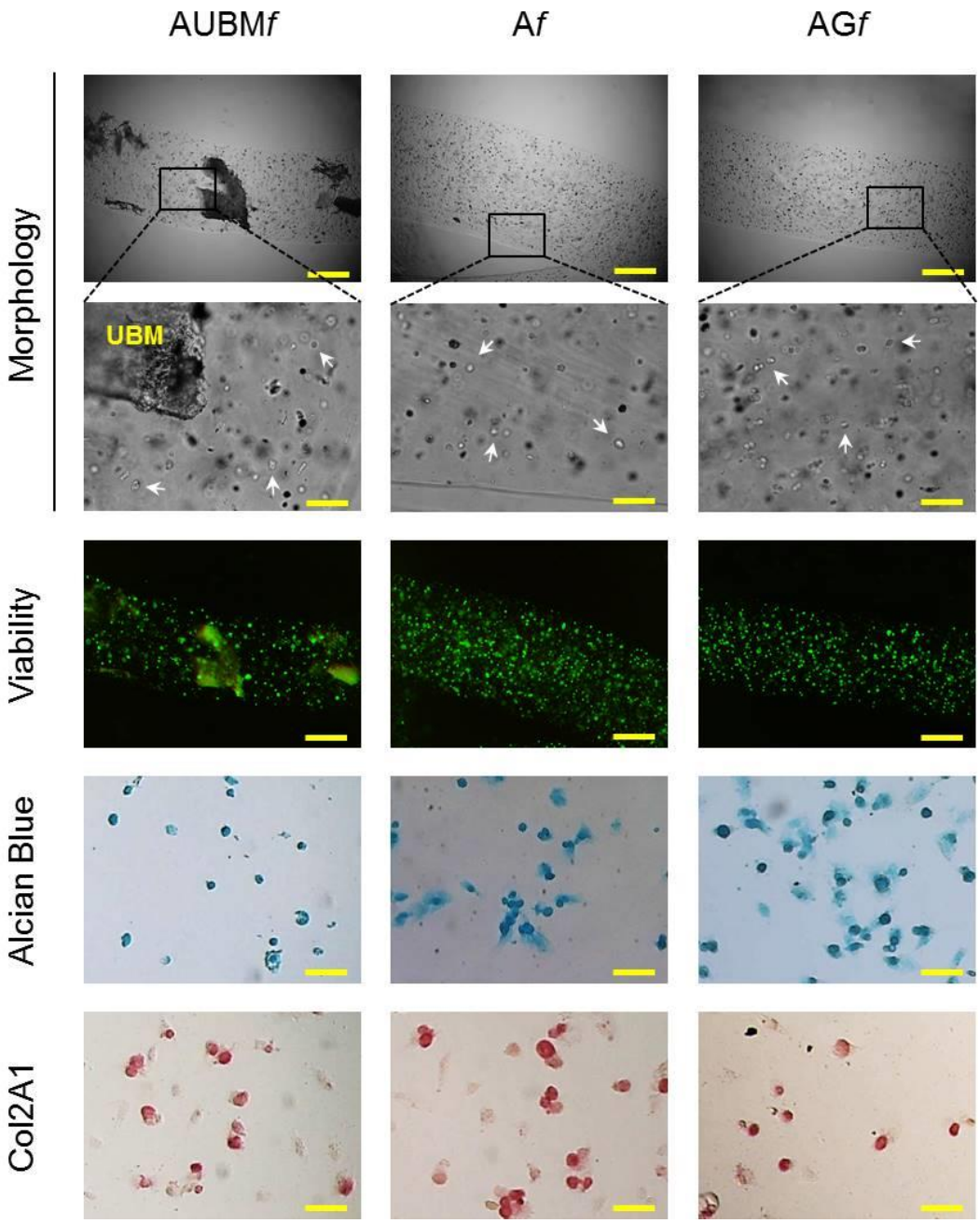

Figure 2.2.8: Properties of thawed AUBM*f*, A*f*, and AG*f* embedded chondrocytes after freezing procedure. AUBM*f*, A*f*, and AG*f* embedded chondrocytes were frozen, stored in liquid nitrogen, thawed and assessed for cell morphology, viability and chondrogenic properties. Optical images of microfibers show the rounded shape of thawed embedded cells (particularly evident at higher magnification: see white arrows). Fluorescence merged images of the Calcein-AM/PI double staining demonstrated the high cell viability. The presence of GAGs and Col2A1 was confirmed by Alcian Blue staining and immunocytochemical analysis on recovered chondrocytes grown in monolayer for 24 h. Bar corresponds to: 300 µm in lower magnification images of morphology and viability, 60 µm in higher magnification, 50 µm in Alcian Blue staining and Col2A1 immunocytochemical analysis.

To our knowledge few reports focused on the effect of ECM-derived biomaterials in cartilage regeneration (*Jin et al, 2007; Yang et al, 2008; Baugé et al, 2014; Grogan et al, 2014; Lee et al, 2014; Youngstrom et al, 2015*) and in any case the combination with alginate properties has not been described. This interaction is an essential feature for the success of a tissue engineering strategy, allowing to maintain the low friction and the load bearing characteristics of the native cartilage (*Moutos and Guilak, 2008; Grogan et al, 2014*). Therefore, the hypothesis to guide cartilage neo-formation *in vivo* by such cell-based microfibrous constructs is worth further consideration, especially given that fibrous versus non-fibrous scaffolds offer interesting advantages for cell delivery in biomedical application since guided growth, alignment and migration of cells are favored (*Blaney et al, 2007; Yang et al, 2008; Grogan et al, 2014; Youngstrom et al, 2015*). In conclusion, our results provide a proof of concept for developing a next experimental design based on the implantation of microfibers or recovered re-differentiated chondrocytes on animal models with critical size defect affecting the whole joint.

Chapter 2 – section 3

A 3D dynamic osteoblasts-osteoclasts co-culture model

Outline of the work

Even though biomaterial represents a critical component in the design of a tissue engineering approach, it remains an exogenous structure which could directly or indirectly affect the metabolic and molecular responses of the cellular counterpart: this feature should be largely exploited to increase the regenerative potential of implanted cells, but could be detrimental for the study of the molecular interplay sustaining tissue homeostasis or pathological conditions. Furthermore this scenario becomes more complex if we think to the tissue microenvironment as the house of several cell types (in particular in bone) continuously talking to each other to obtain a strict regulation between external stimuli and biological responses. The reproduction of an *in vitro* system able to reproduce this unique crosstalk is highly desirable, in order to study cellular and molecular phenomenon occurring. At this aim, the development of a 3D scaffold-free osteoblasts/osteoclasts co-culture system requiring limited amounts of human primary cells was hypothesized, as useful platform to 1. recapitulate an "oral bone microenvironment" in healthy or pathological condition, and 2. produce potential implantable cell constructs for regeneration of jawbone. The work reported in this chapter provide the employment of osteoblasts from normal bone chips (hOBs) or from pathologic jawbone of patients taking bisphosponates (hnOBs), that were co-cultured with monocytes (hMCs) either in static (3D-C) or dynamic (3D-DyC) condition using the RCCS-4™ bioreactor. In all tested conditions hOBs supported the formation of mature osteoclasts (hOCs), without differentiating agents or exogenous scaffolds, but 3D-DyC condition associated with a ground based condition (Xg) rather than modeled microgravity (μXg) produced aggregates with high level of osteogenic markers including OPN, OSX, Runx2 and appreciable bone mineral matrix. In this best culture condition, also hnOBs co-cultured with hMCs generated OPN and mineral matrix positive aggregates. The feasibility to obtain from poor-quality bone sites viable osteoblasts able to form aggregates when co-cultured with hMCs, allows to study the development of

autologous implantable constructs to overcome jawbone deficiency in patients affected by MRONJ (Medication-Related Osteonecrosis of the Jaws).

Introduction

Three-dimensional co-culture systems have been developed greatly within the last decade in an effort to recreate the physiological cellular microenvironment of a specific tissue, and extend cell culture longevity and functionality (*Kaji et al, 2011; Sekine et al, 2013; Knight and Przyborski, 2014*). Regarding bone tissue, several *in vitro* co-culture systems based on bone-forming cells (OBs)/bone-resorbing cells (OCs) have been proposed (*Bloemen et al, 2009; Jones et al, 2009; Heinemann et al, 2011; Kuttenberger et al, 2013; Gamblin et al, 2014; Widbiller et al, 2015*), with the aim of creating the Basic Multicellular Unit (BMU). Different parameters such as cell sources and culture conditions may influence the establishment of the complex interactions and intimate crosstalk that naturally occur *in vivo* between OBs, OCs and their precursors (*Tortelli et al, 2009; Papadimitropoulus et al, 2011; Halai et al, 2014; Sims and Martin, 2014*). In an effort to make the results of these studies the most informative and reproducible, the majority of the evidence were so far obtained using a substantial number of cells that could guarantee the formation of an appreciable cellular aggregate. For this reason cell lines, such as MC3T3-E1, MG63 and SaOS-2 for the osteoblastic lineage and RAW264.7 for the osteoclast lineage are widely used. However, cell lines often fail mimicking the primary counterparts. Considering osteoclastic lineage, peripheral blood mononuclear cells (PBMCs), bone marrow and spleen-derived cell populations are good precursors for adequate amount of primary OCs (*Zhang and Huang, 2012; Jacome-Galarza et al, 2013*). Setting up abundant primary cultures of OBs from human tissues is more challenging. In many cases a limited number of precursors or mature cells from a given source can be obtained with a noninvasive procedure and, consequently, few cells are available for *in vitro* or *in vivo* experiments. This occurs when the cells are harvested from atrophic tissue, with insufficient bone quality and volume, or in sites lacking of stem and progenitor cells due to extensive trauma, radiation therapy, or medications such as bisphosphonates (BPs) antiresorptive drugs. BPs promote proliferation and differentiation of OBs and inhibit OCs (*Reszka and Rodan, 2003*). Sometimes these conditions hesitate in adverse non-healing lesions, such as Medication-Related Osteonecrosis of the Jaws (MRONJ), a condition of exposed bone in the maxillofacial region compromising the quality of life with significant morbility (*Ruggiero et al, 2014; Rosini et al, 2015*). The optimal treatment strategy for MRONJ is still to be established. BPs treatment cessation is not sufficient to restore reparative process, conversely, targeted interventions of regenerative medicine could be an attractive option

(*Albanese et al, 2013; Gonzálvez-García et al, 2013; Cardemil et al, 2015; Huang et al, 2015*). In this context, the replacement of healthy bone in necrotic lesions represents an important bone tissue engineering challenge (*Devaki et al, 2012; Barba-Recreo et al, 2015*). These considerations led us to study the minimal combination of OBs/OCs able to promote cell aggregation and differentiation mimicking a bone microenvironment in a 3D static or dynamic co-culture system. Different culture conditions with limited amount of human primary bone cells in a perfusion bioreactor (*Clarke et al, 2013; Vecchiatini et al, 2015*) have been explored in order to set up a protocol exportable to critical situations. Specifically, the possibility to obtain vital bone specimens from jaw bone of patients taking BPs was evaluated, in order to investigate the potential of cells from such a compromised tissue area, assuming that the approach here described could be helpful to generate an autologous implantable construct.

Materials and methods

Cell culture and harvesting procedure

Human normal osteoblasts (hOBs) were obtained from nasal septum. Bone fragments from nasal septum (*Torreggiani et al, 2011*) were obtained from healthy donors between 25-60 years old undergoing septoplasty surgery procedures after informed consent and approval of the Ethics Committee of the University of Ferrara and S. Anna Hospital. Briefly, bone chips were dissected into smaller pieces and plated in T-25 culture flasks in 50% DMEM high-glucose/50% DMEM F-12/20% FCS (Euroclone S.p.A., Milan, Italy) supplemented with 1 mM L-Glutamine, antibiotics (penicillin 100 μg/mL and streptomycin 10 μg/mL) at 37 °C in a humidified atmosphere of 5% CO_2. At 70–80% of confluence, cells were scraped off by treatment with 0.05 % trypsin- EDTA (Sigma-Aldrich, St. Louis, MO, USA), washed, plated and allowed to proliferate in standard conditions (10% FCS DMEM high-glucose). hOBs (p0) were characterized for the presence of alkaline phosphatase activity (ALP Leukocyte kit; Sigma-Aldrich). OPN and Runx2 expression was assessed by immunostaining. For osteogenic differentiation, hOBs were cultured up to 21 days in osteogenic medium consisting of 10% FCS DMEM high-glucose supplemented with 10 mM β-glycerophosphate, 10^{-7} M dexamethasone and 100 μM ascorbate (Sigma-Aldrich). The osteogenic medium was refreshed twice a week and the extent of mineralized matrix in the plates was determined by Alizarin Red-S staining (Sigma-Aldrich). For co-culture experiments hOBs were used until passage 3.

Human osteoblasts from jawbone of patients taking BPs at risk for "necrotic" lesions (hnOBs) were obtained as described below. Harvesting procedures of autogenous bone were conducted in full accordance with the "Declaration of Helsinki" as adopted by the 18th World Medical Assembly in 1964 and revised in Edinburgh (2000) and the Good Clinical Practice guidelines. Before surgery, each subject provided an informed consent. All surgical extractions and treatments were performed by the same clinician, according to standard surgical and anaesthetic protocols of University Dental Clinic, University of Ferrara.

Bone specimens were harvested from alveolar process during surgical planned treatments in different patients:

- patients previously treated with antiresorptive agents, such as Zoledronate or Alendronate, for metastatic disease or osteoporosis, undergoing to routinary tooth extraction;
- patients previously treated with antiresorptive agents, such as Zoledronate or Alendronate, for metastatic disease or osteoporosis, undergoing to surgical treatment of MRONJ.

There was no history of radiation therapy to the head and neck region in any of these patients.

Before surgical treatment mepivacaine 3% was locally administered, as needed. Buccal flaps were raised, lingual tissues were retracted and protected. After tooth extraction, buccal and distal alveolar bone was harvested with bone scraper (Safescraper® Twist Cortical Bone Collector, Meta, Italy).

Considering the risk for MRONJ onset, each patient received same standard preoperative therapy (amoxicillin 1 g 2 times a day starting 3 days before surgery; metronidazole 250 mg 3 times a day starting 3 days before surgery) and postoperative instructions for Nonsteroidal anti-inflammatory drugs (NSAIDs) and antibiotics prescription (amoxicillin 1 g 2 times a day for 10 days; ketoprofen 80 mg 3 times a day for day 1, 2 and 3). Chlorhexidine 0.20% mouthrinses were prescribed from day 2 until day 14. A post-operative meeting was scheduled for day 7 and day 10, to check swelling and primary wound closure. During the second meeting sutures were removed.

During surgical treatment of MRONJ, bone specimens were collected with the use of a Modified Trephine Bur n. TRE040M (Hu-Friedy Mfg. Co., LLC).

As proposed by Cardemil et al., the alveolar bone samples were collected some distance away from exposed necrotic bone (Figure 6A), within the considered boundary bone. The boundary of the MRONJ lesion was defined where vital, light, and bleeding jawbone replaced grayish, brittle, and necrotic bone (*Cardemil et al, 2015*).

Considering the presence of MRONJ, each patient received same standard preoperative therapy (amoxicillin 1 g twice a day starting 6 days before surgery; metronidazole 250 mg 3 times a day starting 3 days before surgery) and postoperative instructions for non-steroidal anti-inflammatory drugs (NSAIDs) and antibiotics prescription (amoxicillin 1 g twice a day for 10 days; metronidazole

250 mg 3 times a day for 10 days; ketoprofen 80 mg 3 times a day for day 1, 2 and 3. Chlorhexidine 0.20% mouthrinses were prescribed from day 2 until day 14. A post-operative meeting was scheduled for day 7 and day 10, to check swelling and primary wound closure. During the second meeting sutures were removed.

After specimens collections, in all cases surgical area was treated with piezo-electric surgery, and it was cleaned with either a diamond (piezo) or a round diamond-burr drill, at low speed and with generous saline irrigation, leaving dense, highly mineralized bone. Finally the wound space was thoroughly debrided then closed with interrupted sutures (Vicryl 4-0, Ethicon Spa, Pomezia, Italy), to achieve a primary closure, as appropriate. The samples were dissected into smaller pieces, plated and cultured in T-25 culture flasks as already described. The culture medium for hnOBs was further supplemented with a 5-fold increased concentration of antibiotics (penicillin 500 μg/mL and streptomycin 50 μg/mL, gentamicin 50 μg/mL) and antimycotic (fungizone 10 μg/mL): we adopted these conditions given the derivation of the samples and the consequent possibility of contaminations. hnOBs were characterized by immunocytochemical analysis for OPN and Runx2 and ARS staining after osteogenic induction, as already described.

Human monocytes (hMCs) were obtained from peripheral blood (PB) of healthy volunteers (different from the donors of hOBs) after informed consent (median age 37.5 years, range 25-50 that is approximately the same age range of the hOBs donors). PBMCs were obtained from diluted peripheral blood (1:2 in Hanks solution), separated by Histopaque®-1077 (Sigma-Aldrich). hMCs were purified from PBMCs by adhesion selection on polystyrene plates: $1x10^6$ PBMCs/cm^2 were plated in T-25 culture flasks, allowed to settle for 4 h at 37° and flasks were then rinsed to remove non-adherent cells (lymphocytes, platelets, red blood cells, polymorphonuclear cells) (*Piva et al, 2005*). The purity of hMCs population was verified by cytofluorimetric analysis. Briefly, $1x10^5$ cells were resuspended in PBS and incubated with fluorescein isothiocyanate (FITC) conjugated anti-human CD14 antibody (ImmunoTools GmbH, Friesoythe, Germany) for 15 min at 4°C. A monoclonal antibody with no specificity was used as negative control. Cells were then washed and resuspended in 400 μL of PBS. The fluorescence levels were measured using the FACS Scan flow cytometer (Becton Dickinson, Franklin Lakes, NJ, USA) and CELLQUEST software (Becton Dickinson European HQ, Erembodegem Aalst, Belgium). Only the samples that after FACS analysis were CD14 positive ≥95% were used. In order to confirm the ability of isolated hMCs to differentiate into mature osteoclasts, M-CSF (25 ng/mL) and RANKL (30 ng/mL) (PeproTech EC Ltd, London, UK) were added to the culture medium. After 7-10 days, tartrate-resistant acid phosphatase (TRAP) staining was carried out with the Acid Phosphatase Leukocyte (TRAP) Kit (Sigma-Aldrich) according to the manufacturer's protocol. The expression levels of the

osteoclast-specific markers MMP-9 and Cathepsin K (CK) were assessed by immunocytochemistry. Furthermore in order to verify their resorbing ability, hMCs were plated into a calcium phosphate-coated OAAS (OAAS, Osteoclast Activity Assay Substrate, Oscotect Inc., Seoul, Korea) at the density of $1x10^6$ cells/well, and maintained in the same culture condition indicated above. After 7 days, when TRAP-positive hOCs appeared, the cells were removed with a solution of 5% sodium hypochlorite. Bone resorption activity was measured by direct observation under phase contrast microscopy.

Indirect hOBs/hOCs co-culture system

$1.5x10^5$ hOBs were pre-cultured on polystyrene 24 well plates until confluence, then 0.45 μm Cell Culture Inserts (Becton Dickinson, NJ, USA) seeded with hMCs ($0,5x10^5$, hOBs/hMCs 3:1 cell ratio) were added. Cells were cultured in 10% FCS DMEM high-glucose in the absence of osteoclastogenic inducers (M-CSF and RANKL). This method established a co-culture condition with the two cell types not coming into contact, but allowing the interaction with the soluble factors produced by the cells. Co-cultures exposed to M-CSF (25 ng/mL) and RANKL (30 ng/mL) were used as positive control, while hMCs cultured in the absence of hOBs were employed as negative control. After 7 days, TRAP staining and immunocytochemistry analysis for CK were carried out on cells cultured in the upper chamber in order to verify the presence of mature hOCs. After 14 day of osteogenic induction, the expression levels of OPN, OSX and Runx2, the ALP activity and the presence of mineralized matrix deposition (ARS staining) were analyzed. Each individual experiment was entirely performed with hMCs from PBMCs from the same identical donor.

hOBs/hOCs three-dimensional co-culture systems

hOBs/hOCs aggregates were generated in the absence of exogenous scaffolds by using two different experimental approaches: 3D co-culture system obtained in static condition (*3D-C*) and in dynamic condition (*3D-Dyc*).

For *3D-C* culture condition, $0.5\text{-}1x10^6$ hMCs were incubated with $1\text{-}2x10^6$ hOBs in agarose coated polystyrene 6 well plate, in 2 mL of 10% FCS DMEM high-glucose at 37°C (humidified atmosphere, 5% CO_2), with the medium being changed twice a week. After 24h, the presence of spheroids with a diameter >500 μm was observed. After 7 days, a first set of aggregates were collected, fixed in 4% formalin, embedded in paraffin, sectioned and processed for TRAP analysis.

3D-C aggregates were maintained in osteogenic medium (see above) for further 14 days of co-culture. The aggregates were then fixed, embedded in paraffin, sectioned and processed for histochemisty.

The 3D dynamic culture (*3D-DyC*) condition was set up by using the RCCS-4TM bioreactor (Synthecon™, Inc., Houston, TX, USA), with a High Aspect Ratio Vessel (HARV^{TM}; Synthecon™, Inc., Houston, TX, USA). The HARV vessel consists of a horizontally rotated culture chamber, where the cells are suspended, and a perfusion system with media continuously flowing through the culture chamber. The culture chamber can rotate in the X-axis at certain speeds (rpm): higher rpm are associated to lower gravity. 0.5-1x10^6 hMCs and 1-2x10^6 hOBs were inoculated in 2 mL HARV vessels filled with 10% FCS DMEM high-glucose and all air bubbles were removed from the culture chamber. HARV vessels were then inserted into the RCCS-4TM rotary bioreactor and placed in an incubator at 37°C, for the indicated times, in a humidified atmosphere with 5% CO_2. After 7 days, a first set of aggregates were collected for TRAP assay and the others were maintained for further 14 days in osteogenic medium. The rotation speed used for the bioreactor was 4 rpm for the Ground Based dynamic culture at 1xg (Xg) and 14-16 rpm for the Modeled Microgravity condition (μXg), where the aggregate floated in suspension. Medium was refreshed twice a week. At the end-point of co-culture (21 days), the aggregates were collected, 4% formalin fixed and embedded in paraffin for further analysis. All the tested experimental conditions are reported in Figure 2.3.3.

The hnOBs/hMCs aggregate was obtained after incubation of 0.5x10^6 hMCs and 1x10^6 hnOBs, inoculated in 2 mL HARV vessel, inserted into the RCCS-4TM rotary bioreactor (37°C, humidified atmosphere, 5% CO_2), cultured in the absence of modeled microgravity (3DyC/Xg condition) and collected after 21 days (of which 14 days in osteogenic medium) for viability and histological analysis.

Cell viability

Viability of the cells was analyzed by double staining with propidium iodide and Calcein-AM assay (Sigma-Aldrich), according to the manufacturer's instructions. Cells were observed under a fluorescence microscope (Nikon, Optiphot-2; Nikon Corporation, Tokyo, Japan) using the filter block for fluorescein. Dead cells were stained in red, whereas viable ones appeared in green.

Immunocytochemistry and histology

Immunocytochemistry analysis was performed employing the ImmPRESS (Vectorlabs, Burlingame, CA) or 4plus AP universal (Biocare Medical, Concord, CA) detection kit. Briefly, cells grown in 12-wells plate or from indirect co-culture were fixed in cold 100% methanol and permeabilized with 0.2% (v/v) Triton X-100 (Sigma-Aldrich) in TBS. Cells were treated with 3 % H_2O_2 in TBS 1x and incubated in 2 % normal horse serum (Vectorlabs, Burlingame, CA) for 15 min at RT. After the incubation in blocking serum, the different primary antibodies were added and incubated at 4 °C overnight: polyclonal antibodies for MMP-9 (H-129), OPN (LF-123), Runx2 (M-70), OSX (M-15), Cathepsin K (E-7) (rabbit anti-human, 1:200 dilution, Santa Cruz Biotechnology, Dallas TX USA). Cells were then incubated in Vecstain ABC (Vectorlabs, Burlingame, CA) or Universal AP detection (Biocare Medical, Concord, CA) reagents for 30 min and stained, respectively, with DAB solution (Vectorlabs, Burlingame, CA) or Vulcan Fast Red chromogen kit (Biocare Medical, Concord, CA). After washing, cells were mounted in glycerol and observed using the Nikon Esclipse 50i optical microscope.

Histological sections (5 µm) of *3D-C* and *3D-Dyc* aggregates were subjected to immunohistochemistry. To this aim, non-consecutive sections were immunostained with a primary antibody against Cathepsin K (E-7), OPN (LF-123), OSX (M-15) and Runx2 (M-70) (rabbit anti-human, 1:100 dilution, Santa Cruz biotec.). Histological sections were deparaffinized, rehydrated and enzymatic treated with 1 mg/mL pronase and 10 mg/mL hyaluronidase (Sigma-Aldrich) for antigen retrieval and permeabilization. Slides were then incubated overnight with the primary antibody in a humid chamber at 4°C. Alkaline phosphatase-labeled secondary antibody was used (4plus Universal AP Detection, Biocare Medical, Concord, CA, USA) in combination with the Vulcan Fast Red Chromogen Kit (Biocare Medical, Concord, CA, USA), resulting in a red staining. The sections were counterstained with hematoxylin, mounted in glycerol and observed using the Nikon Esclipse 50i optical microscope. TRAP staining was carried out with the Acid Phosphatase Leukocyte (TRAP) Kit (Sigma-Aldrich) according to the manufacturer's protocol. For Alizarin Red-S staining, cells cultured in monolayer or 3D aggregates (*3D-C* and *3D-Dyc*) were fixed in 4% formalin, and then stained with 40 mM ARS solution (pH 4.2) at RT for 10 min. Samples were rinsed five times with distilled water and washed three times in PBS on an orbital shaker at 40 rpm for 5 min each, to reduce non-specific binding. The stainings were quantified by a computerised video camera-based image analysis system (NIH, USA ImageJ software, public domain available at: http://rsb.info.nih.gov/nih-image/) under brightfield microscopy (Nikon Eclipse 50i; Nikon Corporation, Tokyo, Japan). For the analysis of sections obtained from *3D-C* and *3D-Dyc*

aggregates, the positive immunostaining was expressed as % of positive area (three replicates per donors were acquired; five sections per sample; n = 3).

Statistical analysis

Statistical significance was analysed by one-way analysis of variance (ANOVA) and Bonferroni post hoc test if the values followed a normal distribution, or by Kruskal–Wallis analysis (nonparametric one-way ANOVA) and Dunn's post hoc test if the values were not normally distributed. For all statistical analysis, differences were considered statistically significant for p-values ≤ 0.05.

Results

Phenotypical characterization of hOBs and hOCs monotype cell cultures.

hOBs were characterized for their osteogenic potential, in terms of ALP activity, OPN and Runx2 expression and deposition of mineral matrix after 21 days of culture (Figure 2.3.1A). hMCs from human peripheral blood were used as osteoclast progenitors source. hMCs purification by adhesion selection on polystyrene plates (4 h, 37°C) allows to remove contaminating blood cells (lymphocytes, platelets, red blood cells, polymorphonuclear cells), as confirmed by microscopic observations and flow cytometric characterization. As shown in Figure 2.3.1B we obtained more than 95% of purified hMCs, as calculated on the basis of forward and side light scatter profiles and cell surface display pattern (CD14). The ability of the purified hMCs to differentiate into mature multinucleated osteoclasts after exposure to osteoclastogenic inducers (M-CSF and RANKL) was tested, by evaluating the positivity for the TRAP, immunostaining for the osteoclast-specific matrix MMP-9 and Cathepsin K, and the pit formation ability.

Indirect hOBs/hOCs co-culture system

An indirect hOBs/hMCs co-culture system was used to validate the differentiation potential of our experimental model to be used in subsequent 3D co-culture systems. The ability of hOBs to support osteoclastogenesis was investigated seeding hMCs on polystyrene culture plate inserts in the simultaneous presence of hOBs (lower chamber) and without any osteoclastogenic inducers. We

found that 1:3 hMCs/hOBs ratio was the optimal seeding condition allowing the induction of a high percentage of mature TRAP and Cathepsin K positive multinucleated hOCs already detectable after 7 days of culture (Figure 2.3.2, panels a,b,g).

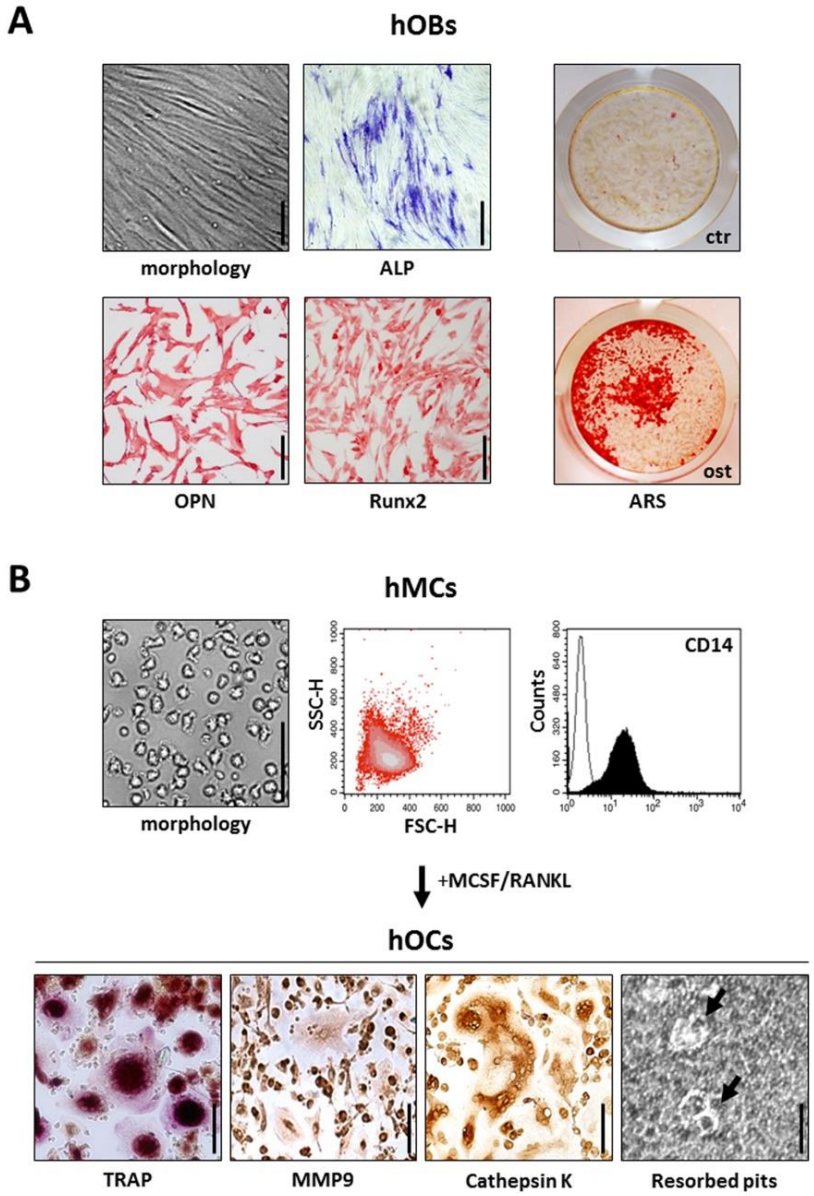

Figure 2.3.1: isolation and characterization of human osteoblasts and monocytes for the co-culture system. (A) Human primary osteoblasts (hOBs) were isolated from bone specimens and characterized in terms of morphology, ALP activity and expression of OPN and Runx2 by immunocytochemistry. hOBs were assayed for mineralization capacity by Alizarin Red S (ARS) staining after culture in osteogenic medium (ost) for 21 days (ctr = cells cultured in basal medium). (B) Human primary monocytes (hMCs) were isolated from peripheral blood and characterized in terms of morphology and CD14 expression by FACS analysis (CD14 positive cells ≥95%). The ability of hMCs to differentiate into mature osteoclasts (hOCs) was confirmed in terms of TRAP-positivity, MMP9 and Cathepsin K expression after stimulation with MCSF (25ng/mL) and RANKL (30 ng/mL) for 7 days. Bars: 250 μm. The pit formation ability of hOCs is also reported. Bars: 20 μm.

The hOCs formation observed in these conditions was comparable with that found when osteoclastogenic inducers were added in the medium (Figure 2.3.2, panels c,d,h). On the contrary, when hOBs were omitted no hOCs were generated (Figure 2.3.2, panels e,f,i). With the progression of culture in osteogenic medium the expression of OPN, OSX, Runx2, the ALP activity and the deposition of mineralized matrix were observed at day 21, indicating that the conventional 2D indirect co-culture system also supported osteoblast maturation.

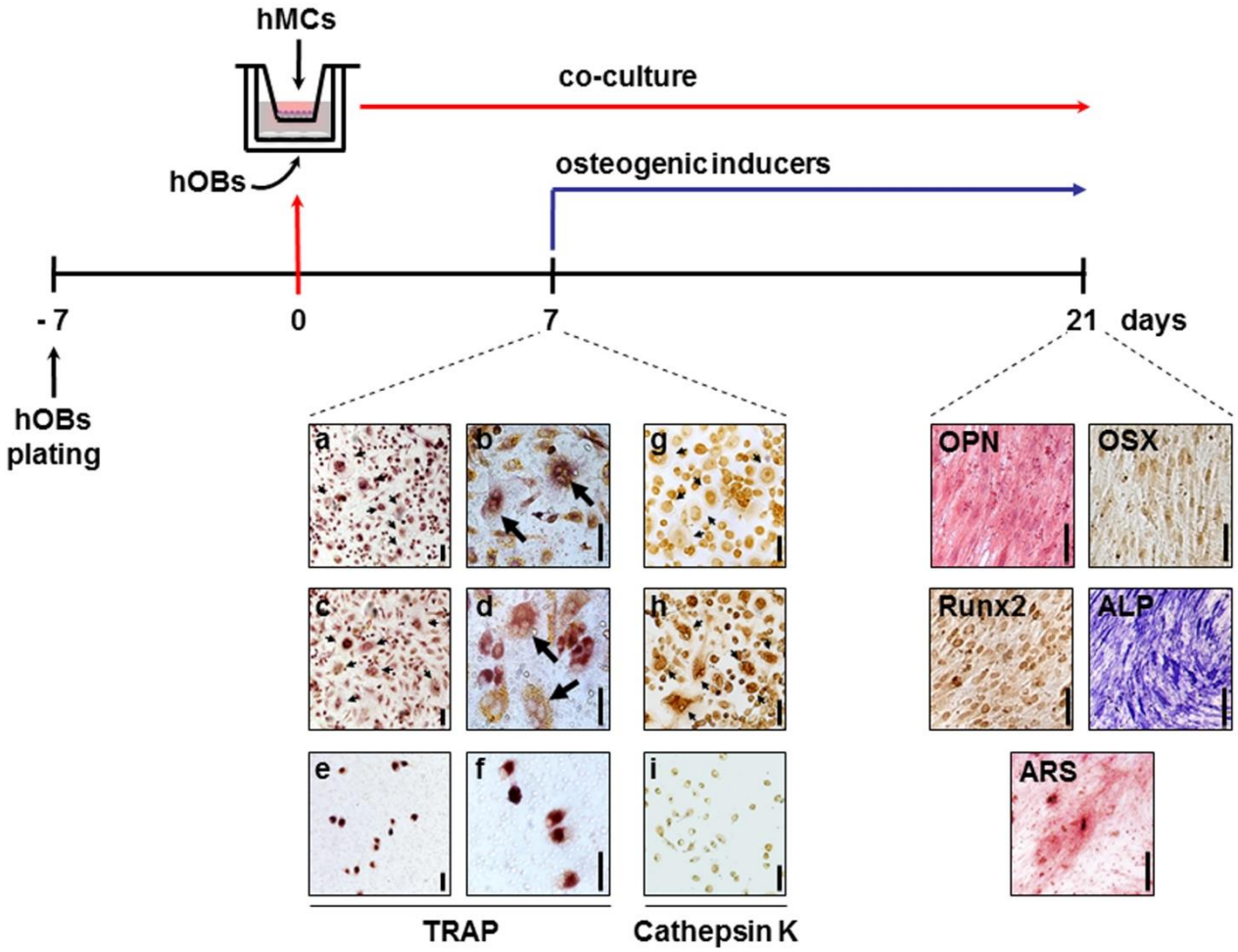

Figure 2.3.2: experimental set-up of in vitro hOBs/hMCs co-culture system. In order to establish a hOBs/hMCs co-culture system, hOBs were plated and after 7 days hMCs were seeded on the apical side of culture plate inserts (day 0). At day 7 of co-culture, the presence of differentiated hOCs (indicated by arrows) was evaluated by TRAP assay (a, b) and Cathepsin K expression (g). The analysis was also performed after stimulation with M-CSF/RANKL (c, d, h: positive control) and in the absence of hOBs (e, f, i: negative control). Bars: 50 μm. Afterwards, osteogenic differentiation of hOBs was induced by replacing the basal medium with osteogenic medium. At day 21 of co-culture, the presence of osteogenic markers was assessed by immunostaining for OPN, OSX, Runx2, ALP activity and ARS staining for mineralized bone matrix. Bars: 20 μm.

hOBs/hOCs three-dimensional co-culture systems

Two different types of 3D environments were then used comparing the effect of static culture (*3D-C*) and dynamic flow (*3D-DyC*) conditions on co-culture systems (Figure 2.3.3A). *3D-C* condition was obtained by direct combination of hMCs and hOBs in agarose coated polystyrene wells, while *3D-DyC* by growing the same cells in the horizontally rotated culture chamber High Aspect Ratio Vessels (HARV) applied to the Rotary Cell Culture System (RCCS). In *3D-DyC* the cells were maintained up to 21 days in controlled microgravity condition - Modeled Microgravity (μXg) - where the aggregate floated in suspension (14-16 rpm), or in 1x g condition - Ground Based dynamic culture (Xg) - where the aggregate was in continuous falling rotation close to the bottom of the vessel (4 rpm). To valuate the optimal condition to generate spontaneously cellular aggregates, the tests reported in the insert of Figure 2.3.3A have been performed. These included the variation of i. cell number and ratio; ii. exposure to differentiating agents (M-CSF and RANKL); iii. rotation rate and modeled microgravity; and iiii. days in culture. Despite it is difficult to characterize the aggregation process, microscopic observations revealed an initial formation of cell assemblies that over time formed spherical aggregates both in *3D-C* and *3D-DyC* condition, mostly when $3x10^6$ cells/mL was used. Cell ratio had no effect for *3D-C*, but appeared relevant for *3D-DyC* condition where cell aggregation process is favored by 1:2 hMCs/hOBs ratio. The presence of inducers (M-CSF/RANKL) was negligible to osteoclastogenic process. Interestingly, already after 7 days of culture, *3D-DyC* condition supported the formation of a functional aggregate exhibiting TRAP positivity (Figure 2.3.3B). Together these findings suggest that all tested environments are favorable to aggregate formation.

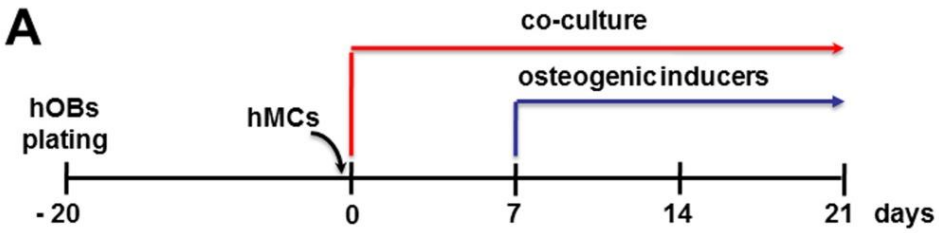

Co-culture system	Cell number	hMCs/hOBs ratio	MCSF/ RANKL	Rpm	Days
3D-C					
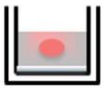	$3x10^6$	1:2	-	-	7
	$3x10^6$	1:2	-	-	21
	$3x10^6$	1:3	-	-	21
	$2x10^6$	1:2	-	-	21
	$2x10^6$	1:2	+	-	21
3D-DyC					
	$3x10^6$	1:2	-	14 (µXg)	7
	$3x10^6$	1:2	+	14 (µXg)	21
	$3x10^6$	1:2	-	14 (µXg)	21
	$3x10^6$	1:3	-	14 (µXg)	21
	$2x10^6$	1:2	-	14 (µXg)	21
	$2x10^6$	1:2	-	4 (Xg)	21
	$3x10^6$	1:2	-	4 (Xg)	21

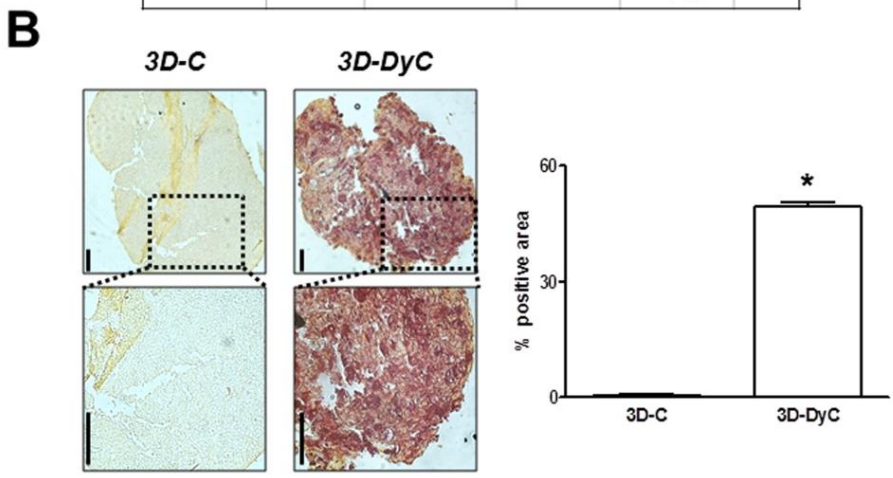

Figure 2.3.3: establishment of three-dimensional (3D) hOBs/hMCs co-culture models. (A) After expansion in monolayer, hOBs were trypsinized and seeded with hMCs (day 0) in agarose-coated wells (3D static condition = 3D-C) or inoculated in HARV culture vessels with the dynamic RCCS bioreactor culture system (3D dynamic condition = 3D-DyC). All the tested experimental conditions are reported in the inset as cell number and ratio (hOBs/hMCs), exposure to differentiating agents (MCSF/RANKL), rotation rate (rpm) and presence or not of controlled microgravity (µXg – modelled microgravity), days of co-culture. (B) At day 7 of co-culture, the presence of mature hOCs was evaluated by TRAP assay in 3D-C and 3D-DyC condition. Higher magnification fields are reported. Bars: 50 µm. TRAP activity was quantified by densitometric analysis using ImageJ software and expressed as percentage of positive area (5 sections per sample, n=3). Data are presented as means ±sem. Statistical analysis was performed: *= $p \leq 0.0001$.

Functionality of the cells within 3D-C and 3D-DyC aggregates

Considering that the overall function of the aggregate depends on the architecture that it achieved in culture, the next experiments were performed at day 21 of culture after allowing the cells to better organize within the aggregate. Before processing for histological analysis, aggregates were subjected to Calcein AM/PI double staining for cell viability assessment. As shown in Figure 2.3.4, both *3D-C* and *3D-DyC* conditions generated aggregates that appeared highly viable at comparable level. Evidently, more than 95% of the cells were viable and remained intact within the aggregate up to day 21 of culture. Interestingly, haematoxylin staining of histological sections revealed appreciable different organization. In both conditions, after 21 days of culture the mass appeared more compact when compared with the cellular aggregate at day 7. This suggests that intercellular crosstalk, cell-stroma interactions and arrangements of the cells change over time, promoting the formation of a cell aggregate progressively better organized. However, in comparison with *3D-DyC*, cells within aggregates from *3D-C* appeared poorly organized. In fact, *3D-DyC* aggregates displayed a layered structure with an appreciable cellular organization: an outer region (arrows) surrounding the aggregate, an intermediate region with a trabecular-like structure and an inner region with different morphological characteristics (Figure 2.3.4).

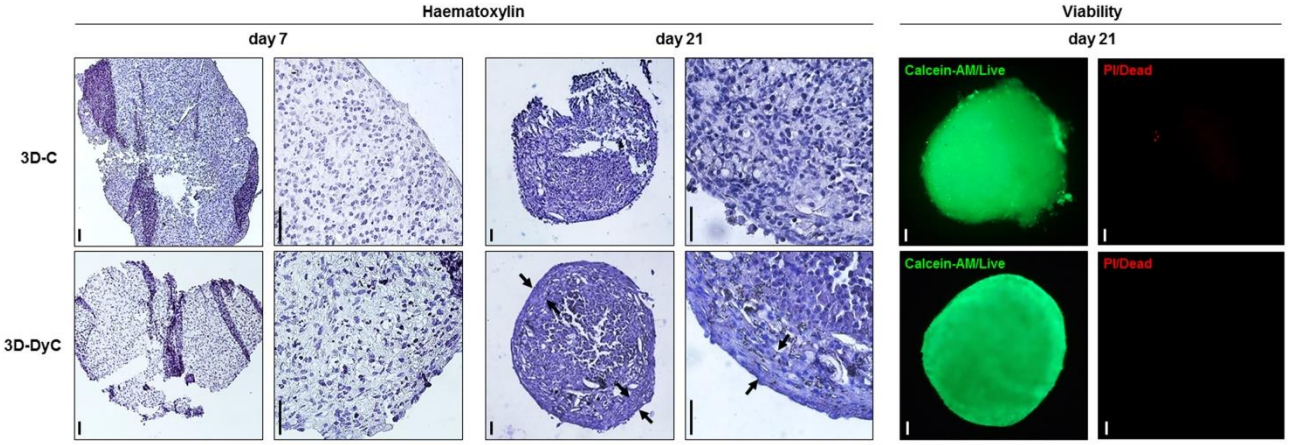

Figure 2.3.4: morphological features and viability of 3D-C and 3D-DyC aggregates generated at day 7 and day 21 of co-culture. It is appreciable by haematoxylin staining that only 3D-DyC constructs at day 21 displayed a noticeable cellular organization in three different cell layers: an outer region (arrows) surrounding the construct, an intermediate region with a trabecular-like structure and an inner region. Representative Calcein-AM fluorescence images of live cells and Propidium iodide (PI) fluorescence images of dead cells at day 21 of co-culture have been reported. Bars: 50 μm.

The functional properties of the cells within the aggregates were then investigated. As shown in Figure 2.3.5A, *3D-C* and *3D-DyC* conditions revealed substantial TRAP and CK positivity

demonstrating the presence of functional osteoclasts in the aggregates. For what concerns the osteoblastic cellular component (Figure 2.3.5B), *3D-C* aggregates clearly exhibited a low expression of OPN, OSX and Runx2 and a faint ARS staining compared to *3D-DyC* aggregates. Detailed analysis of *3D-DyC* conditions revealed that functionality of the hOBs grown in Xg seems to be better that those maintained in μXg. Xg condition induced a more solid cellular organization with numerous osteogenic markers positive areas than found in *3D-DyC* aggregates subjected to Modeled Microgravity. The presence of the hMCs in the culture is critical to the formation of a functional aggregate. In fact, a 3D-monoculture of hOBs alone failed to organize in a well-defined cellular aggregate as well as to deposit mineral matrix even in the most favorable condition (*3D-DyC Xg)* (Supplemental Figure 2.3.1).

Human primary osteoblasts from jawbone of patients taking BPs with or without MRONJ lesion (hnOBs)

After demonstrating the feasibility to produce a construct mimicking the bone microenvironment from a small number of cells, we investigated the possibility to apply the same approach with cells from anatomic critical conditions. In a first step, we investigated if a suitable, although low, number of osteoblasts could be obtained from jawbone of patients taking BPs (hnOBs). Bone chips were collected from 6 patients undergoing oral surgery for different reasons (see Table 2.3.1 for clinical parameters). Considering donors, they were all female subjects, as reflection of higher prevalence of BPs prescription in the female population as consequence of indications to BPs treatment for specific underling diseases (i.e. osteoporosis, breast cancer, multiple myeloma). Recently co-morbid conditions among cancer patients were inconsistently reported to be associated with an increased risk for MRONJ, include anemia and diabetes (*Ruggiero et al, 2014*). Considering anatomic factors, all samples were harvested from mandible, while one sample was harvested during MRONJ surgical treatment. Nowadays limited new information regarding anatomic risk factors for MRONJ is available. MRONJ is more likely to appear in the mandible (73%) than the maxilla (22.5%) but can appear in both jaws (4.5%) (*Ruggiero et al, 2014*).

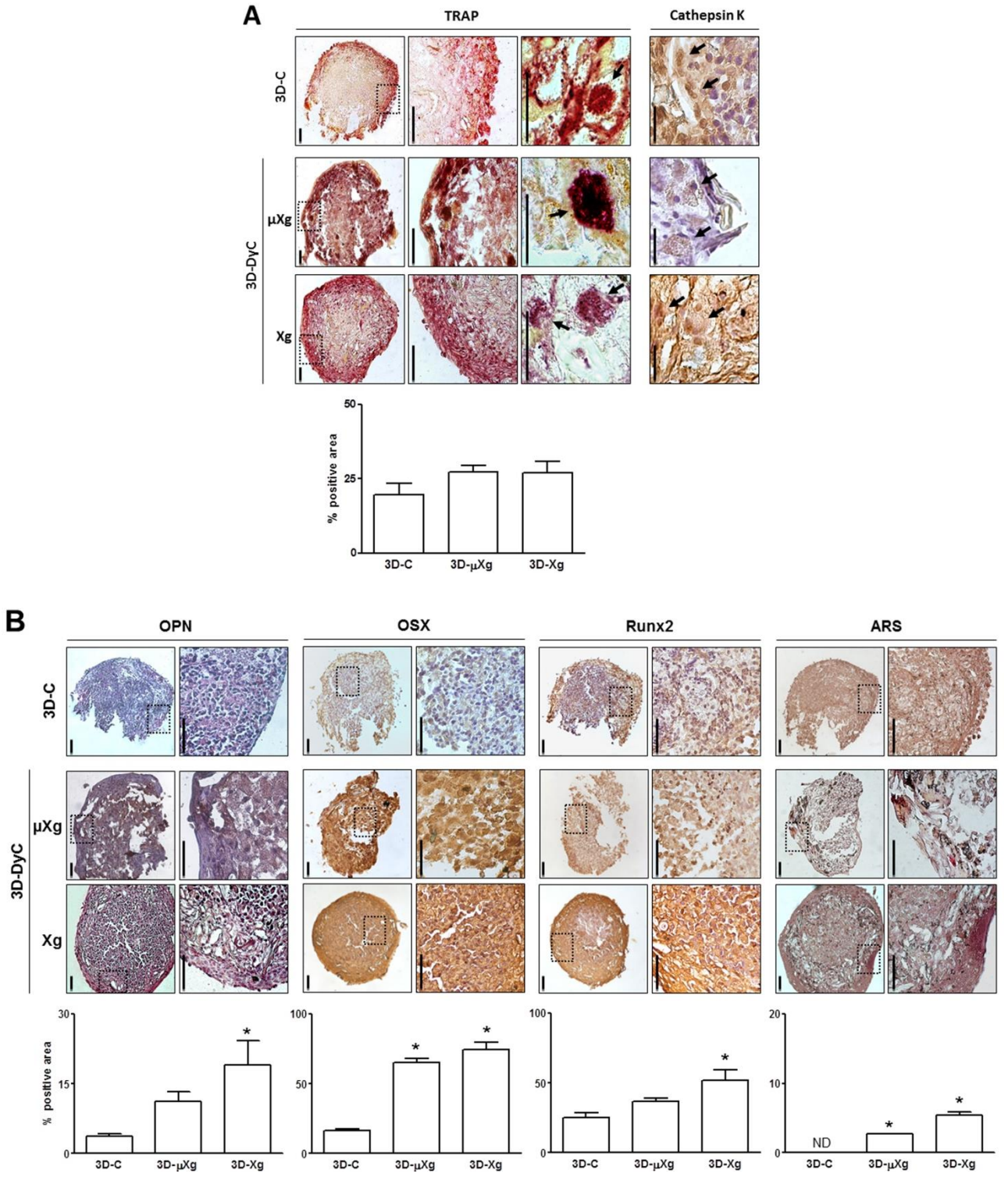

Figure 2.3.5: histochemical characterization of 3D-C and 3D-DyC aggregates, cultured under Modeled Microgravity (µXg) or Ground Based dynamic culture (Xg). (A) The aggregates were characterized to determine hOCs activity by TRAP assay and Cathepsin K. Higher magnification fields are indicated by the boxed areas and reported in the flanking columns. Bars: 50 µm. Multinucleated mature hOCs are arrowed. (B) The aggregates were characterized to determine hOBs activity by the analysis of OPN, OSX, Runx2 expression levels together with ARS staining. Higher magnification fields are indicated by the boxed areas and reported in the flanking columns. Bars: 50 µm. All microphotographs illustrate representative results of the different experimental conditions. The stainings were quantified by ImageJ software and expressed as % of positive area (mean value ± sem, 5 sections per sample, n=3). ND: not detectable. *$p<0.05$ vs 3D-C.

Table 2.3.1: clinical parameters of the patients included in the study

Sample	Age	Gender	BP	Treatment indication	Drug administration	Therapy duration	Co-morbidities	Indication for referral	Jaw	ONJ onset*	Cell attachment	Cell proliferation
1	73	F	ALN[a]	Osteoporosis	Oral	10 yrs	None	Surgical extraction	Mand[a]	None	+	-
2	80	F	ZOL[a]	Multiple myeloma	i.v.[a]	24 months	None	Surgical extraction	Mand[a]	None	+	Contaminated
3	70	F	ALN[a]	Osteoporosis	Oral	5 yrs	Takotsubo syndrome	Surgical extraction	Mand[a]	None	-	-
4	64	F	ALN[a]	Osteoporosis	Oral	5 yrs	Type I diabetes	Surgical extraction	Mand[a]	None	+	Contaminated
5	70	F	ZOL[a] CLO[a]	Multiple myeloma	i.v.[a] i.m.[a]	4 months 6 months	Osteoporosis Type I diabetes Former smoker	Surgical treatment for MRONJ	Mand[a]	Complete healing (within 2 months)	+	+
6	67	F	ALN[a]	Osteoporosis	Oral	7 yrs	Type I diabetes Smoker	Surgical extraction	Mand[a]	None	+	+

*within 12 months; [a]ALN= alendronate, ZOL = zoledronate, CLO = clodronate, i.v. = intravenous; i.m. = intramuscular, mand = mandible

Once harvested, bone chips were maintained in basal medium condition without adding growth factors for the time required (thirty days at least) so that the cells spread out and grow as small clusters until confluence is reached. We observed that these cells required a higher expansion time than hOBs. One out of six samples failed to give cells in culture. From the other five samples the cells spread out, attached to the plastic surface and assumed spindle-shape morphology. However, due to the peculiarity of the source, two samples encountered bacterial contamination, while another has not proliferated. Therefore, positive outcomes have been obtained from two samples (sample n. 5 and sample n. 6) which gave rise to proliferating and viable cells. These cells were recognizable as hnOBs since retained high OPN and Runx2 expression levels, as revealed by immunocytochemical analysis after (Figure 2.3.6A). Furthermore, the positive staining for extracellular calcium deposition at day 21 of culture in osteogenic medium demonstrated the functional ability of hnOBs to deposit mineral matrix. Despite the limitations related to the number and quality of the cells, we tried to combine these hnOBs from sample n. 5 and sample n. 6 with hMCs in the most favorable condition represented by *3D-DyC* in Xg. An appreciable aggregate consisting of viable cells were formed in both cases (Figure 2.3.6B). Therefore, despite starting from hnOBs of poor quality, these cells were able to interact with hMCs contributing to give rise to a substantial aggregate characterized by TRAP positive areas associated with osteoblasts expressing OPN and producing Alizarin Red stained small noduli.

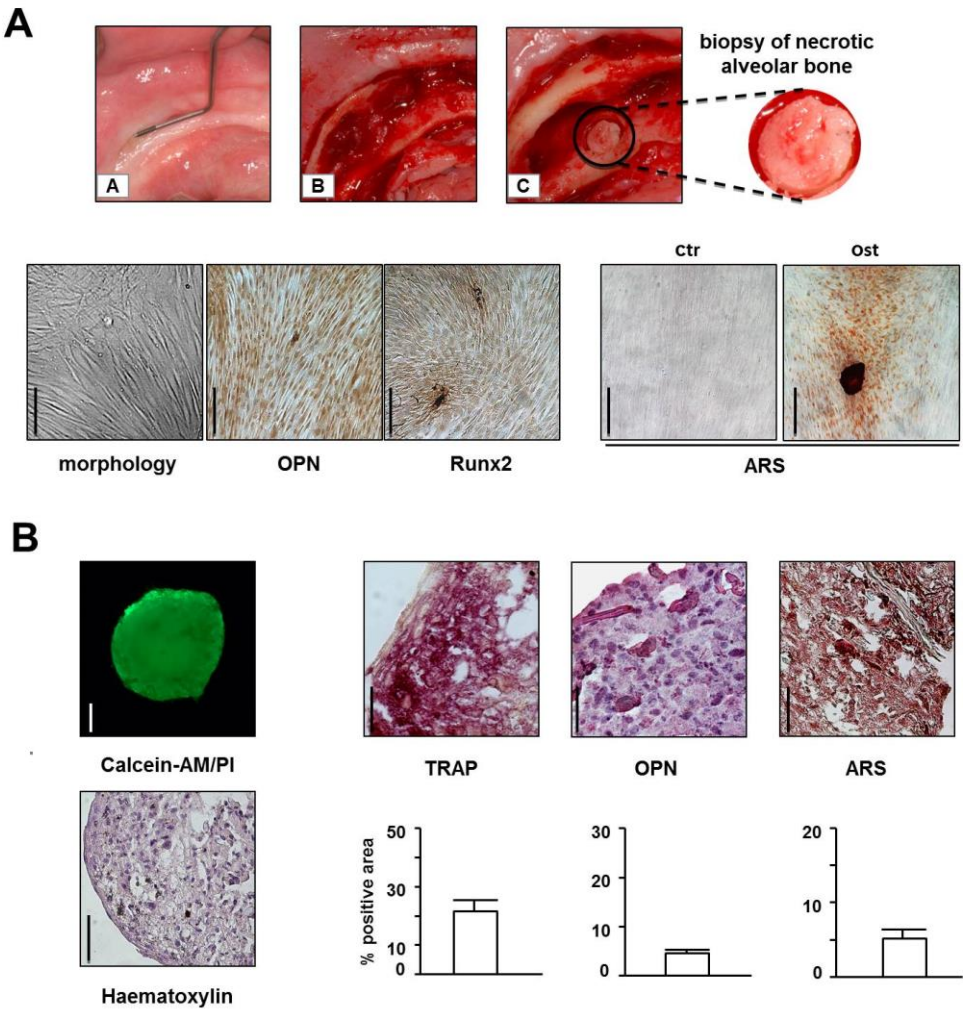

Figure 2.3.6: isolation and characterization of human primary osteoblasts obtained from alveolar bone samples of patients taking BPs (hnOBs). (A) Sample from patient with a potential diagnosis of MRONJ was harvested (abc) and characterized in term of cell morphology, expression of OPN and Runx2 by immunocytochemistry. hnOBs were also assayed for mineralization capacity by ARS staining after culture in osteogenic medium (ost) for 21 days (ctr = cells cultured in basal medium). (B) Viability and histochemical characterization of hnOBn/hMC 3D-DyC aggregates generated after 21 days in Xg condition (4rpm). Fluorescence photomicrograph is representative merged image and shows the presence of green fluorescence (Calcein-AM)-labelled live cells and the absence of red fluorescence (PI)-labelled dead cells. Analysis of the histological sections confirmed the presence of TRAP positive multinucleated osteoclasts. OPN positive staining localized the presence of functional osteoblasts. ARS staining is also reported. TRAP activity, ARS staining and OPN levels were quantified by ImageJ software and expressed as % of positive area (mean value ± sem, 5 sections per sample, n=2). Bars: 50 μm.

Discussion

To date, several *in vitro* experimental models have been proposed for basic research aimed to investigate bone diseases and bone repair. A great opportunity comes from 3D co-culture systems of different cells in combination with natural or synthetic scaffolds, generating cell-based constructs that potentially resemble the bone microenvironment *in vitro* (*Heinemann et al, 2013; Hayden et al,*

2014). To be easily handled and well characterized cell aggregates need to be formed by a substantial number of cells, and, for these reasons, most of the evidence from literature refers to human or murine cell lines (*Li et al, 2009a; Nishi et al, 2011*). As a consequence, while this approach may be useful to standardize and optimize culture conditions, it is hardly exportable to human primary cells. On the other hand, the use of cells obtained from the patient is an essential step towards a better elucidation of the pathogenetic mechanisms and the development of novel treatments inspired by the principle of "personalized medicine". In the present study, we aimed to establish an *in vitro* 3D hOBs/hOCs co-culture model requiring a minimal amount of cells, and therefore particularly suitable to apply to primary bone cells that cannot be obtained in a large amount, since harvested from compromised tissue areas such as from jawbone osteonecrotic specimens. In order to establish culture conditions that could be as close as possible to the *in vivo* microenvironment, we used a rotational culture bioreactor as a physiological stimulus to promote cell aggregation and interaction. Importantly, it has been shown that this strategy may be efficiently employed to induce the production of bone-like matrix in the cell aggregates (*Clarke et al, 2013*) without exogenous scaffolds the use of which may not always be desired since affecting cell metabolism and response to stimuli. The scaffold free system by us developed has the advantage to investigate and monitor the real endogenous properties of the cells. Therefore, besides being one step closer to the *in vivo* microenvironment, culture system here adopted facilitates a fine tuning of the biophysical, biochemical and biomechanical cues, while potentially allowing the monitoring of different parameters and the measurement of soluble factors. Notably, we showed that co-culturing hOBs and osteoclast progenitors (hMCs) in 3D dynamic flow condition (*3D-DyC*) using the RCCS bioreactor led to the formation of cell aggregates that preserved cell viability and exhibited a well-defined structure over the entire period of culture. On the contrary, 3D static condition (*3D-C*) is less favorable to produce cell aggregates with a well-defined matrix, confirming that the mechanical forces induced by rotational culture are important to promote and maintain the integrity and structure of cellular aggregates, mainly in Xg condition. In fact, the application of modeled gravity (μXg) seems to prevent the osteoblastic cellular component to reach those levels of differentiation showed by cellular aggregates cultured in Xg. This is supported by the expression levels of Osteopontin, Osterix, Runx2 as well as the production of bone mineral matrix at day 21 of culture. This interesting aspect deserves to be investigated in more detail with further experiments to determine the signaling pathways or bioactive molecules leading to the aforementioned phenomena. Regardless the level of osteoblastic maturation, the histochemical and functional analysis confirmed the presence of mature multinucleated hOCs in all the different 3D co-culture models analyzed, without the addition of osteoclastogenic inducers (M-CSF/RANKL). Cell aggregates formation

without the employment of external osteoclastogenic inducers is relevant since indicates the potency of osteoblastic cellular component and supports the hypothesis of a possible in vivo use of this system to prime endogenous repair phenomena and bone remodeling process in its entirety.

Therefore, as a whole these preliminary data demonstrate the feasibility to establish a 3D dynamic co-culture system keeping the viability and functionality of cellular component (hOBs and hMCs – hOCs) despite a few cells. This condition produced stable cell aggregates exhibiting active matrix remodeling and potentially implantable without scaffold. After these observations, we aimed to adopt the same conditions to recreate an *in vitro* "oral bone microenvironment" with hOBs from jawbone necrotic area. To the best of our knowledge, an experimental model with this specific purpose is still lacking. In this regards, one of the major challenges that must be overcome is the obtainment of vital and expandable cell populations from compromised tissues such as jawbone of patients taking BPs. For this reason, we tried to isolate osteoblasts from alveolar bone specimens of BPs treated patients, harvested from either boundary bone during surgical treatment of MRONJ lesion or during teeth extraction (hnOBs). Despite the extremely poor quality of the biological specimens, demonstrated by the relatively high incidence of sample contamination or insufficient cell growth (see Table 2.3.1), we showed that it is possible to obtain a sufficient number of primary hnOBs able to form an aggregate with hMCs. We hypothesize that optimization of the culture conditions could help to further improve the isolation of hnOBs from the bone chips, in terms of cell number and growth potential. Nevertheless, we confirmed by immunocytochemical analysis that hnOBs prior and after 3D co-culture condition maintain the properties of osteogenic lineage ability producing a typical bone matrix protein such as OPN and mineral matrix.

Our findings, together with previous reports, evidenced the need for deepened studies on local tissue primary cells from patients treated with antiresorptive agents, such as BPs, to determine each cell type specific role in MRONJ onset and development. Pathophysiology of MRONJ is still not fully understood and only few clinical studies have addressed the influence of antiresorptive agents on the cellular mechanisms involved in bone tissue healing/lack of healing in the human oral cavity (*Otto et al, 2012; Ruggiero et al, 2014*). Intravenous administration of a single dose of BPs leads on the other hand to rapid accumulation of drug in bone tissue, approximately 60% in 1 hour (*Lin et al, 1994*). Once incorporated into the bone, BPs are liberated again only when the bone is resorbed, ideally never again, due to the compromised bone turnover (*Lin, 1996*). Although length of exposure seems to be a very important risk factor for MRONJ development, early cases were reported also after few doses (*Bamias et al, 2005; Barasch et al, 2011*). Barasch and coworkers showed that the risk for development of MRONJ begins within 2 years of treatment, for both cancer

and noncancer patients, showing that even the less potent BPs are linked to MRONJ after a relatively brief treatment period (*Bamias et al, 2005*).

Considering clinical conditions of patients involved in this study, limitations are the small group of patients, different indications for treatment with antiresorptive agents, different ways of administration (oral and I.V.), and the fact that specimen were taken from different mandible sites during different surgical procedures. Another confounding factor is the large number of other medicines taken by such patients. Generally the risk for developing MRONJ after oral treatment has to be carefully considered for patients with osteoporosis or oncologic diseases and severely compromised tissues. However, although our results must be cautiously interpreted, they are suggestive of possible cell-based tissue engineering approach when associated with surgical procedures for treatment or prevention of MRONJ. To confirm our evidence, further studies with a large sample size are urgently needed even if it is reasonable to think that our data will eventually lead to the in vitro development of smart cell-based constructs with regenerative properties, and therefore potentially able to trigger and promote tissue repair once implanted in the site of the oral defect.

Conclusions

In conclusion, we demonstrated the feasibility of a 3D co-culture system with limited amounts of cells preserving viability and functionality of bone cellular components and generating bone-like aggregates also by using cells from jawbone compromised areas. The approach here described will allow to develop in the future a platform useful both to study the molecular mechanisms sustaining the osteonecrosis and test drugs potentially able to revert the aberrant phenotype of pathological OBs. Nonetheless, depending on the cell populations chosen for the co-culture system, such a tool could be exploited not only for diseases affecting the alveolar bone but also other tissues of the oral cavity, such as the jaw muscles or the temporomandibular joint.

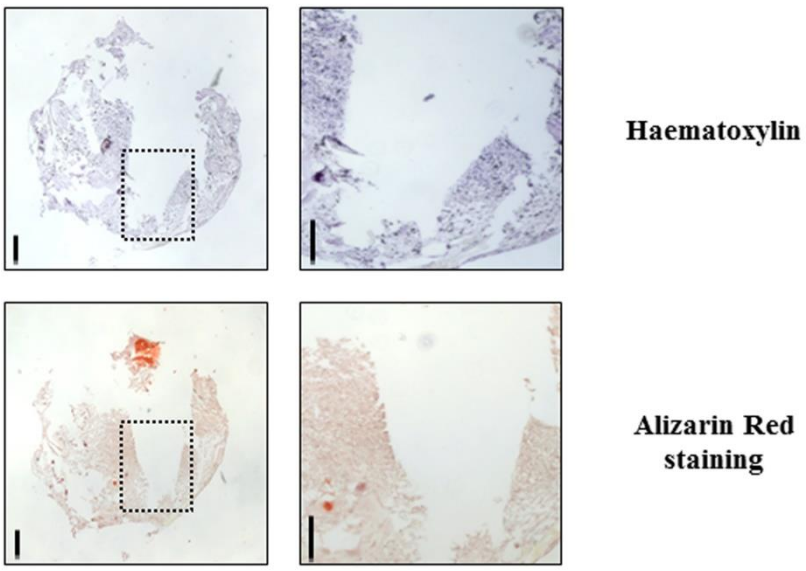

Supplemental Figure 2.3.1: after expansion in monolayer, 3x106 hOBs were trypsinized and inoculated in HARV culture vessels with the dynamic RCCS bioreactor in Ground Based dynamic culture (Xg, at 4 rpm). The observation of the smashed aggregates generated after 21 days in osteogenic medium revealed a poor cellular organization (haematoxylin) and a limited ability to mineral matrix deposition (ARS). Bars: 50 µm.

Chapter 2 – section 4

Collagen type 15 and the osteogenic status

Outline of the work

It is well known that the complex mixture of multiple components present in ECM can help either to maintain stemness or to promote differentiation of stromal cells following change of qualitative characteristics or concentrations. We have previously demonstrated that Collagen type XV (ColXV) is a novel bone extracellular matrix protein, but its role was still unexplored. For this reason we investigated the possible correlation between ColXV expression and mineral matrix deposition by hMSCs with different osteogenic potential and by osteoblasts that are able to grow in culture medium with or without calcium. Analyzing the osteogenic process we have shown that ColXV basal levels are lower in cells less prone to osteo-induction such as hMSCs from Wharton Jelly (hWJMSCs), compared to hMSCs that are prone to osteo-induction such as those from the bone marrow (hBMMSCs). In the group of samples identified as "mineralized MSCs", during successful osteogenic induction, ColXV protein continued to be detected at substantial levels until early stage of differentiation, but it significantly decreased, and then disappeared at the end of culture when the matrix formed was completely calcified. The possibility to grow hOBs in culture medium without calcium corroborated the results obtained with hMSCs demonstrating that calcium deposits organized in a calcified matrix, and not calcium "per se", negatively affected ColXV expression. As a whole our data suggest that ColXV may participate to ECM organization in the early phases of the osteogenic process, and that this is a prerequisite to promote the subsequent deposition of mineral matrix.

Introduction

Mesenchymal stromal cells can differentiate into cells of mesodermal lineages such as cartilage, bone, and adipose tissue (*Pittenger et al, 1999*). MSCs with different proliferation rate and differentiation potential can be isolated from various adult stem cell niches and extraembryonic tissues (*Kern et al, 2006; Hass et al, 2011; Pevsner-Fischer, 2011; Pozzobon et al, 2013*). The donor-related variability in MSCs differentiation potential has been well documented (*Wagner et al, 2009; Hass et al, 2011; Pevsner-Fischer, 2011; Zaim et al, 2012; Pozzobon et al, 2013; Mindaye et al, 2013; Billing et al, 2016*). This is a significant/problematic issue, because it can affect the interpretation of the data and limit the applicability and efficiency of cell-based therapeutic approaches. Recently, a particular attention has been given to the identification of predictive markers for selecting MSCs with high differentiation potential and other desirable characteristics that would allow to obtain useful information for a therapeutic success (*Sotiropoulou et al, 2006; Phinney, 2012; Pozzobon et al, 2013; Bianco et al, 2013; Squillaro et al, 2016*). This is an important issue in the field of bone regenerative medicine concerning the production of tissue-engineered constructs (*Meijer et al, 2007; Siddappa et al, 2007a; Siddappa et al, 2007b; Mentink et al, 2013; Davies et al, 2015*). Osteogenic differentiation is a complex, tightly regulated process that is critical for proper bone formation during development and repair processes (*Komori, 2006; Chen et al, 2016*). As MSCs pass through a temporal sequence of events towards differentiation, they lose their proliferative capacity, acquire the ability to respond to osteogenic stimuli, and become committed to osteoblast lineage. They also support nascent osteoblast environment by extracellular matrix maturation and mineralization under a stringent control that is only partially understood (*Watt and Huck, 2013*). At the same time, MSCs must keep their ability to respond to the need of bone physiological remodeling. This condition is supported by ECM which is one of the major determinants of the structural integrity and functional properties of a stem cell niche, providing specific signals through different kind of molecular interactions with the cell surface. It is in fact widely understood that changes in ECM composition exert powerful control over many cellular phenomena, including stem cell differentiation and tissue remodeling (*Scadden, 2006; Khatiwala et al, 2009; Watt and Huck, 2013*). We are interested in studying still little investigated bone ECM components, in order to understand their possible participation to osteogenic differentiation and their potential role in sustaining bone repair. In this context, there is still much to understand about the role of certain collagens present in the matrix, their interactions with partner molecules or binding to specific receptors. Non-fibrillar collagen (Col) XV is a chondroitin sulphate modified glycoprotein belonging to the multiplexin subfamily (multiple triple helix domains with interruptions) (*Myers et al, 1996*). Its expression is associated with vascular, neuronal,

mesenchymal and some epithelial Basement Membrane (BM) in many tissues, indicating a probable function in the adhesion between BM and the underlying connective tissue stroma (*Myers et al, 1996, Amenta et al, 2005*). Its precise functions remain to be fully elucidated, even if evidence so far suggests that ColXV is involved in more sophisticated roles than just the molecular architecture of BM, particularly in the context of ECM organization and degradation (*Rasi et al, 2010; Clementz and Harris, 2013; Guillon et al, 2016*). By gene array profile and immunohistological analysis we have previously identified ColXV as a novel human osteoblast matrix protein (*Lisignoli et al, 2009*), and our interest is now to investigate a possible involvement of this type of collagen in triggering bone intracellular signaling pathways and regulating osteogenic cell growth and differentiation. In the present study we have investigated the impact of the presence of ColXV on mineral matrix deposition by hMSCs with different osteogenic potential and on hOBs.

Material and methods

Cell culture

hMSCs were isolated from two sources, human bone marrow (hBMMSC) and Wharton's jelly of umbilical cords (hWJMSC). hBMMSCs were obtained, as previously reported (*Lisignoli et al, 2014*), from bone marrow aspirates harvested by the iliac crest, after obtaining the patients' informed consent and the approval of the Istituto Ortopedico Rizzoli Ethics Committee. hWJMSCs were isolated from human umbilical cords collected after the mothers' informed consent and the approval of the University of Ferrara and S. Anna Hospital Ethics Committee; samples were processed within 4 hours, as already reported (Torreggiani et al, 2012). Considering that osteogenic potential of hWJMSCs is usually related to the obstetric parameters (*Penolazzi et al, 2009*), samples homogeneous for duration of the pregnancy (≥ 38 weeks) and birth weight (≥ 3.00 Kg) were chosen. At subconfluence, cells were trypsinized and expanded or used immediately for in vitro experiments.

Flow cytometry analysis was performed on hBMMSC and hWJMSCs (at passage 1), fixed in 4% paraformaldehyde and incubated at 4°C for 30 min, with 5 μg/mL of the following monoclonal antibodies: anti-human –CD34, –CD45 (DAKO Cytomation, Glostrup, Denmark), –CD31 (Chemicon International, Temecula, CA), –CD73, –CD90, –CD146 (Becton Dickinson, Mountaine View, CA, USA), –CD105 (produced from the hybridoma cell line, clone SH2; ATCC, Rochville, MD, USA), –Runx2 (R&D System, Minneapolis, MN, USA), –alkaline phosphatase (ALP, Developmental Studies Hybridoma Bank, Iowa City, IA, USA), –osteocalcin (OC, R&D System), –

bone sialoprotein (BSP, Immunodiagnostik, Bensheim, Germany), –Collagen type 1 (Coll.1, Millipore, Temecula, CA, USA). Cells were washed twice and incubated with 2.4 μg/mL of a polyclonal rabbit anti-mouse (DAKO Cytomation) or goat anti-rat (AbD Serotec, Oxford, UK) immunoglobulins/FITC conjugate antibody at 4°C for 30 min. After two final washes, cells were analyzed using a FACStar plus Cytometer (Becton Dickinson). For isotype control, FITC-coupled non-specific mouse IgG was used instead of the primary antibody. Data were expressed as mean percentage of positive cells.

hWJMSC and hBMMSC were induced to osteogenic differentiation in DMEM high glucose (Euroclone S.p.A.) supplemented with 10% FCS (Euroclone S.p.A., Milan, Italy), 100 mM ascorbic acid, 0.1 mM dexamethasone, and 10 mM β-glycerol phosphate (Sigma–Aldrich, St. Louis, MO). For ARS staining, samples were fixed in ethanol 70%, stained with 40 mM, pH 4.2 Alizarin Red-S solution (Sigma–Aldrich), for 10 min at RT, rinsed in distilled water and washed in PBS on an orbital shaker at 40 rpm, to reduce nonspecific binding.

Human osteoblasts were isolated from trabecular bone chips and grown in DMEM/F12K (Gibco, Invitrogen Corporation, Indianapolis, IN) without calcium supplementation with antibiotics, 25 μg/mL ascorbic acid, 4mM glutamine (Sigma-Aldrich) with or without 0.5, 1.3 and 2.6 mM extracellular $CaCl_2$, as previously reported (*Gabusi et al, 2012*).

Western blotting

For western blot analysis, cells were washed twice with ice-cold PBS and cell lysates were prepared as previously reported (*Torreggiani et al, 2012*). For the processing of the media fractions, non-induced or osteogenic induced cells (≥90% confluence) were starved in 0.1% FCS for 72 h before collection. Medium was clarified for 10 min at 4000 rpm and concentrated up to 50 fold by using Amicon Ultra-15, 100 KDa (Millipore, Billerica, MA). The chondroitinase ABC digestions were performed for 90 min at 37°C using 20 mU of enzyme as previously reported (*Li et al, 2000*). 30 μg of each sample were electrophoresed on a 5-12% SDS polyacrylamide gel. Proteins were then transferred onto an Immobilon-P PVDF membrane (Millipore, Billerica, MA). After blocking with TBS-0.1 % Tween-20 and 5% nonfat dried milk, the membrane was probed with goat anti-human collagen type 15 (ColXV) (1:200, clone C-20, Santa Cruz, CA), rabbit anti-human Runx2 antibody (1:1000, clone M-70, Santa Cruz, CA) washed, and incubated with peroxidase conjugated anti-goat or anti rabbit secondary antibody (Dako, Glostrup, Denmark) in 5% nonfat dried milk. Immunocomplexes were detected using Immobilon Western Chemiluminescent HRP Substrate

(Merck-Millipore, Darmstadt, Germany). GAPDH, Actin or IP3K were used to confirm equal protein loading. Densitometric analysis was performed by ImageJ software (NIH, USA, public domain available at: http://rsb.info.nih.gov/nih-image/). RNA extraction and qRT-PCR Total RNA was extracted using the RNeasy Plus Micro Kit (Qiagen, Hilden, Germany), according to the manufacturer's instructions. Briefly, cDNA was synthesized from total RNA (500 ng) in a 20 μL reaction volume using the TaqMan High Capacity cDNA Reverse Transcription kit (Thermofisher) as previously described (*Lisignoli et al, 2014*). Quantitative real-time PCR was performed using gene expression master mix (Thermofisher) and analyzed on CFX96 Real-Time detection System (Bio-Rad laboratories, Hercules, CA, USA). Assays-On-Demand kits (Life Technologies) for human COLXV and Runx2 were used. The expression level of cDNA samples was normalized to the expression of GAPDH, used as reference, with the formula $2^{-\Delta Ct}$. All reactions were performed in triplicate and the experiments were repeated at least three times.

Statistical analysis

The normal distribution of data was verified using the Kolmogorov-Smirnov test. In the case of single comparison, statistical significance was determined by unpaired Student's t-test for normally distributed data and Mann-Whitney test for non-normally distributed data. In the case of multiple comparisons, statistical significance was analyzed by one-way analysis of variance (ANOVA) and Bonferroni post hoc test. Differences were considered statistically significant for p-values ≤ 0.05.

Results and discussion

Collagen type XV and osteogenic potential of hMSCs

51 samples of hBMMSCs and 65 samples of hWJMSCs were evaluated. Cells were characterized by using conventional flow cytometric analysis with CD34, CD45, CD73, CD90, CD105, CD146 antibodies. Moreover, for each sample the percentage of Runx2, ALP, OC, BSP and Collagen type 1 positive cells was also investigated. As reported in the Supplemental Figure 2.4.1, all samples analyzed showed a comparable phenotype except CD146, ALP and Collagen type 1 which were expressed at significantly lower levels in the hWJMSCs compared to hBMMSCs. We had previously found that osteogenically differentiated hBMMSCs and hWJMSCs showed a comparable increase of typical osteogenic markers such as Runx2, BSP, OC and Collagen type 1 (*Manferdini et al, 2011; Torreggiani et al, 2012*).

However, when the functional *in vitro* endpoint reflecting advanced cell differentiation and osteogenic potential was assessed in terms of ECM mineralization, substantial differences between the various samples cultured in osteogenic medium were observed. Alizarin red staining (ARS) was used to evaluate the secreted mineralized matrix and showed differences among samples. We found samples creating a mineralizing microenvironment after 21-28 days, which we called ARS positive samples (ARS+) and samples that after 28 days were still not able to secrete mineralized matrix, which we called ARS negative samples (ARS-) (Figure 2.4.1A). These experiments demonstrated a higher percentage of ARS+ samples in hBMMSCs (82.35%) compared to hWJMSCs (57.15%) (Figure 2.4.1B).

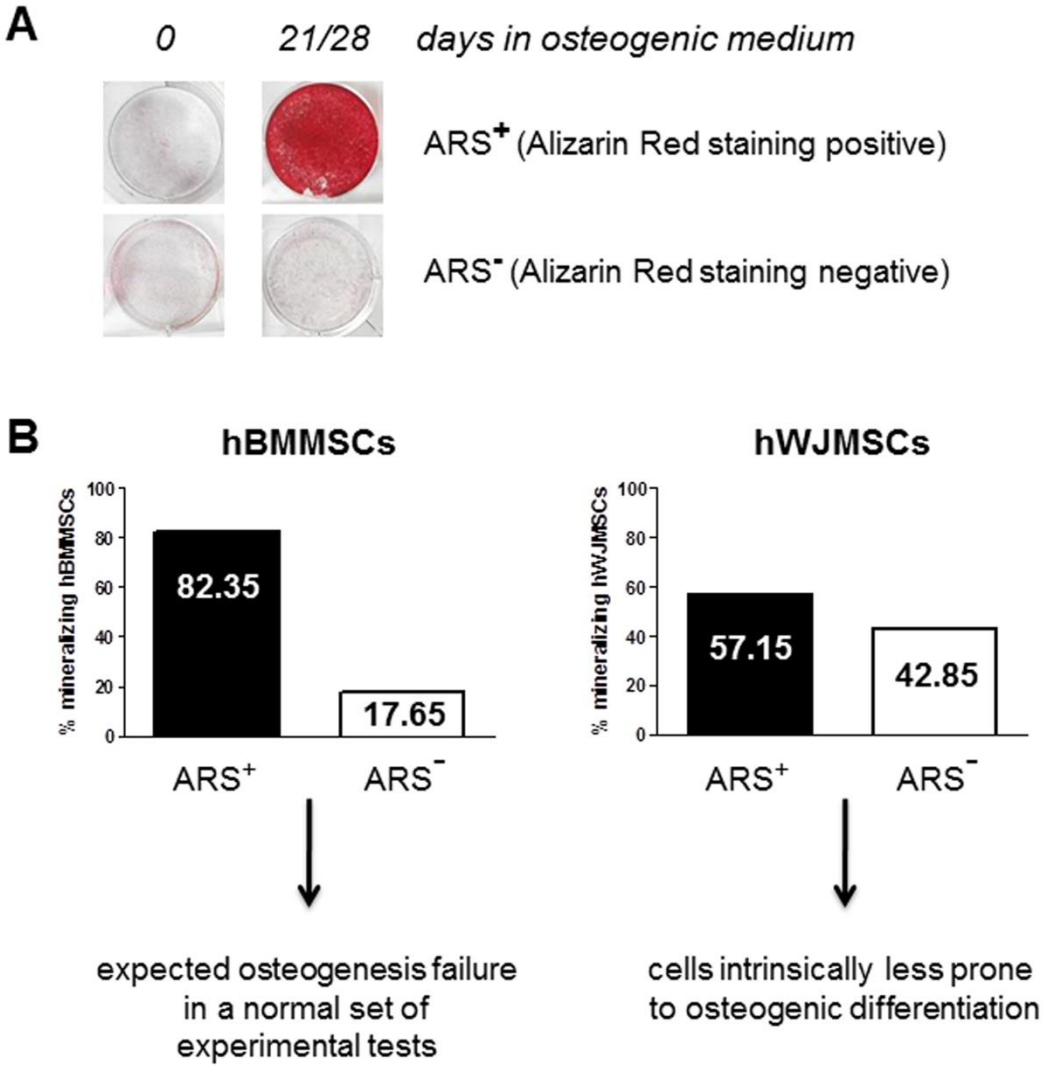

Figure 2.4.1: secreted mineralized matrix by hMSCs. (A) hMSCs from bone marrow (hBMMSCs, N=51) and from Wharton's jelly of umbilical cord (hWJMSCs, N=65) were cultured for 21-28 days in osteogenic medium and analyzed for their ability to secrete mineralized matrix by Alizarin Red staining (ARS). Samples were defined ARS+ when they reached a red peak staining at 21-28 days of culture, or ARS- when they remained unstained. (B) Graphical representation of the percentage of mineralizing hBMMSCs and hWJMSCs samples that were ARS+ or ARS- .

These observations are not a new concept since various evidences in literature highlighted interindividual and source-dependent differences in the osteogenic potential of MSCs (*Phinney et al, 1999; Siddappa et al, 2007a; Phinney, 2012; Heo et al, 2016*). Therefore, it is reasonable to assume that hWJMSCs are intrinsically less prone to osteogenic differentiation compared to hBMMSCs for which the unsatisfactory results for mineralized ECM deposition may be ascribed to a normal variability in primary culture setting. In order to understand which elements and molecular mechanisms can contribute to the inability of the cells to develop mineralized matrix, it may be useful to identify new functional roles of specific molecules. It is known that when cells are unable to reach mineralization, ECM is disorganized, and this probably represents a restriction point for cell maturation. In this scenario we focused on ColXV to understand if it had a role in guiding the fate of MSCs and the mineral nodule formation. A first evidence for this hypothesis came from the analysis of ColXV basal levels which are significantly lower, both at mRNA and protein level, in cells less prone to osteo-induction such as hWJMSCs, than in cells which are prone to osteo-induction such as hBMMSCs (Figure 2.4.2A). The expression of ColXV protein evaluated by Western blot of cell extracts corresponded to a band of the expected size (250-kDa) for the α1(XV) core protein (*Li et al, 2000*).

To evaluate a possible correlation between the level of expression of ColXV and the ability of the cells to secrete mineralized matrix, we grouped together all hMSCs samples independently from their source (hBM or hWJ). Samples were then divided in two groups: mineralized ARS+ samples (Min group) and non-mineralized ARS- samples (Non Min group) (Figure 2.4.2B). We found that ColXV mRNA levels remained substantially unchanged between the two groups (Min versus Non Min group) while α1(XV) core protein level was significantly higher in the Min versus the Non Min group (Figure 2.4.2C), highlithing that mRNA does not correlate with the same changes at protein level. This gave us the opportunity to make the following important observation. When we considered each case individually, we found an appreciable amount of the α1(XV) core protein also in samples with very low or scarcely measurable levels of mRNA (Supplemental Figure 2.4.2A and B, see samples n. 6, 7). Likewise, the sample with the higher level of mRNA (sample n. 4) is not the one with the highest protein content. This approach, based on the parallel evaluation of ColXV at mRNA and protein level, allows to reduce false positive or negative samples and increases the possibility of finding a functional correlation between the expression of a putative marker, such as ColXV, and a specific osteo-phenotype. Therefore, we confirmed that mRNA levels cannot be used as surrogates for corresponding protein levels without protein evaluation (*Vogel and Marcotte, 2012; Clarke et al, 2012*). In particular, we showed that the more informative analysis for the expression of matrix proteins is once again represented by investigation of their protein level. We

also tested Runx2 expression since it has been shown that MSCs with higher basal level of mRNA for this factor have higher osteogenic differentiation ability (*Loebel et al, 2015*). We found that both Min and Non Min samples did not show a correlation between basal level of Runx2 expression and osteogenic potential of the cells (Supplemental Figure 2.4.2B and C). Moreover, Runx2 expression did not follow the same trend of ColXV expression. These evidences confirm the importance of considering different parameters simultaneously in order to have a reliable prediction of the osteogenic potential (*Murgia et al, 2016*).Interestingly, we have not found any ColXV negative hMSC sample. Considering that ECM components including proteoglycans are often directly or indirectly involved in the regulation of the cell fate (*Bi et al, 2005*), our evidence supports the view that ColXV may contribute to the retention of features of a stromal cell phenotype by hMSCs.

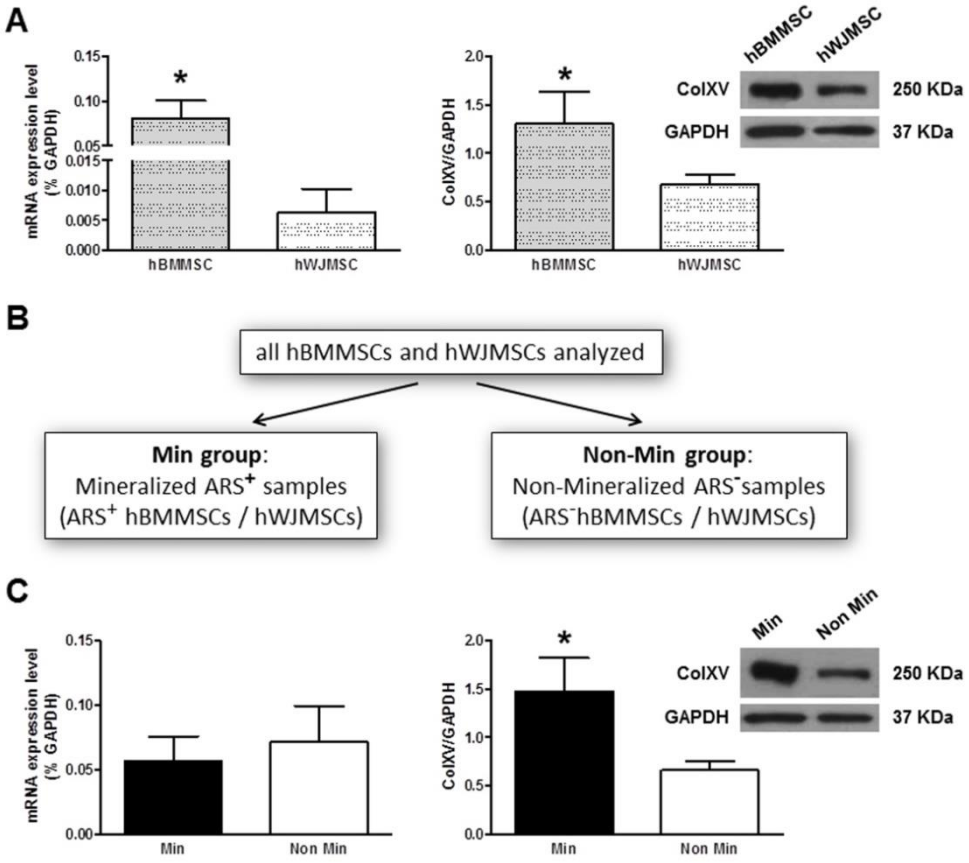

Figure 2.4.2: analysis of ColXV basal levels performed by qRT-PCR and Western blot. (A) ColXV evaluation in hBMMSCs and hWJMSCs at mRNA and protein level. mRNA data were expressed as % of the housekeeping gene GAPDH, Western blot data were expressed as ColXV/GAPDH ratio. Representative Western blots are reported with densitometric analysis of all samples analyzed. (B, C) ColXV expression was evaluated in the Min group (mineralized ARS+ hBMMSCs / hWJMSCs) and in the Non Min group (non mineralized ARS- hBMMSCs / hWJMSCs). mRNA data were expressed as % of the housekeeping gene GAPDH, Western blot data were expressed as ColXV/GAPDH ratio. Representative Western blots are reported with densitometric analysis of all samples analyzed. Statistical analysis was performed comparing hBMMSCs versus hWJMSCs, or Min versus Non Min groups. *$p \leq 0.05$ was considered statistically significant.

Collagen type XV expression and mineral matrix deposition

We also monitored the expression of ColXV during the osteogenic induction of hMSCs to verify a possible relationship with the extent of deposition of mineralized matrix in hMSCs from the Min group. Considering the heterogeneity of hMSC cultures and donor variability, it is not surprising that even within the Min group there is some difference in the degree of mineralization, as it is highlighted by a different ARS intensity. By comparing the level of mineralization by ARS and the expression of ColXV by Western blot on the same sample at different culture time points, we clearly evidenced that the α1(XV) core protein was maintained at levels comparable to baseline, until the early stage of differentiation (Figure 2.4.3A), and it significantly decreased and finally disappeared in samples reaching a high degree of mineralization (Figure 2.4.3B). The baseline expression of ColXV has also been detected in the medium fraction from hMSCs cultured in presence of 0.1% FCS after chondroitinase digestion. This confirmed that ColXV is present as chondroitin sulfate proteoglycan functional molecule in ECM following secretion (*Li et al, 2000*) (see "Material and Methods" and the insert in Figure 2.4.3). We could not perform Western blot analysis of medium fraction during the 4-weeks of osteodifferentiation as it precluded the use of serum-low culture conditions. Therefore, to evaluate ColXV expression we have to rely on core protein signal from cell extracts.

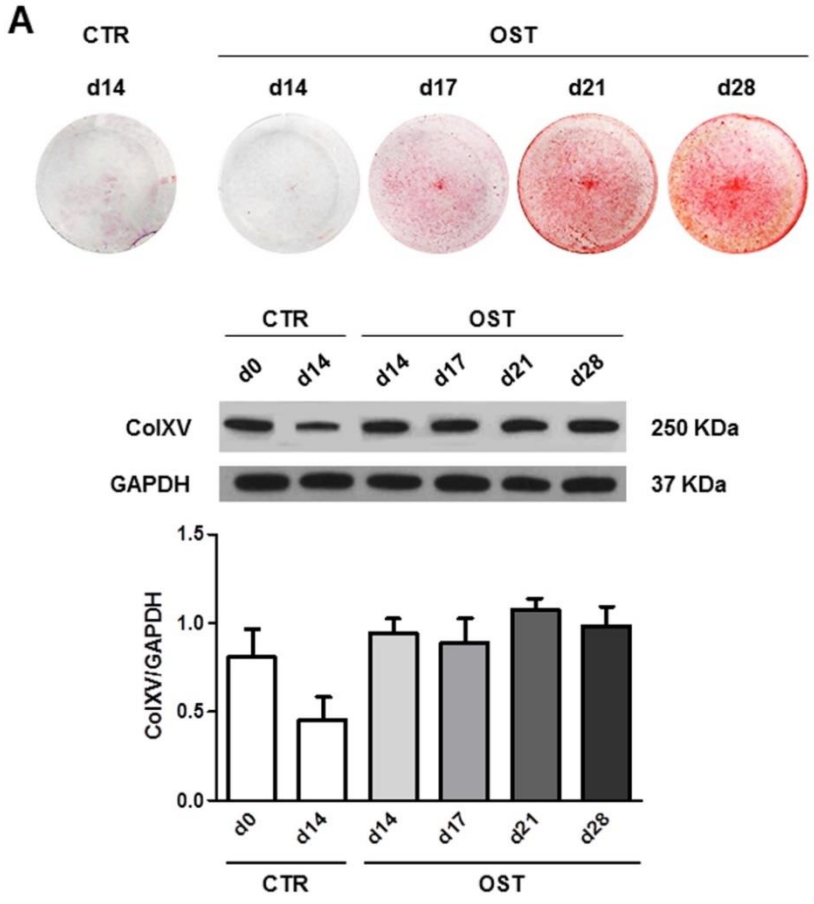

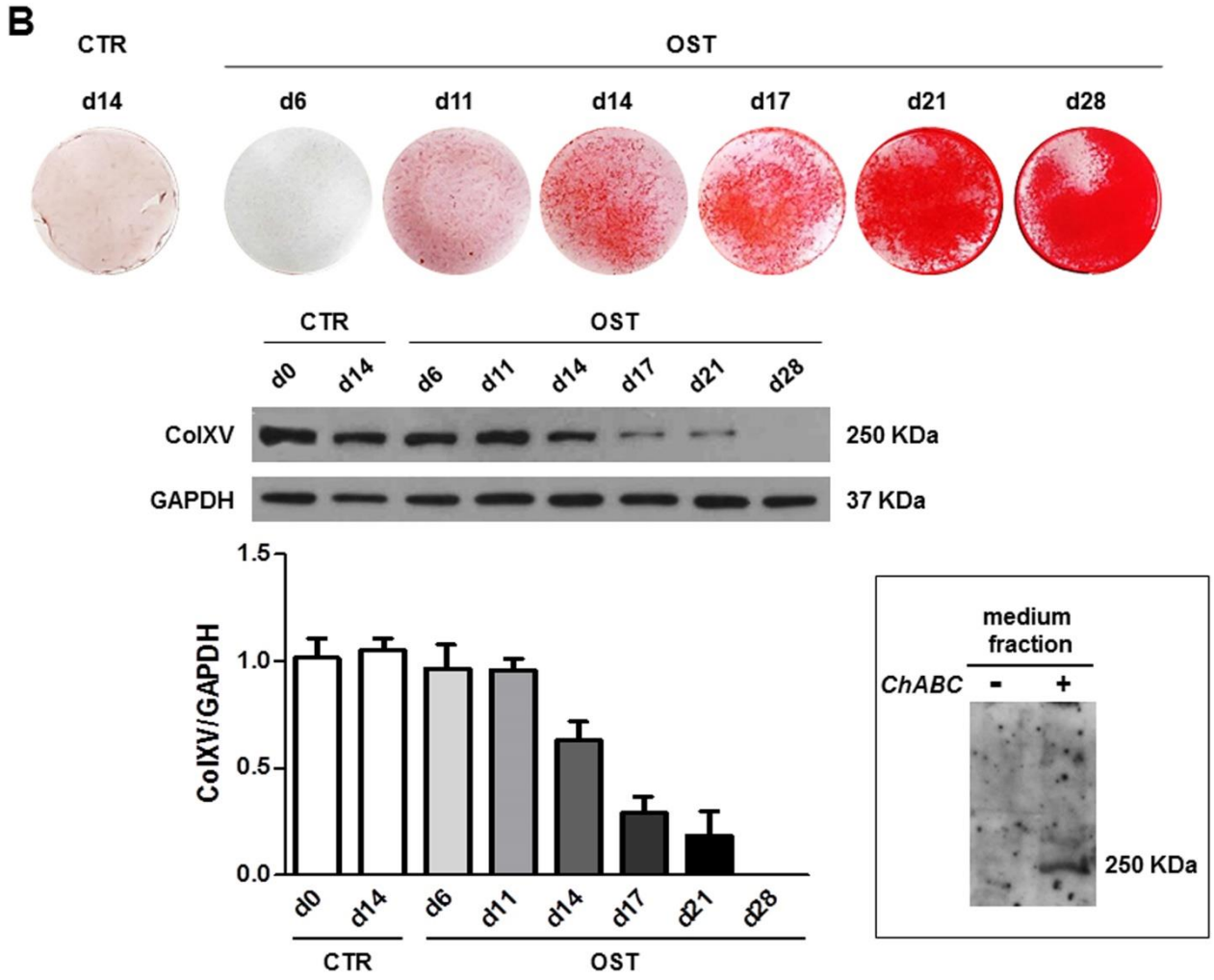

Figure 2.4.3: ColXV expression during osteogenic induction of hMSCs from Min group. The expression of ColXV was monitored at protein level during osteogenic induction (OST) at different time points until day 28 of culture, and compared to the corresponding matrix mineralization status. The analysis of two Min representative samples with different degree of mineralization has been reported. The α1(XV) core protein expression was maintained stable in osteodifferentiated hMSCs which did not reach a high degree of mineralization (A), while it significantly decreased when a mineralization was reached by a different sample (B). The densitometric analysis of each Western blot is reported and data were expressed as ColXV/GAPDH ratio. CTR, control hMSCs from the same sample but not subjected to osteogenic induction. In the insert, the evaluation of ColXV expression in the medium fraction has been reported. Medium from hMSCs cultured for 72h in presence of 0.1% FCS was processed and electrophoresed on a 5% SDS-polyacrylamide gel after incubation with (+) or without (-) chondroitinase ABC (ChABC).

These evidences suggest that ColXV might act as an ECM organizer in the early phases of the osteogenic process, and that this should be a prerequisite to promote the subsequent deposition of mineral matrix. At the end of in vitro osteogenic differentiation when the microenvironment is completely calcified, α1(XV) core protein disappeared. These data, together with our previous immunohistological analysis (*Lisignoli et al, 2009*) support the hypothesis that ColXV expression

must be downmodulated in presence of high amounts of extracellular calcium deposits in the mineralized matrix. In fact, as we previously demonstrated in bone tissue biopsies, ColXV was positive on osteoblasts lining bone trabeculae and negative on osteocytes (*Lisignoli et al, 2009*). Moreover, this hypothesis is also supported by our previous data on human osteoblasts (hOBs) isolated directly from bone chips. These cells, when chronically stimulated with different calcium concentrations, showed a significant increase of osteocalcin-osteogenic marker and extracellular matrix mineralization, whereas ColXV mRNA was down-modulated (*Gabusi et al, 2012*). We also confirmed these data at protein level by Western blot analysis (Figure 2.4.4A) on hOBs after exposure to increasing concentrations of extracellular CaCl2 (0.5, 1.3, and 2.6 mM). Moreover, we took advantage of the ability of hOBs to grow in culture medium with or without calcium to better understand the influence of calcium on ColXV. As shown in Figure 2.4.4B, we found that hOBs cultured in medium without calcium expressed high amounts of ColXV both at mRNA and protein level compared to hOBs obtained in the same manner but grown in conventional culture medium containing calcium.

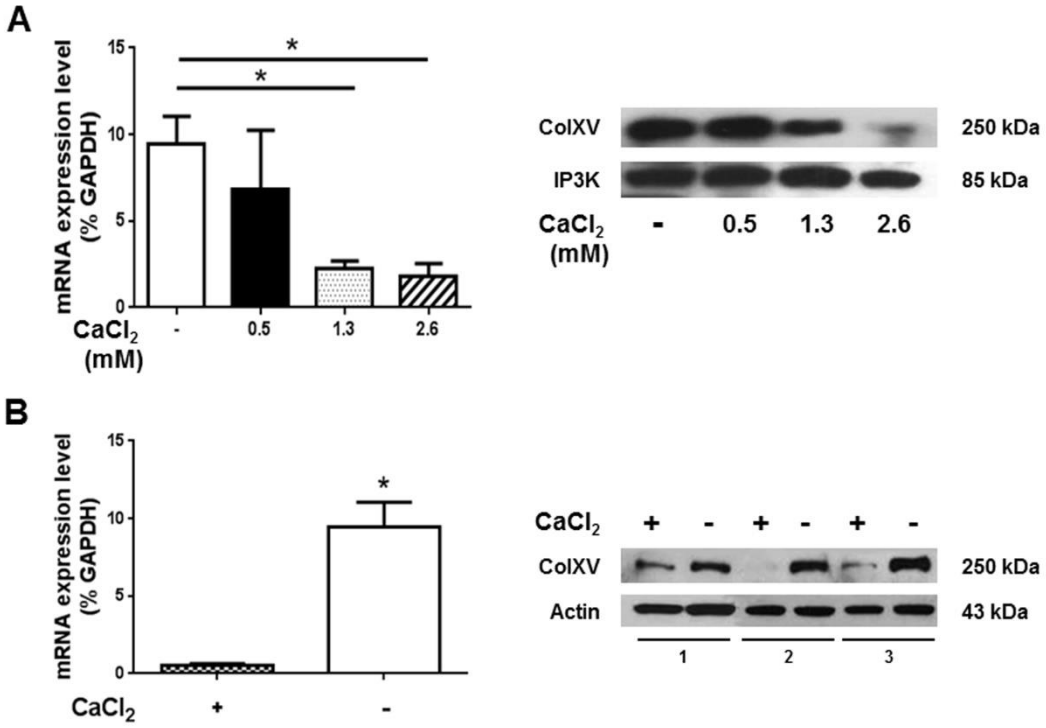

Figure 2.4.4: ColXV expression in osteoblasts. The analysis was performed by qRT-PCR and Western blot in hOBs isolated and exposed to increasing concentrations of extracellular CaCl2 (0.5, 1.3, and 2.6 mM) for 48 h (A) or chronically maintained in calcium-containing (1.3 mM) (+) or calcium-free (-) medium for 7 days (B). Statistical analysis was performed in calcium-free versus calcium containing medium condition. *$p \leq 0.05$ was considered statistically significant.

By contrast, hMSCs showed a different scenario. The inability of hMSCs to proliferate and differentiate in culture medium without calcium has been in fact established (*Neuhuber et al, 2008*). This indicates that the presence of calcium is "per se" essential to allow hMSCs to grow and move towards the osteogenic lineage, but it has no influence on the expression of ColXV and the osteogenic potential of hMSCs. In fact, we demonstrated that hMSCs grown in the same culture medium have different ColXV levels and exhibit different performance in terms of ability to deposit mineral matrix (see Figure 2.4.2 and Supplemental Figure 2.4.2). Conversely, when calcium deposits in the extracellular calcified matrix were abundantly produced by mature cells (terminally osteo-differentiated MSCs, Figure 2.4.3B, or OBs (*Gabusi et al, 2012*), Figure 2.4.4) we observed a substantial decrease of α1(XV) core protein expression.

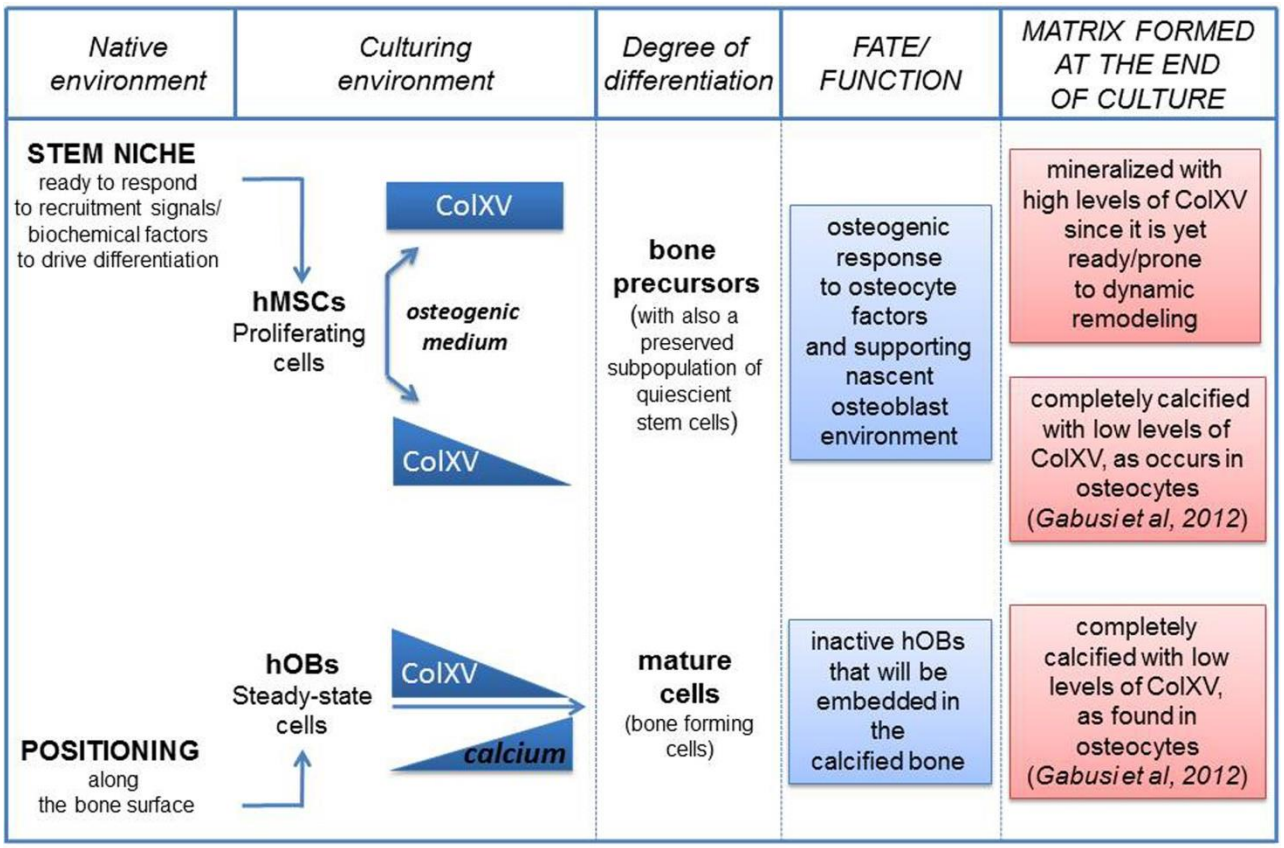

Figure 2.4.5: schematic representation of a possible correlation between ColXV expression levels and mineral matrix deposition in hMSCs with different status of maturation and in hOBs that are able to grow in culture medium with or without calcium. Nearly constant expression of ColXV in those hMSCs which osteodifferentiated but did not produce a completely calcified matrix could be useful to keep cells in a prone and responsive state to osteogenic differentiation stimuli, allowing bone remodeling or regeneration. Conversely, cells at the end of differentiation, such as osteoblasts or completely osteo-differentiated hMSCs, are present in a completely calcified extracellular matrix with low or undetectable levels of ColXV.

In Figure 2.4.5, we summarized in a cartoon our hypothesis on the degree of mineralization associated to ColXV expression, evidencing a peculiar fate of MSCs and OBs in favoring dynamic bone remodeling or in maintaining mature cell in calcified bone areas. In particular, we believe that the nearly constant levels of ColXV during the osteogenic process could be useful to keep the hMSCs prone to dynamic remodeling and capable of responding to those signals supporting nascent osteoblast environment or repair of a damage. It is in fact well established that the complex mixture of multiple components present in ECM helps maintaining MSCs stemness in the MSC niche or to promote differentiation following changes of qualitative characteristics or concentrations (*Kolf et al, 2007; Lai et al, 2010; Birmingham et al, 2012; Watt and Huck, 2013*).

On the basis of our preliminary data, it will be interesting to understand how ColXV interacts with the extracellular environment, in particular, whether ColXV is a key accessory protein involved in cell-extracellular matrix interactions, or a crucial component directly involved in MSCs or OBs behavior. Moreover, it will be interesting to explore how ColXV can affect intracellular signaling in response to differentiation signals, injury, physiological bone remodeling and development, and proper mineralization process initiated as an intracellular event. It is known that collagens and their bioactive fragments (released by proteolytic cleavage) play critical functional roles in many physiological and pathological processes such as development, angiogenesis, tissue repair, tumor growth and metastasis (*Ricard-Blum and Ballut, 2011*), supporting the hypothesis that ColXV is a multifunctional collagen-proteoglycan with characteristics different from what originally believed. Therefore, further studies are needed to understand which signals control the expression of ColXV and the production of its proteolytically processed C-terminal fragment that functions as an endostatin by inhibiting endothelial cell migration and angiogenesis (Ramchandran et al, 1999).

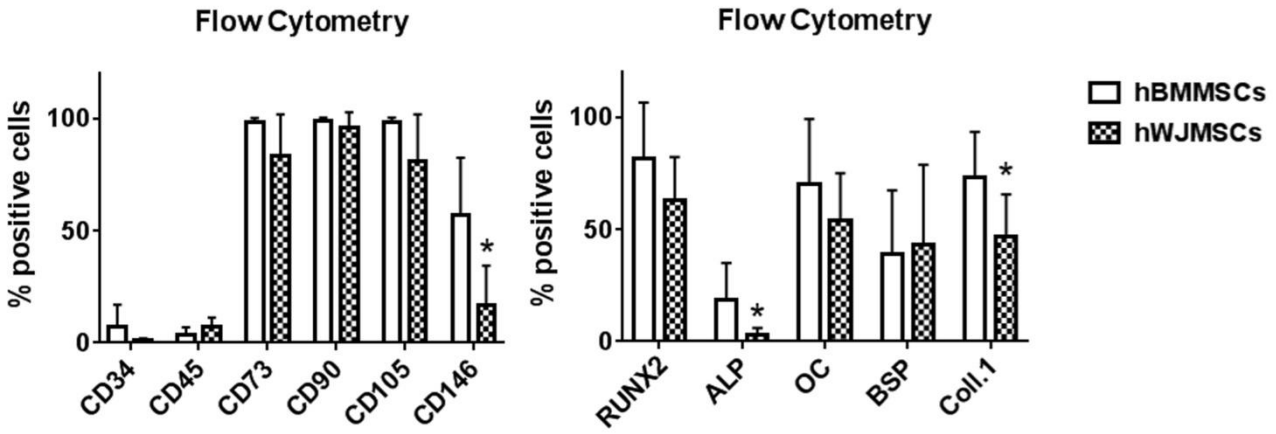

Supplemental Figure 2.4.1: hBMMSCs and hWJMSCs were characterized by flow cytometry for the expression of mesenchymal markers (CD73, CD90, CD105, CD146), hematopoietic markers (CD34, CD45) and typical osteogenic markers (Runx2, ALP, OC, BSP and Coll.1). The percentage of positive cells for each indicated protein is reported in the graphs.

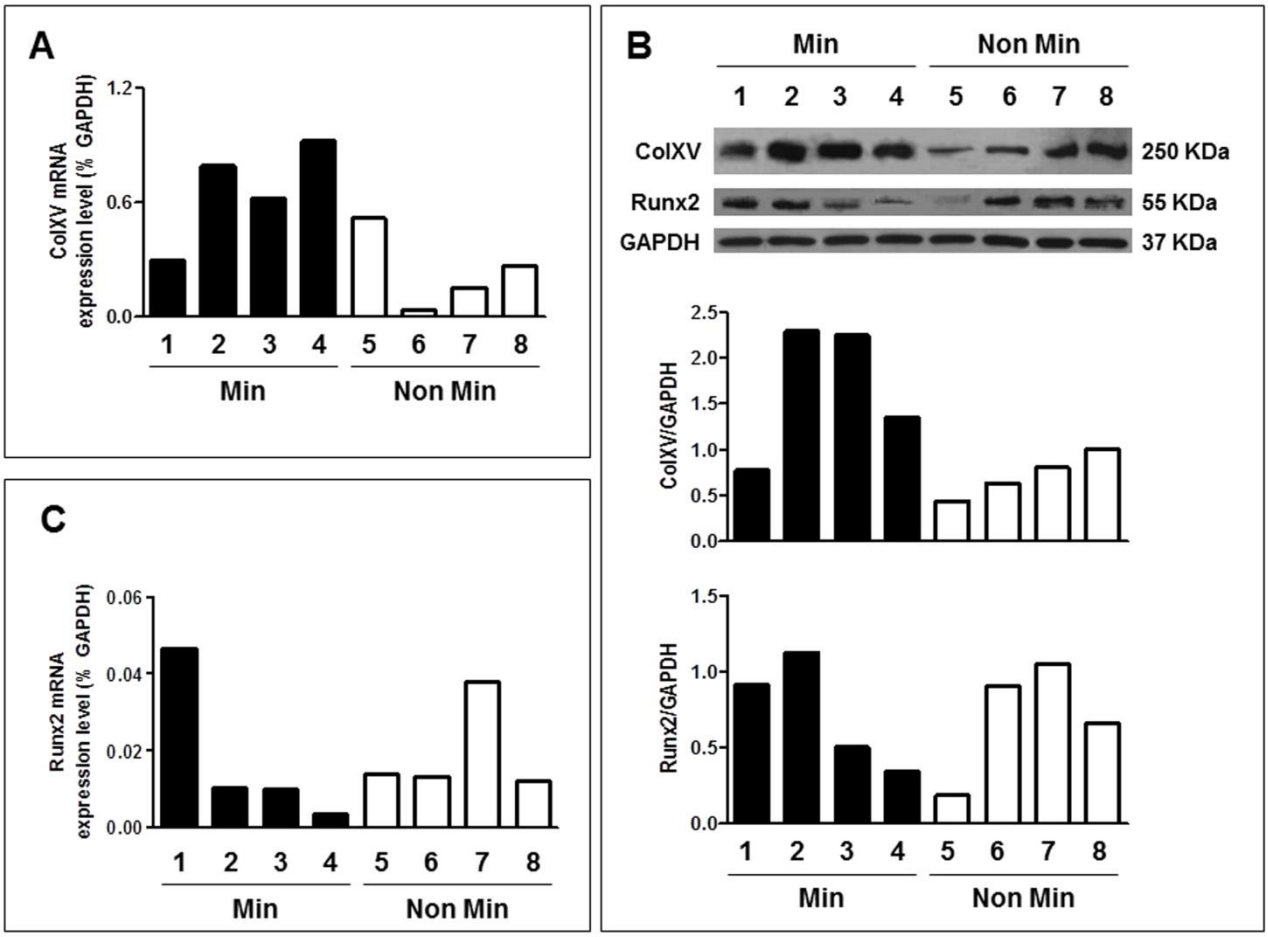

Supplemental Figure 2.4.2: Analysis of ColXV and Runx2 basal levels performed by qRT-PCR (A, C) and Western blot (B) on individual representative cases (4 Min and 4 Non Min). mRNA data were expressed as % of the housekeeping gene GAPDH, Western blot data were expressed as ColXV/GAPDH ratio. The analysis evidenced substantial differences between the detection of ColXV or Runx2 at mRNA and protein level.

Chapter 2 – section 5

Discussion and conclusions

Since its birth in the early 1990s, tissue engineering has raised a great amount of promises and expectations, with encouraging impact on biomedical and clinical fields. In 1993, in the first publication stating the foundation of the tissue engineering discipline, Langer and Vacanti asserted: "…*Tissue engineering offers the possibility of substantial future savings by providing substitutes that are less expensive than donor organs and by providing a means of intervention before patients are critically ill. In addition, cell transplant systems may complement gene therapy approaches in facilitating transfer of large populations of cells expressing a desired phenotype. Few areas of technology will require more interdisciplinary research than tissue engineering or have the potential to affect more positively the quality and length of life.*" (*Langer and Vacanti, 1993*). Although scientific progresses led by tissue engineering have produced relevant repercussions in different fields (from biology to engineering), clinical applications have come out with a great delay respect to expectations and only in recent years first TE-based products have been employed (see Table 1.2 in Chapter 1). The slowing down of the delivery of tissue engineering approaches in medical routine has depended by different issues, which, in the years of TE origin, weren't taken into account (e.g. the need for coupling more disciplines into a unique proposal, the difficulty in obtaining an off-the-shelf product, immunogenicity of biological constructs, the need for vascularization and innervation, advancements in stem cell biology research) (*Oerlemans et al, 2014*). One of the main challenges to face is the ability to reproduce during the *in vitro*/*ex vivo* cell culture a microenvironment as similar as possible to the *in vivo* cellular condition, in order to obtain the best biological performances from implantable cells in terms of newly tissue formation and integration with the host tissue (*Barthes et al, 2014*). Cell-cell and cell-ECM interactions represent the fundamental networking in the *in vivo* microenvironment, also in bone and cartilage, where ECM is an essential component of these tissues and different kind of cells (MSCs, osteoblasts, osteoclasts, chondrocytes) continuously communicate, directly or indirectly, among them and

within ECM (*Pirraco et al, 2010; Gao et al, 2014*). Thus, the realization of constructs able to mimic these sophisticated interactions is of great interest for bone and cartilage tissue engineering, in order to obtain products supporting cell functionality and, consequently, tissue regeneration *in vivo*.

Effect of decellularized ECM on cell behavior

ECM is composed of a great variety of molecules, including collagens, elastic fibers, GAGs and proteoglycans, which are differently distributed and organized in the diverse body tissues and organs. Each one of these complex configurations gives rise to diverse interaction with cells, guiding their differentiation and functionality; thus the comprehension of the cell-ECM relationship is essential to deeply understand how regenerative potential of the cells could be guided and exploited (*Rosso et al, 2004*). The reproduction of the ECM complexity *in vitro* is an arduous task, but the decellularization procedures developed in tissue engineering advancements allowed the direct use of native ECM in combination with implantable cells: decellularized matrices retain their characteristic biological cues impacting on cell behavior and functionality, and at the same time present a reduced immunogenicity, allowing the use of allogenic or xenogenic matrices, too (*Fitzpatrick and McDevitt, 2015*). UBM (porcine urinary bladder matrix) is a FDA approved ECM-derived material, known as MicroMatrix® (ACell, Columbia, MD, USA) and employed in wound regeneration (*https://acell.com/micromatrix*). However beneficial effect of UBM have been reported for others tissues, such as bladder (*Rosario et al, 2008*), brain (*Zhang et al, 2013a*), muscle (*Song et al, 2014*), cardiac tissue (*Remlinger et al, 2013*), even though clinical evidences are still lacking. In the Section 2 of this chapter we demonstrated how UBM exerts positive effects also on human de-differentiated chondrocytes, sustaining the re-acquisition of the differentiated phenotype and, thus, the expression of typical chondrogenic markers (e.g. Col2a1, aggrecan) and ECM synthesis. However evidences reported in this thesis didn't show a direct effect on chondrocytes re-differentiation, rather it seems like exposure to UBM could help in the maintenance of the re-differentiated status. This effect could be attractive both for ACI/MACI procedures, where the loss of phenotype is one of the major issue leading to implantation failure, but also in hMSCs chondrogenic differentiation, where the obtainment of a stable differentiated phenotype and the advancement toward hypertrophy represent two relevant drawbacks. The mechanism throughout UBM exerts its role has not been elucidated in this work, but two main hypotheses could be advanced: i) the release of growth factors entrapped in the ECM structure or ii) the direct interaction with binding proteins on cell surface. Both mechanisms of action have been reported for other decellularized matrices (*Hoganson et al, 2010; Sun et al, 2013*) and it is well established the

important role of both growth factors (e.g. TGF-β, FGF, IGF, Wnt signaling) and adhesion molecules in chondrogenesis and cartilage formation. Interestingly a work by Kim and Lee demonstrated how the interruption of integrin signaling pathway negatively affected chondrocyte re-differentiation in alginate beads functionalized with collagen type 2 fibers (*Kim and Lee, 2009*), letting suppose the importance of this molecular signaling induced by ECM components in sustaining the chondrogenic phenotype. In support of a protective effect of UBM on cartilage, two interesting works have demonstrated how treatment with UBM could reduce cartilage degradation in OA animals, specifically in a dog and a mouse models (*Rose et al, 2009; Jacobs et al, 2016*). Authors speculate that UBM possesses not only a pro-chondrogenic effect, but also an anti-inflammatory role on osteoarthritic tissues with positive repercussion on cartilage tissue loss; since inflammation represents a relevant element in different cartilage diseases and in traumatic damages, this anti-inflammatory property of UBM could be exploited in several tissue engineering approaches.

Interestingly, we demonstrated that UBM has beneficial effects not only on human chondrocytes, but also on biomineralization process by SaOS-2 cell line (see Figure 2.1.16 in Section 1), confirming the pro-regenerative properties of these decellularized matrices on different tissues (*Aulino et al, 2015*). Even though SaOS-2 cells are not eligible candidate for TE strategies, we obtained a proof of concept of the pro-osteogenic effect of UBM, which was confirmed by a previous study conducted by our group, where we demonstrated the osteogenic differentiation and release of mineralized ECM by hMSCs seeded on UBM flakes (*Penolazzi et al, 2012*). These "multipotent" characteristics make UBM an ideal material for tissue engineering of articular system, where the involvement of different tissues (in particular cartilage and subchondral bone) generally occurs. The work reported in this chapter, specifically in Sections 1 and 2, formed the basis for moving towards the *in vivo* demonstration of the beneficial effects of UBM in osteochondral defects and articular diseases, like osteoarthritis.

Novel ECM molecules for tissue engineering approaches

Although decellularized matrices represent optimal candidates as TE products, it is important to keep in mind that each tissue possesses an ECM with a specific molecular and structural signature which is significant for tissue functionality and homeostasis. For this reason the realization of autologous decellularized ECM or, at least, decellularized matrices obtained from the same tissue which is aimed to regenerate has been proposed, although several limitations have been evidenced,

in particular for bone and cartilage whose compact nature make them harder to decellularize (*Lu et al, 2011; Ghanavi et al, 2012; Cheng et al, 2014*). Fortunately, the development of new techniques, such as bioprinting, has allowed the production of scaffolds/matrices composed of specific components, resembling native ECM of the tissue. However a deeper characterization of the expression, disposition and functionality of all the components present in a determinate extracellular matrix is highly needed, in order to synthetize the most suitable scaffold for a specific tissue (*Murphy and Atala, 2014*). The work described in Section 4 falls within this context: for the first time we demonstrated a relationship between collagen type 15 (ColXV) and the osteogenic status of hMSCs. ColXV was previously identified as a novel molecule expressed by hMSCs and osteoblasts (*Lisignoli et al, 2009*), but here we evidenced how its expression was higher in the early phases of the osteogenic differentiation, suggesting an essential role in maintaining cells prone to osteogenesis and in guiding the proper initial commitment (see Figure 2.4.3 in Section 4). Certainly, further investigations to confirm and better understand this possible role of ColXV are needed, in particular *in vivo* (e.g. evaluation of ColXV expression in newly forming bone or effect of ColXV knock-out on bone development): however previous immunohistochemical analysis on bone tissue supported our hypothesis, demonstrating the presence of ColXV in osteoblasts in lining bone trabeculae, but not in terminal differentiated osteocytes (*Lisignoli et al, 2009*). Furthermore, additional analysis regarding the molecular interplay in which ColXV is involved (e.g. interaction with other ECM proteins, binding with cell surface molecules, TFs regulating its expression) will be necessary to obtain a deeper comprehension of its function in ECM produced by hMSCs. If the involvement of ColXV in osteogenic commitment will be confirmed, it could become a new component in TE scaffolds for hMSCs delivery in bone damaged tissue.

Scaffold-based *versus* scaffold-free approach

The *in vitro* mimicking of the *in vivo* extracellular matrix is an essential feature for the development of adequate 3D culture systems as close as possible to the natural cell microenvironment. Two main strategies can be adopted: the first consists in the employment of specific scaffolds that act as matrix templates onto/into which cells are seeded, while the second rely on the ECM produced by the same cells and to which cells attach. These concepts are at the basis of the scaffold-based or the scaffold-free approaches, respectively. Each one has its advantages and limitations, as it has already been described in Chapter 1: scaffolds help cell delivery and give mechanical support to damaged tissue during regeneration period, but at the same time biomaterials and their degradation products may affect cell metabolism and responses, which, if occurring as a non-controlled process, could

negatively impact on cell regenerative potential. Thus, a real predominance of an approach over the other doesn't exist, and the employment of the scaffold-based rather than scaffold-free approach depends from experimental needs and final aim of the construct. On the contrary new trends of opinion have proposed the possibility to combine the two different technologies, in order to complement each one with the other (*Ozbolat, 2015*). In this chapter we reported the use of scaffold-based (Section 2) and scaffold-free (Section 3) strategies, with the obtainment of positive results from both approaches.

In particular, in our experimental models, it should be noted how for the scaffold-based approach the best outcomes have been obtained from the combination of different biomaterials, namely alginate and UBM. Alginate was chosen since its chemical structure resembles glycosaminoglycans, which are one of the main components in cartilage ECM. Furthermore, it ensured optimal morphological and structural characteristics of microfibers, which could be modulated on the basis of need, as demonstrated in Section 1: changes in production parameters (i.e. pumping rate, microchip design, material and dimensions of the outlet, cross-linking ion) highly influence dimensions and morphological features of the microfibers with possible repercussions on cell viability and functionality. UBM, instead, supplied biological cues to direct cell behavior, as already discussed. Composite materials, and in particular polymer-based composite scaffolds, have emerged as suitable candidates in load bearing application such as in cartilage, taking advantages from the better properties of the combined starting materials (*Gloria et al, 2010*). However, the effective beneficial effect of our composite microfibers, in terms of both biological and mechanical properties, must be verified in a cartilage defect model *in vivo*. Instead, an interesting result was the possibility to cryopreserve re-differentiated chondrocytes within the scaffolds: alginate demonstrated cryoprotective properties, as already reported (*Katsen-Globa et al, 2007; Malpique et al, 2010; Pravdyuk et al, 2013*), ensuring the recovery of highly viable and functional cells after thawing (see Figure 2.2.8 in Section 2). Cryopreservation is an important step in translational regenerative medicine and for the obtainment of off-the-shelf products: the realization of cryo-banked materials will be essential to match patient need against supply, distribute tissue-engineered cell products between treatment centers, and provide a bank of regulatory-tested cells for application (*Pravdyuk et al, 2013*).

Regarding the scaffold-free approach it was employed to obtain a construct able to reproduce bone microenvironment, and in particular the crosstalk between osteoblasts and osteoclasts, which is at the basis of bone tissue homeostasis. In order to not impair or enhance functionality of one of the two cell lineages, the use of scaffold was avoided, and strategies favoring cell-cell contact and ECM

production were adopted for the realization of a self-sustaining cell construct. In particular, we demonstrated how a dynamic microenvironment, created thanks to the use of the Rotary Cell Culture System (RCCS) bioreactor, better supports the formation of a "tissue-like microarchitecture" and the functionality of the cell construct respect to the static condition (see Figures 2.3.4 and 2.3.5 in Section 3). Continuous rotation of the bioreactor chambers prevents cell seeding and encourages their aggregation within the formation of 3D spheroids, which could be cultured also for a considerable period; furthermore dynamic rotation allows the high mass transfer of nutrients in media preventing cell death within spheroid core, and maintaining their viability and functionality (*Breslin and O'Driscoll, 2013; http://synthecon.com*). Evidences reported in this thesis also demonstrated how ground-based gravity (Xg) better supports structural and bio-functional features of the cell construct respect to modeled microgravity (μXg) (see Figure 2.3.5 in Section 3). It could be speculated that the negative impact of microgravity on cell aggregates may be related to a superior osteoclast activity in this condition: previous works demonstrated how microgravity supported the resorption ability of OCs, and contemporarily impaired osteoblasts cellular integrity; furthermore osteoporosis-like loss of bone mass has been reported in astronauts and cosmonauts after extended microgravity exposure (*Loomer, 2001; Nabavi et al, 2011; Chatani et al, 2015*). However the central point of the work described in Section 3 is the possibility to recreate in vitro a miniaturized bone microenvironment through the only use of cells producing their own ECM and without exogenous additions: it seems like osteoblasts and osteoclasts are able to coordinate themselves through the instauration of a molecular cross-talk. For instance OBs activated and supported OCs functionality without the need for exogenous inducers (M-CSF and RANKL), and at the same time resorption activity did not prevail on the bone-like ECM formation and mineralization by osteoblasts. More interestingly when we cultured osteoblast from compromised areas, namely from necrotic jaw bone (hnOBs), in a balanced bone-like microenvironment like that one realized, these cells recovered their functionality: they were able to produce mineralized ECM, positively stained for OPN, and to sustain the osteoclast activity, also in absence of classical inducers (see Figure 2.3.6B in Section 3). These results are particularly relevant for tissue engineering, supporting the possibility to obtain autologous cells (remaining the gold standard) also from not fully healthy tissues, reestablish their regenerative potential and re-implant them in the patient. Furthermore we demonstrated how the realization of an implantable cell construct could be obtained from a limited amount of starting material and cells, which remains a major issue in the employment of autologous cells (*Ikada, 2006*). Definitely the regenerative potential of these constructs must be assessed *in vivo*; additionally it is important to underline how they have been thought for small size defects where an imbalance between osteoblasts and osteoclasts occurred,

such as in osteonecrosis of the jaw. Finally depending on the source from which OBs are harvested it is reasonable to apply these cell aggregates in anatomical districts different from the jaw.

3D *in vitro* systems as screening platforms

Technological progresses in tissue engineering field allow to obtain 3D *in vitro* living surrogates of the *in vivo* tissues/organs: this is relevant not only for regenerative medicine, but in recent years also pharmaceutical sciences benefit from these three-dimensional cell-based constructs. In fact, the development of the 3D culture systems will allow to test a great number of bioactive molecules (e.g morphogens, drugs, miRNAs) directly on human cells maintained in a microenvironment more similar to *in vivo*. It will be possible to obtain more predictive and precise information about the biological effect of a potential therapeutic molecule, reducing false positive or negative outcomes, and reducing also the use of animal models, which, however, will remain essential before moving towards clinic (*Ranga et al, 2014; Edmondson et al, 2014*). Substantially, 3D cell-based constructs will fill the gap present between classical 2D cell cultures and animal tests (Figure 2.5.1).

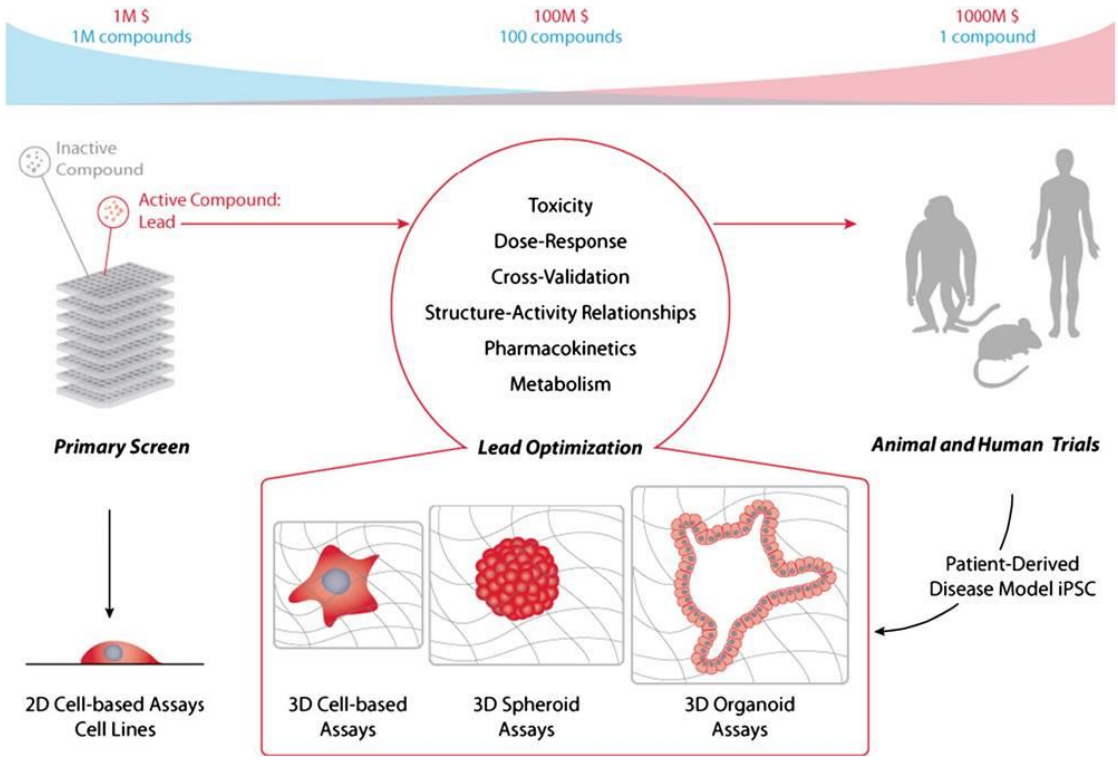

Figure 2.5.1: role of 3D in vitro systems as a bridge filling the gap between classical 2D screening and animal and human trials. Drug discovery pipeline typically proceeds from multiple compounds tested at relatively low cost to few compounds in high-cost high-risk trials, a process which could benefit from increasingly representative *in vitro* technologies (*Ranga et al, 2014*).

Specifically, the 3D cell-based constructs described in this thesis, and mainly planned for possible tissue engineering strategies, could conveniently be used also as screening platforms for pro- or anti- chondrogenic/osteogenic molecules (composite microfibers of Section 2 and OBs/OCs aggregate of Section 3, respectively). The realization of miniaturized cell-based constructs is a central point, since it will allow the screening of larger number of molecules contemporarily, reducing time and costs of the analysis. The realization of a bone-like microenvironment through the use of human osteoblasts from necrotic jaw bone is another significant issue, since it theoretically paves the way to the possibility to reproduce *in vitro* bone disease models to test the effect of drugs on a specific disorder. Furthermore the low amount of cells used in the 3D systems here reported supports the feasibility of the employment of autologous cells from the patient, which could help in the realization of a personalized therapy.

Even though the 3D cell-based constructs reported in this chapter have shown promising results as bone and cartilage models, they could be further improved to obtain *in vitro* systems always more similar to *in vivo* conditions, and thus, more suitable to resemble tissue responses to exogenous bioactive molecules. For example the vascularization of the *in vitro* bone is a crucial issue since vascular network and endothelial cells represent a fundamental component of the *in vivo* bone: vasculature and mineralization are interconnected and impinge on each other, and several studies have demonstrated the influence of endothelial cells on osteoblasts and *vice versa* (*Dariima et al, 2013; Shah et al, 2014; Ben Shoham et al, 2016*). For this reason several attempts have been reported in literature for the *in vitro* vascularization of bone grafts (*Grellier et al, 2009; Santos et al, 2009; Correia et al, 2011; Park et al, 2016*); however the majority of the works employing primary cells in 3D systems focused on the co-culture of osteoblasts and endothelial cells, omitting the use of the osteoclast component.

Another interesting improvement could be the realization of an *in vitro* miniaturized osteochondral model, where bone and cartilage are considered as singular unit, since articular diseases frequently affect both tissues. Actually, different groups have tried to recapitulate the osteochondral environment *in vitro*, but, due to its high complexity and the difficulty in reproducing mechanical, cellular and molecular features, an ideal model have not been produced yet (*Alexander et al, 2014*). Currently in most cases MSCs cultured into/onto multiphasic scaffolds have been employed for replicating the osteochondral unit (*Alexander et al, 2014*); however it should be taken into account that not only osteoblasts and chondroblasts participate in the homeostasis of osteochondral tissue but also other kind of cells, such as osteoclasts, endothelial cells or synoviocytes. For this reason the set-up of complex 3D co-culture systems with several cell types and the employment of bioreactors,

for an adequate mechanical stimulation, should be encouraged to obtain a more adequate *in vitro* osteochondral model. Lozito and colleagues described in a recent work the realization of an osteochondral unit which represents a step towards this direction: they cultured endothelial cells, osteogenic and chondrogenic pre-differentiated MSCs and synovial-committed MSCs into a miniaturized perfusion system, fitting in 96-well plate, with controlled mechanical stimulation. However the effectiveness of this system in a drug screening approach or to study biological processes of healthy or pathological tissue needs to be validated yet (*Lozito et al, 2013*).

Conclusions and future perspectives

The work described in this chapter demonstrated the functionality of *in vitro* cell-based products produced for a potential use in bone or cartilage tissue engineering. Cells included in the devices here described showed good biological performances in terms of differentiated phenotype maintenance and ECM synthesis. In particular we demonstrated how composite microfibrous scaffolds could sustain re-differentiation of human de-differentiated chondrocytes (Section 2), while scaffold-free culture in bioreactor allow the realization of cell-aggregates mimicking bone microenvironment (Section 3). The positive results obtained in this thesis pave the way to test the effectiveness of these constructs *in vivo* in animal models of bone and cartilage defects.

Beyond the *in vivo* tests, an improvement of these cell-based devices will be taken into account, in order to obtain *in vitro* constructs more similar to the *in vivo* tissue environment, with the purpose to increase a possible tissue regeneration and integration in the host. The realization of a construct able to better resemble the *in vivo* cellular condition passes through the characterization of the biological signaling in the tissue environment. With respect to this consideration, we demonstrated for the first time the involvement of a new ECM protein, namely collagen type 15, in the osteogenic commitment of hMSCs, in particular in the early phases of the differentiation process (Section 4). A deeper characterization of the role and the molecular interaction involving ColXV in the osteogenic process will be necessary, but the data here reported suggest the employment of this collagen in tissue engineering-based strategies for bone defects.

Chapter 3

Molecular regulation in hMSCs

Mesenchymal stem cells (MSCs) have emerged as attractive candidates in many cell-based tissue engineering approaches, thanks to their proliferative ability and multilineage differentiation potential. The prospect of monitoring MSC differentiation is a crucial regulatory and clinical requirement, and, even though great progresses have been done, the molecular regulation underlying differentiation process has not been completely understood: the proper role of several transcription factors and microRNAs needs to be still identified. For this reason a deeper characterization of the molecular signaling occurring during MSC differentiation is highly desirable. The opportunity to work in a laboratory of molecular biology gave me the chance to deepen also this aspect during my PhD period. In particular, this chapter describes the study carried out on two regulatory molecules, namely the transcription factor NFATc1 and the microRNA-221, in the control of the osteogenic and chondrogenic fate of hMSCs, respectively.

NFATc1 is one of the main transcription factors involved in osteoclast differentiation and functionality. It is also implicated in the osteogenic process, but its role is still poorly understood, since both positive and negative effects on osteogenesis have been reported. For the first time we demonstrated a new role of NFATc1 in osteo-differentiated hMSCs, as a transcription factor of the mitochondrial DNA and, thus, as a regulator of the metabolic state of the cells during osteogenesis (***Section 1***).

In ***Section 2***, an ongoing work is presented about the molecular regulation by miR-221 during hMSC chondrogenesis. In fact, miR-221 has been recently identified by our group as an anti-chondrogenic factor, but its molecular targets and the pathways in which it is implicated, have not been still elucidated. Thus, here we reported some preliminary data about the study of the molecular network of miR-221 in hMSCs.

The significance and relevance for tissue engineering of the results described in this chapter will be finally discussed in ***Section 3***.

Chapter 3 – section 1

A novel role of NFATc1 in mitochondria

Outline of the work

Cellular metabolism has been recognized as a fundamental aspect in osteogenic differentiation of hMSCs: changes in mitochondrial morphology and function have been reported during the transition towards mature osteoblasts and the production of mineralized ECM. Molecular mechanisms regulating these metabolic alterations are still poorly understood, but the existence of an interplay between nucleus and mitochondria has recently emerged. This crosstalk is finely governed by an extensive network of molecules moving from nucleus to mitochondria and *vice versa* and, among these, nuclear transcription factors have gained new roles in the regulation of mitochondrial pathways. In this scenario, the aim of the work described in this section is to evidence the alternative function of TFs involved in osteogenic differentiation in guiding mitochondrial and metabolic changes occurring during hMSCs differentiation. In particular our attention have focused on two factors, namely Slug and NFATc1, evaluating their localization into the mitochondrial compartment and their recruitment at the D-loop regulatory region of mitochondrial DNA (mtDNA) in osteogenic differentiated hMSCs. For the first time, we demonstrated that NFATc1, but not Slug, is present inside mitochondria and acts as a mitochondrial transcription factor (mitoTF): by chromatin immunoprecipitation (ChIP) assay we found that NFATc1 is "*in vivo*" recruited at mtDNA when the highest differentiation and calcification levels are reached. Furthermore, the occupancy of the mtDNA by NFATc1 is associated with a decreased expression of crucial mitochondrial genes. This suggests a negative role for NFATc1 on the transcription of these molecules, associated with the interruption of aerobic energy demand, during the calcification process.

Introduction

It is well known that variations of number, structure, function and intracellular distribution of mitochondria are correlated with cell functionality and different cell energy demand (*Kuznetsov and Margreiter, 2009*). These variations, which are strictly associated with a finely tuned crosstalk between the mitochondrial and nuclear genomes, have only been recently appreciated as essential events during the differentiation process of stem cells and cell fate switch (*Parker et al., 2009; Mandal et al., 2011; Folmes et al., 2012; Bukowiecki et al., 2014; Wanet et al., 2014*). While numerous efforts have been made to uncover the mechanisms of mitochondrial biogenesis as well as to characterize energy metabolism and redox status during cell differentiation (*Chen et al., 2008; Chen et al., 2010; Madeira, 2012*), little is known about mitochondria transcription regulation by lineage-specific factors and signaling demands. In particular, molecular regulatory circuits that govern mitochondrial dynamics together with mitochondrial contribution to differentiation potential of stem cells remain poorly understood. Thus it is important to explore the properties of mitochondria during differentiation of cellular progenitors. This may add new information on stem cell biology, and may help developing new pharmacologic strategies in regenerative medicine. In addition, this may facilitate the understanding of maintenance of cell culture homeostasis and the optimization of in vitro cell differentiation protocols by adjusting some biochemical properties, such as energy production or redox status of mitochondria. These improvements may provide high quality stem cells to be used for cell therapy. In this scenario, mitochondrial properties might thus be used as a quality measure of cell-based products for several clinical uses. Recent studies showed that mitochondrial DNA copy number, protein subunits of the respiratory enzymes, and intracellular ATP content, increased together with the efficiency of oxidative phosphorylation during osteogenic differentiation of adult hMSCs (*Chen et al., 2008; Pietilä et al., 2010*). Growing evidence supports the bifunctional role of many transcription factors in the control of both nuclear and mitochondrial gene expression (*Szczepanek et al., 2012; Leigh-Brown et al., 2010*).

Two nuclear TFs, Slug/Snail2 (*Cobaleda et al., 2007*) and NFATc1 (nuclear factor of activated T cells complex 1) (*Horsley and Pavlath, 2002*), have been recently described as osteogenic modulators (*Lambertini et al., 2009; Deng et al., 2008; Koga et al., 2005; Penolazzi et al., 2011*).

Slug belongs to the highly conserved Slug/Snail family of transcription factors with an essential role in development and in many cellular functions including control of stem cell properties (*Cobaleda et al., 2007*). NFAT proteins comprise a family of transcription factors (NFAT 1-5) that, after calcium/calcineurin-dependent dephosphorylation, are activated and regulate the expression of many genes involved in a wide range of cellular processes (*Hogan et al., 2003*).

Up to now it is unexplored if Slug and NFATc1 are possible mitoTFs in the mitochondrial pool of nuclear TFs. Several evidences indicate that these TFs are associated with mitochondria functions. In particular, Slug interferes with the mitochondria-dependent apoptotic pathway (*Wu et al., 2005*), may regulate mitochondrial ROS production (*Kim et al., 2011*), and supports the propagation of stress signaling transcriptional network organized by CREB and HMGA2 in mitochondrial dysfunction (*Shibanuma et al., 2012*). NFATc1, through calcineurin and calmodulin, is implicated in the regulation of gene expression by calcium signaling, the control of which involves the mitochondria (*Kim et al., 2009; Chen et al., 2007; Stern, 2006*).

Starting from these evidences, we aimed to further characterize mitochondria during differentiation of hMSCs towards osteogenesis, and examine whether osteogenic TFs are also present in the mitochondria. Furthermore, we studied whether Slug and NFATc1 can be good candidates in the communication between mitochondrial and nuclear genomes, and can contribute to the behavior of MSCs in differentiating towards osteogenic lineage through the regulation of mitochondrial gene expression.

Materials and methods

Cell Culture and differentiation

Human mesenchymal stem cells were isolated from human adipose tissues of five healthy women and 5 healty men (age: 21-36) undergoing cosmetic surgery procedures at the University of Padova's Plastic Surgery Clinic. The adipose tissues were digested with 0.075% collagenase (type 1A; Sigma-Aldrich Chemical Co., St. Louis, MO) in a modified Krebs-Ringer buffer (KRB) [125 mM NaCl, 5mM KCl, 1mM Na_3PO_4, 1mM $MgSO_4$, 5.5 mM glucose, and 20mM Hepes (pH 7.4)] for 60 min at 37°C, followed by 10 min with 0.25% trypsin. Floating adipocytes were discarded, and cells from the stromal-vascular fraction were pelleted, rinsed with media, and centrifuged (*Gardin et al., 2011*). The resulting viable cells were counted using the trypan blue exclusion assay and seeded at a density of 10^6 cells per cm^2 for *in vitro* expansion, in DMEM low-glucose supplemented with 10% FBS (Euroclone S.p.A., Milan, Italy), 2mM L-glutamine, antibiotics (penicillin 100 μg/mL; streptomycin 10 μg/mL), at 37 °C in a humidified atmosphere of 5% CO_2.

hMSCs were used at passage 3 and characterized by testing a panel of surface markers using flow cytometry as previously described (*Torreggiani et al., 2012*). hMSC from all samples were positive for CD90, CD73, CD105 (mesenchymal cell markers), but negative for CD34, and CD45 (haematopoietic cell markers) (Supplemental Figure 3.1.1A). Multilineage differentiation potentials

in response to specific differentiating agents have been confirmed in all samples analyzed. As reported in Supplemental Figure 3.1.1B, Alizarin Red-S staining revealed the ability of the cells to deposit mineral matrix that is a characteristic of osteoblastic lineage, Alcian Blue stains sulfated proteoglycans deposits that are indicative of chondrogenic differentiation, and Oil Red-O staining demonstrated the formation of lipid droplets after induction of adipogenic differentiation. For osteogenic differentiation, hMSCs were cultured up to 28 days in DMEM high Glucose (Euroclone S.p.A.) supplemented with 10% FBS, 10mM β-glycerophosphate, 10^{-7} M dexamethasone and 100 mM ascorbate (Sigma-Aldrich). For ARS staining, the cells were fixed with 70% ethanol for 1 h and then stained with 40 mM Alizarin Red-S solution (pH 4.2) at RT for 10 min. Cells were microphotographed by an optical Leitz microscope.

Quantitative Real-Time RT-PCR

Cells were harvested and total RNA was extracted using an RNeasy Mini Kit (Qiagen, Hilden, Germany) in accordance with the manufacturer's instruction. Quantitative real-time PCR was performed using gene expression Master mix (Life Technologies, Carlsbad, CA, USA) and analyzed on CFX96 Real-Time detection System (Bio-Rad laboratories, Hercules, CA, USA). Assays-On-Demand kits (Life Technologies) for human OC, ON, OPN, Runx2, COL1A1, ALP, BMP2, BMP7, Slug, NFATc1, ND1 and CYTB were used. The expression level of cDNA samples was normalized to the expression of reference GAPDH using the formula $2^{-\Delta Ct}$ or as fold change using the formula $2^{-\Delta\Delta Ct}$. Data are the mean values of n=6 hMSC samples performed in triplicate.

Immunocytochemistry

hMSC grown in chamber slides were fixed in ice-cold methanol and then permeabilized with 0.2% (v/v) Triton X-100 (Sigma-Aldrich) in TBS. After blocking with 2% normal horse serum (Vectorlabs, Burlingame, CA, USA), hMSCs were incubated with primary antibody for 16 h at 4°C. The following primary antibodies were used: rabbit anti-human Col1a1 (H-197, 1:100), rabbit anti-human OPN (LF-123, 1:100) and rabbit anti-human Runx2 (M-70, 1:100) (Santa Cruz Biotechnology, Dallas, TX, USA). Cells were then rinsed and incubated with ImmPRESS™ (Peroxidase) Polymer Universal Anti-Mouse/Rabbit Ig Reagent (Vectorlabs) for 30 min. After washing, the cells were stained with Vectastain ABC reagent and DAB substrate kit for peroxidase (Vectorlabs), mounted in glycerol/TBS 9:1 and observed using a Leitz microscope.

Immunofluorescence and confocal analysis

hMSC were stained with 100 nM Mitotracker Orange CMTMRos (Life Technologies) for 15 min at 37°C and fixed in 4% paraformaldehyde/PBS. After three washes with TBS, the cells were permeabilized with 0.2% Triton X-100 and then blocked with TBS 2.5% FCS. Cells were then incubated over night at 4°C with antibodies (Santa Cruz) against human NFATc1 (clone H-110, 1:20), Slug (clone H-140, 1:20), TFAM (clone H-203, 1:100). Finally primary antibodies were revealed by means of Alexa Fluor® 488 Goat Anti-Rabbit IgG (H+L) (1:100) (Life Technologies). Images were acquired on Axiovert 220M microscope equipped with a x100 oil immersion Plan-Neofluar objective (NA 1.3, from Carl Zeiss, Jena, Germany) and a CoolSnap HQ CCD camera. The acquired images were background corrected, and Pearson's coefficient for co-localization was analyzed using JACOP plugin of the open source Fiji software (http://fiji.sc/Fiji).

Immunogold labeling and electron microscopy

hMSCs were fixed in 1% glutaraldehyde in 0.1 M phosphate buffer (pH 7.4) for 1 h, partially dehydrated up to 70% ethanol and embedded in LR White Resin at 0°C. Thin sections were pre-incubated with 5% normal goat serum in 0.05 M Tris-Cl (pH 7.6), 0.14 M NaCl, 0.1% BSA in TBS and then incubated overnight at 4°C with rabbit anti-human NFATc1 (Santa Cruz, clone H-110, 1:10 dilution in TBS I); and then with a goat anti-rabbit conjugated with 15-nm colloidal gold particles (BBInternational, Cardiff, UK) diluted 1:20 in 0.02 M Tris–HCl (pH 8.2), 0.14M NaCl and 0.1% BSA for 1 h at RT. Thin sections were stained with aqueous uranyl acetate and lead citrate and observed with a Zeiss EM109 transmission electron microscope. Images were captured using a Nikon digital camera Dmx 1200F, and ACT-1 software.

Subcellular fractionation and western blot analysis

hMSCs were harvested and gently disrupted by homogenization as reported (*Bononi and Pinton, 2015*). The homogenate was centrifuged twice at 1000 g for 5 min to remove nuclei and unbroken cells (nuclear fraction) and then the supernatant was centrifuged 10000 g for 10 min. The resultant supernatant was used for cytosolic fraction isolation, while the pellet, consisting in the mitochondrial fraction, was subjected to 100 μM Proteinase K (Sigma-Aldrich) for 30 min on ice. Proteins from the three subcellular fractions were electrophoresed on 12% SDS-polyacrylamide gel and transferred onto an Immobilon-P PVDF (Millipore, Billerica, MA). After blocking the

following primary antibodies were used: VDAC (mouse anti-human, 1:2000, Millipore, Billerica, MA), Lamin B1 (mouse anti-human, 1:1000, Santa Cruz) and NFATc1 (rabbit anti-human, 1:500, Santa Cruz Biotechnology). After washing, the membranes were incubated with HRP-conjugated anti-mouse (1:2000) or anti-rabbit (1:50000) antibodies (Dako, Glostrup, Denmark) and signals were detected by SupersignalWest Femto Substrate (Pierce, Rockford, IL, USA).

Chromatin Immunoprecipitation (ChIP)

ChIP assay was done using a ChIP Assay Kit (catalog no. 17-295) from Upstate following procedures provided by the manufacturer. Briefly, after crosslinking the chromatin with 1% formaldehyde at 37°C for 10 min, cells were washed with cold PBS, scraped and collected on ice, lysed and sonicated. An equal amount of chromatin was immunoprecipitated at 4°C overnight with 5 μg of the following antibodies: TFAM, Slug, NFATc1, or non-specific IgG (Santa Cruz). Immunoprecipitated products were collected after incubation with Protein A-agarose beads. The beads were washed, and the bound chromatin was eluted in ChIP Eluition Buffer. The samples were incubated at 65°C overnight to reverse the crosslinking. Then the proteins were digested with Proteinase K for 1 h at 45°C and DNA was purified in 50 μL of Tris–EDTA with a PCR purification kit (Qiagen) according to the manufacturer's instructions. The DNA precipitates and Input (1% of total chromatin used for the immunoprecipitation) were further subjected to semi-quantitative or quantitative PCR using the following primers for amplification of 286-bp fragment of the D-loop region (d-loop forward, 5'-CCC CTC ACC CACTAGGATAC-3', and d-loop, reverse, 5'-ACG TGT GGG CTA TTT AGG C-3'). PCR products were analyzed by agarose gel electrophoresis and visualized by UV light apparatus. Real-time PCR analyses of the ChIP samples were carried with CFX96 Real-Time detection System (Bio-Rad labs) using iTaq Universal SYBR Green SuperMix (Bio-Rad). We analyzed ChIP-qPCR data relative to Input signal and presented as fold increase in signal relative to the background signal (IgG).

Statistical analysis

The Student's t test was used for comparisons between the groups. $p \leq 0.05$ was considered significant.

Results and discussion

hMSC osteogenic differentiation and mitochondria

We focused on the ability of hMSCs to differentiate towards osteoblastic lineage in order to add informations on functional link between mitochondria and osteogenic differentiation. As shown in Figure 3.1.1A and B, osteogenic induced cells increased the expression of typical osteogenic markers. These include: the main constituent of the organic part of the bone ECM, collagen type 1, ALP which is responsible for the ECM mineralization, the master regulator of osteogenic differentiation Runx2, three non-collagenous ECM proteins, osteopontin, osteonectin and osteocalcin, three osteogenic growth factors (BMP2, BMP7 and WNT3). Moreover, the cells produced Alizarin red positive nodular aggregates at the end of differentiation (day 28). The mitochondrial morphology has been then assessed by Mitotracker Orange staining at early stage of osteogenic differentiation (day 14) when oxidative demand induced by osteogenic medium is high. As shown in Figure 3.1.1C, relative mitochondrial network area per cell was significantly increased in osteogenic induced cells, while no significant alterations were observed in average particle area or form factor.

There are many open questions regarding the signaling pathways and key molecules supporting mitochondria changes in response to specific cell processes such as osteogenic differentiation. The need to respond to this issue is important both for defining the complexity of human mitochondrial transcription machinery, and for understanding the increasing number of diseases associated with mitochondrial dysfunction. Specifically, this approach may be useful to provide new information toward the development of novel therapeutics for bone disorders and bone tissue regeneration.

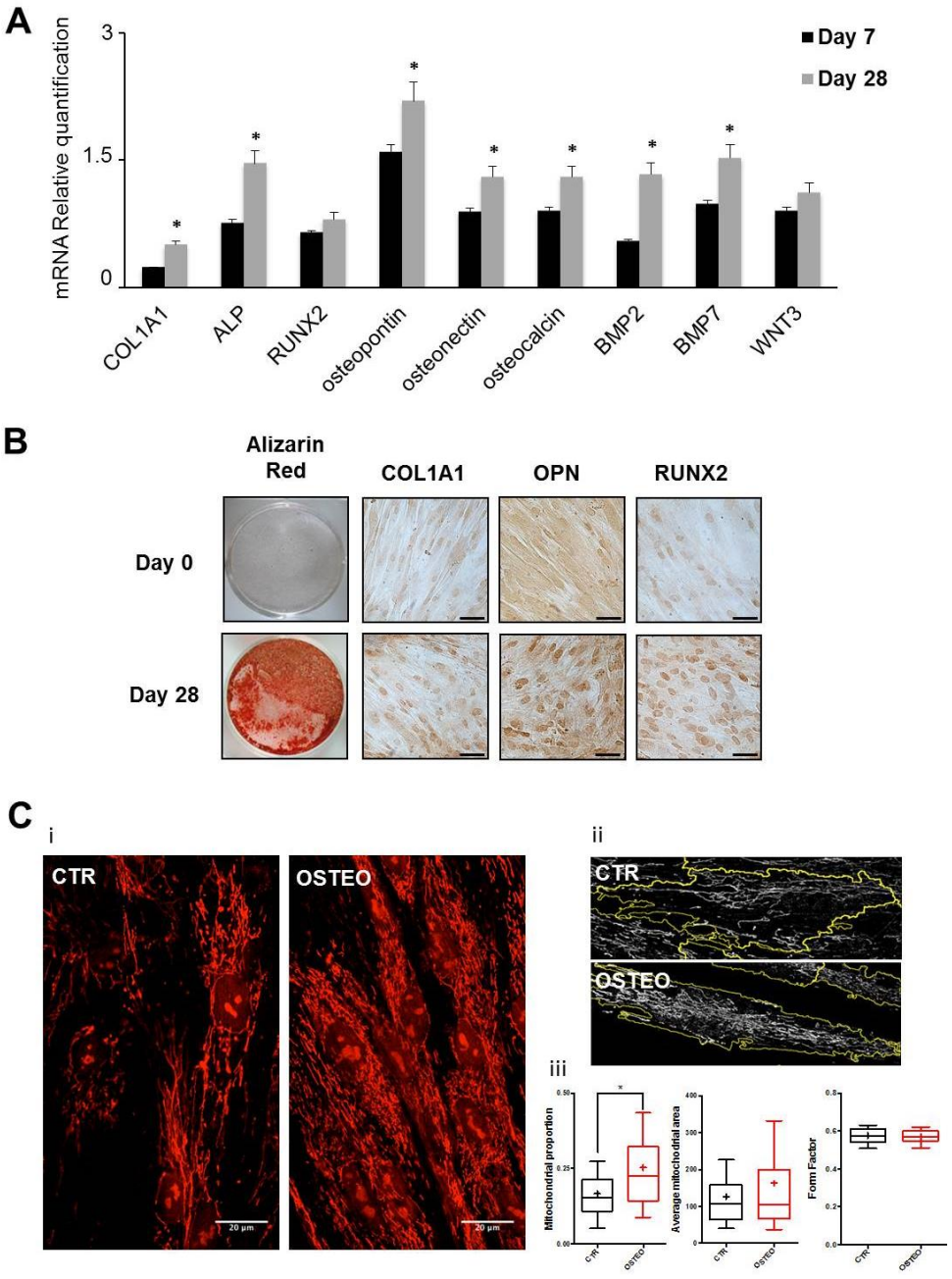

Figure 3.1.1: osteogenic differentiation of human mesenchymal stem cells (hMSCs) and evaluation of specific markers. (A) Quantitative gene expression analysis of specific osteogenic markers was performed in hMSC induced towards osteogenic differentiation for 28 days. For each cDNA sample, the Ct of the reference gene GAPDH was subtracted from the Ct of the target sequence to obtain the ΔCt. Relative gene expression was then calculated using the $2^{-\Delta Ct}$ method. Error bars represent means ± standard deviation for n=6. *p-value <0.05 compared to Day 7 sample group. (B) Mineral matrix deposition was evaluated by ARS staining in hMSCs at day 0 and after 28 days of culture in osteogenic medium. The expression levels of Collagen type 1 (COL1A1), osteopontin (OPN) and RUNX2 were analysed by immunocytochemistry. Scale bar 50 µm. (C) Morphological aspect of hMSC mitochondria. The amount of mitochondria was evaluated by optical microscopy **(i)** on hMSC stained with Mitotracker Orange after 14 days of culture in presence (OSTEO) or absence (CTR) of osteogenic inducers. Images were segmented for cell surface and mitochondrial area (see representative sample in ii) to allow quantitation of relative mitochondrial amount, mitochondrial area and morphology (iii). *Significant at $p < 0.05$; line = median, cross = mean, bars = maximum and minimum values. The boxes envelop the 10^{th} to the 90^{th} percentile of the assayed population.

NFATc1, but not Slug, is associated with mitochondria

By qRT-PCR analysis we confirmed that hMSCs express substantial levels of Slug and NFATc1 transcription factors both at basal condition (day 0) and after osteogenic differentiation. In particular, mRNA for Slug significantly increased in osteogenic differentiated hMSCs compared to undifferentiated ones (Figure 3.1.2A).

In-silico analysis allows prediction of NFATc1 and Slug localization to mitochondria. Such predictions were performed by two different informatical tools, MitoProt and TargetP. Both these tools predict high probability for mitochondrial localization of some NFATc1 isoforms, while only MitoProt predicts a slight probability for Slug to reach mitochondria (Table 3.1.1).

Table 3.1.1: prediction of mitochondrial localization of the known NFATc1 isoforms and Slug by the informatical tools MitoProt and TargetP.

	TargetP	**MitoProt**	
Target	**Predicted subcellular localization**	**Probability of export**	**Cleavage sequence**
NFATc1 A-alpha	Mitochondria	0.1448	MPSTSFPVPSKFPLGPAAAVFGRGETLGPAPRA
NFATc1 A-alpha'	/	0.0599	NA
NFATc1 B-alpha	Mitochondria	0.1444	MPSTSFPVPSKFPLGPAAAVFGRGETLGPAPRA
NFATc1 B-beta	/	0.0052	NA
NFATc1 C-alpha	Mitochondria	0.1343	MPSTSFPVPSKFPLGPAAAVFGRGETLGPAPRA
NFATc1 C-beta	/	0.0054	NA
NFATc1 1A-deltaIX	Mitochondria	0.1433	MPSTSFPVPSKFPLGPAAAVFGRGETLGPAPRA
NFATc1 1B-deltaIX	/	0.0053	NA
SNAI2	/	0.5571	NA

NFATc1 and Slug localization were then investigated by immunostaining and confocal microscopy co-localization analysis (Figure 3.1.2B). Interestingly, NFATc1 displays significant co-localization with the mitochondrial marker Mitotracker Orange (as indicated by Pearson's coefficient) to an extent comparable to the Transcription factor A mitochondrial (TFAM) which is a crucial activator of mitochondrial transcription and genome duplication. On the contrary, Slug remains predominantly localized to the nucleus. Immunogold labeling and Western blot analysis confirmed

the association of NFATc1 with the mitochondria (Figure 3.1.2C and D). Treatment with osteogenic inducers did not affect the localization of these two bone associated transcription factors (data not shown).

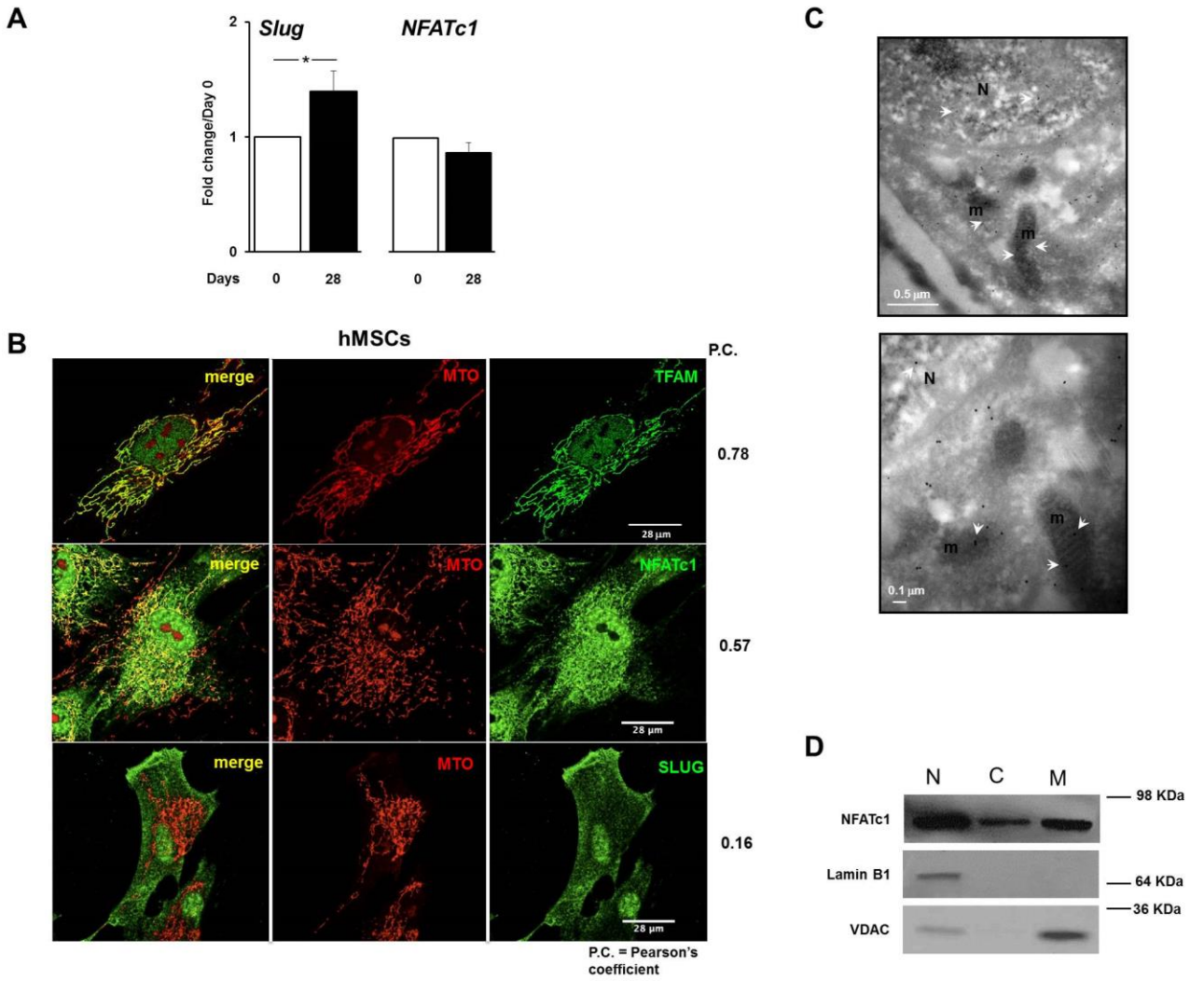

Figure 3.1.2: mitochondrial localization of NFATc1 and Slug. (A) Slug, and NFATc1 gene expression was determined at mRNA level in hMSCs induced towards osteogenic differentiation for 28 days, and revealed by quantitative RT-PCR. Data were normalized to GAPDH according to the formula 2-ΔΔCt and scaled relative to day 0 expression levels. Results represent means ± SEM of six independent experiments. *p-value <0.05 were considered statistically significant. (B) hMSCs were treated with Mitotracker Orange (MTO, red staining) and antibodies (green staining) against TFAM, NFATc1 or Slug. Merge images represent an overlay of the two channels where co-localization is indicated by a color change (yellow). (C) Immunogold labeling of NFATc1 in mitochondria of hMSC cells. Arrows indicate gold particles; m, mitochondria; n, nucleus. (D) Nuclear (N), cytoplasmic (C) and mitochondrial (M) fractions were analyzed by Western blot for NFATc1 expression. Lamin B1 and VDAC1 were used as markers for the purity of the nuclear and mitochondrial fractions, respectively. The data are representative of three independent fractionation experiments.

NFATc1 is recruited at mtDNA

In order to explore functional regulatory role of Slug and NFATc1 nuclear transcription factors in mitochondria, we performed a chromatin immunoprecipitation assay to analyze the "*in vivo*" recruitment of Slug and NFATc1 at the non-coding displacement loop (D-loop) regulatory region of mtDNA (*Hock and Kralli, 2009*). It is well known that mitochondrial genes are densely packed along the genome with the exception of D-loop which is devoted to transcription initiation carried out by the mitochondrial-specific RNA polymerase (*Shutt et al., 2011; Marinov et al., 2014*). Multiple reports have suggested that TFs, that typically act in the nucleus, might also have regulatory functions in mitochondrial transcription (*Leigh-Brown et al., 2010; Hock and Kralli, 2009; Szczepanek et al., 2012*). These include: CREB, NF-kB, ER, MEF2D, STAT1, T3 receptor p43, p53, IRF3, and STAT3. However, a direct evidence of *in vivo* protein-DNA contacts in mitochondria has been provided by ChIP analysis only for p53, CREB, and MEFD2 (*Leigh-Brown et al., 2010*). By using the programs Transcription Element Search Software (TESS) for TF search, and MatInspector 7.4, we identified the presence of one putative Slug binding site (E-box motifs, 5'-CACCTG/CAGGTG-3') and three NFAT binding sites (5'-GGAAA-3') in the D-loop region (Figure 3.1.3A). The results from ChIP assays demonstrated that in all examined conditions Slug is not recruited at appreciable levels. Interestingly, in hMSC samples that fail osteogenic differentiation the D-loop region chromatin was not immunoprecipitated by neither Slug nor by NFATc1 (see the n.2 representative sample in Figure 3.1.3A). Conversely, the D-loop region is highly occupied by NFATc1 in hMSCs that undergo osteogenesis and this recruitment increased when the cells reach the end of the differentiation process (day 28). TFAM, which is required for initiation and regulation of mitochondrial transcription, was properly recruited by its recognition site at a very high level regardless of the presence of differentiating agents. Recent studies demonstrated that mitochondria are maintained at a low activity state in hMSCs. Upon osteogenic induction, their functions increased to fulfill a higher degree of energy demand or to facilitate other biochemical reactions that take place within the organelles. However, the high energy aerobic demand by osteoblasts at the early stages of differentiation, is necessarily slowed down during the progress of calcified matrix deposition and, even more, at the end of differentiation when the cells become apoptotic or quiescent. The regulation of these dynamics is still poorly studied even if it is reasonable that specific signals are sent from the nucleus to mitochondria to change their activities (*Cagin and Enriquez, 2015*). Our data are consistent with this hypothesis, suggesting that one of these signals could be represented by NFATc1 acting as negative regulator of mtDNA transcription. Therefore, NFATc1 could contribute to the calcification process participating in the interruption of aerobic energy demand when is no longer needed (see the scheme in Figure 3.1.3B). This

hypothesis is furthered by the expression levels of crucial mitochondrial genes. As shown in Figure 3.1.3C, we observed a decrease of CytB (Cytochrome B) and ND1 (NADH dehydrogenase 1) expression at the end of the osteogenic differentiation.

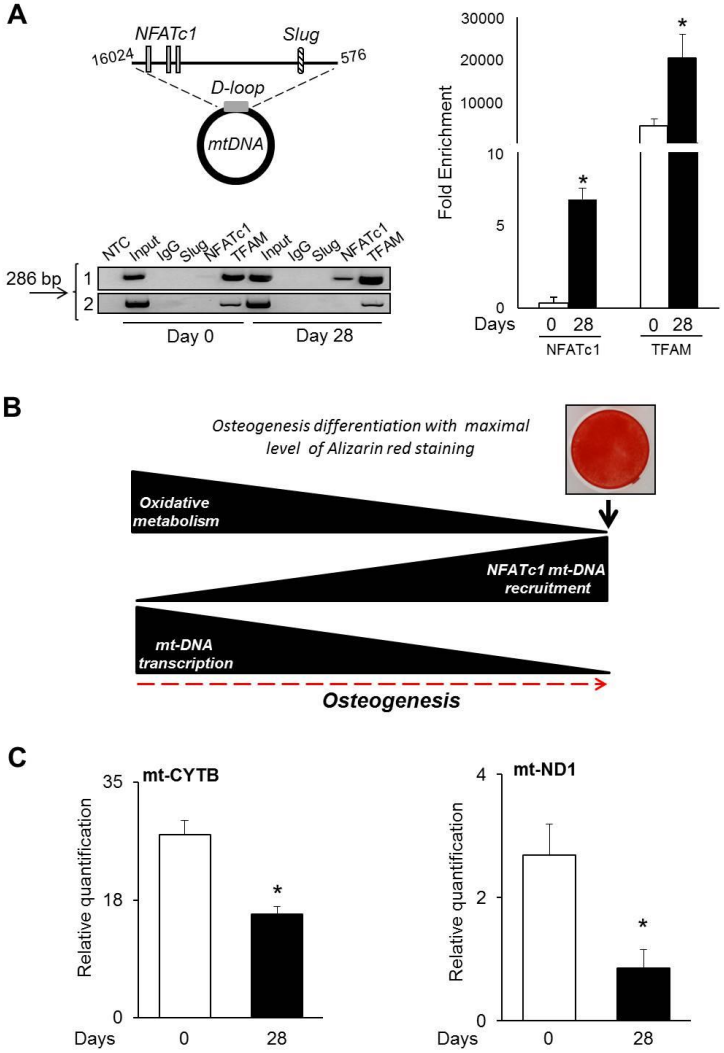

Figure 3.1.3: recruitment of Transcription factors (TFs) to the non-coding region (D-Loop) of hMSC mitochondrial DNA. (A) Schematic representation of D-Loop region with binding sites for NFAT and Slug TFs is reported. hMSCs at day 0 and after 28 days of culture in osteogenic medium were subjected to Chromatin immunoprecipitation (ChIP) assay using antibodies against Slug, NFATc1 and TFAM TFs. A non-specific IgG antibody was used as control. Representative semiquantitative PCRs after ChIP assay are shown. NTC, no template control; Input, positive control; 1, osteogenic differentiated hMSCs sample; 2, hMSCs sample unable to differentiate toward osteogenic lineage. In order to evaluate the fold enrichment relative to the IgG control, quantitative PCR was performed on osteogenic differentiated hMSCs samples. Data represent mean ± S.E.M. (n=6). (B) The hypothesis of relationship between NFATc1 and mitochondrial activity during osteogenic differentiation of hMSCs is schematized. (C) Analysis of mt-DNA transcription in osteogenic differentiated hMSCs. Cells were cultured in presence of osteogenic inducers for 28 days and mRNA expression level of mt-CYTB and mt-ND1 was determined by quantitative RT-PCR. For each cDNA sample, the Ct of the reference gene GAPDH was subtracted from the Ct of the target sequence to obtain the ΔCt. Relative gene expression was then calculated using the $2^{-\Delta Ct}$ method. Data represent mean ± S.E.M of six independent experiments. *p-value <0.05 compared to Day 0 sample group.

Concerning NFATc1 in osteoblasts, our preliminary evidences can shed light on the controversial role of NFATc1 in osteoblastic differentiation and function. Recent studies have demonstrated that activation of NFATc1 promotes osteoblast differentiation in vitro and in vivo (*Koga et al., 2005; Fromigue et al., 2010, Ogasawara et al., 2013*). Other evidences support the inhibitory effects of NFATc1 on osteoblast differentiation through different pathways (*Yeo et al., 2007; Zanotti et al., 2011*). Therefore, the role of NFATc1 in osteoblasts could be different, depending on its interaction with other specific molecules. In addition, concerning the potential involvement of NFATc1 in mineralization process, our data are in agreement with recent evidences that indicate the implication of this transcription factor in vascular calcification (*Goettsch et al., 2011*).

In conclusion, our data suggest a new role of NFATc1, even if further studies are required for a better understanding of its involvement in the regulatory machinery of mitochondria in relation to osteoblast function and energetic metabolism.

A

Surface protein abbreviation	*Surface protein description*	*Mean percentage ± SD*
CD45	Leucocyte common antigen	1±1
CD34	Siamolucin-like adhesion molecule	2±2
CD90	Thy-1	99±1
CD73	Ecto 5' nucleotidase	98±2
CD105	SH-2, endoglin	95±5

B

Alizarin Red *Alcian Blue* *Oil Red O*

Supplemental Figure 3.1.1: characterization of hMSC from adipose tissues. (A) The expression of the reported surface markers was analyzed by flow cytometry (FACS). Data from three different hMSC samples are presented as mean percentage ± SD. (B) Multilineage differentiation potential of hMSC was tested by alizarin red, alcian blue and oil red O staining positivity after exposure to osteogenic, chondrogenic and adipogenic inducers respectively.

Chapter 3 – section 2

Molecular interplay of miR-221 in hMSCs

Outline of the work

hMSCs have been recognized as a promising cellular component in bone and cartilage tissue engineering approaches. However successful clinical outcomes have not yet been achieved due to issues related to a strictly controlled differentiation process and the achievement of stable differentiated phenotypes. In order to overcome these limitations, the identification of novel factors and a deeper understanding of the molecular mechanisms guiding cell differentiation should be obtained. Regarding hMSCs chondrogenesis, our group recently identified microRNA-221 (miR-221) as a new antichondrogenic molecule, whose depletion supported chondrogenesis process and cartilage ECM formation both *in vitro* and *in vivo*. Nonetheless molecular pathways involved in hMSCs chondrogenesis guided by miR-221 depletion are still under investigation. The research presented in this section is a preliminary study towards the identification of these mechanisms, in order to find new possible targets for cartilage therapeutic strategies. The work was performed in collaboration with the molecular medicine laboratory of Prof. Mauro Giacca at the Internation Centre for Genetic Engineering and Biotechnology (ICGEB), where I spent three months during my Ph.D. training.

Herein an initial systemic study of the transcriptome of the miR-221 silenced hMSCs was performed by RNA-sequencing technology, with the aim to highlight possible miR-221 target genes with pro-chondrogenic function. To facilitate the realization of this purpose a chondrogenic screening system in hMSCs was hypothesized and the design of this procedure, which is still in a preliminary phase, is here presented.

Introduction

Mesenchymal stromal cells (hMSCs) have been identified as an attractive cell source for cartilage regeneration due to their chondrogenic potential (*Xian and Foster, 2006; Gordeladze et al, 2011; Johnstone et al, 2013; Demoor et al, 2014*). Many studies demonstrating that cartilage tissue can be created from hMSCs have paid special attention to growth factors that are involved in promoting chondrogenesis: in particular the members of the TGF-β family induce hMSCs to acquire a chondrogenic phenotype, and synthesize specific extracellular matrix proteins such as collagen type 2 and aggrecan (*Mackay et al, 1998; de Crombrugghe et al, 2001; Liao et al, 2014*). The use of TGF-β, however, revealed contradictory findings and undesired off target effects on the synthesis and functionality of cartilage matrix components. In fact, during chondrogenesis release of high levels of TGF-β may drive progenitor cells to become hypertrophic or induce fibrosis (*van Beuningen et al, 2000; Hellingman et al, 2011*). The presence of TGF-β during chondrocyte proliferation may be detrimental for the redifferentiation process and may promote the rapid and undesirable differentiation into fibroblast-like cells (*Narcisi et al, 2012a*). Additionally, recent studies have demonstrated that TGF-β signaling plays a critical role in the development and progression of osteoarthritis (OA) (*Baugé et al, 2014*). This emerging body of evidence has stimulated researchers to pay special attention to feasible alternatives, including the removing of potentially anti-chondrogenic factors. As part of this effort, we previously demonstrated that silencing of an anti-chondrogenic microRNA, namely miR-221, induced the expression of chondrogenic markers and the production of cartilage-like ECM in hMSCs cultured in 3D *in vitro* culture and in an osteochondral defect model *in vivo*, without TGF-β (*Lolli et al, 2016*). Even though the effectiveness of the approach has been demonstrated, the proper role of miR-221 in the chondrogenic process and in cartilage homeostasis and the molecular mechanisms sustaining this function have not yet been established. In literature only the cyclin-dependent kinase inhibitor 1B (p27) and mouse double-minute 2 homolog (MDM2) have been experimentally validated as relevant miR-221 chondro-targets: p27 up-regulation after miR-221 suppression has been associated to chondrocyte proliferation, while removing the inhibition by miR-221 on MDM2 expression resulted in an increased degradation of the anti-chondrogenic transcription factor Slug in chick limb mesenchymal cells (*Kim et al, 2010; Yang et al, 2015*). Thus, this work focused on the research of miR-221 target genes implicated in the chondrogenic commitment of hMSCs, with the intent of deepening the comprehension of the molecular regulation sustaining cartilage homeostasis and formation.

Materials and methods

hMSCs culture

hMSCs were isolated from Wharton's jelly of human umbilical cord, as previously reported (*Penolazzi et al, 2012*). Human umbilical cords (all from natural deliveries) were collected after mothers' consent and approval of the Ethics Committee of the University of Ferrara and S. Anna Hospital (protocol approved on November 19, 2006). Harvesting procedures of Wharton's jelly from umbilical cord were conducted in full accordance with the Declaration of Helsinki, as adopted by the 18th World Medical Assembly in 1964 and successively revised in Edinburgh (2000), and the Good Clinical Practice guidelines. Cords were processed within 4 hours and stored in sterile saline until use. Typically, the cord was rinsed several times with sterile phosphate-buffered saline (PBS) before processing and cut into pieces (2–4 cm in length). Blood and clots were drained from vessels with PBS to avoid any contamination. Single pieces were dissected, after separating the epithelium of each section along its length, to expose the underlying Wharton's jelly. Subsequently, cord vessels were pulled away and the soft gel tissue was finely chopped. The same tissue (2–3 mm^2 pieces) was placed directly into 75 cm^2 flasks in DMEM low-glucose 10% FCS (Euroclone S.p.A., Milan, Italy), supplemented with 100 μg/mL penicillin and 10 μg/mL streptomycin), at 37°C in a humidified atmosphere of 5% CO_2. After 5–7 days, the culture medium was removed and then changed twice a week. At subconfluence, cells were trypsinized, and thereafter expanded and used at passage 3 or 4.

miR-221 silencing and RNA-seq analysis

2 samples of hMSCs were transfected with 30 nM antagomiR-221 through Lipofectamine RNAiMAX reagent (Thermo Fisher Scientific, Waltham, MA) as delivering agent (0.43 μL/mL of culture medium), by combination with the oligonucleotides for 20 min at RT. Monolayered hMSCs were transfected twice, the day after the plating and again after 3 days. The transfected cells were cultured at 37°C in a humidified atmosphere of 5% CO_2 and after other 3 days were detached and used for RNA extraction. Total RNA was extracted through miRNeasy Mini Kit (Qiagen,Hilden, Germany) according to the manufacturer's instruction. RNA concentration and quality was measured using a NanoDrop ND-1000 spectrophotometer (Thermo Fisher Scientific, Waltham, MA); RNA integrity was checked by gel electrophoresis. TruSeq Stranded mRNA Sample Prep kit (Illumina, San Diego, CA) has been used for library preparation following the manufacturer's instructions, starting with 1-2 μg of good quality RNA (R.I.N. >7) as input. The poly-A mRNA was

fragmented 3 minutes at 94°C and every purification step has been performed by using 1X (or 0.6X if paired end reads) Agencourt AMPure XP beads. Both RNA samples and final libraries were quantified by using the Qubit 2.0 Fluorometer (Thermo Fisher Scientific, Waltham, MA) and quality tested by Agilent 2100 Bioanalyzer RNA Nano assay (Agilent technologies, Santa Clara, CA). Libraries were then processed with Illumina cBot for cluster generation on the flowcell, following the manufacturer's instructions and sequenced on single-end (or paired-end if required) mode at the multiplexing level requested on HiSeq2500 (Illumina, San Diego, CA). The CASAVA 1.8.2 version of the Illumina pipeline was used to processed raw data for both format conversion and de-multiplexing. Data were finally analyzed through Cufflinks bioinformatics program (*http://cole-trapnell-lab.github.io/cufflinks*).

Bioinformatics analysis for the research of miR-221 seed sequence

Seed sequence for miR-221 (5'-GCUACAU-3') was searched in the 3'UTR, coding sequence (CDS), 5'UTR and promoter of the up-regulated genes identified by RNA-seq analysis. The research was performed through the bioinformatics database miRWalk 2.0 (*http://zmf.umm.uni-heidelberg.de/apps/zmf/mirwalk2*): predicted targets are originated from its own algorithm and are also collected from datasets of 12 established miRNA target prediction programs.

HeLa cells culture

HeLa cell line was maintained in DMEM high glucose with 10% FCS, supplemented with 100 μg/mL penicillin and 10 μg/mL streptomycin, at 37°C in a humidified atmosphere of 5% CO_2. At subconfluence, cells were trypsinized, and thereafter expanded or used for transfection experiments.

Cell transfection and luciferase assay

HeLa cells or hMSCs were plated at specific cell density in basal medium: $5x10^5$ HeLa cells/cm^2 and $1.5x10^5$ hMSCs/cm^2. After 24 hours culture medium was removed and cells were transfected with pGL3 control vector (Promega, Madison, WI) or pGL2-4ECol2luc vector (from Dr. Kenji Hata) with or without expression plasmid for human Sox9 (from Dr. Elisabeth Sock). Two Sox9/pGL2-4ECol2luc ratios were tested, that is 1:2 and 1:1. Lipofectamine 2000 (Thermo Fisher Scientific, Waltham, MA) was used as delivering agent by the combination with plasmids for 20

min at RT. After 72 hours cells were detached and were lysed in Reporter Lysis Buffer (Promega, Madison, WI). Cells were then centrifuged at 12500 rpm for 2 min and the supernatant was collected in a new tube. Subsequently 20 μL of cell lysate were incubated with 50 μL of the luciferin substrate provided by Luciferase Assay System (Promega, Madison, WI) and the light emission was detected through a luminometer (Turner Biosystem, Sunnyvale, CA). Luciferase activity was then normalized on the total protein amount, quantified by Bradford reagent (Sigma-Aldrich, Saint Louis, MO).

hMSCs transduction with AAV vectors

hMSCs were plated at a density of $1.5x10^5$ cells/cm^2 and after 24 hours cells were transduced with AAV-2 or AAV-DJ vectors containing the transgene for the green fluorescent protein (GFP) expression at two different multiplicity of infection (10^4 or 10^5). Contemporarily hMSCs were transfected with an expression plasmid for GFP using Lipofectamine 2000 as delivering agent. After 72 cells transduced with AAV vectors or transfected were collected and the percentage of GFP positive cells was determined by FACS Scan (Becton Dickinson, Franklin Lakes, NJ) and CellQuest software (Becton Dickinson European HQ, Erembodegem Aalst, Belgium).

Results and discussion

In a first attempt to identify possible targets of miR-221, a study of the already validated and predicted ones in literature was performed. In particular, the attention was focused on those genes for which an implication in chondrogenesis was already evidenced and the result was schematized in a complex scenario reported in Figure 3.2.1. As notable, the feasible targets of miR-221 could belong to different molecular pathways (i.e. cartilage ECM synthesis, cartilage hypertrophy and ECM degradation, Wnt signaling, cell cycle and proliferation, cytoskeleton organization and inflammation) which could be positively or negatively implicated in the regulation of chondrogenic markers espression, such as collagen type 2 or aggrecan. It is highly reasonable that anti-chondrogenic role of miR-221 acts through the inhibition of multiple molecules, and thus the pro-chondrogenic effect of the silencing in hMSCs could depend from the re-expression of several factors. It is important to underline that, actually, only 2 of the genes presented in Figure 1 have been already reported as chondro-targets of miR-221, namely MDM2 and p27 (*Kim et al, 2010;*

Yang et al, 2015). It is therefore possible that not yet identified targets of miR-221 may be involved in the chondrogenic process by alternative and unexplored molecular pathways.

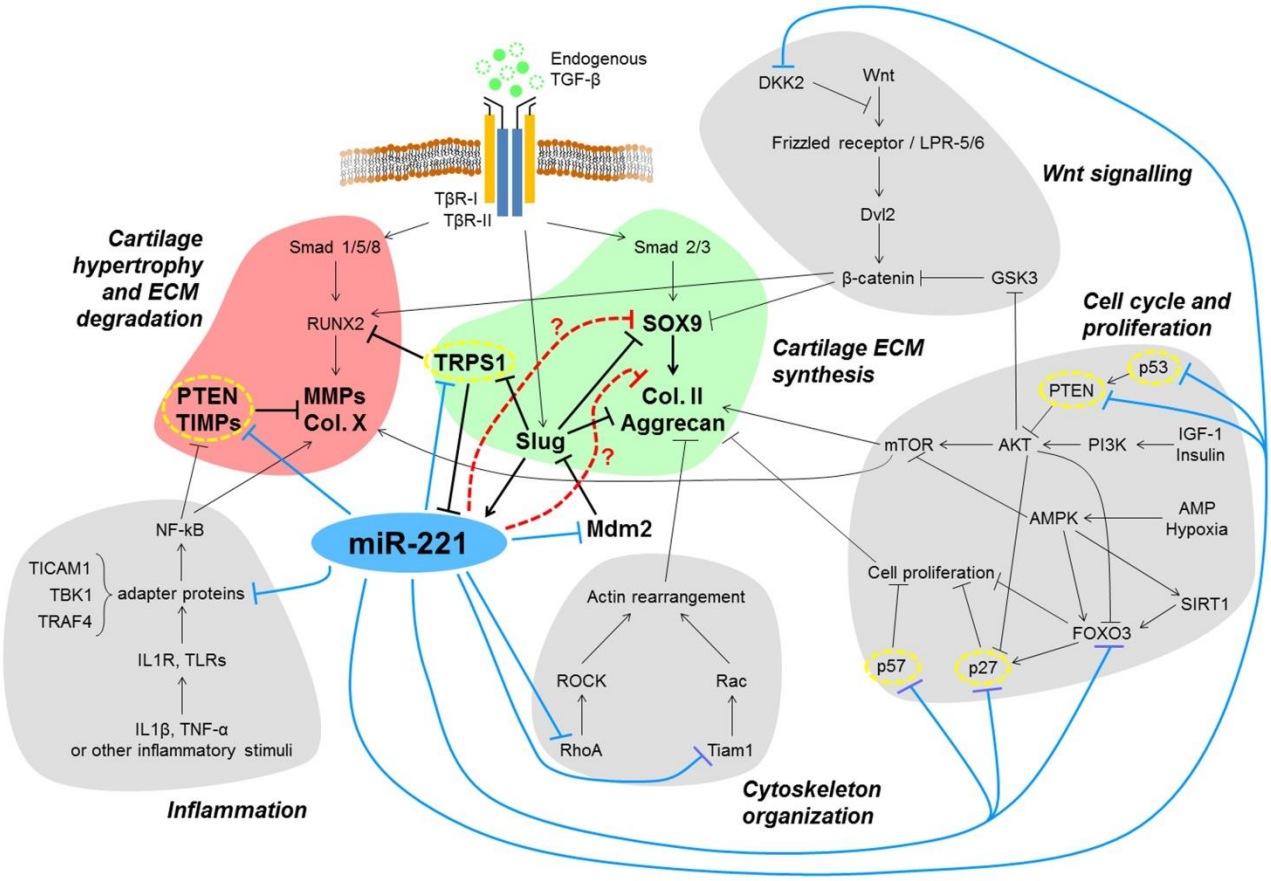

Figure 3.2.1: general overview of miR-221 targets and downstream effects potentially affecting the synthesis and maintenance of cartilage ECM. Six possible scenarios have been considered: cartilage hypertrophy and ECM degradation, cartilage ECM synthesis, Wnt signaling, cell cycle and proliferation, cytoskeleton organization and inflammation (for the references of target genes see Supplemental Table 3.2.1). Among the experimentally validated targets of miR- 221 (blue lines) are transcription factors and regulators involved in signaling pathways that directly or indirectly affect cartilage ECM remodeling: the implications of miR-221 into molecular pathways directly involved in ECM synthesis (green backdrop) or degradation (red backdrop) were evidenced. Common targets of miR-221 and miR-222 are circled in yellow.

In order to shed light onto this intricate scenario, we decided to submit miR-221 depleted hMSCs to a high-throughput screening system based on RNA-sequencing (RNA-seq) approach: this technique allows the study of the whole transcriptome of cells giving an accurate quantification of the expression levels of the detected targets (*Wang et al, 2009*). A first analysis was performed on 2 samples of hMSCs and for each sample the comparison between the transcriptome of untreated and miR-221 silenced cells was carried out. From this investigation 110 genes were found up-regulated in cells where miR-221 was depleted respect to control cells: as reported in Figure 3.2.2A, these

genes were implicated in different cellular functions, such as mitosis and proliferation, DNA replication and modification, signaling transduction, adhesion and ECM interaction, cytoskeleton organization, transcriptional regulation, ubiquitination and inflammation. Among the up-regulated genes, some of them were already reported in literature as factors implicated in chondrogenesis and cartilage tissue formation/maintenance: they include CD44, GDF5, HAS2, MKI67, MMP1, SOX9, STMN1, WNT5A and WNT5B (Figure 3.2.2B).

A

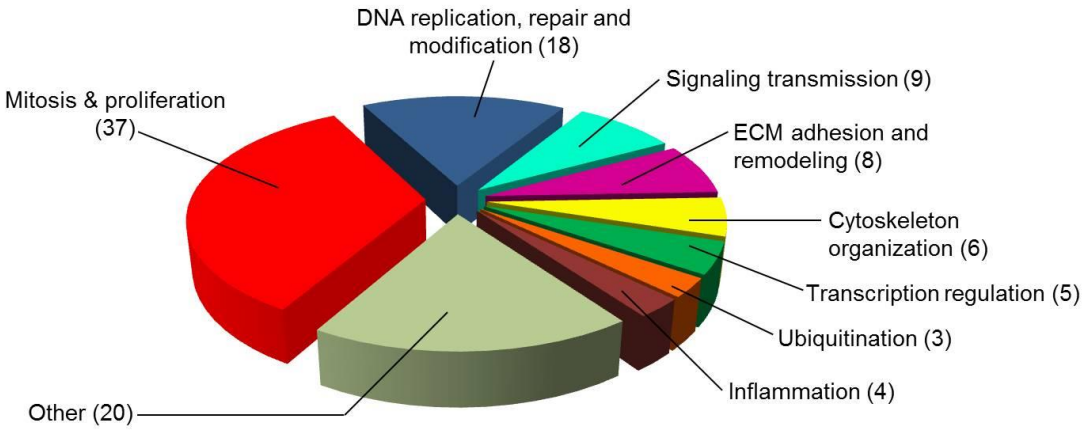

B

Gene	Protein name	Cellular function	Implication in chondrogenesis and cartilage tissue	References
CD44	CD44, receptor for hyaluronic acid	ECM binding	Involved in cartilage development and chondrogenesis intitation	*Knudson, 2003; Wu et al, 2013*
GDF5	Growth/differentiation factor 5	BMP signaling	Involved in chondrogenesis and endochondral ossification	*Coleman et al, 2013*
HAS2	Hyaluronan synthase 2	Hyaluronan biosynthesis	Its knockout has been associated with chondrogenesis and joint defects	*Liu et al, 2013*
MKI67	Antigen KI-67	Cell proliferation	Associated to chondrocytes proliferation	*Apte and Athanasou, 1992*
MMP1	Interstitial collagenase	ECM degradation	Cartilage ECM degradation in osteoarthritis	*Wu et al, 2008; Troeberg and Nagase, 2012*
SOX9	Transcription factor Sox9	Transcription regulation	Master regulator of chondrogenic differentiation	*Akiyama et al, 2002*
STMN1	Stathmin	Microtubule organization	Involved in chondrocytes proliferation and differentiation state	*Hummert et al, 2000; Hummert et al, 2001*
WNT5A	Protein Wnt-5a	Wnt signaling	Involved in chondrogenesis and chondrocyte hypertrophy	*Bradley and Drissi, 2010*
WNT5B	Protein Wnt-5b	Wnt signaling	Sustain chondrocyte proliferation and inhibit chondrocyte hypertrophy	*Bradley and Drissi, 2011; Wu et al, 2015*

Figure 3.2.2: candidate miR-221 target genes identified by RNA-seq analysis. (A) The study of the transcriptome of 2 sample of hMSCs revealed the up-regulation of 110 genes in hMSCs depleted for miR-221 expression respect to untreated cells. In the graph the main cellular pathways in which these genes are involved are reported: mitosis and proliferation, DNA replication, repair and modification, signaling transduction, ECM adhesion and remodeling, cytoskeletal organization, transcription regulation, ubiquitination and inflammation. For each pathway the number of implicated genes is reported in brackets. (B) List of up-regulated genes in miR-221 silenced hMSCs for which an association with chondrogenesis and cartilage development/homeostasis is already reported in literature.

Notably, the master regulator of chondrogenesis Sox9 resulted as one of the up-regulated genes in mir-221 depleted hMSCs: this evidence is in agreement with our previous studies (*Lolli et al, 2014; Lolli et al, 2016*) and with a recent paper where the investigation of the 3'UTRome showed Sox9 as a candidate target of miR-221 (*Kotagama et al, 2015*). It is interesting also the presence of molecules involved in the hyaluronan pathway in the group of up-regulated genes, including the binding protein CD44 and the hyaluronan synthase 2 (Has2): hyaluronic acid is one of the main GAG in the cartilage ECM with relevant structural and metabolic roles and its presence is essential for normal development and function of the cartilage. In fact, the knock-out of Has2 has been associated with defects in chondrogenesis and cartilage development and issues in joint positioning (*Liu et al, 2013*), while the inhibition of CD44-hyaluronan binding resulted in a reduced chondrogenesis of hMSCs, indicating the importance of this signaling pathway in triggering the initiation of the chondrogenic process (*Wu et al, 2013*). Finally it is not really surprising that also genes associated to the Wnt signaling, such as Wnt-5a and -5b, are up-regulated in miR-221 silenced hMSCs, since this molecular pathway in one of the main involved in cartilage development and formation, even though its role has not yet been fully elucidated and controversial results have been obtained depending on the activation of different signaling cascades (*Hartmann and Tabin, 2000; Usami et al, 2016*).

To further select the candidate miR-221 target genes, a bioinformatic analysis has been performed to search the presence of the homologous miR-221 sequence (seed sequence) in the 3'UTR of the RNA-seq identified genes. The binding to canonical seed sequence in the 3'UTR is a well-known mechanism throughout microRNAs regulate the post-transcriptional expression of target genes; however more recently the presence of seed sites also in other mRNA region have emerged (*Lytle et al, 2007; Hafner et al, 2010; Fang and Rajewski, 2011*): for this reason the research of the seed sequence was extended also to the promoter, the coding sequence (CDS) and the 5' untranslated region (5'UTR). Bioinformatic analysis was carried out through the miRWalk 2.0 (*http://zmf.umm.uni-heidelberg.de/apps/zmf/mirwalk2*), a comprehensive database of predicted and validated miRNA-target interactions which allows the prediction of miRNA binding sites comparing the outcomes from 12 existing programs (*Dweep and Gretz, 2015*). In Table 3.2.1 the up-regulated genes which contain a predicted binding site for miR-221 were reported, indicating also where the homologous sequence was estimated (i.e. 3'UTR, CDS, 5'UTR or promoter): only 2 of the listed genes (highlighted in blue) were already validated in literature as miR-221 targets,

namely MYBL1 (*Pineau et al, 2009*) and STMN1 (*Liu et al, 2015*), beyond the context of chondrogenesis.

Table 3.2.1: predicted miR-221 binding site by miRWalk 2.0 program in genes identified by RNA-seq analysis.

		Binding site position			
Gene	**Protein name**	**3'UTR***	**CDS***	**5'UTR***	**Promoter**
AK5	Adenylate kinase isoenzyme 5	-	-	-	*Yes*
BRCA1	Breast cancer type 1 susceptibility protein	*Yes*	*Yes*	-	-
BUB1	Mitotic checkpoint serine/threonine protein kinase BUB1	-	-	-	*Yes*
C14orf80	Uncharacterized protein C14orf80	-	-	*Yes*	-
CD44	CD44, receptor for hyaluronic acid	*Yes*	-	-	-
CDC6	Cell division control protein 6 homolog	-	-	-	*Yes*
CENPA	Histone H3-like centromeric protein A	*Yes*	-	-	-
CIT	Citron Rho interacting kinase	*Yes*	-	-	*Yes*
CNIH3	Protein cornichon homolog 3	*Yes*	-	-	-
DEPDC1	DEP domain-containing protein 1A	*Yes*	-	-	-
ESPL1	Separin	-	*Yes*	-	*Yes*
FAM65C	Protein FAM65C	*Yes*	-	-	-
FAM83D	Protein FAM83D	-	*Yes*	-	-
FANCG	Fanconi anemia complementation group G	*Yes*	-	-	-
HAS2	Hyaluronan synthase 2	-	*Yes*	-	-
HAUS8	HAUS augmin-like complex subunit 8	*Yes*	-	-	-
IDNK	Probable gluconokinase	-	*Yes*	-	-
KIF20A	Kinesin-like protein KIF20A	*Yes*	-	-	-
KIF4A	Chromosome-associated kinesin KIF4A	-	*Yes*	-	-
MKI67	Antigen KI-67	*Yes*	-	-	-
MMP1	Interstitial collagenase	*Yes*	-	-	-
MYBL1	Myb-related protein A	*Yes*	*Yes*	-	*Yes*

Gene	Protein name	3'UTR*	CDS*	5'UTR*	Promoter
PAQR4	Progestin and adipoQ receptor family member 4	-	*Yes*	-	-
PLAU	Urokinase-type plasminogen activator	-	-	-	*Yes*
RAD54L	DNA repair and recombination protein RAD-54 like	*Yes*	-	-	-
RECQL4	ATP-dependent DNA helicase Q4	-	-	-	*Yes*
RFX8	DNA-binding protein RFX8	*Yes*	-	-	-
S100A4	Protein S100-A4	-	-	-	*Yes*
SEMA3A	Semaphorin-3A	-	-	-	*Yes*
SOX9	Transcription factor Sox9	*Yes*	-	-	-
SPOCD1	SPOC domain-containing protein 1	-	*Yes*	-	-
STMN1	Stathmin	*Yes*	-	-	-
TIAF1	TGFβ1-induced anti-apoptotic factor 1	-	-	-	*Yes*
TMEM158	Transmembrane protein 158	-	-	-	*Yes*
WNT5A	Protein Wnt-5a	-	*Yes*	-	-
WNT5B	Protein Wnt-5b	-	-	*Yes*	-

* 3'UTR = 3' untranslated region; CDS = coding sequence; 5'UTR = 5' untranslated region
Validated targets

It is interesting to underline how, among genes associated with chondrogenesis and cartilage formation, previously mentioned in Figure 3.2.2B, all of them presented a predicted binding site for miR-221, apart from GDF5. It is surprising the identification of a binding site in the Sox9 3'UTR, since our previous investigations didn't evidence the presence of the miR-221 seed sequence in this region (*Lolli et al, 2016*). Through a deeper examination of the Sox9 3'UTR, a 6-bp homologous sequence was found which differs from the 7-bp miR-221 seed sequence for 1 base: the advancement in computational programs allowed the recognition of this not-fully complementary sequence as a probable binding site for miR-221. In fact recent evidences demonstrated that the full complementarity between miRNA and seed sequence is not always requested for miRNA-target interaction, suggesting that miRNA function could be carried out also through these non-canonical sites (*Hausser and Zavolan, 2014*). Even though these data are promising for the identification of

miR-221 chondro-targets, the experimental validation need to be performed (e.g. luciferase reporter assay, western blot analysis) and the work is currently in progress.

A relevant aspect of the employment of miRNA-binding site prediction algorithms is the high percentage of false positive and false negative in the resulting outcomes and this situation is further complicated by the possibility of new miRNA-target interaction mechanisms which have not yet been elucidated and, thus, can't be taken into account in prediction programs (*Witkos et al, 2011*). Thus, even if computational analysis are really useful, they could not be the only evidence to identify miRNA targets and furthermore we could not completely exclude miR-221 interaction with unidentified binding sites in the other genes highlighted by RNA-seq analysis. Another important aspect is that expression and, consequently, interactions of miRNAs and target genes are strictly dependent from the cellular model and microenvironment (*Jacobsen et al, 2013*): thus experimental validation of the miR-221 targets should be performed in hMSCs, possibly in pro-chondrogenic conditions.

With respect to these considerations, we decided to set up a miniaturized chondrogenic screening system in hMSCs, in order to identify which genes have effectively a pro-chondrogenic effect and subsequently validate them as miR-221 chondro-targets. The miniaturization of the system should allow the simultaneous study of a large number of genes with the employment of a reduced amount of cells that is a relevant aspect being hMSCs primary cells with relatively limited expansion potential. An essential feature of a screening system should be the easy survey of a specific and quantifiable reporter signal linked to the effect of external stimuli into the cells: in our case we decided to use a luciferase based system, through the employment of a reporter vector, namely pGL2-4ECol2luc vector (Figure 3.2.3A). This vector, previously employed in literature (*Hata et al, 2008*), consists in a luciferase gene under the control of specific chondrogenic responsive elements, which include a short sequence (from -108 to +16 bp) of the proximal promoter of the collagen type 2 and four repeated enhancer sequences which correspond to consensus sites for Sox9: the exposure to chondrogenic stimuli should increase Sox9 expression, which, in turn, should stimulate the expression of the luciferase through the binding at the consensus sequences. Two experimental strategies were designed, as reported in Figure 3.2.3B: in the first case (i) hMSCs were seeded in flat-bottom 96-well plates and after 24 hours cells were co-transfected with the pGL2-4ECol2luc vector and an expression vector for one of the candidate pro-chondrogenic gene; after 72 hours cells were lysed and the luciferase expression levels were assessed. In the second strategy (ii) a 3D culture system was approached through the realization of hMSCs micro-pellet in round-bottom 96-well plates: the transfection step was performed contemporarily to micro-pellet formation and the

luciferase assay was performed after 72 hours. Through a progressive decrease of cell number, the minimal amount of hMSCs to obtain the micro-pellet formation was determined at $1.5x10^4$ cells (data not shown).

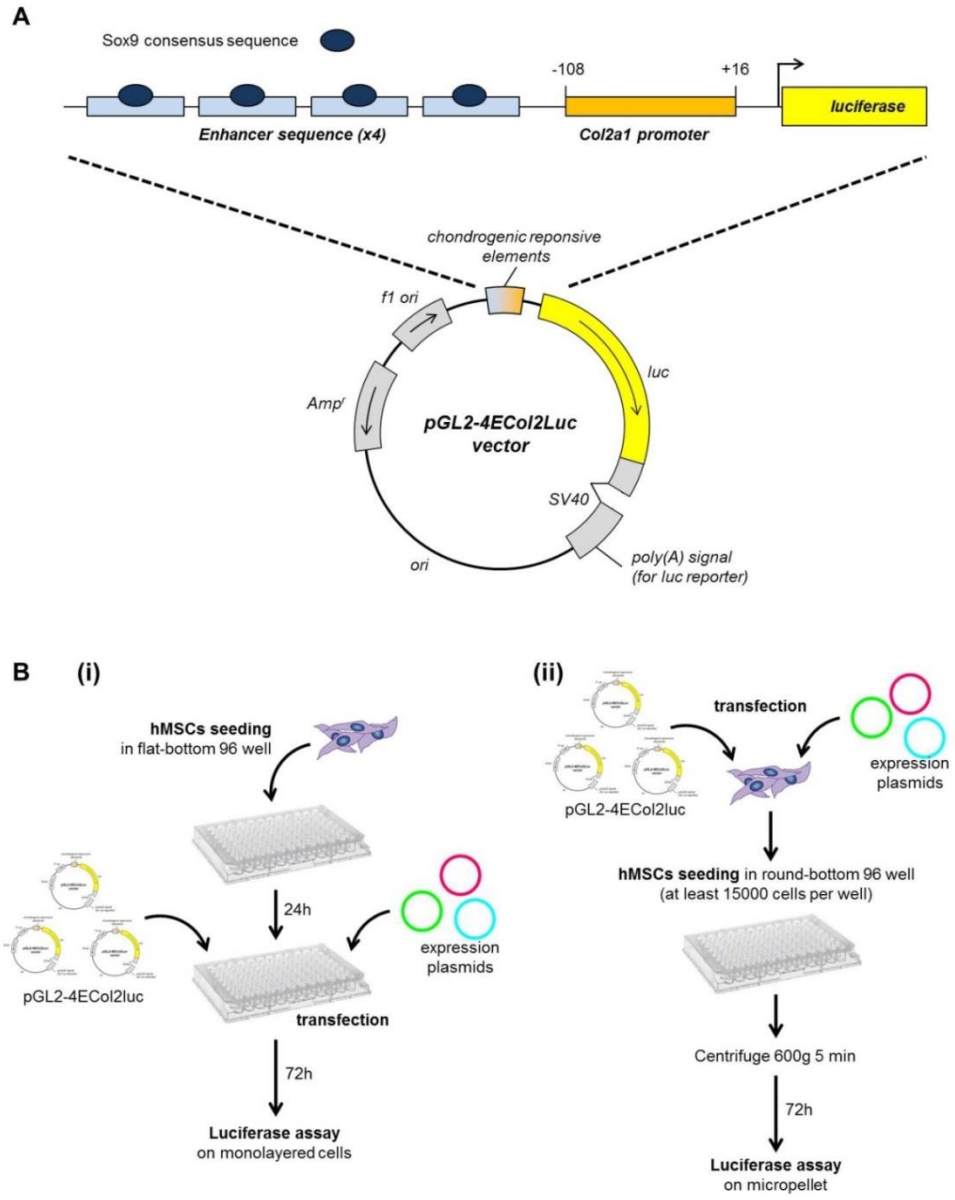

Figure 3.2.3: set-up of the chondrogenic screening system in hMSCs. (A) pGL2-4ECol2luc vector was employed as the reporter system for the chondrogenic screening. The vector consists in a luciferase gene (in yellow) under the control of a short sequence (from -106 to +16 bp) of the proximal promoter of collagen type 2 (Col2a1) (in orange) and four tandem-repeated consensus sequences for Sox9 (in blue) (*Hata et al, 2008*). (B) Schematic representation of the two experimental strategies designed for the chondrogenic screening system. In (i) hMSCs were cultured in monolayer in flat-bottom 96-well plates and transfected after 24 h with the pGL2-4ECol2luc vector and the expression plasmid for the candidate pro-chondrogenic gene. After 72 h luciferase assay was performed. In (ii) $1,5x10^4$ hMSCs were seeded in round-bottom 96-well plate and centrifugated to allow the formation of micro-pellets. Transfection step was performed contemporarily to cell seeding and luciferase expression was assessed after 72 h.

The establishment of a 3D screening system is a relevant point since a proper hMSCs chondrogenesis occurs only in a three-dimensional microenvironment and, thus, this type of culture could highly influence cell response to the pro- or anti-chondrogenic stimuli (*Tortelli and Cancedda, 2009*). In literature few reports about chondrogenic screening are present: some of these (*Hata et al, 2008; Kan et al, 2009*) used monolayered ATDC5 cells (a chondrogenic cell line) as cellular model with the risk of obtaining artificial results for the aforementioned reasons. Regarding the employment of MSCs, Huang and colleagues described a high-throughput screening system based on bovine MSCs micro-pellets where the chondrogenic effect was measured through the content of GAGs by DMMB (*Huang et al, 2008*): even though this approach is low cost, GAG quantification by this method is poor sensitive and lack of specificity respect to the analysis of proper chondrogenic markers, as in pGL2-4ECol2luc vector. In a more elegant work, Occhetta et al. developed an innovative microfluidic platform to culture micromasses made of few tens of hMSCs that could subsequently be used to test effect of drugs or morphogens on chondrogenesis: authors demonstrated the feasibility to use this platform as a tool to study molecular mechanisms implicated in chondrogenesis, however a true screening was not performed and, in addition, the system currently lacks of a suitable reporter marker which could help in the outcomes comprehension (*Occhetta et al, 2015*).

In the first phase of our study, we decided to test (i) the ability of the pGL2-4ECol2luc vector to respond to Sox9 and (ii) the practicability to successfully transfect the vector in hMSCs. To this aim pGL2-4ECol2luc vector was co-transfected both in HeLa cell line and in hMSCs together with two ratio of the expression plasmid for human Sox9 (1:2 and 1:1 respect to pGL2-4ECol2luc). Results are shown in Figure 4 and demonstrated: (i) pGL2-4ECol2luc is highly responsive to Sox9 over-expression in HeLa cells but not in hMSCs in a dose-dependent manner (Figure 3.2.4A) and (ii) the poor responsiveness in hMSCs is probably related to the difficulty in transfecting this kind of cells with classical liposome-based approach (*Halim et al, 2014*). In fact, when cells were transfected with a control vector which constitutively express luciferase, HeLa cells showed high and appreciable levels of luciferase, differently from hMSCs (Figure 3.2.4B). These evidences sustain the scarce feasibility into applying this transfection approach in hMSCs, particularly if we think to a 3D screening system as our final aim: in fact 3D high cell-density culture represents a further hindrance to transfection success.

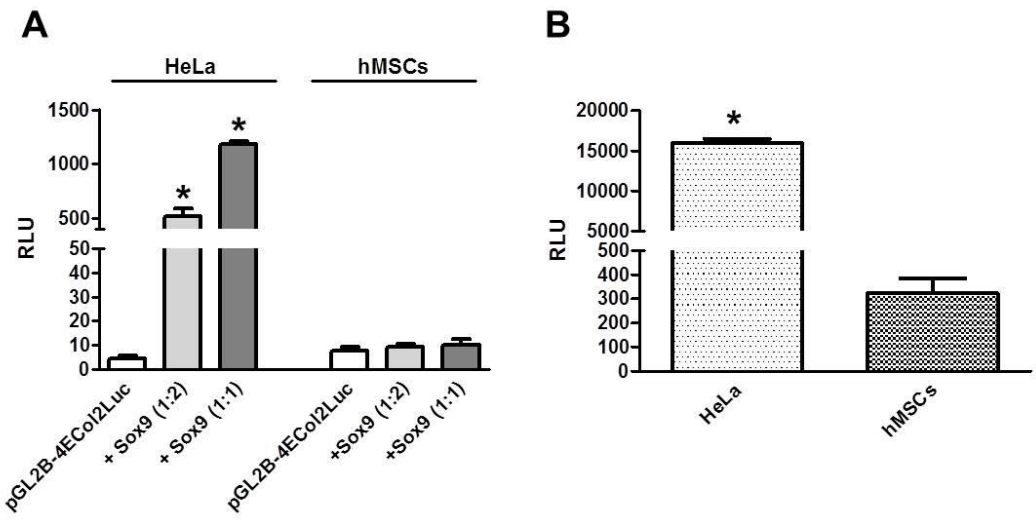

Figure 3.2.4: responsiveness of pGL2B-4ECol2 vector to Sox9 and transfection efficiency in HeLa cell line and hMSCs. (A) HeLa cells or hMSCs were co-transfected with pGL2B-4ECol2luc vector and the expression plasmid for human Sox9. Two amount ratios of Sox9/pGL2B-4ECol2luc were employed (1:2 and 1:1). (B) HeLa cells or hMSCs were transfected with the pGL3 control vector which allows the constitutive expression of the luciferase gene. The lower levels of luciferase expression in hMSCs, indicating a reduced efficiency of transfection, should be noted. Luciferase activity was normalized on total protein amount and data are presented as mean ± SEM. *p≤0.05 were considered significant.

For this reason an alternative gene transfer approach was conceived. Viral vectors have shown high superiority in the delivery of exogenous DNA into hMSCs and, among them, adeno-associated virus (AAV) have emerged as a promising strategy thanks to their greater safety, the possibility to employ different serotype exploiting their specific tropism and the ability to sustain long-term transgene expression (*Stender et al, 2007; Daya and Berns, 2008*). A preliminary experiment was conducted on one sample of hMSCs in order to evaluate the transduction efficiency: at this purpose AAV vectors containing green fluorescent protein (GFP) gene were employed and after 72 hours the percentage of GFP-positive cells was evaluated and compared with that one of hMSCs transfected with GFP through liposome-based approach. Two AAV serotypes were tested, namely AAV-2, being the main employed in gene therapy (*Daya and Berns, 2008*), and AAV-DJ, an artificial pseudoserotype demonstrating higher gene delivery efficiency (*Lakhan et al, 2015*). As shown in Figure 3.2.5, at a multiple of infection (MOI) of 10^5 both AAV-2 and AAV-DJ vectors highly increase (more than twofold) the percentage of hMSCs positive for GFP-expression, indicating, as expected, an increased efficiency in transgene delivery.

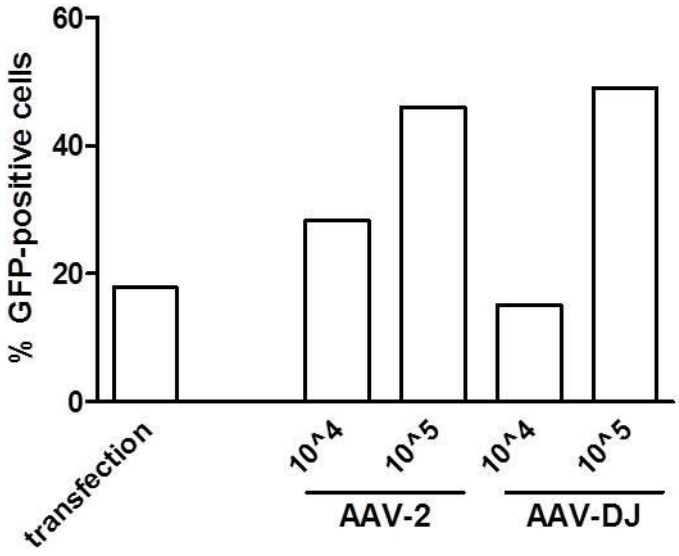

Figure 3.2.5: efficiency of transduction of hMSCs with adeno-associated viral (AAV) vectors. A GFP transgene was delivered into one sample of hMSCs through liposome-based transfection or through the employment of AAV vectors. Two AAV serotype were used (AAV-2 and AAV-DJ) at two different MOI (10^4 and 10^5). The percentage of GFP-positive cells after 72 hours was reported.

Conclusion

Although data here reported are still in progress, they are really promising regarding the two main aims of this work: (i) the identification of miR-221 chondro-targets and (ii) the development of a chondrogenic screening system. RNA-seq analysis evidenced 110 up-regulated genes in miR-221 depleted hMSCs, and 9 of these have already been implicated in chondrogenesis and cartilage development, sustaining a possible involvement in hMSCs chondrogenic differentiation guided by miR-221 silencing. However a new chondrogenic role for the other identified genes could not be excluded and for this reason the development of a 3D miniaturized chondrogenic screening system based on hMSCs is extremely advantageous. AAV vectors seems to be a good choice for the development of this screening system, which in future could be helpful also as a platform to test a high number of morphogens, drugs and other bioactive molecules to apply in cartilage tissue engineering strategies.

Supplemental Table 3.2.1: validated targets of miR-221 reported in Figure 3.2.1

Target gene	Cell signaling pathway	Reference
Validated targets by strong evidences*		
CDKN1B (p27)	Oncogenesis	*Galardi et al, 2007*
CDKN1C (p57)	Cell cycle	*Fornari et al, 2008*
DKK2	Wnt signaling	*Pineau et al, 2010*
FOXO3	Oncogenesis/Apoptosis	*Garofalo et al, 2012*
MDM2	Cell cycle	*Kim et al, 2010*
PTEN	Cell cycle	*Garofalo et al, 2009*
TBK1	Oncogenesis/Inflammation	*Pineau et al, 2010*
TICAM1	Inflammation	*Gong et al, 2011*
TIMP2	Oncogenesis	*Xu et al, 2015*
TIMP3	Oncogenesis	*Garofalo et al, 2009*
TP53 (p53)	Cell cycle	*Yang et al, 2011b*
TRPS1	Epithelial-mesenchymal transition	*Stinson et al, 2011*
Validated targets by NGS*: RHOA, TIAM1, TRAF4 (*from http://www.mirbase.org*)		

* strong evidences = reporter assay, Western blot and qPCR; NGS = next generation sequencing

Chapter 3 – section 3

Discussion and conclusions

Multipotency of MSCs is an important feature that made these cells ideal candidates for bone and cartilage tissue engineering. However their differentiation is still scarcely controlled and inefficient for TE application, and for this reason the control of stem cell fate has become a major area of interest (*Griffin et al, 2015*). The differentiation of hMSCs into a lineage rather than another one depends by the coordination of a plethora of molecular signals, governed by growth factors, transcription factors and microRNAs, leading to different transcriptional signatures characterizing each type of differentiated cells (*Ng et al, 2013; Bombonato-Prado et al, 2015*). Thus, the identification of these specific factors and their role in hMSCs is an essential step to obtain a complete control on the differentiation towards a precise lineage and, consequently, the best outcomes in tissue engineering approaches: the ability to modulate biological effectors to maintain a desired differentiation program, or possibly to prevent spurious differentiation of MSCs, is needed for effective clinical application (*Kolf et al, 2007*).

MitoTFs and metabolic state of hMSCs

Metabolism is a finely controlled process in hMSCs and recent studies have evidenced its active role in determining cell fate and adaptation to external microenvironment: for example it has been shown how glycolysis is able to sustain stem cell proliferation and self-renewal, while metabolic reconfigurations occur during differentiation allowing to meet increasing energy demand of the differentiated phenotype (Figure 3.3.1) (*Liu and Ma, 2014*). Thus, the understanding of the metabolic cues controlling MSC fate provides new ways for the improvement of therapeutic effects of cell-based TE approaches. In this context the discovery of an alternative role in mitochondria for nuclear transcription factors is of high interest in regenerative medicine field, since this mitoTFs act

as regulator of the mitochondrial DNA and, consequently, of the metabolic responses of the cells: it could be hypothesize that controlling the expression and localization of these factors, we could direct MSC metabolism and their fate.

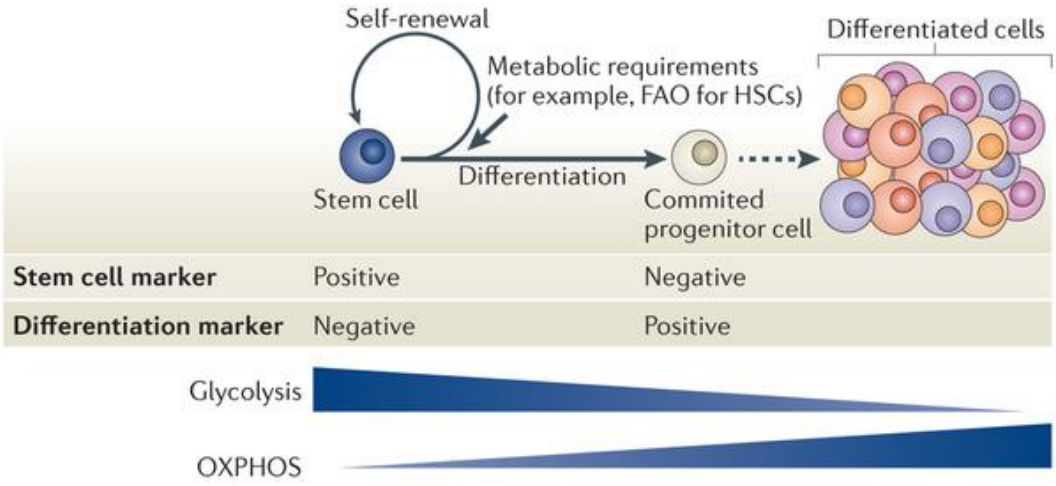

Figure 3.3.1: coordinated regulation between stem cell function and metabolism. Mitochondria in stem cells are relatively inactive and their energetic metabolism is heavily based on anaerobic glycolysis, whereas oxidative phosphorylation (OXPHOS) is associated with differentiation, as well as impaired stem cell function (*Ito and Suda, 2014*).

As described in Section 1 of this chapter, for the first time we demonstrated the presence of NFATc1 in mitochondria of osteo-differentiated hMSCs and its recruitment at the regulatory region D-loop of the mitochondrial DNA, where it acts as a negative regulator of the mitochondrial genes when the energetic request is lowered during calcification process. This is the first time that a mitoTF was directly correlated to osteogenesis, even though its specific role needs to be better clarified. Other transcription factors, more or less directly implicated in osteogenic differentiation, have been also found in mitochondria, but in cellular models different from osteogenesis. For example the signal transducer and activator of transcription 3 (STAT3) is a pro-osteogenic TF (*Nicolaidou et al, 2012; Huh and Lee, 2013*), which has been found in the mitochondria of several cell lines (*Zhang et al, 2013b; Kramer et al, 2015; Luo et al, 2016*). Similarly, estrogen receptor is an important factor sustaining bone remodeling process and preventing bone loss related to osteoporosis (*Nakamura et al, 2007; Manolagas et al, 2013*): its presence in mitochondria was firstly evidenced in rabbit uterus and ovary and, subsequently, in various cell lines (*Monje and Boland, 2001; Pedram et al, 2006; Milanesi et al, 2008*). These evidences suggested that NFATc1 is not the only transcription factor present in the mitochondria of osteo-differentiated hMSCs, but it

is highly probable that its action is coordinated with that one of other mitoTFs, which have not been identified yet.

Since mature osteogenic, chondrogenic and adipogenic lineages have distinct metabolic phenotypes, understanding the underlying metabolic regulation during hMSC differentiation is important in refining the lineage-specific commitment conditions: for example osteogenic differentiation is associated to an increase of bioenergetic demand and mitochondrial metabolism to sustain the switch from glycolysis to oxidative phosphorylation, while chondrogenesis is supported by an increment of the glycolytic activity. Thus, therapeutic strategies improving or reducing mitochondrial biogenesis and metabolism could be adopted to move MSC differentiation towards the osteogenic or chondrogenic lineage, respectively (*Liu and Ma, 2014*). In this context, the overexpression or inhibition of the mitoTFs controlling energetic metabolism in hMSCs and differentiated cells could be an alternative approach for directing the regenerative properties of implantable cells in tissue engineering therapies. However a more precise characterization of their role both in the nucleus and in mitochondria is surely needed to obtain the expected outcomes.

miRNA regulation in MSC differentiation

A demonstration of the key role of miRNAs in regenerative medicine derived from the fact that an intact miRNA biogenesis pathway is required for correct tissue development and regeneration: the knock-out of Dicer protein, an endoribonuclease with a central role in miRNA synthesis, causes the lack of almost all pluripotent stem cells and, consequently, embryonic death in mice (*Bernstein et al, 2003*). Furthermore it has been highlighted how only a small subset of miRNAs is expressed in stem cells, while the number increases as cells differentiate into specific tissues and organs (*Houbaviy et al, 2003; Hatfield et al, 2005; Wienholds and Plasterk, 2005*). The key role of miRNAs has emerged also in controlling cell fate of mesenchymal stem cells: for instance Oskowitz and colleagues demonstrated how silencing the expression of Dicer and Drosha, and consequently reducing miRNA biogenesis, highly impacted on osteogenic and adipogenic differentiation of hMSCs (*Oskowitz et al, 2008*). Successively, *in vitro* and *in vivo* analyses have identified miRNA expression patterns associated with a specific type of MSC differentiation, as reported in Figure 3.3.2 and as already discussed in paragraph 3.3 of Chapter 1. Thus, novel therapeutic strategies have emerged for cell-based tissue engineering approaches, exploiting the effect of specific miRNAs as positive or negative regulator of osteogenic/chondrogenic differentiation and the resulting tissue formation.

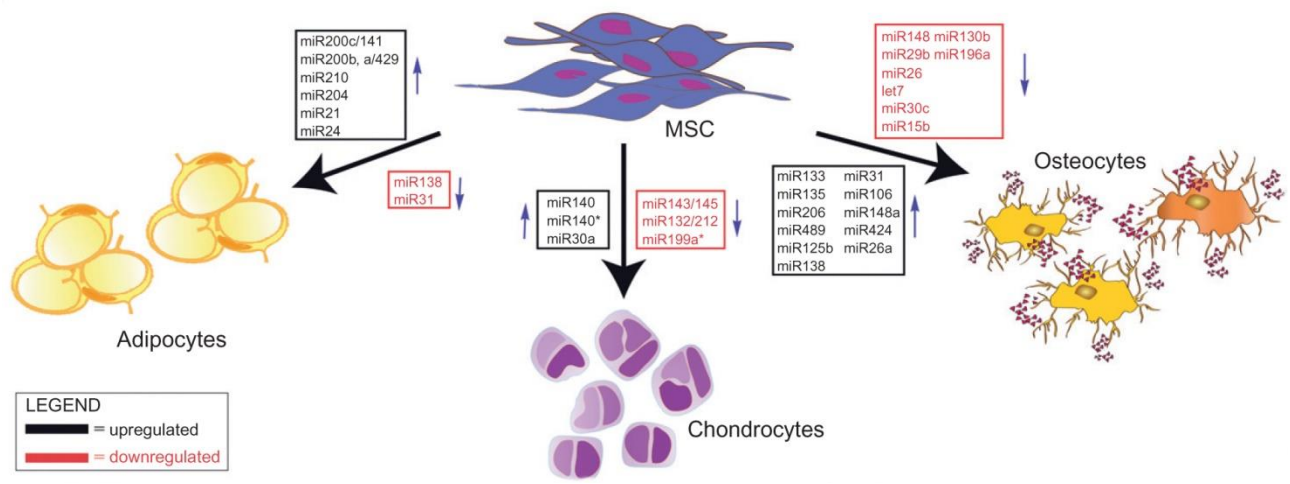

Figure 3.3.2: miRNA expression patterns in MSCs differentiating towards adipogenic, chondrogenic and osteogenic lineage. Red-labeled miRNAs are down-regulated, while black-labeled ones are up-regulated during differentiation process (*Collino et al, 2011*).

In this context, our group recently demonstrated how miR-221 is associated with chondrocyte de-differentiation and acts as an anti-chondrogenic factor in hMSCs: we showed how its inhibition is able to guide the formation of newly cartilage-like tissue both *in vitro* and *in vivo* (*Lolli et al, 2014; Lolli et al, 2016*). These evidences are at the basis of the work reported in Section 2 of this chapter, which aimed to investigate the mechanism of action throughout miR-221 silencing sustains chondrogenic differentiation of hMSCs. The RNA-seq analysis performed on two samples of miR-221 silenced hMSCs highlighted 110 over-expressed genes and, thus, possible targets of miR-221. Obviously they need to be validated as effective targets of the examined microRNA and their pro-chondrogenic role must be confirmed; however among these genes, some of them have been already related to chondrogenesis and cartilage formation, that is CD44, GDF5, HAS2, MKI67, MMP1, SOX9, STMN1, WNT5A and WNT5B (for the references see Figure 3.2.2B in Section 2). Nonetheless, each one of the up-regulated genes could be considered a miR-221 candidate target with a new and unrevealed role in chondrogenesis; furthermore the identification of the targets is complicated by novel or unexplored mechanisms of action of miRNAs, which are not considered by prediction programs: for example we found in Sox9 3'UTR a 6-bp homologous sequence which differs from the 7-bp miR-221 seed sequence for 1 base.

Mechanisms of miRNA-target interaction

In order to play their function, miRNAs need to recognize and bind their mRNA targets. The first discovered mechanism guiding this recognition is based on the perfect pairing between a short sequence centered between nucleotides 2-8 in the 5' end of the miRNA, called seed sequence, and the complementary sequence in the 3'UTR of the target mRNA (*Bartel, 2009*). However it has been demonstrated how the presence of seed site in a mRNA does not ensure the occupancy by a selected miRNA, and conversely many functional miRNA binding sites exist outside the 3'UTR (*Cloonan, 2015*). For instance, it has been demonstrated that some miRNAs can modulate the expression of target mRNAs through the binding to 5'UTR, the coding region or, even, the promoter of target genes (*Lee et al, 2009; O'Connell, 2012; Reczko et al, 2012*). Furthermore, as reported in Figure 3.3.3, non-canonical (non-seed mediated) binding sites have been identified and functionally validated: for instance Chi and colleagues were able to identify novel sites characterized by the presence of an extra G in the mRNA causing an imperfect match with the miRNA and the formation of a "G-bulge" (*Chi et al, 2012*). Also the matching with the 3' sequence of the miRNA has been identified: nucleotides 13-16 could pair to mRNA to strengthen the interaction through the seed-site (3' supplementary binding) or the G-bulge model (3' compensatory binding) (*Bartel, 2009*). Finally an extension of the nucleotides (up to nucleotides 13-17) involved in the target recognition has been reported (perfect centered binding), but the match between the miRNA and mRNA sequences could be frequently not perfect (imperfect centered binding) (*Martin et al 2014*). The identification of these alternative interaction mechanisms complicates the panorama of the miRNA-mRNA networks, but it will help us to identify new possible targets and unexplored biological pathways. There is no doubt that prediction tools and databases should evolve to take in consideration these novel mechanisms, in order to sustain the recognition of new miRNA targets.

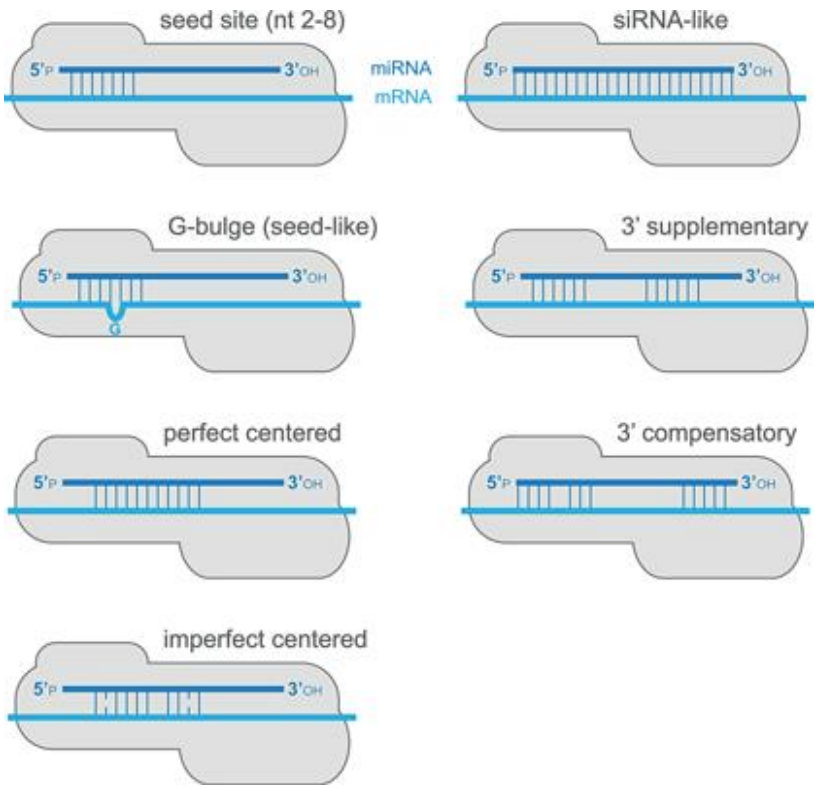

Figure 3.3.3: novel mechanisms for miRNA-mRNA interactions (*Cloonan, 2015*).

Conclusions and future perspectives

Evidences reported in this chapter are of great interest for the study of hMSC differentiation towards osteogenic and chondrogenic lineage, and also for tissue engineering applications, suggesting the identification of novel therapeutic targets in MSC-based approaches.

In particular, we demonstrated a new role for the transcription factor NFATc1 in the mitochondria of osteo-differentiated hMSCs (Section 1), indicating its involvement in the control of cell metabolism during osteogenic differentiation. The specific contribution of NFATc1 should be better characterized and also the mechanism of transport into mitochondria will be studied. It will be interesting exploring how the presence or the absence (inhibiting its transport) of NFATc1 into mitochondria could affect not only hMSC metabolism, but also the osteogenic and calcification processes. More detailed analysis about the function of NFATc1 and its cooperation with other mitoTFs during osteogenic differentiation will be helpful in the realization of new strategies able to improve the regenerative potential of hMSCs and their specific commitment towards the osteoblastic lineage.

Regarding the work presented in the Section 2, it will be our interest validating the effective targets of miR-221 in chondrogenic hMSCs, through luciferase assay or Western blot analysis after miR-221 depletion or overexpression. Furthermore it will be intriguing to achieve the complicated set-up of the MSC-based chondrogenic screening system, in order to identify miR-221 targets involved in chondrogenesis: these molecules could be employed as new molecular targets in pharmacological or genetic treatments or to improve the chondro-regenerative ability of hMSCs for tissue engineering. Finally the screening system could be employed as a reliable *in vitro* platform to assess the pro- or anti-chondrogenic properties of a large amount of drugs and bioactive molecules.

Chapter 4

References

Achilli, T.M., Meyer, J., and Morgan, J.R. (2012). Advances in the formation, use and understanding of multi-cellular spheroids. Expert Opinion on Biological Therapy *12*, 1347–1360.

Akiyama, H., Chaboissier, M.C., Martin, J.F., Schedl, A., and de Crombrugghe, B. (2002). The transcription factor Sox9 has essential roles in successive steps of the chondrocyte differentiation pathway and is required for expression of Sox5 and Sox6. Genes & Development *16*, 2813–2828.

Albanese, A., Licata, M.E., Polizzi, B., and Campisi, G. (2013). Platelet-rich plasma (PRP) in dental and oral surgery: from the wound healing to bone regeneration. Immunity & Ageing *10*, 23.

Alexander, P.G., Gottardi, R., Lin, H., Lozito, T.P., and Tuan, R.S. (2014). Three-dimensional osteogenic and chondrogenic systems to model osteochondral physiology and degenerative joint diseases. Experimental Biology and Medicine *239*, 1080–1095.

Alvarez, K., and Nakajima, H. (2009). Metallic scaffolds for bone regeneration. Materials *2*, 790–832.

do Amaral, R.J.F.C., Pedrosa, C. da S.G., Kochem, M.C.L., Silva, K.R. da, Aniceto, M., Claudio-da-Silva, C., Borojevic, R., and Baptista, L.S. (2012). Isolation of human nasoseptal chondrogenic cells: a promise for cartilage engineering. Stem Cell Res *8*, 292–299.

Amenta, P.S., Scivoletta, N.A., Newman, N.D., Sciancalepore, J.P., Li, D., and Myers, J.C. (2005). Proteoglycan-collagen XV in human tissues is seen linking banded collagen fibers subjacent to the basement membrane. Journal of Histochemistry and Cytochemistry *53*, 165–176.

An, J., Teoh, J.E.M., Suntornnond, R., and Chua, C.K. (2015). Design and 3D printing of scaffolds and tissues. Engineering *1*, 261–268.

Angelozzi, M., Miotto, M., Penolazzi, L., Mazzitelli, S., Keane, T., Badylak, S.F., Piva, R., and Nastruzzi, C. (2015). Composite ECM-alginate microfibers produced by microfluidics as scaffolds with biomineralization potential. Mater Sci Eng C Mater Biol Appl *56*, 141–153.

Apte, S.S., and Athanasou, N.A. (1992). An immunohistological study of cartilage and synovium in primary synovial chondromatosis. The Journal of Pathology *166*, 277–281.

Aulino, P., Costa, A., Chiaravalloti, E., Perniconi, B., Adamo, S., Coletti, D., Marrelli, M., Tatullo, M., and Teodori, L. (2015). Muscle extracellular matrix scaffold is a multipotent environment. International Journal of Medical Sciences *12*, 336–340.

Badylak, S., Freytes, D., and Gilbert, T. (2009). Extracellular matrix as a biological scaffold material: structure and function. Acta Biomaterialia *5*, 1–13.

Baino, F., Novajra, G., and Vitale-Brovarone, C. (2015). Bioceramics and scaffolds: a winning combination for tissue engineering. Frontiers in Bioengineering and Biotechnology *3*.

Balmayor, E.R., and van Griensven, M. (2015). Gene therapy for bone engineering. Frontiers in Bioengineering and Biotechnology *3*.

Bamias, A., Kastritis, Bamia, Moloupolous, Melakopolous, and Bozas (2005). Osteonecrosis of the jaw in cancer after treatment with bisphosphonates: incidence and risk factors. Journal of Clinical Oncology *23*, 8580–8587.

Barasch, A., Cunha-Cruz, J., Curro, F.A., Hujoel, P., Sung, A.H., Vena, D., Voinea-Griffin, A.E., the CONDOR Collaborative Group, Beadnell, S., Craig, R.G., et al. (2011). Risk factors for osteonecrosis of the jaws: a case-control study from the CONDOR Dental PBRN. Journal of Dental Research *90*, 439–444.

Barba-Recreo, P., Del Castillo Pardo de Vera, J.L., Georgiev-Hristov, T., Ruiz Bravo-Burguillos, E., Abarrategi, A., Burgueño, M., and García-Arranz, M. (2015). Adipose-derived stem cells and platelet-rich plasma for preventive treatment of bisphosphonate-related osteonecrosis of the jaw in a murine model. Journal of Cranio-Maxillofacial Surgery *43*, 1161–1168.

Baret, J.C. (2009). A remote syringe for cells, beads and particle injection in microfluidic channels. Chips and Tips.

Bartel, D.P. (2009). MicroRNAs: target recognition and regulatory functions. Cell *136*, 215–233.

Barthes, J., Özçelik, H., Hindié, M., Ndreu-Halili, A., Hasan, A., and Vrana, N.E. (2014). Cell microenvironment engineering and monitoring for tissue engineering and regenerative medicine: The Recent Advances. BioMed Research International *2014*, 1–18.

Baugé, C., Girard, N., Lhuissier, E., Bazille, C., and Boumediene, K. (2014). Regulation and role of TGFβ signaling pathway in aging and osteoarthritis joints. Aging and Disease *5*, 394–405.

Beavers, K.R., Nelson, C.E., and Duvall, C.L. (2015). MiRNA inhibition in tissue engineering and regenerative medicine. Advanced Drug Delivery Reviews *88*, 123–137.

Bellido, M., Lugo, L., Roman-Blas, J.A., Castañeda, S., Caeiro, J.R., Dapia, S., Calvo, E., Largo, R., and Herrero-Beaumont, G. (2010). Subchondral bone microstructural damage by increased remodelling aggravates experimental osteoarthritis preceded by osteoporosis. Arthritis Research & Therapy *12*, R152.

Ben Shoham, A., Rot, C., Stern, T., Krief, S., Akiva, A., Dadosh, T., Sabany, H., Lu, Y., Kadler, K.E., and Zelzer, E. (2016). Deposition of collagen type I onto skeletal endothelium reveals a new role for blood vessels in regulating bone morphology. Development *143*, 3933–3943.

Benders, K.E.M., Weeren, P.R. van, Badylak, S.F., Saris, D.B.F., Dhert, W.J.A., and Malda, J. (2013). Extracellular matrix scaffolds for cartilage and bone regeneration. Trends in Biotechnology *31*, 169–176.

Berenbaum, F. (2013). Osteoarthritis as an inflammatory disease (osteoarthritis is not osteoarthrosis!). Osteoarthritis and Cartilage *21*, 16–21.

Bernhard, J.C., and Vunjak-Novakovic, G. (2016). Should we use cells, biomaterials, or tissue engineering for cartilage regeneration? Stem Cell Research & Therapy *7*.

Bernstein, E., Kim, S.Y., Carmell, M.A., Murchison, E.P., Alcorn, H., Li, M.Z., Mills, A.A., Elledge, S.J., Anderson, K.V., and Hannon, G.J. (2003). Dicer is essential for mouse development. Nature Genetics *35*, 215–217.

van Beuningen, H.M., Glansbeek, H.L., van der Kraan, P.M., and van den Berg, W.B. (2000). Osteoarthritis-like changes in the murine knee joint resulting from intra-articular transforming growth factor-beta injections. Osteoarthr. Cartil. *8*, 25–33.

Bhattacharjee, M., Coburn, J., Centola, M., Murab, S., Barbero, A., Kaplan, D.L., Martin, I., and Ghosh, S. (2015). Tissue engineering strategies to study cartilage development, degeneration and regeneration. Advanced Drug Delivery Reviews *84*, 107–122.

Bi, Y., Stuelten, C.H., Kilts, T., Wadhwa, S., Iozzo, R.V., Robey, P.G., Chen, X.-D., and Young, M.F. (2005). Extracellular matrix proteoglycans control the fate of bone marrow stromal cells. Journal of Biological Chemistry *280*, 30481–30489.

Bianco, P., Cao, X., Frenette, P.S., Mao, J.J., Robey, P.G., Simmons, P.J., and Wang, C.-Y. (2013). The meaning, the sense and the significance: translating the science of mesenchymal stem cells into medicine. Nature Medicine *19*, 35–42.

Bidarra, S.J., Barrias, C.C., and Granja, P.L. (2014). Injectable alginate hydrogels for cell delivery in tissue engineering. Acta Biomaterialia *10*, 1646–1662.

Billing, A.M., Ben Hamidane, H., Dib, S.S., Cotton, R.J., Bhagwat, A.M., Kumar, P., Hayat, S., Yousri, N.A., Goswami, N., Suhre, K., et al. (2016). Comprehensive transcriptomic and proteomic characterization of human mesenchymal stem cells reveals source specific cellular markers. Scientific Reports *6*, 21507.

Birk, D.E., and Silver, F.H. (1984). Collagen fibrillogenesis *in vitro*: comparison of types I, II, and III. Arch. Biochem. Biophys. *235*, 178–185.

Birmingham, E., Niebur, G.L., McHugh, P.E., Shaw, G., Barry, F.P., and McNamara, L.M. (2012). Osteogenic differentiation of mesenchymal stem cells is regulated by osteocyte and osteoblast cells in a simplified bone niche. Eur Cell Mater *23*, 13–27.

Blaney Davidson, E.N., van der Kraan, P.M., and van den Berg, W.B. (2007). TGF-β and osteoarthritis. Osteoarthritis and Cartilage *15*, 597–604.

Bloemen, V., Schoenmaker, T., de Vries, T.J., and Everts, V. (2009). Direct cell–cell contact between periodontal ligament fibroblasts and osteoclast precursors synergistically increases the expression of genes related to osteoclastogenesis. Journal of Cellular Physiology n/a-n/a.

Boccaccio, A., Uva, A.E., Fiorentino, M., Mori, G., and Monno, G. (2016). Geometry Design Optimization of functionally graded scaffolds for bone tissue engineering: a mechanobiological approach. PLoS ONE *11*, e0146935.

Bombonato-Prado, K.F., Rosa, A.L., Oliveira, P.T., Dernowsek, J.A., Fontana, V., Evangelista, A.F., and Passos, G.A. (2014). Transcriptome analysis during normal human mesenchymal stem cell differentiation. In Transcriptomics in Health and Disease, G.A. Passos, ed. (Cham: Springer International Publishing), pp. 109–119.

Bonaventure, J., Kadhom, N., Cohen-Solal, L., Ng, K.H., Bourguignon, J., Lasselin, C., and Freisinger, P. (1994). Reexpression of cartilage-specific genes by dedifferentiated human articular chondrocytes cultured in alginate beads. Exp. Cell Res. *212*, 97–104.

Bononi, A., and Pinton, P. (2015). Study of PTEN subcellular localization. Methods *77–78*, 92–103.

Boonrungsiman, S., Gentleman, E., Carzaniga, R., Evans, N.D., McComb, D.W., Porter, A.E., and Stevens, M.M. (2012). The role of intracellular calcium phosphate in osteoblast-mediated bone apatite formation. Proceedings of the National Academy of Sciences *109*, 14170–14175.

Boskey, A.L. (2013). Bone composition: relationship to bone fragility and antiosteoporotic drug effects. BoneKEy Reports *2*.

Boushell, M.K., Hung, C.T., Hunziker, E.B., Strauss, E.J., and Lu, H.H. (2016). Current strategies for integrative cartilage repair. Connective Tissue Research 1–14.

Bozec, A., Zaiss, M.M., Kagwiria, R., Voll, R., Rauh, M., Chen, Z., Mueller-Schmucker, S., Kroczek, R.A., Heinzerling, L., Moser, M., et al. (2014). T cell costimulation molecules CD80/86 inhibit osteoclast differentiation by inducing the IDO/tryptophan pathway. Science Translational Medicine *6*, 235ra60-235ra60.

Bradley, E.W., and Drissi, M.H. (2010). WNT5A regulates chondrocyte differentiation through differential use of the CaN/NFAT and IKK/NF-κB pathways. Molecular Endocrinology *24*, 1581–1593.

Bradley, E.W., and Drissi, M.H. (2011). Wnt5b regulates mesenchymal cell aggregation and chondrocyte differentiation through the planar cell polarity pathway. Journal of Cellular Physiology *226*, 1683–1693.

Brakke, R., Singh, J., and Sullivan, W. (2012). Physical therapy in persons with osteoarthritis. PM&R *4*, S53–S58.

Breslin, S., and O'Driscoll, L. (2013). Three-dimensional cell culture: the missing link in drug discovery. Drug Discovery Today *18*, 240–249.

Bretcanu, O., Misra, S., Roy, I., Renghini, C., Fiori, F., Boccaccini, A.R., and Salih, V. (2009). *In vitro* biocompatibility of 45S5 Bioglass ® -derived glass-ceramic scaffolds coated with poly(3-hydroxybutyrate). Journal of Tissue Engineering and Regenerative Medicine *3*, 139–148.

Brown, B.N., and Badylak, S.F. (2014). Extracellular matrix as an inductive scaffold for functional tissue reconstruction. Transl Res *163*, 268–285.

Bukowiecki, R., Adjaye, J., and Prigione, A. (2014). Mitochondrial function in pluripotent stem cells and cellular reprogramming. Gerontology *60*, 174–182.

Burra, S., Nicolella, D.P., Francis, W.L., Freitas, C.J., Mueschke, N.J., Poole, K., and Jiang, J.X. (2010). Dendritic processes of osteocytes are mechanotransducers that induce the opening of hemichannels. Proceedings of the National Academy of Sciences *107*, 13648–13653.

Bush, J.R., and Beier, F. (2013). TGF-β and osteoarthritis—the good and the bad. Nature Medicine *19*, 667–669.

Cagin, U., and Enriquez, J.A. (2015). The complex crosstalk between mitochondria and the nucleus: What goes in between? The International Journal of Biochemistry & Cell Biology *63*, 10–15.

Camarero-Espinosa, S., Rothen-Rutishauser, B., Foster, E.J., and Weder, C. (2016). Articular cartilage: from formation to tissue engineering. Biomater. Sci. *4*, 734–767.

Campisi, J., and d'Adda di Fagagna, F. (2007). Cellular senescence: when bad things happen to good cells. Nature Reviews Molecular Cell Biology *8*, 729–740.

Cancedda, R., Dozin, B., Giannoni, P., and Quarto, R. (2003). Tissue engineering and cell therapy of cartilage and bone. Matrix Biol. *22*, 81–91.

Capretto, L., Mazzitelli, S., Focaroli, S., and Nastruzzi, C. (2010). Wall plug inspired connectors for macro to microfluidic interfacing. Chips and Tips.

Cardemil, C., Thomsen, P., and Larsson Wexell, C. (2015). Jaw bone samples from bisphosphonate-treated patients: a pilot cohort study. Clinical Implant Dentistry and Related Research *17*, e679–e691.

Caron, M.M.J., Emans, P.J., Coolsen, M.M.E., Voss, L., Surtel, D.A.M., Cremers, A., van Rhijn, L.W., and Welting, T.J.M. (2012). Redifferentiation of dedifferentiated human articular chondrocytes: comparison of 2D and 3D cultures. Osteoarthritis and Cartilage *20*, 1170–1178.

Cartmell, S., Rupani, and Balint (2012). Osteoblasts and their applications in bone tissue engineering. Cell Health and Cytoskeleton 49.

Chang, C.H., Lin, F.H., Kuo, T.F., and Liu, H.C. (2005). Cartilage tissue engineering. Biomedical Engineering: Applications, Basis and Communications *17*, 61–71.

Chatani, M., Mantoku, A., Takeyama, K., Abduweli, D., Sugamori, Y., Aoki, K., Ohya, K., Suzuki, H., Uchida, S., Sakimura, T., et al. (2015). Microgravity promotes osteoclast activity in medaka fish reared at the international space station. Scientific Reports *5*, 14172.

Chen, C.T., Shih, Y.R.V., Kuo, T.K., Lee, O.K., and Wei, Y.H. (2008). Coordinated changes of mitochondrial biogenesis and antioxidant enzymes during osteogenic differentiation of human mesenchymal stem cells. Stem Cells *26*, 960–968.

Chen, C.T., Hsu, S.H., and Wei, Y.H. (2010). Upregulation of mitochondrial function and antioxidant defense in the differentiation of stem cells. Biochimica et Biophysica Acta (BBA) - General Subjects *1800*, 257–263.

Chen, H., Zhou, X., Fujita, H., Onozuka, M., and Kubo, K.Y. (2013). Age-related changes in trabecular and cortical bone microstructure. International Journal of Endocrinology *2013*, 1–9.

Chen, Q., Shou, P., Zheng, C., Jiang, M., Cao, G., Yang, Q., Cao, J., Xie, N., Velletri, T., Zhang, X., et al. (2016). Fate decision of mesenchymal stem cells: adipocytes or osteoblasts? Cell Death and Differentiation *23*, 1128–1139.

Chen, W.H., Lai, M.T., Wu, A.T.H., Wu, C.-C., Gelovani, J.G., Lin, C.T., Hung, S.C., Chiu, W.T., and Deng, W.P. (2009). *In vitro* stage-specific chondrogenesis of mesenchymal stem cells committed to chondrocytes. Arthritis & Rheumatism *60*, 450–459.

Chen, Y., Yuen, W.H., Fu, J., Huang, G., Melendez, A.J., Ibrahim, F.B.M., Lu, H., and Cao, X. (2007). The mitochondrial respiratory chain controls intracellular calcium signaling and NFAT activity essential for heart formation in Xenopus laevis. Molecular and Cellular Biology *27*, 6420–6432.

Chen, Y.C., Chen, R.N., Jhan, H.J., Liu, D.Z., Ho, H.O., Mao, Y., Kohn, J., and Sheu, M.T. (2015). Development and characterization of acellular extracellular matrix scaffolds from porcine menisci for use in cartilage tissue engineering. Tissue Engineering Part C: Methods *21*, 971–986.

Cheng, L., and Changyong, L. (2015). Advantages, limitations, and future trends for biofabrication techniques in tissue engineering. (Atlantis Press).

Cheng, C.W., Solorio, L.D., and Alsberg, E. (2014). Decellularized tissue and cell-derived extracellular matrices as scaffolds for orthopaedic tissue engineering. Biotechnology Advances *32*, 462–484.

Chevalier, E., Chulia, D., Pouget, C., and Viana, M. (2008). Fabrication of porous substrates: a review of processes using pore forming agents in the biomaterial field. J Pharm Sci *97*, 1135–1154.

Chi, S.W., Hannon, G.J., and Darnell, R.B. (2012). An alternative mode of microRNA target recognition. Nature Structural & Molecular Biology *19*, 321–327.

Christensen, R., Astrup, A., and Bliddal, H. (2005). Weight loss: the treatment of choice for knee osteoarthritis? A randomized trial. Osteoarthritis and Cartilage *13*, 20–27.

Clarke, B. (2008). Normal bone anatomy and physiology. Clinical Journal of the American Society of Nephrology *3*, S131–S139.

Clarke, B.L., and Khosla, S. (2010). Physiology of bone loss. Radiologic Clinics of North America *48*, 483–495.

Clarke, C., Henry, M., Doolan, P., Kelly, S., Aherne, S., Sanchez, N., Kelly, P., Kinsella, P., Breen, L., Madden, S.F., et al. (2012). Integrated miRNA, mRNA and protein expression analysis reveals the role of post-transcriptional regulation in controlling CHO cell growth rate. BMC Genomics *13*, 656.

Clarke, M.S.F., Sundaresan, A., Vanderburg, C.R., Banigan, M.G., and Pellis, N.R. (2013). A three-dimensional tissue culture model of bone formation utilizing rotational co-culture of human adult osteoblasts and osteoclasts. Acta Biomaterialia *9*, 7908–7916.

Clementz, A.G., and Harris, A. (2013). Collagen XV: exploring its structure and role within the tumor microenvironment. Molecular Cancer Research *11*, 1481–1486.

Cloonan, N. (2015). Re-thinking miRNA-mRNA interactions: intertwining issues confound target discovery. BioEssays *37*, 379–388.

Cobaleda, C., Pérez-Caro, M., Vicente-Dueñas, C., and Sánchez-García, I. (2007). Function of the zinc-finger transcription factor *SNAI2* in cancer and development. Annual Review of Genetics *41*, 41–61.

Coleman, C.M., Vaughan, E.E., Browe, D.C., Mooney, E., Howard, L., and Barry, F. (2013). Growth differentiation factor-5 enhances *in vitro* mesenchymal stromal cell chondrogenesis and hypertrophy. Stem Cells and Development *22*, 1968–1976.

Correia, C., Grayson, W.L., Park, M., Hutton, D., Zhou, B., Guo, X.E., Niklason, L., Sousa, R.A., Reis, R.L., and Vunjak-Novakovic, G. (2011). *In vitro* model of vascularized bone: synergizing vascular development and osteogenesis. PLoS ONE *6*, e28352.

Crane, J.L., and Cao, X. (2014). Bone marrow mesenchymal stem cells and TGF-β signaling in bone remodeling. Journal of Clinical Investigation *124*, 466–472.

Crapo, P.M., Gilbert, T.W., and Badylak, S.F. (2011). An overview of tissue and whole organ decellularization processes. Biomaterials *32*, 3233–3243.

de Crombrugghe, B., Lefebvre, V., and Nakashima, K. (2001). Regulatory mechanisms in the pathways of cartilage and bone formation. Curr. Opin. Cell Biol. *13*, 721–727.

Cucchiarini, M. (2016). Human gene therapy: novel approaches to improve the current gene delivery systems. Discov Med *21*, 495–506.

Cucchiarini, M., Henrionnet, C., Mainard, D., Pinzano, A., and Madry, H. (2015). New trends in articular cartilage repair. Journal of Experimental Orthopaedics *2*.

Cunniffe, G.M., Vinardell, T., Murphy, J.M., Thompson, E.M., Matsiko, A., O'Brien, F.J., and Kelly, D.J. (2015). Porous decellularized tissue engineered hypertrophic cartilage as a scaffold for large bone defect healing. Acta Biomaterialia *23*, 82–90.

Dalheim, M.Ø., Vanacker, J., Najmi, M.A., Aachmann, F.L., Strand, B.L., and Christensen, B.E. (2016). Efficient functionalization of alginate biomaterials. Biomaterials *80*, 146–156.

Dariima, T., Jin, G.Z., Lee, E.J., Wall, I.B., and Kim, H.W. (2013a). Cooperation between osteoblastic cells and endothelial cells enhances their phenotypic responses and improves osteoblast function. Biotechnology Letters *35*, 1135–1143.

Das, T., Chakraborty, D., and Chakraborty, S. (2009). Interfacing of microfluidic devices. Chips and Tips.

Davies, O.G., Cooper, P.R., Shelton, R.M., Smith, A.J., and Scheven, B.A. (2015). A comparison of the *in vitro* mineralisation and dentinogenic potential of mesenchymal stem cells derived from adipose tissue, bone marrow and dental pulp. Journal of Bone and Mineral Metabolism *33*, 371–382.

Dawson, J.I., and Oreffo, R.O.C. (2008). Bridging the regeneration gap: Stem cells, biomaterials and clinical translation in bone tissue engineering. Archives of Biochemistry and Biophysics *473*, 124–131.

Daya, S., and Berns, K.I. (2008). Gene therapy using adeno-associated virus vectors. Clinical Microbiology Reviews *21*, 583–593.

Dehne, T., Schenk, R., Perka, C., Morawietz, L., Pruss, A., Sittinger, M., Kaps, C., and Ringe, J. (2010). Gene expression profiling of primary human articular chondrocytes in high-density micromasses reveals patterns of recovery, maintenance, re- and dedifferentiation. Gene *462*, 8–17.

Dell'Accio, F., Cosimo De Bari, and Luyten, F.P. (2001). Molecular markers predictive of the capacity of expanded human articular chondrocytes to form stable cartilage *in vivo*. Arthritis & Rheumatism *44*, 1608–1619.

Demoor, M., Ollitrault, D., Gomez-Leduc, T., Bouyoucef, M., Hervieu, M., Fabre, H., Lafont, J., Denoix, J.-M., Audigié, F., Mallein-Gerin, F., et al. (2014). Cartilage tissue engineering: Molecular control of chondrocyte differentiation for proper cartilage matrix reconstruction. Biochimica et Biophysica Acta (BBA) - General Subjects *1840*, 2414–2440.

Denduluri, S.K., Idowu, O., Wang, Z., Liao, Z., Yan, Z., Mohammed, M.K., Ye, J., Wei, Q., Wang, J., Zhao, L., et al. (2015). Insulin-like growth factor (IGF) signaling in tumorigenesis and the development of cancer drug resistance. Genes & Diseases *2*, 13–25.

Deng, Z.L., Sharff, K.A., Tang, N., Song, W.X., Luo, J., Luo, X., Chen, J., Bennett, E., Reid, R., Manning, D., et al. (2008). Regulation of osteogenic differentiation during skeletal development. Front. Biosci. *13*, 2001–2021.

Devaki, V., Balu, K., Ramesh, S., Arvind, R., and Venkatesan (2012). Pre-prosthetic surgery: mandible. Journal of Pharmacy and Bioallied Sciences *4*, 414.

Dey, A., Bomans, P.H.H., Müller, F.A., Will, J., Frederik, P.M., de With, G., and Sommerdijk, N.A.J.M. (2010). The role of prenucleation clusters in surface-induced calcium phosphate crystallization. Nature Materials *9*, 1010–1014.

Di Luca, A., Lorenzo-Moldero, I., Mota, C., Lepedda, A., Auhl, D., Van Blitterswijk, C., and Moroni, L. (2016). Tuning cell differentiation into a 3D scaffold presenting a pore shape gradient for osteochondral regeneration. Advanced Healthcare Materials *5*, 1753–1763.

Dimitriou, R., Tsiridis, E., and Giannoudis, P.V. (2005). Current concepts of molecular aspects of bone healing. Injury *36*, 1392–1404.

Downey, P.A., and Siegel, M.I. (2006). Bone biology and the clinical implications for osteoporosis. Phys Ther *86*, 77–91.

DuRaine, G.D., Brown, W.E., Hu, J.C., and Athanasiou, K.A. (2015). Emergence of scaffold-free approaches for tissue engineering musculoskeletal cartilages. Annals of Biomedical Engineering *43*, 543–554.

Dweep, H., and Gretz, N. (2015). miRWalk2.0: a comprehensive atlas of microRNA-target interactions. Nature Methods *12*, 697–697.

Edmondson, R., Broglie, J.J., Adcock, A.F., and Yang, L. (2014). Three-dimensional cell culture systems and their applications in drug discovery and cell-based biosensors. ASSAY and Drug Development Technologies *12*, 207–218.

El Haj, A.J., and Cartmell, S.H. (2010). Bioreactors for bone tissue engineering. Proceedings of the Institution of Mechanical Engineers, Part H: Journal of Engineering in Medicine *224*, 1523–1532.

Elloumi-Hannachi, I., Yamato, M., and Okano, T. (2010). Cell sheet engineering: a unique nanotechnology for scaffold-free tissue reconstruction with clinical applications in regenerative medicine. Journal of Internal Medicine *267*, 54–70.

Fakhry, M. (2013). Molecular mechanisms of mesenchymal stem cell differentiation towards osteoblasts. World Journal of Stem Cells *5*, 136.

Fang, Z., and Rajewsky, N. (2011). The impact of miRNA target sites in coding sequences and in 3'UTRs. PLoS ONE *6*, e18067.

Feng, X., and McDonald, J.M. (2011). Disorders of bone remodeling. Annual Review of Pathology: Mechanisms of Disease *6*, 121–145.

Findlay, D.M., and Kuliwaba, J.S. (2016). Bone–cartilage crosstalk: a conversation for understanding osteoarthritis. Bone Research *4*, 16028.

Fini, M., Giavaresi, G., Aldini, N.N., Torricelli, P., Botter, R., Beruto, D., and Giardino, R. (2002). A bone substitute composed of polymethylmethacrylate and alpha-tricalcium phosphate: results in terms of osteoblast function and bone tissue formation. Biomaterials *23*, 4523–4531.

Fitzgerald, K.A., Malhotra, M., Curtin, C.M., O' Brien, F.J., and O' Driscoll, C.M. (2015). Life in 3D is never flat: 3D models to optimise drug delivery. Journal of Controlled Release *215*, 39–54.

Fitzpatrick, L.E., and McDevitt, T.C. (2015). Cell-derived matrices for tissue engineering and regenerative medicine applications. Biomater. Sci. *3*, 12–24.

Focaroli, S., Mazzitelli, S., Falconi, M., Luca, G., and Nastruzzi, C. (2014). Preparation and validation of low cost microfluidic chips using a shrinking approach. Lab Chip *14*, 4007–4016.

Folmes, C.D.L., Dzeja, P.P., Nelson, T.J., and Terzic, A. (2012). Mitochondria in control of cell fate. Circulation Research *110*, 526–529.

Fondi, C., and Franchi, A. (2007). Definition of bone necrosis by the pathologist. Clin Cases Miner Bone Metab. *4*, 21–26.

Fornari, F., Gramantieri, L., Ferracin, M., Veronese, A., Sabbioni, S., Calin, G.A., Grazi, G.L., Giovannini, C., Croce, C.M., Bolondi, L., et al. (2008). MiR-221 controls CDKN1C/p57 and CDKN1B/p27 expression in human hepatocellular carcinoma. Oncogene *27*, 5651–5661.

Fromigue, O., Hay, E., Barbara, A., and Marie, P.J. (2010). Essential role of Nuclear Factor of Activated T cells (NFAT)-mediated Wnt signaling in osteoblast differentiation induced by strontium ranelate. Journal of Biological Chemistry *285*, 25251–25258.

Furukawa, K.S., Imura, K., Tateishi, T., and Ushida, T. (2008). Scaffold-free cartilage by rotational culture for tissue engineering. Journal of Biotechnology *133*, 134–145.

Furumatsu, T., Tsuda, M., Taniguchi, N., Tajima, Y., and Asahara, H. (2005). Smad3 induces chondrogenesis through the activation of SOX9 via CREB-binding protein/p300 recruitment. Journal of Biological Chemistry *280*, 8343–8350.

Gabusi, E., Manferdini, C., Grassi, F., Piacentini, A., Cattini, L., Filardo, G., Lambertini, E., Piva, R., Zini, N., Facchini, A., et al. (2012). Extracellular calcium chronically induced human osteoblasts effects: specific modulation of osteocalcin and collagen type XV. Journal of Cellular Physiology *227*, 3151–3161.

Gadjanski, I., and Vunjak-Novakovic, G. (2015). Challenges in engineering osteochondral tissue grafts with hierarchical structures. Expert Opinion on Biological Therapy *15*, 1583–1599.

Galardi, S., Mercatelli, N., Giorda, E., Massalini, S., Frajese, G.V., Ciafre, S.A., and Farace, M.G. (2007). miR-221 and miR-222 expression affects the proliferation potential of human prostate carcinoma cell lines by targeting p27Kip1. Journal of Biological Chemistry 282, 23716–23724.

Gallagher, J.C., and Sai, A.J. (2010). Molecular biology of bone remodeling: implications for new therapeutic targets for osteoporosis. Maturitas *65*, 301–307.

Gamblin, A.L., Renaud, A., Charrier, C., Hulin, P., Louarn, G., Heymann, D., Trichet, V., and Layrolle, P. (2014). Osteoblastic and osteoclastic differentiation of human mesenchymal stem cells and monocytes in a miniaturized three-dimensional culture with mineral granules. Acta Biomaterialia *10*, 5139–5147.

Gardin, C., Vindigni, V., Bressan, E., Ferroni, L., Nalesso, E., Puppa, A.D., D'Avella, D., Lops, D., Pinton, P., and Zavan, B. (2011). Hyaluronan and fibrin biomaterial as scaffolds for neuronal differentiation of adult stem cells derived from adipose tissue and skin. International Journal of Molecular Sciences *12*, 6749–6764.

Gariboldi, M.I., and Best, S.M. (2015). Effect of ceramic scaffold architectural parameters on biological response. Frontiers in Bioengineering and Biotechnology *3*.

Garofalo, M., Di Leva, G., Romano, G., Nuovo, G., Suh, S.-S., Ngankeu, A., Taccioli, C., Pichiorri, F., Alder, H., Secchiero, P., et al. (2009). miR-221&222 regulate TRAIL resistance and enhance tumorigenicity through PTEN and TIMP3 downregulation. Cancer Cell *16*, 498–509.

Garofalo, M., Quintavalle, C., Romano, G., Croce, C.M., and Condorelli, G. (2012). miR221/222 in cancer: their role in tumor progression and response to therapy. Curr. Mol. Med. *12*, 27–33.

Gattazzo, F., Urciuolo, A., and Bonaldo, P. (2014). Extracellular matrix: a dynamic microenvironment for stem cell niche. Biochimica et Biophysica Acta (BBA) - General Subjects *1840*, 2506–2519.

Gavasane, A.J. (2014). Synthetic biodegradable polymers used in controlled drug delivery system: an overview. Clinical Pharmacology & Biopharmaceutics *3*.

Gentili, C., and Cancedda, R. (2009). Cartilage and bone extracellular matrix. Curr. Pharm. Des. *15*, 1334–1348.

Ghanavi, P., Kabiri, M., and Doran, M.R. (2012). The rationale for using microscopic units of a donor matrix in cartilage defect repair. Cell and Tissue Research *347*, 643–648.

Ghone, N.V., and Grayson, W.L. (2012). Recapitulation of mesenchymal condensation enhances *in vitro* chondrogenesis of human mesenchymal stem cells. Journal of Cellular Physiology *227*, 3701–3708.

Gilbert, S.F. (2000). Developmental biology (Sunderland, Mass: Sinauer Associates).

Gilbert, T., Sellaro, T., and Badylak, S. (2006). Decellularization of tissues and organs. Biomaterials *27*, 3675–3683.

Gimble, J.M., Guilak, F., Nuttall, M.E., Sathishkumar, S., Vidal, M., and Bunnell, B.A. (2008). *In vitro* differentiation potential of mesenchymal stem cells. Transfusion Medicine and Hemotherapy *35*, 228–238.

Gloria, A., De Santis, R., and Ambrosio, L. (2010). Polymer-based composite scaffolds for tissue engineering. J Appl Biomater Biomech *8*, 57–67.

Glyn-Jones, S., Palmer, A.J.R., Agricola, R., Price, A.J., Vincent, T.L., Weinans, H., and Carr, A.J. (2015). Osteoarthritis. The Lancet *386*, 376–387.

Goettsch, C., Rauner, M., Hamann, C., Sinningen, K., Hempel, U., Bornstein, S.R., and Hofbauer, L.C. (2011). Nuclear factor of activated T cells mediates oxidised LDL-induced calcification of vascular smooth muscle cells. Diabetologia *54*, 2690–2701.

Goldring, S.R., and Goldring, M.B. (2016). Changes in the osteochondral unit during osteoarthritis: structure, function and cartilage–bone crosstalk. Nature Reviews Rheumatology *12*, 632–644.

Goldring, M.B., Tsuchimochi, K., and Ijiri, K. (2006). The control of chondrogenesis. Journal of Cellular Biochemistry *97*, 33–44.

Gómez-Guillén, M.C., Giménez, B., López-Caballero, M.E., and Montero, M.P. (2011). Functional and bioactive properties of collagen and gelatin from alternative sources: A review. Food Hydrocolloids *25*, 1813–1827.

Gong, A.-Y., Hu, G., Zhou, R., Liu, J., Feng, Y., Soukup, G.A., and Chen, X.-M. (2011). MicroRNA-221 controls expression of intercellular adhesion molecule-1 in epithelial cells in response to Cryptosporidium parvum infection. International Journal for Parasitology *41*, 397–403.

Gonzalez-Fernandez, T., Tierney, E.G., Cunniffe, G.M., O'Brien, F.J., and Kelly, D.J. (2016). Gene Delivery of TGF-β3 and BMP2 in an MSC-laden alginate hydrogel for articular cartilage and endochondral bone tissue engineering. Tissue Engineering Part A *22*, 776–787.

Gonzálvez-García, M., Rodríguez-Lozano, F.J., Villanueva, V., Segarra-Fenoll, D., Rodríguez-González, M.A., Oñate-Sánchez, R., Blanquer, M., and Moraleda, J.M. (2013). Cell therapy in bisphosphonate-related osteonecrosis of the jaw. Journal of Craniofacial Surgery *24*, e226–e228.

Gordeladze, J.O., Reseland, J.E., Karlsen, T.A., Jakobsen, R.B., Engebretsen, L., Lyngstadaas, S.P., Duroux-Richard, I., Jorgensen, C., and Brinchmann, J.E. (2011). Bone and cartilage from stem cells: growth optimalization and stabilization of cell phenotypes. In Regenerative Medicine and Tissue Engineering - Cells and Biomaterials, D. Eberli, ed. (InTech).

Grellier, M., Granja, P.L., Fricain, J.C., Bidarra, S.J., Renard, M., Bareille, R., Bourget, C., Amédée, J., and Barbosa, M.A. (2009). The effect of the co-immobilization of human osteoprogenitors and endothelial cells within alginate microspheres on mineralization in a bone defect. Biomaterials *30*, 3271–3278.

Griffin, M.F. (2015). Control of stem cell fate by engineering their micro and nanoenvironment. World Journal of Stem Cells *7*, 37.

Grogan, S.P., Chen, X., Sovani, S., Taniguchi, N., Colwell, C.W., Lotz, M.K., and D'Lima, D.D. (2014). Influence of cartilage extracellular matrix molecules on cell phenotype and neocartilage formation. Tissue Engineering Part A *20*, 264–274.

Guillon, E., Bretaud, S., and Ruggiero, F. (2016). Slow muscle precursors lay down a collagen XV matrix fingerprint to guide motor axon navigation. Journal of Neuroscience *36*, 2663–2676.

Guo, J., Jourdian, G.W., and Maccallum, D.K. (1989). Culture and growth characteristics of chondrocytes encapsulated in alginate beads. Connective Tissue Research *19*, 277–297.

Hafner, M., Landthaler, M., Burger, L., Khorshid, M., Hausser, J., Berninger, P., Rothballer, A., Ascano, M., Jungkamp, A.C., Munschauer, M., et al. (2010). Transcriptome-wide identification of RNA-binding protein and microRNA target sites by PAR-CLIP. Cell *141*, 129–141.

Halai, M., Ker, A., Meek, R.D., Nadeem, D., Sjostrom, T., Su, B., McNamara, L.E., Dalby, M.J., and Young, P.S. (2014). Scanning electron microscopical observation of an osteoblast/osteoclast co-culture on micropatterned orthopaedic ceramics. Journal of Tissue Engineering *5*.

Halim, N., Fakiruddin, K., Ali, S., and Yahaya, B. (2014). A comparative study of non-viral gene delivery techniques to human adipose-derived mesenchymal stem cell. International Journal of Molecular Sciences *15*, 15044–15060.

Hartmann, C., and Tabin, C.J. (2000). Dual roles of Wnt signaling during chondrogenesis in the chicken limb. Development *127*, 3141–3159.

Hass, R., Kasper, C., Böhm, S., and Jacobs, R. (2011). Different populations and sources of human mesenchymal stem cells (MSC): a comparison of adult and neonatal tissue-derived MSC. Cell Communication and Signaling *9*, 12.

Hassan, M.Q., Gordon, J.A.R., Beloti, M.M., Croce, C.M., Wijnen, A.J. v., Stein, J.L., Stein, G.S., and Lian, J.B. (2010). A network connecting Runx2, SATB2, and the miR-23a 27a 24-2 cluster regulates the osteoblast differentiation program. Proceedings of the National Academy of Sciences *107*, 19879–19884.

Hata, K., Nishimura, R., Muramatsu, S., Matsuda, A., Matsubara, T., Amano, K., Ikeda, F., Harley, V.R., and Yoneda, T. (2008). Paraspeckle protein p54nrb links Sox9-mediated transcription with RNA processing during chondrogenesis in mice. Journal of Clinical Investigation *118*, 3098–3108.

Hatfield, S.D., Shcherbata, H.R., Fischer, K.A., Nakahara, K., Carthew, R.W., and Ruohola-Baker, H. (2005). Stem cell division is regulated by the microRNA pathway. Nature *435*, 974–978.

Häuselmann, H.J., Masuda, K., Hunziker, E.B., Neidhart, M., Mok, S.S., Michel, B.A., and Thonar, E.J. (1996). Adult human chondrocytes cultured in alginate form a matrix similar to native human articular cartilage. Am. J. Physiol. *271*, C742-752.

Hausser, J., and Zavolan, M. (2014). Identification and consequences of miRNA–target interactions — beyond repression of gene expression. Nature Reviews Genetics *15*, 599–612.

Haycock, J.W. (2011). 3D cell culture: a review of current approaches and techniques. In Methods Mol Biol., J.W. Haycock, ed. (Totowa, NJ: Humana Press), pp. 1–15.

Hayden, R.S., Quinn, K.P., Alonzo, C.A., Georgakoudi, I., and Kaplan, D.L. (2014). Quantitative characterization of mineralized silk film remodeling during long-term osteoblast–osteoclast co-culture. Biomaterials *35*, 3794–3802.

Hayrapetyan, A., Jansen, J.A., and van den Beucken, J.J.J.P. (2015). Signaling pathways involved in osteogenesis and their application for bone regenerative medicine. Tissue Engineering Part B: Reviews *21*, 75–87.

Heath, C.A. (2000). Cells for tissue engineering. Trends in Biotechnology *18*, 17–19.

Heinemann, C., Heinemann, S., Worch, H., and Hanke, T. (2011). Development of an osteoblast/osteoclast co-culture derived by human bone marrow stromal cells and human monocytes for biomaterials testing. Eur Cell Mater *21*, 80–93.

Heinemann, S., Heinemann, C., Wenisch, S., Alt, V., Worch, H., and Hanke, T. (2013). Calcium phosphate phases integrated in silica/collagen nanocomposite xerogels enhance the bioactivity and ultimately manipulate the osteoblast/osteoclast ratio in a human co-culture model. Acta Biomaterialia *9*, 4878–4888.

Hellingman, C.A., Davidson, E.N.B., Koevoet, W., Vitters, E.L., van den Berg, W.B., van Osch, G.J.V.M., and van der Kraan, P.M. (2011). Smad signaling determines chondrogenic differentiation of bone-marrow-derived mesenchymal stem cells: inhibition of Smad1/5/8P prevents terminal differentiation and calcification. Tissue Engineering Part A *17*, 1157–1167.

Henrotin, Y., Pesesse, L., and Sanchez, C. (2012). Subchondral bone and osteoarthritis: biological and cellular aspects. Osteoporosis International *23*, 847–851.

Heo, J., Choi, Y., Kim, H.-S., and Kim, H. (2015). Comparison of molecular profiles of human mesenchymal stem cells derived from bone marrow, umbilical cord blood, placenta and adipose tissue. International Journal of Molecular Medicine.

Hersel, U., Dahmen, C., and Kessler, H. (2003). RGD modified polymers: biomaterials for stimulated cell adhesion and beyond. Biomaterials *24*, 4385–4415.

Hock, M.B., and Kralli, A. (2009). Transcriptional control of mitochondrial biogenesis and function. Annual Review of Physiology *71*, 177–203.

Hogan, P.G. (2003). Transcriptional regulation by calcium, calcineurin, and NFAT. Genes & Development *17*, 2205–2232.

Hoganson, D.M., O'Doherty, E.M., Owens, G.E., Harilal, D.O., Goldman, S.M., Bowley, C.M., Neville, C.M., Kronengold, R.T., and Vacanti, J.P. (2010). The retention of extracellular matrix proteins and angiogenic and mitogenic cytokines in a decellularized porcine dermis. Biomaterials *31*, 6730–6737.

Hojo, H., Ohba, S., and Chung, U. (2015). Signaling pathways regulating the specification and differentiation of the osteoblast lineage. Regenerative Therapy *1*, 57–62.

Homicz, M.R., Chia, S.H., Schumacher, B.L., Masuda, K., Thonar, E.J., Sah, R.L., and Watson, D. (2003). Human septal chondrocyte redifferentiation in alginate, polyglycolic acid scaffold, and monolayer culture: The Laryngoscope *113*, 25–32.

Hong, E., and Reddi, A.H. (2012). MicroRNAs in chondrogenesis, articular cartilage, and osteoarthritis: implications for tissue engineering. Tissue Engineering Part B: Reviews *18*, 445–453.

Horsley, V., and Pavlath, G.K. (2002). NFAT: ubiquitous regulator of cell differentiation and adaptation. The Journal of Cell Biology *156*, 771–774.

Houbaviy, H.B., Murray, M.F., and Sharp, P.A. (2003). Embryonic stem cell-specific MicroRNAs. Dev. Cell *5*, 351–358.

Howard, D., Buttery, L.D., Shakesheff, K.M., and Roberts, S.J. (2008). Tissue engineering: strategies, stem cells and scaffolds. Journal of Anatomy *213*, 66–72.

Hu, Y.C. (2014). Gene therapy for cartilage and bone tissue engineering (Heidelberg ; New York: Springer).

Huang, F., and Chen, Y.G. (2012). Regulation of TGF-β receptor activity. Cell & Bioscience *2*, 9.

Huang, A.H., Motlekar, N.A., Stein, A., Diamond, S.L., Shore, E.M., and Mauck, R.L. (2008). High-throughput screening for modulators of mesenchymal stem cell chondrogenesis. Annals of Biomedical Engineering *36*, 1909–1921.

Huang, Y.F., Chang, C.T., Muo, C.H., Tsai, C.H., Shen, Y.F., and Wu, C.Z. (2015). Impact of bisphosphonate-related osteonecrosis of the jaw on osteoporotic patients after dental extraction: a population-based cohort study. PLoS ONE *10*, e0120756.

Huh, J.E., and Lee, S.Y. (2013). IL-6 is produced by adipose-derived stromal cells and promotes osteogenesis. Biochimica et Biophysica Acta (BBA) - Molecular Cell Research *1833*, 2608–2616.

Hultberg, B., Lundblad, A., Masson, P.K., and Ockerman, P.A. (1975). Specificity studies on alpha-mannosidases using oligosaccharides from mannosidosis urine as substrates. Biochim. Biophys. Acta *410*, 156–163.

Hummert, T.W., Schwartz, Z., Sylvia, V.L., Dean, D.D., Hardin, R.R., and Boyan, B.D. (2000). Expression and production of stathmin in growth plate chondrocytes is cell-maturation dependent. J. Cell. Biochem. *79*, 150–163.

Hummert, T.W., Schwartz, Z., Sylvia, V.L., Dean, D.D., and Boyan, B.D. (2001). Stathmin levels in growth plate chondrocytes are modulated by vitamin D3 metabolites and transforming growth factor-β1 and are associated with proliferation. Endocrine *15*, 093–102.

Hutmacher, D.W. (2000). Scaffolds in tissue engineering bone and cartilage. Biomaterials *21*, 2529–2543.

Ikada, Y. (2006). Challenges in tissue engineering. Journal of The Royal Society Interface *3*, 589–601.

Ilan, D.I., and Ladd, A.L. (2002). Bone graft substitutes. Operative Techniques in Plastic and Reconstructive Surgery *9*, 151–160.

Ito, K., and Suda, T. (2014). Metabolic requirements for the maintenance of self-renewing stem cells. Nature Reviews Molecular Cell Biology *15*, 243–256.

Itokazu, M., Wakitani, S., Mera, H., Tamamura, Y., Sato, Y., Takagi, M., and Nakamura, H. (2016). Transplantation of scaffold-free cartilage-like cell-sheets made from human bone marrow mesenchymal stem cells for cartilage repair: a preclinical study. Cartilage *7*, 361–372.

Izadifar, Z., Chen, X., and Kulyk, W. (2012). Strategic design and fabrication of engineered scaffolds for articular cartilage repair. Journal of Functional Biomaterials *3*, 799–838.

Jacobs, H.N., Rathod, S., Wolf, M.T., and Elisseeff, J.H. (2016). Intra-articular injection of urinary bladder matrix reduces osteoarthritis development. The AAPS Journal *19*, 141–149.

Jacobsen, A., Silber, J., Harinath, G., Huse, J.T., Schultz, N., and Sander, C. (2013). Analysis of microRNA-target interactions across diverse cancer types. Nature Structural & Molecular Biology *20*, 1325–1332.

Jacome-Galarza, C.E., Lee, S.-K., Lorenzo, J.A., and Aguila, H.L. (2013). Identification, characterization, and isolation of a common progenitor for osteoclasts, macrophages, and dendritic cells from murine bone marrow and periphery. Journal of Bone and Mineral Research *28*, 1203–1213.

Jayakumar, P., and Di Silvio, L. (2010). Osteoblasts in bone tissue engineering. Proceedings of the Institution of Mechanical Engineers, Part H: Journal of Engineering in Medicine *224*, 1415–1440.

Jin, C.Z., Park, S.R., Choi, B.H., Park, K., and Min, B.H. (2007). *In vivo* cartilage tissue engineering using a cell-derived extracellular matrix scaffold. Artif Organs *31*, 183–192.

Jo, J.-I., and Tabata, Y. (2015). How controlled release technology can aid gene delivery. Expert Opinion on Drug Delivery *12*, 1689–1701.

Johnstone, B., Alini, M., Cucchiarini, M., Dodge, G.R., Eglin, D., Guilak, F., Madry, H., Mata, A., Mauck, R.L., Semino, C.E., et al. (2013). Tissue engineering for articular cartilage repair--the state of the art. Eur Cell Mater *25*, 248–267.

Jones, G.L., Motta, A., Marshall, M.J., El Haj, A.J., and Cartmell, S.H. (2009). Osteoblast: osteoclast co-cultures on silk fibroin, chitosan and PLLA films. Biomaterials *30*, 5376–5384.

Juréus, J., Lindstrand, A., Geijer, M., Robertsson, O., and Tägil, M. (2013). The natural course of spontaneous osteonecrosis of the knee (SPONK): a 1- to 27-year follow-up of 40 patients. Acta Orthopaedica *84*, 410–414.

Kaji, H., Camci-Unal, G., Langer, R., and Khademhosseini, A. (2011). Engineering systems for the generation of patterned co-cultures for controlling cell–cell interactions. Biochimica et Biophysica Acta (BBA) - General Subjects *1810*, 239–250.

Kaklamani, G., Cheneler, D., Grover, L.M., Adams, M.J., and Bowen, J. (2014). Mechanical properties of alginate hydrogels manufactured using external gelation. Journal of the Mechanical Behavior of Biomedical Materials *36*, 135–142.

Kan, A., Ikeda, T., Saito, T., Yano, F., Fukai, A., Hojo, H., Ogasawara, T., Ogata, N., Nakamura, K., Chung, U.-I., et al. (2009). Screening of chondrogenic factors with a real-time fluorescence-monitoring cell line ATDC5-C2ER: identification of sorting nexin 19 as a novel factor. Arthritis & Rheumatism *60*, 3314–3323.

Kang, H., Lu, S., Peng, J., Yang, Q., Liu, S., Zhang, L., Huang, J., Sui, X., Zhao, B., Wang, A., et al. (2015). *In vivo* construction of tissue-engineered cartilage using adipose-derived stem cells and bioreactor technology. Cell and Tissue Banking *16*, 123–133.

Karageorgiou, V., and Kaplan, D. (2005). Porosity of 3D biomaterial scaffolds and osteogenesis. Biomaterials *26*, 5474–5491.

Karim, A.R., Cherian, J.J., Jauregui, J.J., Pierce, T., and Mont, M.A. (2015). Osteonecrosis of the knee: review. Ann Transl Med *3*, 6.

Katsen-Globa, A., Ehrhart, F., Zimmermann, H., Feilen, P., and Weber, M.M. (2007). Alginate encapsulation improves viability and integrity of cryopreserved pancreatic islets and multicellular spheroids: combined fluorescence, scanning and block-face scanning electron microscopy. Microscopy and Microanalysis *13*.

Kawai, M., Mödder, U.I., Khosla, S., and Rosen, C.J. (2011). Emerging therapeutic opportunities for skeletal restoration. Nature Reviews Drug Discovery *10*, 141–156.

Kawakami, Y., Rodriguez-León, J., and Belmonte, J.C.I. (2006). The role of TGFβs and Sox9 during limb chondrogenesis. Current Opinion in Cell Biology *18*, 723–729.

Kern, S., Eichler, H., Stoeve, J., Klüter, H., and Bieback, K. (2006). Comparative analysis of mesenchymal stem cells from bone marrow, umbilical cord blood, or adipose tissue. Stem Cells *24*, 1294–1301.

Kerschnitzki, M., Akiva, A., Ben Shoham, A., Asscher, Y., Wagermaier, W., Fratzl, P., Addadi, L., and Weiner, S. (2016). Bone mineralization pathways during the rapid growth of embryonic chicken long bones. Journal of Structural Biology *195*, 82–92.

Khaghani, S.A., Denyer, M.C.T., and Youseffi, M. (2012). Effect of transforming growth factor-β1 in biological regulation of primary chondrocyte. American Journal of Biomedical Engineering *2*, 1–8.

Khatiwala, C.B., Kim, P.D., Peyton, S.R., and Putnam, A.J. (2009). ECM compliance regulates osteogenesis by influencing MAPK signaling downstream of RhoA and ROCK. Journal of Bone and Mineral Research *24*, 886–898.

Kim, S. (2003). Stat1 functions as a cytoplasmic attenuator of Runx2 in the transcriptional program of osteoblast differentiation. Genes & Development *17*, 1979–1991.

Kim, M.S., and Usachev, Y.M. (2009). Mitochondrial Ca^{2+} cycling facilitates activation of the transcription factor NFAT in sensory neurons. Journal of Neuroscience *29*, 12101–12114.

Kim, Y.H., and Lee, J.W. (2009). Targeting of focal adhesion kinase by small interfering RNAs reduces chondrocyte redifferentiation capacity in alginate beads culture with type II collagen. Journal of Cellular Physiology *218*, 623–630.

Kim, C.H., Jeon, H.M., Lee, S.Y., Ju, M.K., Moon, J.Y., Park, H.G., Yoo, M.A., Choi, B.T., Yook, J.I., Lim, S.C., et al. (2011). Implication of Snail in metabolic stress-induced necrosis. PLoS ONE *6*, e18000.

Kim, D., Song, J., and Jin, E.J. (2010). MicroRNA-221 regulates chondrogenic differentiation through promoting proteosomal degradation of Slug by targeting Mdm2. Journal of Biological Chemistry *285*, 26900–26907.

Kimelman Bleich, N., Kallai, I., Lieberman, J.R., Schwarz, E.M., Pelled, G., and Gazit, D. (2012). Gene therapy approaches to regenerating bone. Advanced Drug Delivery Reviews *64*, 1320–1330.

Kini, U., and Nandeesh, B.N. (2012). Physiology of bone formation, remodeling, and metabolism. In Radionuclide and Hybrid Bone Imaging, I. Fogelman, G. Gnanasegaran, and H. van der Wall, eds. (Berlin, Heidelberg: Springer Berlin Heidelberg), pp. 29–57.

Kleinman, H.K., Philp, D., and Hoffman, M.P. (2003). Role of the extracellular matrix in morphogenesis. Current Opinion in Biotechnology *14*, 526–532.

Knight, E., and Przyborski, S. (2015). Advances in 3D cell culture technologies enabling tissue-like structures to be created *in vitro*. Journal of Anatomy *227*, 746–756.

Knudson, C.B. (2003). Hyaluronan and CD44: strategic players for cell-matrix interactions during chondrogenesis and matrix assembly. Birth Defects Research Part C: Embryo Today: Reviews *69*, 174–196.

Kobayashi, T., Lu, J., Cobb, B.S., Rodda, S.J., McMahon, A.P., Schipani, E., Merkenschlager, M., and Kronenberg, H.M. (2008). Dicer-dependent pathways regulate chondrocyte proliferation and differentiation. Proceedings of the National Academy of Sciences *105*, 1949–1954.

Koga, T., Matsui, Y., Asagiri, M., Kodama, T., de Crombrugghe, B., Nakashima, K., and Takayanagi, H. (2005). NFAT and Osterix cooperatively regulate bone formation. Nature Medicine *11*, 880–885.

Kolf, C.M., Cho, E., and Tuan, R.S. (2007). Mesenchymal stromal cells. Biology of adult mesenchymal stem cells: regulation of niche, self-renewal and differentiation. Arthritis Res. Ther. *9*, 204.

Komori, T. (2006). Regulation of osteoblast differentiation by transcription factors. Journal of Cellular Biochemistry *99*, 1233–1239.

Kon, E., Filardo, G., Di Martino, A., and Marcacci, M. (2012). ACI and MACI. Journal of Knee Surgery *25*, 017–022.

Kong, L., Gao, Y., Lu, G., Gong, Y., Zhao, N., and Zhang, X. (2006). A study on the bioactivity of chitosan/nano-hydroxyapatite composite scaffolds for bone tissue engineering. European Polymer Journal *42*, 3171–3179.

Kotagama, K., Babb, C.S., Wolter, J.M., Murphy, R.P., and Mangone, M. (2015). A human 3′UTR clone collection to study post-transcriptional gene regulation. BMC Genomics *16*.

Kotwica, Z., and Brzeziński, J. (1989). Intracerebral hematoma as the complication of the surgical removal of chronic subdural hematoma. Case report. Neurol Psychiatr (Bucur) *27*, 167–169.

Kramer, A.H., Edkins, A.L., Hoppe, H.C., and Prinsloo, E. (2015). Dynamic mitochondrial localisation of STAT3 in the cellular adipogenesis model 3T3-L1. Journal of Cellular Biochemistry *116*, 1232–1240.

Kulkarni, N.H., Onyia, J.E., Zeng, Q., Tian, X., Liu, M., Halladay, D.L., Frolik, C.A., Engler, T., Wei, T., Kriauciunas, A., et al. (2006). Orally bioavailable GSK-3α/β dual inhibitor increases markers of cellular differentiation *in vitro* and bone mass *in vivo*. Journal of Bone and Mineral Research *21*, 910–920.

Kuo, C.K., and Ma, P.X. (2001). Ionically crosslinked alginate hydrogels as scaffolds for tissue engineering: part 1. Structure, gelation rate and mechanical properties. Biomaterials *22*, 511–521.

Kuttenberger, J., Polska, E., and Schaefer, B.M. (2013). A novel three-dimensional bone chip organ culture. Clinical Oral Investigations *17*, 1547–1555.

Kuznetsov, A.V., and Margreiter, R. (2009). Heterogeneity of mitochondria and mitochondrial function within cells as another level of mitochondrial complexity. International Journal of Molecular Sciences *10*, 1911–1929.

Kwan Tat, S., Amiable, N., Pelletier, J.-P., Boileau, C., Lajeunesse, D., Duval, N., and Martel-Pelletier, J. (2009). Modulation of OPG, RANK and RANKL by human chondrocytes and their implication during osteoarthritis. Rheumatology *48*, 1482–1490.

Kwon, H., Paschos, N.K., Hu, J.C., and Athanasiou, K. (2016). Articular cartilage tissue engineering: the role of signaling molecules. Cellular and Molecular Life Sciences *73*, 1173–1194.

Lai, Y., Sun, Y., Skinner, C.M., Son, E.L., Lu, Z., Tuan, R.S., Jilka, R.L., Ling, J., and Chen, X.-D. (2010). Reconstitution of marrow-derived extracellular matrix *ex vivo*: a robust culture system for expanding large-scale highly functional human mesenchymal stem cells. Stem Cells and Development *19*, 1095–1107.

Lakhan, R., Baylink, D.J., Lau, K.-H.W., Tang, X., Sheng, M.H.C., Rundle, C.H., and Qin, X. (2015). Local administration of AAV-DJ pseudoserotype expressing COX2 provided early onset of transgene expression and promoted bone fracture healing in mice. Gene Therapy *22*, 721–728.

Lambertini, E., Lisignoli, G., Torreggiani, E., Manferdini, C., Gabusi, E., Franceschetti, T., Penolazzi, L., Gambari, R., Facchini, A., and Piva, R. (2009). Slug gene expression supports human osteoblast maturation. Cellular and Molecular Life Sciences *66*, 3641–3653.

Lambertini, E., Lolli, A., Vezzali, F., Penolazzi, L., Gambari, R., and Piva, R. (2012). Correlation between Slug transcription factor and miR-221 in MDA-MB-231 breast cancer cells. BMC Cancer *12*.

Langer, R., and Vacanti, J. (1993). Tissue engineering. Science *260*, 920–926.

Leach, J.K., Kaigler, D., Wang, Z., Krebsbach, P., and Mooney, D. (2006). Coating of VEGF-releasing scaffolds with bioactive glass for angiogenesis and bone regeneration. Biomaterials *27*, 3249–3255.

Lee, H.S., and Salter, D.M. (2015). Biomechanics of cartilage and osteoarthritis. In Osteoarthritis - Progress in Basic Research and Treatment, Q. Chen, ed. (InTech).

Lee, K.Y., and Mooney, D.J. (2001). Hydrogels for tissue engineering. Chem. Rev. *101*, 1869–1879.

Lee, L.K., and Roth, C.M. (2003). Antisense technology in molecular and cellular bioengineering. Curr. Opin. Biotechnol. *14*, 505–511.

Lee, E.J., Kasper, F.K., and Mikos, A.G. (2014a). Biomaterials for tissue engineering. Annals of Biomedical Engineering *42*, 323–337.

Lee, I., Ajay, S.S., Yook, J.I., Kim, H.S., Hong, S.H., Kim, N.H., Dhanasekaran, S.M., Chinnaiyan, A.M., and Athey, B.D. (2009). New class of microRNA targets containing simultaneous 5'-UTR and 3'-UTR interaction sites. Genome Research *19*, 1175–1183.

Lee, J.I., Sato, M., Kim, H.W., and Mochida, J. (2011). Transplantatation of scaffold-free spheroids composed of synovium-derived cells and chondrocytes for the treatment of cartilage defects of the knee. Eur Cell Mater *22*, 275–290; discussion 290.

Lee, J.M., Kim, J.D., Oh, E.J., Oh, S.H., Lee, J.H., and Im, G.-I. (2014b). PD98059-impregnated functional PLGA scaffold for direct tissue engineering promotes chondrogenesis and prevents hypertrophy from mesenchymal stem cells. Tissue Engineering Part A *20*, 982–991.

Lee, K.Y., Rowley, J.A., Eiselt, P., Moy, E.M., Bouhadir, K.H., and Mooney, D.J. (2000). Controlling mechanical and swelling properties of alginate hydrogels independently by cross-linker type and cross-linking density. Macromolecules *33*, 4291–4294.

Lee, P., Tran, K., Chang, W., Shelke, N.B., Kumbar, S.G., and Yu, X. (2014c). Influence of chondroitin sulfate and hyaluronic acid presence in nanofibers and its alignment on the bone marrow stromal cells: cartilage regeneration. J Biomed Nanotechnol *10*, 1469–1479.

Lee, Y.H., Lee, J.H., An, I.-G., Kim, C., Lee, D.S., Lee, Y.K., and Nam, J.-D. (2005). Electrospun dual-porosity structure and biodegradation morphology of Montmorillonite reinforced PLLA nanocomposite scaffolds. Biomaterials *26*, 3165–3172.

Leigh-Brown, S., Enriquez, J., and Odom, D.T. (2010). Nuclear transcription factors in mammalian mitochondria. Genome Biology *11*, 215.

Leong, K.F., Cheah, C.M., and Chua, C.K. (2003). Solid freeform fabrication of three-dimensional scaffolds for engineering replacement tissues and organs. Biomaterials *24*, 2363–2378.

Li, D., Clark, C.C., and Myers, J.C. (2000). Basement membrane zone type XV collagen is a disulfide-bonded chondroitin sulfate proteoglycan in human tissues and cultured cells. Journal of Biological Chemistry *275*, 22339–22347.

Li, G., Wu, P., Xu, Y., Yu, Y., Sun, L., Zhu, L., and Ye, D. (2009a). The effect of Lipoxin A4 on the interaction between macrophage and osteoblast: possible role in the treatment of aseptic loosening. BMC Musculoskeletal Disorders *10*.

Li, H., Zheng, Y., and Qin, L. (2014). Progress of biodegradable metals. Progress in Natural Science: Materials International *24*, 414–422.

Li, H., Sun, S., Liu, H., Chen, H., Rong, X., Lou, J., Yang, Y., Yang, Y., and Liu, H. (2016a). Use of a biological reactor and platelet-rich plasma for the construction of tissue-engineered bone to repair articular cartilage defects. Experimental and Therapeutic Medicine *12*, 711–719.

Li, J., Liu, X., zuo, B., and Zhang, L. (2016b). The role of bone marrow microenvironment in governing the balance between osteoblastogenesis and adipogenesis. Aging and Disease *7*, 514.

Li, X., Ominsky, M.S., Warmington, K.S., Morony, S., Gong, J., Cao, J., Gao, Y., Shalhoub, V., Tipton, B., Haldankar, R., et al. (2009b). Sclerostin antibody treatment increases bone formation, bone mass, and bone strength in a rat model of postmenopausal osteoporosis. Journal of Bone and Mineral Research *24*, 578–588.

Li, Y., Wei, X., Zhou, J., and Wei, L. (2013). The age-related changes in cartilage and osteoarthritis. BioMed Research International *2013*, 1–12.

Lian, J.B., Stein, G.S., van Wijnen, A.J., Stein, J.L., Hassan, M.Q., Gaur, T., and Zhang, Y. (2012). MicroRNA control of bone formation and homeostasis. Nature Reviews Endocrinology *8*, 212–227.

Liao, J., Shi, K., Ding, Q., Qu, Y., Luo, F., and Qian, Z. (2014). Recent developments in scaffold-guided cartilage tissue regeneration. J Biomed Nanotechnol *10*, 3085–3104.

Lin, J.H. (1996). Bisphosphonates: a review of their pharmacokinetic properties. Bone *18*, 75–85.

Lin, J.H., Chen, I.W., and deLuna, F.A. (1994). On the absorption of alendronate in rats. J Pharm Sci *83*, 1741–1746.

Lindner, U., Kramer, J., Rohwedel, J., and Schlenke, P. (2010). Mesenchymal stem or stromal cells: toward a better understanding of their biology? Transfusion Medicine and Hemotherapy *37*, 75–83.

Lisignoli, G., Codeluppi, K., Todoerti, K., Manferdini, C., Piacentini, A., Zini, N., Grassi, F., Cattini, L., Piva, R., Rizzoli, V., et al. (2009). Gene array profile identifies collagen type XV as a novel human osteoblast-secreted matrix protein. Journal of Cellular Physiology *220*, 401–409.

Liu, Y., and Ma, T. (2015). Metabolic regulation of mesenchymal stem cell in expansion and therapeutic application. Biotechnology Progress *31*, 468–481.

Liu, J., Li, Q., Kuehn, M.R., Litingtung, Y., Vokes, S.A., and Chiang, C. (2013). Sonic hedgehog signaling directly targets Hyaluronic Acid Synthase 2, an essential regulator of phalangeal joint patterning. Developmental Biology *375*, 160–171.

Liu, J., Cao, J., and Zhao, X. (2015). miR-221 facilitates the TGFbeta1-induced epithelial-mesenchymal transition in human bladder cancer cells by targeting STMN1. BMC Urology *15*.

Liu, Y.Y., Yu, H.C., Liu, Y., Liang, G., Zhang, T., and Hu, Q.X. (2016). Dual drug spatiotemporal release from functional gradient scaffolds prepared using 3D bioprinting and electrospinning. Polymer Engineering & Science *56*, 170–177.

Loeser, R.F. (2006). Molecular mechanisms of cartilage destruction: mechanics, inflammatory mediators, and aging collide. Arthritis & Rheumatism *54*, 1357–1360.

Loeser, R.F., Shanker, G., Carlson, C.S., Gardin, J.F., Shelton, B.J., and Sonntag, W.E. (2000). Reduction in the chondrocyte response to insulin-like growth factor 1 in aging and osteoarthritis: Studies in a non-human primate model of naturally occurring disease. Arthritis & Rheumatism *43*, 2110–2120.

Loeser, R.F., Collins, J.A., and Diekman, B.O. (2016). Ageing and the pathogenesis of osteoarthritis. Nature Reviews Rheumatology *12*, 412–420.

Lolli, A., Lambertini, E., Penolazzi, L., Angelozzi, M., Morganti, C., Franceschetti, T., Pelucchi, S., Gambari, R., and Piva, R. (2014). Pro-chondrogenic effect of miR-221 and slug depletion in human MSCs. Stem Cell Rev *10*, 841–855.

Lolli, A., Narcisi, R., Lambertini, E., Penolazzi, L., Angelozzi, M., Kops, N., Gasparini, S., van Osch, G.J.V.M., and Piva, R. (2016). Silencing of antichondrogenic microRNA-221 in human mesenchymal stem cells promotes cartilage repair *in vivo*. Stem Cells *34*, 1801–1811.

Long, F. (2011). Building strong bones: molecular regulation of the osteoblast lineage. Nature Reviews Molecular Cell Biology *13*, 27–38.

Longo, U.G., Petrillo, S., Franceschetti, E., Berton, A., Maffulli, N., and Denaro, V. (2012). Stem Cells and Gene Therapy for Cartilage Repair. Stem Cells International *2012*, 1–9.

Longobardi, L., O'Rear, L., Aakula, S., Johnstone, B., Shimer, K., Chytil, A., Horton, W.A., Moses, H.L., and Spagnoli, A. (2005). Effect of IGF-I in the chondrogenesis of bone marrow mesenchymal stem cells in the presence or absence of TGF-β signaling. Journal of Bone and Mineral Research *21*, 626–636.

Loomer, P.M. (2001). The impact of microgravity on bone metabolism *in vitro* and *in vivo*. Crit. Rev. Oral Biol. Med. *12*, 252–261.

López-Ruiz, E., Jiménez, G., García, M.Á., Antich, C., Boulaiz, H., Marchal, J.A., and Perán, M. (2016). Polymers, scaffolds and bioactive molecules with therapeutic properties in osteochondral pathologies: what's new? Expert Opinion on Therapeutic Patents *26*, 877–890.

Lott Carvalho, J., de Carvalho, P.H., Assis, D., and de Goes, A.M. (2013). Innovative strategies for tissue engineering. In Advances in Biomaterials Science and Biomedical Applications, R. Pignatello, ed. (InTech).

Lozito, T.P., Alexander, P.G., Lin, H., Gottardi, R., Cheng, A., and Tuan, R.S. (2013). Three-dimensional osteochondral microtissue to model pathogenesis of osteoarthritis. Stem Cell Research & Therapy *4*, S6.

Lu, H., Hoshiba, T., Kawazoe, N., and Chen, G. (2011). Autologous extracellular matrix scaffolds for tissue engineering. Biomaterials *32*, 2489–2499.

Lu, T., Li, Y., and Chen, T. (2013). Techniques for fabrication and construction of three-dimensional scaffolds for tissue engineering. International Journal of Nanomedicine 337.

Luo, X., Ribeiro, M., Bray, E.R., Lee, D.-H., Yungher, B.J., Mehta, S.T., Thakor, K.A., Diaz, F., Lee, J.K., Moraes, C.T., et al. (2016). Enhanced transcriptional activity and mitochondrial localization of STAT3 co-induce axon regrowth in the adult central nervous system. Cell Reports *15*, 398–410.

Luria, A., and Chu, C.R. (2014). Articular cartilage changes in maturing athletes: new targets for joint rejuvenation. Sports Health: A Multidisciplinary Approach *6*, 18–30.

Lytle, J.R., Yario, T.A., and Steitz, J.A. (2007). Target mRNAs are repressed as efficiently by microRNA-binding sites in the 5’ UTR as in the 3’ UTR. Proc. Natl. Acad. Sci. U.S.A. *104*, 9667–9672.

Ma, B., Leijten, J.C.H., Wu, L., Kip, M., van Blitterswijk, C.A., Post, J.N., and Karperien, M. (2013). Gene expression profiling of dedifferentiated human articular chondrocytes in monolayer culture. Osteoarthritis and Cartilage *21*, 599–603.

Mackay, A.M., Beck, S.C., Murphy, J.M., Barry, F.P., Chichester, C.O., and Pittenger, M.F. (1998). Chondrogenic differentiation of cultured human mesenchymal stem cells from marrow. Tissue Engineering *4*, 415–428.

Madeira, V.M.C. (2012). Overview of mitochondrial bioenergetics. In Mitochondrial Bioenergetics, C.M. Palmeira, and A.J. Moreno, eds. (Totowa, NJ: Humana Press), pp. 1–6.

Mahamid, J., Sharir, A., Gur, D., Zelzer, E., Addadi, L., and Weiner, S. (2011). Bone mineralization proceeds through intracellular calcium phosphate loaded vesicles: a cryo-electron microscopy study. Journal of Structural Biology *174*, 527–535.

Maianskiĭ, A.N. (1975). Immunological polyfunctionality of proteins and its meaning for the analysis of an allergen-active bacterial substrate. Zh. Mikrobiol. Epidemiol. Immunobiol. 127–132.

Malkin, A.Y., Goncharenko, V.V., and Malinovskii, V.V. (1977). Barus effect in polymer flows through cylindrical and flat dies. Polymer Mechanics *12*, 439–444.

Malpique, R., Osório, L.M., Ferreira, D.S., Ehrhart, F., Brito, C., Zimmermann, H., and Alves, P.M. (2010). Alginate encapsulation as a novel strategy for the cryopreservation of neurospheres. Tissue Engineering Part C: Methods *16*, 965–977.

Mandal, S., Lindgren, A.G., Srivastava, A.S., Clark, A.T., and Banerjee, U. (2011). Mitochondrial function controls proliferation and early differentiation potential of embryonic stem Cells. Stem Cells *29*, 486–495.

Manferdini, C., Gabusi, E., Grassi, F., Piacentini, A., Cattini, L., Zini, N., Filardo, G., Facchini, A., and Lisignoli, G. (2011). Evidence of specific characteristics and osteogenic potentiality in bone cells from tibia. Journal of Cellular Physiology *226*, 2675–2682.

Manolagas, S.C., O'Brien, C.A., and Almeida, M. (2013). The role of estrogen and androgen receptors in bone health and disease. Nature Reviews Endocrinology *9*, 699–712.

Mao, A.S., and Mooney, D.J. (2015). Regenerative medicine: current therapies and future directions. Proceedings of the National Academy of Sciences *112*, 14452–14459.

Mariani, E., Pulsatelli, L., and Facchini, A. (2014). Signaling pathways in cartilage repair. International Journal of Molecular Sciences *15*, 8667–8698.

Marie, P.J. (2010). Osteoporosis: a disease of bone formation. Medicographia *32*, 10–17.

Marinov, G.K., Wang, Y.E., Chan, D., and Wold, B.J. (2014). Evidence for site-specific occupancy of the mitochondrial genome by nuclear transcription factors. PLoS ONE *9*, e84713.

Marion, N.W., and Mao, J.J. (2006). Mesenchymal stem cells and tissue engineering. In Methods in Enzymology, (Elsevier), pp. 339–361.

Marrella, A., Aiello, M., Quarto, R., and Scaglione, S. (2016). Chemical and morphological gradient scaffolds to mimic hierarchically complex tissues: from theoretical modeling to their fabrication. Biotechnology and Bioengineering *113*, 2286–2297.

Martin, I., Schaefer, D., and Dozin, B. (2005). Repair of Osteochondral Lesions. In Engineered Bone, (Georgetown, Tex.: Landes Bioscience).

Martin, T.J., and Seeman, E. (2008). Bone remodelling: its local regulation and the emergence of bone fragility. Best Practice & Research Clinical Endocrinology & Metabolism *22*, 701–722.

Martin, H.C., Wani, S., Steptoe, A.L., Krishnan, K., Nones, K., Nourbakhsh, E., Vlassov, A., Grimmond, S.M., and Cloonan, N. (2014). Imperfect centered miRNA binding sites are common and can mediate repression of target mRNAs. Genome Biology *15*, R51.

Martin, I., Miot, S., Barbero, A., Jakob, M., and Wendt, D. (2007). Osteochondral tissue engineering. Journal of Biomechanics *40*, 750–765.

Mazzitelli, S., Focaroli, S., and Nastruzzi, C. (2009). "Custom made" production of cheap luer lock adapters for chip-to-syringe interfacing. Chips and Tips.

Mazzitelli, S., Capretto, L., Quinci, F., Piva, R., and Nastruzzi, C. (2013). Preparation of cell-encapsulation devices in confined microenvironment. Advanced Drug Delivery Reviews *65*, 1533–1555.

Meijer, G.J., de Bruijn, J.D., Koole, R., and van Blitterswijk, C.A. (2007). Cell-based bone tissue engineering. PLoS Medicine *4*, e9.

Melero-Martin, J., and Al-Rubeai, M. (2007). *In vitro* expansion of chondrocytes. In Topics in Tissue Engineering, (N Ashammakhi, R Reis & E Chiellini).

Mentink, A., Hulsman, M., Groen, N., Licht, R., Dechering, K.J., van der Stok, J., Alves, H.A., Dhert, W.J., van Someren, E.P., Reinders, M.J.T., et al. (2013). Predicting the therapeutic efficacy of MSC in bone tissue engineering using the molecular marker CADM1. Biomaterials *34*, 4592–4601.

Meyer, U., and Wiesmann, H.P. (2006). Bone and cartilage engineering: from cells to skeletal defect regeneration. In Bone and Cartilage Engineering, (Dordrecht: Springer-Verlag Berlin and Heidelberg & Co. KG).

Michael, J.W.P., Schlüter-Brust, K.U., and Eysel, P. (2010). The epidemiology, etiology, diagnosis, and treatment of osteoarthritis of the knee. Deutsches Aerzteblatt Online *107*, 152–162.

Milanesi, L., de Boland, A.R., and Boland, R. (2008). Expression and localization of estrogen receptor α in the C2C12 murine skeletal muscle cell line. Journal of Cellular Biochemistry *104*, 1254–1273.

Mindaye, S.T., Ra, M., Lo Surdo, J.L., Bauer, S.R., and Alterman, M.A. (2013). Global proteomic signature of undifferentiated human bone marrow stromal cells: evidence for donor-to-donor proteome heterogeneity. Stem Cell Research *11*, 793–805.

Mitani, G., Sato, M., Lee, J.I., Kaneshiro, N., Ishihara, M., Ota, N., Kokubo, M., Sakai, H., Kikuchi, T., and Mochida, J. (2009). The properties of bioengineered chondrocyte sheets for cartilage regeneration. BMC Biotechnology *9*, 17.

Monje, P., and Boland, R. (2001). Subcellular distribution of native estrogen receptor alpha and beta isoforms in rabbit uterus and ovary. J. Cell. Biochem. *82*, 467–479.

Moutos, F.T., and Guilak, F. (2008). Composite scaffolds for cartilage tissue engineering. Biorheology *45*, 501–512.

Mueller, M.B., Fischer, M., Zellner, J., Berner, A., Dienstknecht, T., Prantl, L., Kujat, R., Nerlich, M., Tuan, R.S., and Angele, P. (2010). Hypertrophy in mesenchymal stem cell chondrogenesis: effect of TGF-beta isoforms and chondrogenic conditioning. Cells Tissues Organs (Print) *192*, 158–166.

Muir, H. (1995). The chondrocyte, architect of cartilage. Biomechanics, structure, function and molecular biology of cartilage matrix macromolecules. Bioessays *17*, 1039–1048.

Murgia, A., Veronesi, E., Candini, O., Caselli, A., D'souza, N., Rasini, V., Giorgini, A., Catani, F., Iughetti, L., Dominici, M., et al. (2016). Potency biomarker signature genes from multiparametric osteogenesis assays: will cGMP human bone marrow mesenchymal stromal cells make bone? PLoS ONE *11*, e0163629.

Murphy, S.V., and Atala, A. (2014). 3D bioprinting of tissues and organs. Nature Biotechnology *32*, 773–785.

Murphy, K.C., Hoch, A.I., Harvestine, J.N., Zhou, D., and Leach, J.K. (2016). Mesenchymal stem cell spheroids retain osteogenic phenotype through α2β1 signaling. Stem Cells Translational Medicine *5*, 1229–1237.

Murua, A., Portero, A., Orive, G., Hernández, R.M., de Castro, M., and Pedraz, J.L. (2008). Cell microencapsulation technology: towards clinical application. Journal of Controlled Release *132*, 76–83.

Myers, J.C., Dion, A.S., Abraham, V., and Amenta, P.S. (1996). Type XV collagen exhibits a widespread distribution in human tissues but a distinct localization in basement membrane zones. Cell Tissue Res. *286*, 493–505.

Nabavi, N., Khandani, A., Camirand, A., and Harrison, R.E. (2011). Effects of microgravity on osteoclast bone resorption and osteoblast cytoskeletal organization and adhesion. Bone *49*, 965–974.

Nafea, E.H., Poole-Warren, A.M., L.A., and Martens, P.J. (2011). Immunoisolating semi-permeable membranes for cell encapsulation: focus on hydrogels. Journal of Controlled Release *154*, 110–122.

Nakamura, T., Imai, Y., Matsumoto, T., Sato, S., Takeuchi, K., Igarashi, K., Harada, Y., Azuma, Y., Krust, A., Yamamoto, Y., et al. (2007). Estrogen prevents bone loss via estrogen receptor α and induction of Fas ligand in osteoclasts. Cell *130*, 811–823.

Narcisi, R., Quarto, R., Ulivi, V., Muraglia, A., Molfetta, L., and Giannoni, P. (2012a). TGF β-1 administration during *ex vivo* expansion of human articular chondrocytes in a serum-free medium redirects the cell phenotype toward hypertrophy. Journal of Cellular Physiology *227*, 3282–3290.

Narcisi, R., Signorile, L., Verhaar, J. a. N., Giannoni, P., and van Osch, G.J.V.M. (2012b). TGFβ inhibition during expansion phase increases the chondrogenic re-differentiation capacity of human articular chondrocytes. Osteoarthr. Cartil. *20*, 1152–1160.

Navarro, M., Valle, S. del, Martínez, S., Zeppetelli, S., Ambrosio, L., Planell, J.A., and Ginebra, M.P. (2004). New macroporous calcium phosphate glass ceramic for guided bone regeneration. Biomaterials *25*, 4233–4241.

Naveena, N., Venugopal, J., Rajeswari, R., Sundarrajan, S., Sridhar, R., Shayanti, M., Narayanan, S., and Ramakrishna, S. (2012). Biomimetic composites and stem cells interaction for bone and cartilage tissue regeneration. Journal of Materials Chemistry *22*, 5239.

Nayerossadat, N., Ali, P., and Maedeh, T. (2012). Viral and nonviral delivery systems for gene delivery. Advanced Biomedical Research *1*, 27.

Neogi, T. (2012). Clinical significance of bone changes in osteoarthritis. Therapeutic Advances in Musculoskeletal Disease *4*, 259–267.

Nepple, J., Milewski, M., and Shea, K. (2016). Research in osteochondritis dissecans of the knee: 2016 update. The Journal of Knee Surgery *29*, 533–538.

Ng, V.Y. (2012). Risk of disease transmission with bone allograft. Orthopedics *35*, 679–681.

Ng, F., Boucher, S., Koh, S., Sastry, K.S.R., Chase, L., Lakshmipathy, U., Choong, C., Yang, Z., Vemuri, M.C., Rao, M.S., et al. (2008). PDGF, TGF-β, and FGF signaling is important for differentiation and growth of mesenchymal stem cells (MSCs): transcriptional profiling can identify markers and signaling pathways important in differentiation of MSCs into adipogenic, chondrogenic, and osteogenic lineages. Blood *112*, 295–307.

Nicolaidou, V., Wong, M.M., Redpath, A.N., Ersek, A., Baban, D.F., Williams, L.M., Cope, A.P., and Horwood, N.J. (2012). Monocytes induce STAT3 activation in human mesenchymal stem cells to promote osteoblast formation. PLoS ONE *7*, e39871.

Niethammer, T.R., Pietschmann, M.F., Horng, A., Roßbach, B.P., Ficklscherer, A., Jansson, V., and Müller, P.E. (2014). Graft hypertrophy of matrix-based autologous chondrocyte implantation: a two-year follow-up study of NOVOCART 3D implantation in the knee. Knee Surg Sports Traumatol Arthrosc *22*, 1329–1336.

Nishi, M., Matsumoto, R., Dong, J., and Uemura, T. (2011). Regeneration of bone tissue in a controlled *in vitro* environment with a rotating wall vessel bioreactor. Nano Biomedicine *3*, 267–274.

Nixon, A.J., Rickey, E., Butler, T.J., Scimeca, M.S., Moran, N., and Matthews, G.L. (2015). A chondrocyte infiltrated collagen type I/III membrane (MACI® implant) improves cartilage healing in the equine patellofemoral joint model. Osteoarthritis and Cartilage *23*, 648–660.

Nooeaid, P., Salih, V., Beier, J.P., and Boccaccini, A.R. (2012). Osteochondral tissue engineering: scaffolds, stem cells and applications. Journal of Cellular and Molecular Medicine *16*, 2247–2270.

Nooeaid, P., Schulze-Tanzil, G., and Boccaccini, A.R. (2015). Stratified scaffolds for osteochondral tissue engineering. In Cartilage Tissue Engineering, P.M. Doran, ed. (New York, NY: Springer New York), pp. 191–200.

Nudelman, F., Pieterse, K., George, A., Bomans, P.H.H., Friedrich, H., Brylka, L.J., Hilbers, P.A.J., de With, G., and Sommerdijk, N.A.J.M. (2010). The role of collagen in bone apatite formation in the presence of hydroxyapatite nucleation inhibitors. Nature Materials *9*, 1004–1009.

Nukavarapu, S.P., and Dorcemus, D.L. (2013). Osteochondral tissue engineering: current strategies and challenges. Biotechnology Advances *31*, 706–721.

Occhetta, P., Centola, M., Tonnarelli, B., Redaelli, A., Martin, I., and Rasponi, M. (2015). High-throughput microfluidic platform for 3D cultures of mesenchymal stem cells, towards engineering developmental processes. Scientific Reports *5*, 10288.

O'Connell, R.M. (2012). MicroRNAs function on a new level. Blood *119*, 3875–3876.

Oerlemans, A.J., van Hoek, M.E., van Leeuwen, E., and Dekkers, W.J. (2014). Hype and expectations in tissue engineering. Regenerative Medicine *9*, 113–122.

Ogasawara, T., Ohba, S., Yano, F., Kawaguchi, H., Chung, U., Saito, T., Yonehara, Y., Nakatsuka, T., Mori, Y., Takato, T., et al. (2013). Nanog promotes osteogenic differentiation of the mouse mesenchymal cell line C3H10T1/2 by modulating bone morphogenetic protein (BMP) signaling. Journal of Cellular Physiology *228*, 163–171.

Oh, C.D., and Chun, J.S. (2003). Signaling mechanisms leading to the regulation of differentiation and apoptosis of articular chondrocytes by insulin-like growth factor-1. Journal of Biological Chemistry *278*, 36563–36571.

Oskowitz, A.Z., Lu, J., Penfornis, P., Ylostalo, J., McBride, J., Flemington, E.K., Prockop, D.J., and Pochampally, R. (2008). Human multipotent stromal cells from bone marrow and microRNA: regulation of differentiation and leukemia inhibitory factor expression. Proceedings of the National Academy of Sciences *105*, 18372–18377.

Osterhoff, G., Morgan, E.F., Shefelbine, S.J., Karim, L., McNamara, L.M., and Augat, P. (2016). Bone mechanical properties and changes with osteoporosis. Injury *47*, S11–S20.

Otto, S., Schreyer, C., Hafner, S., Mast, G., Ehrenfeld, M., Stürzenbaum, S., and Pautke, C. (2012). Bisphosphonate-related osteonecrosis of the jaws – Characteristics, risk factors, clinical features, localization and impact on oncological treatment. Journal of Cranio-Maxillofacial Surgery *40*, 303–309.

Ouwerx, C., Velings, N., Mestdagh, M.., and Axelos, M.A.. (1998). Physico-chemical properties and rheology of alginate gel beads formed with various divalent cations. Polymer Gels and Networks *6*, 393–408.

Ozbolat, I.T. (2015). Scaffold-based or scaffold-free bioprinting: competing or complementing approaches? Journal of Nanotechnology in Engineering and Medicine *6*, 24701.

Palmer, L.C., Newcomb, C.J., Kaltz, S.R., Spoerke, E.D., and Stupp, S.I. (2008). Biomimetic systems for hydroxyapatite mineralization inspired by bone and enamel. Chemical Reviews *108*, 4754–4783.

Papadimitropoulos, A., Scherberich, A., Güven, S., Theilgaard, N., Crooijmans, H.J.A., Santini, F., Scheffler, K., Zallone, A., and Martin, I. (2011). A 3D *in vitro* bone organ model using human progenitor cells. Eur Cell Mater *21*, 445–458; discussion 458.

Park, H., Lim, D.J., Sung, M., Lee, S.H., Na, D., and Park, H. (2016). Microengineered platforms for co-cultured mesenchymal stem cells towards vascularized bone tissue engineering. Tissue Engineering and Regenerative Medicine *13*, 465–474.

Parker, G.C., Acsadi, G., and Brenner, C.A. (2009). Mitochondria: determinants of stem cell fate? Stem Cells and Development *18*, 803–806.

Pedram, A. (2006). Functional estrogen receptors in the mitochondria of breast cancer cells. Molecular Biology of the Cell *17*, 2125–2137.

Pelttari, K., Winter, A., Steck, E., Goetzke, K., Hennig, T., Ochs, B.G., Aigner, T., and Richter, W. (2006). Premature induction of hypertrophy during *in vitro* chondrogenesis of human mesenchymal stem cells correlates with calcification and vascular invasion after ectopic transplantation in SCID mice. Arthritis & Rheumatism *54*, 3254–3266.

Pelttari, K., Steck, E., and Richter, W. (2008). The use of mesenchymal stem cells for chondrogenesis. Injury *39*, 58–65.

Penolazzi, L., Vecchiatini, R., Bignardi, S., Lambertini, E., Torreggiani, E., Canella, A., Franceschetti, T., Calura, G., Vesce, F., and Piva, R. (2009). Influence of obstetric factors on osteogenic potential of umbilical cord-derived mesenchymal stem cells. Reproductive Biology and Endocrinology *7*, 106.

Penolazzi, L., Tavanti, E., Vecchiatini, R., Lambertini, E., Vesce, F., Gambari, R., Mazzitelli, S., Mancuso, F., Luca, G., Nastruzzi, C., et al. (2010). Encapsulation of mesenchymal stem cells from Wharton's jelly in alginate microbeads. Tissue Eng Part C Methods *16*, 141–155.

Penolazzi, L., Lisignoli, G., Lambertini, E., Torreggiani, E., Manferdini, C., Lolli, A., Vecchiatini, R., Ciardo, Francesca, Gabusi, E., Facchini, A., et al. (2011). Transcription factor decoy against NFATc1 in human primary osteoblasts. International Journal of Molecular Medicine.

Penolazzi, L., Mazzitelli, S., Vecchiatini, R., Torreggiani, E., Lambertini, E., Johnson, S., Badylak, S.F., Piva, R., and Nastruzzi, C. (2012). Human mesenchymal stem cells seeded on extracellular matrix-scaffold: viability and osteogenic potential. J. Cell. Physiol. *227*, 857–866.

Pesce, V., Speciale, D., Sammarco, G., Patella, S., Spinarelli, A., and Patella, V. (2009). Surgical approach to bone healing in osteoporosis. Clin Cases Miner Bone Metab *6*, 131–135.

Petite, H., Viateau, V., Bensaïd, W., Meunier, A., de Pollak, C., Bourguignon, M., Oudina, K., Sedel, L., and Guillemin, G. (2000). Tissue-engineered bone regeneration. Nat. Biotechnol. *18*, 959–963.

Pevsner-Fischer, M., Levin, S., and Zipori, D. (2011). The origins of mesenchymal stromal cell heterogeneity. Stem Cell Reviews and Reports *7*, 560–568.

Phillips, M.D., Kuznetsov, S.A., Cherman, N., Park, K., Chen, K.G., McClendon, B.N., Hamilton, R.S., McKay, R.D.G., Chenoweth, J.G., Mallon, B.S., et al. (2014). Directed differentiation of human induced pluripotent stem cells toward bone and cartilage: *in vitro versus in vivo* assays. Stem Cells Translational Medicine *3*, 867–878.

Phinney, D.G. (2012). Functional heterogeneity of mesenchymal stem cells: implications for cell therapy. Journal of Cellular Biochemistry *113*, 2806–2812.

Phinney, D.G., Kopen, G., Righter, W., Webster, S., Tremain, N., and Prockop, D.J. (1999). Donor variation in the growth properties and osteogenic potential of human marrow stromal cells. J. Cell. Biochem. *75*, 424–436.

Pietilä, M., Lehtonen, S., Närhi, M., Hassinen, I.E., Leskelä, H.V., Aranko, K., Nordström, K., Vepsäläinen, A., and Lehenkari, P. (2010). Mitochondrial function determines the viability and osteogenic potency of human mesenchymal stem cells. Tissue Engineering Part C: Methods *16*, 435–445.

Pineau, P., Volinia, S., McJunkin, K., Marchio, A., Battiston, C., Terris, B., Mazzaferro, V., Lowe, S.W., Croce, C.M., and Dejean, A. (2010). miR-221 overexpression contributes to liver tumorigenesis. Proceedings of the National Academy of Sciences *107*, 264–269.

Pirraco, R.P., Marques, A.P., and Reis, R.L. (2010). Cell interactions in bone tissue engineering. Journal of Cellular and Molecular Medicine *14*, 93–102.

Pirraco, R.P., Obokata, H., Iwata, T., Marques, A.P., Tsuneda, S., Yamato, M., Reis, R.L., and Okano, T. (2011). Development of osteogenic cell sheets for bone tissue engineering applications. Tissue Engineering Part A *17*, 1507–1515.

Pittenger, M.F., Mackay, A.M., Beck, S.C., Jaiswal, R.K., Douglas, R., Mosca, J.D., Moorman, M.A., Simonetti, D.W., Craig, S., and Marshak, D.R. (1999). Multilineage potential of adult human mesenchymal stem cells. Science *284*, 143–147.

Piva, R., Penolazzi, L., Lambertini, E., Giordano, S., and Gambari, R. (2005). Induction of apoptosis of human primary osteoclasts treated with a transcription factor decoy mimicking a promoter region of estrogen receptor α. Apoptosis *10*, 1079–1094.

Pleumeekers, M.M., Nimeskern, L., Koevoet, W.L.M., Kops, N., Poublon, R.M.L., Stok, K.S., and van Osch, G.J.V.M. (2014). The *in vitro* and *in vivo* capacity of culture-expanded human cells from several sources encapsulated in alginate to form cartilage. Eur Cell Mater *27*, 264-280-280.

Plunkett, N., and O'Brien, F.J. (2011). Bioreactors in tissue engineering. Technol Health Care *19*, 55–69.

Pokrywczynska, M., Drewa, T., Jundzill, A., and Lysik, J. (2008). Alginate is not a good material for growth of rapidly proliferating cells. Transplantation Proceedings *40*, 1664–1667.

Polak, J.M. (2006). Stem cells and tissue engineering: past, present, and future. Annals of the New York Academy of Sciences *1068*, 352–366.

Poole, A.R., Kojima, T., Yasuda, T., Mwale, F., Kobayashi, M., and Laverty, S. (2001). Composition and structure of articular cartilage: a template for tissue repair. Clin. Orthop. Relat. Res. S26-33.

Pozzobon, M., Piccoli, M., and De Coppi, P. (2012). Sources of mesenchymal stem cells: current and future clinical use. In Mesenchymal Stem Cells - Basics and Clinical Application II, B.

Weyand, M. Dominici, R. Hass, R. Jacobs, and C. Kasper, eds. (Berlin, Heidelberg: Springer Berlin Heidelberg), pp. 267–286.

Prasadam, I., Friis, T., Shi, W., van Gennip, S., Crawford, R., and Xiao, Y. (2010). Osteoarthritic cartilage chondrocytes alter subchondral bone osteoblast differentiation via MAPK signalling pathway involving ERK1/2. Bone *46*, 226–235.

Pravdyuk, A.I., Petrenko, Y.A., Fuller, B.J., and Petrenko, A.Y. (2013). Cryopreservation of alginate encapsulated mesenchymal stromal cells. Cryobiology *66*, 215–222.

Pritzker, K.P.H., Gay, S., Jimenez, S.A., Ostergaard, K., Pelletier, J.-P., Revell, P.A., Salter, D., and van den Berg, W.B. (2006). Osteoarthritis cartilage histopathology: grading and staging. Osteoarthritis and Cartilage *14*, 13–29.

Punzi, L., Galozzi, P., Luisetto, R., Favero, M., Ramonda, R., Oliviero, F., and Scanu, A. (2016). Post-traumatic arthritis: overview on pathogenic mechanisms and role of inflammation. RMD Open *2*, e000279.

Rahman, M.S., Akhtar, N., Jamil, H.M., Banik, R.S., and Asaduzzaman, S.M. (2015). TGF-β/BMP signaling and other molecular events: regulation of osteoblastogenesis and bone formation. Bone Research *3*, 15005.

Rainbow, R., Ren, W., and Zeng, L. (2012). Inflammation and joint tissue interactions in OA: implications for potential therapeutic approaches. Arthritis *2012*, 1–8.

Raisin, S., Belamie, E., and Morille, M. (2016). Non-viral gene activated matrices for mesenchymal stem cells based tissue engineering of bone and cartilage. Biomaterials *104*, 223–237.

Raisz, L.G. (2005). Pathogenesis of osteoporosis: concepts, conflicts, and prospects. Journal of Clinical Investigation *115*, 3318–3325.

Ramchandran, R., Dhanabal, M., Volk, R., Waterman, M.J.F., Segal, M., Lu, H., Knebelmann, B., and Sukhatme, V.P. (1999). Antiangiogenic activity of restin, NC10 domain of human collagen XV: comparison to endostatin. Biochemical and Biophysical Research Communications *255*, 735–739.

Ranga, A., Gjorevski, N., and Lutolf, M.P. (2014). Drug discovery through stem cell-based organoid models. Advanced Drug Delivery Reviews *69–70*, 19–28.

Rasi, K., Piuhola, J., Czabanka, M., Sormunen, R., Ilves, M., Leskinen, H., Rysa, J., Kerkela, R., Janmey, P., Heljasvaara, R., et al. (2010). Collagen XV is necessary for modeling of the extracellular matrix and its deficiency predisposes to cardiomyopathy. Circulation Research *107*, 1241–1252.

Rath, S.N., Strobel, L.A., Arkudas, A., Beier, J.P., Maier, A.-K., Greil, P., Horch, R.E., and Kneser, U. (2012). Osteoinduction and survival of osteoblasts and bone-marrow stromal cells in 3D biphasic calcium phosphate scaffolds under static and dynamic culture conditions. Journal of Cellular and Molecular Medicine *16*, 2350–2361.

Ray, J.L., Leach, R., Herbert, J.M., and Benson, M. (2001). Isolation of vascular smooth muscle cells from a single murine aorta. Methods Cell Sci *23*, 185–188.

Reczko, M., Maragkakis, M., Alexiou, P., Grosse, I., and Hatzigeorgiou, A.G. (2012). Functional microRNA targets in protein coding sequences. Bioinformatics *28*, 771–776.

Remlinger, N.T., Gilbert, T.W., Yoshida, M., Guest, B.N., Hashizume, R., Weaver, M.L., Wagner, W.R., Brown, B.N., Tobita, K., and Wearden, P.D. (2013). Urinary bladder matrix promotes site appropriate tissue formation following right ventricle outflow tract repair. Organogenesis *9*, 149–160.

Reszka, A.A., and Rodan, G.A. (2003). Bisphosphonate mechanism of action. Current Rheumatology Reports *5*, 65–74.

Reznikov, N., Steele, J.A.M., Fratzl, P., and Stevens, M.M. (2016). A materials science vision of extracellular matrix mineralization. Nature Reviews Materials *1*, 16041.

Ricard-Blum, S., and Ballut, L. (2011). Matricryptins derived from collagens and proteoglycans. Front Biosci (Landmark Ed) *16*, 674–697.

Rosario, D.J., Reilly, G.C., Ali Salah, E., Glover, M., Bullock, A.J., and MacNeil, S. (2008). Decellularization and sterilization of porcine urinary bladder matrix for tissue engineering in the lower urinary tract. Regenerative Medicine *3*, 145–156.

Rose, W., Wood, J.D., Simmons-Byrd, A., and Spievack, A.R. (2009). Effect of a xenogeneic urinary bladder injectable bioscaffold on lameness in dogs with osteoarthritis of the coxofemoral joint (hip): a randomized, double blinded controlled trial. Intern J Appl Res Vet Med *7*, 13–22.

Rosella, D., Papi, P., Giardino, R., Cicalini, E., Piccoli, L., and Pompa, G. (2016). Medication-related osteonecrosis of the jaw: clinical and practical guidelines. Journal of International Society of Preventive and Community Dentistry *6*, 97.

Rosen, C.J., and Bouxsein, M.L. (2006). Mechanisms of disease: is osteoporosis the obesity of bone? Nature Clinical Practice Rheumatology *2*, 35–43.

Rosini, S., Rosini, S., Bertoldi, I., and Frediani, B. (2015). Understanding bisphosphonates and osteonecrosis of the jaw: uses and risks. Eur Rev Med Pharmacol Sci *19*, 3309–3317.

Ruggiero, S.L., Dodson, T.B., Fantasia, J., Goodday, R., Aghaloo, T., Mehrotra, B., and O'Ryan, F. (2014). American association of oral and maxillofacial surgeons position paper on Medication-Related Osteonecrosis of the Jaw—2014 update. Journal of Oral and Maxillofacial Surgery *72*, 1938–1956.

Saad, F., Brown, J.E., Van Poznak, C., Ibrahim, T., Stemmer, S.M., Stopeck, A.T., Diel, I.J., Takahashi, S., Shore, N., Henry, D.H., et al. (2012). Incidence, risk factors, and outcomes of osteonecrosis of the jaw: integrated analysis from three blinded active-controlled phase III trials in cancer patients with bone metastases. Annals of Oncology *23*, 1341–1347.

Sacchetti, B., Funari, A., Remoli, C., Giannicola, G., Kogler, G., Liedtke, S., Cossu, G., Serafini, M., Sampaolesi, M., Tagliafico, E., et al. (2016). No identical "mesenchymal stem cells" at different times and sites: human committed progenitors of distinct origin and differentiation potential are incorporated as adventitial cells in microvessels. Stem Cell Reports *6*, 897–913.

Saidak, Z., Le Henaff, C., Azzi, S., Marty, C., Da Nascimento, S., Sonnet, P., and Marie, P.J. (2015). Wnt/β-catenin signaling mediates osteoblast differentiation triggered by peptide-induced α5β1 integrin priming in mesenchymal skeletal cells. Journal of Biological Chemistry *290*, 6903–6912.

Sanchez, C., Deberg, M.A., Piccardi, N., Msika, P., Reginster, J.Y.L., and Henrotin, Y.E. (2005a). Osteoblasts from the sclerotic subchondral bone downregulate aggrecan but upregulate metalloproteinases expression by chondrocytes. This effect is mimicked by interleukin-6, -1β and oncostatin M pre-treated non-sclerotic osteoblasts. Osteoarthritis and Cartilage *13*, 979–987.

Sanchez, C., Deberg, M.A., Piccardi, N., Msika, P., Reginster, J.-Y.L., and Henrotin, Y.E. (2005b). Subchondral bone osteoblasts induce phenotypic changes in human osteoarthritic chondrocytes. Osteoarthritis and Cartilage *13*, 988–997.

Santoro, M., Tatara, A.M., and Mikos, A.G. (2014). Gelatin carriers for drug and cell delivery in tissue engineering. J Control Release *190*, 210–218.

Santos, M.I., Unger, R.E., Sousa, R.A., Reis, R.L., and Kirkpatrick, C.J. (2009). Crosstalk between osteoblasts and endothelial cells co-cultured on a polycaprolactone–starch scaffold and the *in vitro* development of vascularization. Biomaterials *30*, 4407–4415.

Scadden, D.T. (2006). The stem-cell niche as an entity of action. Nature *441*, 1075–1079.

Schmoldt, A., Benthe, H.F., and Haberland, G. (1975). Digitoxin metabolism by rat liver microsomes. Biochem. Pharmacol. *24*, 1639–1641.

Schnabel, M., Marlovits, S., Eckhoff, G., Fichtel, I., Gotzen, L., Vécsei, V., and Schlegel, J. (2002). Dedifferentiation-associated changes in morphology and gene expression in primary human articular chondrocytes in cell culture. Osteoarthritis and Cartilage *10*, 62–70.

Schulze-Tanzil, G., Mobasheri, A., de Souza, P., John, T., and Shakibaei, M. (2004). Loss of chondrogenic potential in dedifferentiated chondrocytes correlates with deficient Shc–Erk interaction and apoptosis. Osteoarthritis and Cartilage *12*, 448–458.

Scotti, C., Tonnarelli, B., Papadimitropoulos, A., Scherberich, A., Schaeren, S., Schauerte, A., Lopez-Rios, J., Zeller, R., Barbero, A., and Martin, I. (2010). Recapitulation of endochondral bone formation using human adult mesenchymal stem cells as a paradigm for developmental engineering. Proceedings of the National Academy of Sciences *107*, 7251–7256.

Sekine, H., Shimizu, T., Sakaguchi, K., Dobashi, I., Wada, M., Yamato, M., Kobayashi, E., Umezu, M., and Okano, T. (2013). *In vitro* fabrication of functional three-dimensional tissues with perfusable blood vessels. Nature Communications *4*, 1399.

Sen, C.K. (2014). MicroRNA in regenerative medicine.

Serfontein, W.J., Botha, D., and De Villiers, L. (1975). A rapid g.l.c. procedure for the determination of codeine and norcodeine in biological fluids based on micro-phase extraction techniques. J. Pharm. Pharmacol. *27*, 937–939.

Shah, A.R., Wenke, J.C., and Agrawal, C.M. (2016). Manipulation of human primary endothelial cell and osteoblast coculture ratios to augment vasculogenesis and mineralization. Annals of Plastic Surgery *77*, 122–128.

Sharaf-Eldin, W.E., Abu-Shahba, N., Mahmoud, M., and El-Badri, N. (2016). The modulatory effects of mesenchymal stem cells on osteoclastogenesis. Stem Cells International *2016*, 1–13.

Sharma, A., Jagga, S., Lee, S.-S., and Nam, J.S. (2013). Interplay between cartilage and subchondral bone contributing to pathogenesis of osteoarthritis. International Journal of Molecular Sciences *14*, 19805–19830.

Shibanuma, M., Ishikawa, F., Kobayashi, M., Katayama, K., Miyoshi, H., Wakamatsu, M., Mori, K., and Nose, K. (2012). Critical roles of the cAMP-responsive element-binding protein-mediated pathway in disorganized epithelial phenotypes caused by mitochondrial dysfunction. Cancer Science *103*, 1803–1810.

Shutt, T.E., Bestwick, M., and Shadel, G.S. (2011). The core human mitochondrial transcription initiation complex: It only takes two to tango. Transcription *2*, 55–59.

Siddappa, R., Fernandes, H., Liu, J., van Blitterswijk, C., and de Boer, J. (2007a). The response of human mesenchymal stem cells to osteogenic signals and its impact on bone tissue engineering. Curr Stem Cell Res Ther *2*, 209–220.

Siddappa, R., Licht, R., van Blitterswijk, C., and de Boer, J. (2007b). Donor variation and loss of multipotency during *in vitro* expansion of human mesenchymal stem cells for bone tissue engineering. Journal of Orthopaedic Research *25*, 1029–1041.

Sims, N.A., and Martin, T.J. (2014). Coupling the activities of bone formation and resorption: a multitude of signals within the basic multicellular unit. BoneKEy Reports *3*.

Singh, P., and Schwarzbauer, J.E. (2012). Fibronectin and stem cell differentiation - lessons from chondrogenesis. Journal of Cell Science *125*, 3703–3712.

Sokolove, J., and Lepus, C.M. (2013). Role of inflammation in the pathogenesis of osteoarthritis: latest findings and interpretations. Therapeutic Advances in Musculoskeletal Disease *5*, 77–94.

Solorio, L.D., Dhami, C.D., Dang, P.N., Vieregge, E.L., and Alsberg, E. (2012). Spatiotemporal regulation of chondrogenic differentiation with controlled delivery of transforming growth factor-

β1 from gelatin microspheres in mesenchymal stem cell aggregates. Stem Cells Translational Medicine *1*, 632–639.

Somoza, R.A., Welter, J.F., Correa, D., and Caplan, A.I. (2014). Chondrogenic differentiation of mesenchymal stem cells: challenges and unfulfilled expectations. Tissue Engineering Part B: Reviews *20*, 596–608.

Song, J., Hornsby, P., Stanley, M., AbdelFattah, K.R., and Wolf, S.E. (2014). Porcine urinary bladder extracellular matrix activates skeletal myogenesis in mouse muscle cryoinjury. Journal of Regenerative Medicine and Tissue Engineering *3*, 3.

Sophia Fox, A.J., Bedi, A., and Rodeo, S.A. (2009). The basic science of articular cartilage: structure, composition, and function. Sports Health: A Multidisciplinary Approach *1*, 461–468.

Sotiropoulou, P.A., Perez, S.A., Salagianni, M., Baxevanis, C.N., and Papamichail, M. (2006). Characterization of the optimal culture conditions for clinical scale production of human mesenchymal stem cells. Stem Cells *24*, 462–471.

Squillaro, T., Peluso, G., and Galderisi, U. (2016). Clinical trials with mesenchymal stem cells: an update. Cell Transplantation *25*, 829–848.

Stender, S., Murphy, M., O'Brien, T., Stengaard, C., Ulrich-Vinther, M., Søballe, K., and Barry, F. (2007). Adeno-associated viral vector transduction of human mesenchymal stem cells. European Cells and Materials *13*, 93–99.

Stern, P.H. (2006). The calcineurin-NFAT pathway and bone: intriguing new findings. Molecular Interventions *6*, 193–196.

Stinson, S., Lackner, M.R., Adai, A.T., Yu, N., Kim, H.J., O'Brien, C., Spoerke, J., Jhunjhunwala, S., Boyd, Z., Januario, T., et al. (2011). TRPS1 targeting by miR-221/222 promotes the epithelial-to-mesenchymal transition in breast cancer. Science Signaling *4*, ra41.

Su, J., Zheng, Y., and Wu, H. (2009). Generation of alginate microfibers with a roller-assisted microfluidic system. Lab Chip *9*, 996–1001.

Sun, H., Calle, E., Chen, X., Mathur, A., Zhu, Y., Mendez, J., Zhao, L., Niklason, L., Peng, X., Peng, H., et al. (2014). Fibroblast engraftment in the decellularized mouse lung occurs via a 1-

integrin-dependent, FAK-dependent pathway that is mediated by ERK and opposed by AKT. AJP: Lung Cellular and Molecular Physiology *306*, L463–L475.

Sun, J., Zhong, N., Li, Q., Min, Z., Zhao, W., Sun, Q., Tian, L., Yu, H., Shi, Q., Zhang, F., et al. (2011). MicroRNAs of rat articular cartilage at different developmental stages identified by Solexa sequencing. Osteoarthritis and Cartilage *19*, 1237–1245.

Szczepanek, K., Lesnefsky, E.J., and Larner, A.C. (2012). Multi-tasking: nuclear transcription factors with novel roles in the mitochondria. Trends in Cell Biology *22*, 429–437.

Tanner, K.E. (2010). Bioactive ceramic-reinforced composites for bone augmentation. Journal of The Royal Society Interface *7*, S541–S557.

Thysen, S., Luyten, F.P., and Lories, R.J.U. (2015). Targets, models and challenges in osteoarthritis research. Disease Models & Mechanisms *8*, 17–30.

Torfason, E.G., Reimer, C.B., and Keyserling, H.L. (1987). Subclass restriction of human enterovirus antibodies. J. Clin. Microbiol. *25*, 1376–1379.

Torreggiani, E., Bianchini, C., Penolazzi, L., Lambertini, E., Vecchiatini, R., Canella, A., Gambari, R., Magri, E., Pelucchi, S., Pastore, A., et al. (2011). Osteogenic potential of cells derived from nasal septum. Rhinology *49*, 148–154.

Torreggiani, E., Lisignoli, G., Manferdini, C., Lambertini, E., Penolazzi, L., Vecchiatini, R., Gabusi, E., Chieco, P., Facchini, A., Gambari, R., et al. (2012). Role of Slug transcription factor in human mesenchymal stem cells. Journal of Cellular and Molecular Medicine *16*, 740–751.

Tortelli, F., and Cancedda, R. (2009). Three-dimensional cultures of osteogenic and chondrogenic cells: a tissue engineering approach to mimic bone and cartilage *in vitro*. European Cells and Materials *17*, 1–14.

Tortelli, F., Pujic, N., Liu, Y., Laroche, N., Vico, L., and Cancedda, R. (2009). Osteoblast and osteoclast differentiation in an *in vitro* three-dimensional model of bone. Tissue Eng Part A *15*, 2373–2383.

Tripathi, A., Riddell, J., and Chronis, N. (2013). A Biochip with a 3D microfluidic architecture for trapping white blood cells. Sensors and Actuators B: Chemical *186*, 244–251.

Troeberg, L., and Nagase, H. (2012). Proteases involved in cartilage matrix degradation in osteoarthritis. Biochimica et Biophysica Acta (BBA) - Proteins and Proteomics *1824*, 133–145.

Tseng, L.-F., Mather, P.T., and Henderson, J.H. (2013). Shape-memory-actuated change in scaffold fiber alignment directs stem cell morphology. Acta Biomaterialia *9*, 8790–8801.

Tsumaki, N., Okada, M., and Yamashita, A. (2015). iPS cell technologies and cartilage regeneration. Bone *70*, 48–54.

Turner, N.J., Badylak, J.S., Weber, D.J., and Badylak, S.F. (2012). Biologic scaffold remodeling in a dog model of complex musculoskeletal injury. Journal of Surgical Research *176*, 490–502.

Upton, A.R., Holding, C.A., Dharmapatni, A.A.S.S.K., and Haynes, D.R. (2012). The expression of RANKL and OPG in the various grades of osteoarthritic cartilage. Rheumatology International *32*, 535–540.

Usami, Y., Gunawardena, A.T., Iwamoto, M., and Enomoto-Iwamoto, M. (2016). Wnt signaling in cartilage development and diseases: lessons from animal studies. Laboratory Investigation *96*, 186–196.

Valverde-Franco, G. (2003). Defective bone mineralization and osteopenia in young adult FGFR3-/- mice. Human Molecular Genetics *13*, 271–284.

Vecchiatini, R., Penolazzi, L., Lambertini, E., Angelozzi, M., Morganti, C., Mazzitelli, S., Trombelli, L., Nastruzzi, C., and Piva, R. (2015). Effect of dynamic three-dimensional culture on osteogenic potential of human periodontal ligament-derived mesenchymal stem cells entrapped in alginate microbeads. Journal of Periodontal Research *50*, 544–553.

Vinatier, C., Mrugala, D., Jorgensen, C., Guicheux, J., and Noël, D. (2009). Cartilage engineering: a crucial combination of cells, biomaterials and biofactors. Trends in Biotechnology *27*, 307–314.

Vinatier, C., Merceron, C., and Guicheux, J. (2016). Osteoarthritis: from pathogenic mechanisms and recent clinical developments to novel prospective therapeutic options. Drug Discovery Today.

Vogel, C., and Marcotte, E.M. (2012). Insights into the regulation of protein abundance from proteomic and transcriptomic analyses. Nature Reviews Genetics *13*, 227–232.

de Vos, P., Faas, M.M., Strand, B., and Calafiore, R. (2006). Alginate-based microcapsules for immunoisolation of pancreatic islets. Biomaterials *27*, 5603–5617.

Wagner, W., Bork, S., Horn, P., Krunic, D., Walenda, T., Diehlmann, A., Benes, V., Blake, J., Huber, F.X., Eckstein, V., et al. (2009). Aging and replicative senescence have related effects on human stem and progenitor cells. PLoS ONE *4*, e5846.

Wanet, A., Remacle, N., Najar, M., Sokal, E., Arnould, T., Najimi, M., and Renard, P. (2014). Mitochondrial remodeling in hepatic differentiation and dedifferentiation. The International Journal of Biochemistry & Cell Biology *54*, 174–185.

Wang, W., Rigueur, D., and Lyons, K.M. (2014). TGFβ signaling in cartilage development and maintenance. Birth Defects Research Part C: Embryo Today: Reviews *102*, 37–51.

Wang, X., Kua, H.Y., Hu, Y., Guo, K., Zeng, Q., Wu, Q., Ng, H.H., Karsenty, G., de Crombrugghe, B., Yeh, J., et al. (2006). p53 functions as a negative regulator of osteoblastogenesis, osteoblast-dependent osteoclastogenesis, and bone remodeling. The Journal of Cell Biology *172*, 115–125.

Wang, Z., Gerstein, M., and Snyder, M. (2009). RNA-Seq: a revolutionary tool for transcriptomics. Nature Reviews Genetics *10*, 57–63.

Watt, F.M., and Huck, W.T.S. (2013). Role of the extracellular matrix in regulating stem cell fate. Nature Reviews Molecular Cell Biology *14*, 467–473.

Whitesides, G.M. (2006). The origins and the future of microfluidics. Nature *442*, 368–373.

Widbiller, M., Lindner, S.R., Buchalla, W., Eidt, A., Hiller, K.A., Schmalz, G., and Galler, K.M. (2016). Three-dimensional culture of dental pulp stem cells in direct contact to tricalcium silicate cements. Clinical Oral Investigations *20*, 237–246.

Wienholds, E., and Plasterk, R.H.A. (2005). MicroRNA function in animal development. FEBS Letters *579*, 5911–5922.

Winthrop, Z., Pinkowsky, G., and Hennrikus, W. (2015). Surgical treatment for osteochondritis dessicans of the knee. Current Reviews in Musculoskeletal Medicine *8*, 467–475.

Witkos, T.., Koscianska, E., and Krzyzosiak, W.. (2011). Practical aspects of microRNA target prediction. Current Molecular Medicine *11*, 93–109.

Witte, F., Ulrich, H., Palm, C., and Willbold, E. (2007). Biodegradable magnesium scaffolds: Part II: peri-implant bone remodeling. Journal of Biomedical Materials Research Part A *81A*, 757–765.

Wu, B.T., Wen, S.H., Hwang, S.P.L., Huang, C.J., and Kuan, Y.S. (2015). Control of Wnt5b secretion by Wntless modulates chondrogenic cell proliferation through fine-tuning FGF3 expression. Journal of Cell Science *128*, 2328–2339.

Wu, H., Du, J., and Zheng, Q. (2008). Expression of MMP-1 in cartilage and synovium of experimentally induced rabbit ACLT traumatic osteoarthritis: immunohistochemical study. Rheumatol. Int. *29*, 31–36.

Wu, S.C., Chen, C.H., Chang, J.K., Fu, Y.C., Wang, C.K., Eswaramoorthy, R., Lin, Y.S., Wang, Y.H., Lin, S.Y., Wang, G.J., et al. (2013). Hyaluronan initiates chondrogenesis mainly via CD44 in human adipose-derived stem cells. Journal of Applied Physiology *114*, 1610–1618.

Wu, W.S., Heinrichs, S., Xu, D., Garrison, S.P., Zambetti, G.P., Adams, J.M., and Look, A.T. (2005). Slug antagonizes p53-mediated apoptosis of hematopoietic progenitors by repressing puma. Cell *123*, 641–653.

Xian, C.J., and Foster, B.K. (2006). Repair of injured articular and growth plate cartilage using mesenchymal stem cells and chondrogenic gene therapy. Curr Stem Cell Res Ther *1*, 213–229.

Xiao, G., Jiang, D., Ge, C., Zhao, Z., Lai, Y., Boules, H., Phimphilai, M., Yang, X., Karsenty, G., and Franceschi, R.T. (2005). Cooperative interactions between activating transcription factor 4 and Runx2/Cbfa1 stimulate osteoblast-specific osteocalcin gene expression. Journal of Biological Chemistry *280*, 30689–30696.

Xiao, L., Naganawa, T., Obugunde, E., Gronowicz, G., Ornitz, D.M., Coffin, J.D., and Hurley, M.M. (2004). Stat1 controls postnatal bone formation by regulating fibroblast growth factor signaling in osteoblasts. Journal of Biological Chemistry *279*, 27743–27752.

Xie, F., Kovic, B., Jin, X., He, X., Wang, M., and Silvestre, C. (2016). Economic and humanistic burden of osteoarthritis: a systematic review of large sample studies. PharmacoEconomics *34*, 1087–1100.

Xu, H.H.K., Quinn, J.B., Takagi, S., and Chow, L.C. (2004). Synergistic reinforcement of *in situ* hardening calcium phosphate composite scaffold for bone tissue engineering. Biomaterials *25*, 1029–1037.

Xu, Q., Li, P., Chen, X., Zong, L., Jiang, Z., Nan, L., Lei, J., Duan, W., Zhang, D., Li, X., et al. (2015). miR-221/222 induces pancreatic cancer progression through the regulation of matrix metalloproteinases. Oncotarget *6*, 14153–14164.

Yadav, V.K., Ryu, J.-H., Suda, N., Tanaka, K.F., Gingrich, J.A., Schütz, G., Glorieux, F.H., Chiang, C.Y., Zajac, J.D., Insogna, K.L., et al. (2008). Lrp5 controls bone formation by inhibiting serotonin synthesis in the duodenum. Cell *135*, 825–837.

Yagi, H., Soto-Gutierrez, A., Parekkadan, B., Kitagawa, Y., Tompkins, R.G., Kobayashi, N., and Yarmush, M.L. (2010). Mesenchymal stem cells: mechanisms of immunomodulation and homing. Cell Transplantation *19*, 667–679.

Yamaguchi, Y., Ohno, J., Sato, A., Kido, H., and Fukushima, T. (2014). Mesenchymal stem cell spheroids exhibit enhanced *in-vitro* and *in-vivo* osteoregenerative potential. BMC Biotechnology *14*.

Yamashita, T. (2012). New roles of osteoblasts involved in osteoclast differentiation. World Journal of Orthopedics *3*, 175.

Yan, L.P., Oliveira, J.M., Oliveira, A.L., and Reis, R.L. (2015). Current concepts and challenges in osteochondral tissue engineering and regenerative medicine. ACS Biomaterials Science & Engineering *1*, 183–200.

Yang, B., Guo, H., Zhang, Y., Chen, L., Ying, D., and Dong, S. (2011a). MicroRNA-145 regulates chondrogenic differentiation of mesenchymal stem cells by targeting Sox9. PLoS ONE *6*, e21679.

Yang, C.J., Shen, W.G., Liu, C.J., Chen, Y.W., Lu, H.H., Tsai, M.M., and Lin, S.C. (2011b). miR-221 and miR-222 expression increased the growth and tumorigenesis of oral carcinoma cells: miR-221 and miR-222 in OSCC. Journal of Oral Pathology & Medicine *40*, 560–566.

Yang, J., Yamato, M., Kohno, C., Nishimoto, A., Sekine, H., Fukai, F., and Okano, T. (2005). Cell sheet engineering: recreating tissues without biodegradable scaffolds. Biomaterials *26*, 6415–6422.

Yang, M., Zhang, L., and Gibson, G.J. (2015). Chondrocyte miRNAs 221 and 483-5p respond to loss of matrix interaction by modulating proliferation and matrix synthesis. Connective Tissue Research *56*, 236–243.

Yang, Q., Peng, J., Guo, Q., Huang, J., Zhang, L., Yao, J., Yang, F., Wang, S., Xu, W., Wang, A., et al. (2008). A cartilage ECM-derived 3-D porous acellular matrix scaffold for *in vivo* cartilage tissue engineering with PKH26-labeled chondrogenic bone marrow-derived mesenchymal stem cells. Biomaterials *29*, 2378–2387.

Yang, X., Chen, L., Xu, X., Li, C., Huang, C., and Deng, C.X. (2001). TGF-beta/Smad3 signals repress chondrocyte hypertrophic differentiation and are required for maintaining articular cartilage. J. Cell Biol. *153*, 35–46.

Yavropoulou, M.P., and Yovos, J.G. (2007). The role of the Wnt signaling pathway in osteoblast commitment and differentiation. Hormones (Athens) *6*, 279–294.

Yeo, H., Beck, L.H., Thompson, S.R., Farach-Carson, M.C., McDonald, J.M., Clemens, T.L., and Zayzafoon, M. (2007). Conditional disruption of calcineurin B1 in osteoblasts increases bone formation and reduces bone resorption. J. Biol. Chem. *282*, 35318–35327.

You, L., Temiyasathit, S., Lee, P., Kim, C.H., Tummala, P., Yao, W., Kingery, W., Malone, A.M., Kwon, R.Y., and Jacobs, C.R. (2008). Osteocytes as mechanosensors in the inhibition of bone resorption due to mechanical loading. Bone *42*, 172–179.

Youngstrom, D.W., Cakstina, I., and Jakobsons, E. (2015). Cartilage-derived extracellular matrix extract promotes chondrocytic phenotype in three-dimensional tissue culture. Artificial Cells, Nanomedicine, and Biotechnology 1–8.

Yousefi, A.M., Hoque, M.E., Prasad, R.G.S.V., and Uth, N. (2015). Current strategies in multiphasic scaffold design for osteochondral tissue engineering: a review. Journal of Biomedical Materials Research Part A *103*, 2460–2481.

Yu, B., and Wang, C.Y. (2016). Osteoporosis: the result of an “aged” bone microenvironment. Trends in Molecular Medicine *22*, 641–644.

Yuan, X.L., Meng, H.Y., Wang, Y.C., Peng, J., Guo, Q.Y., Wang, A.Y., and Lu, S.B. (2014). Bone–cartilage interface crosstalk in osteoarthritis: potential pathways and future therapeutic strategies. Osteoarthritis and Cartilage *22*, 1077–1089.

Zadpoor, A.A. (2015). Bone tissue regeneration: the role of scaffold geometry. Biomater. Sci. *3*, 231–245.

Zaim, M., Karaman, S., Cetin, G., and Isik, S. (2012). Donor age and long-term culture affect differentiation and proliferation of human bone marrow mesenchymal stem cells. Annals of Hematology *91*, 1175–1186.

Zanon, G., DI Vico, G., and Marullo, M. (2014). Osteochondritis dissecans of the talus. Joints *2*, 115–123.

Zanotti, S., Smerdel-Ramoya, A., and Canalis, E. (2011). Reciprocal regulation of Notch and Nuclear Factor of Activated T-cells (NFAT) c1 transactivation in osteoblasts. Journal of Biological Chemistry *286*, 4576–4588.

Zhang, M., and Huang, B. (2012). The multi-differentiation potential of peripheral blood mononuclear cells. Stem Cell Research & Therapy *3*, 48.

Zhang, L., Hu, J., and Athanasiou, K.A. (2009). The role of tissue engineering in articular cartilage repair and regeneration. Crit Rev Biomed Eng *37*, 1–57.

Zhang, L., Zhang, F., Weng, Z., Brown, B.N., Yan, H., Ma, X.M., Vosler, P.S., Badylak, S.F., Dixon, C.E., Cui, X.T., et al. (2013a). Effect of an inductive hydrogel composed of urinary bladder matrix upon functional recovery following traumatic brain injury. Tissue Engineering Part A *19*, 1909–1918.

Zhang, Q., Raje, V., Yakovlev, V.A., Yacoub, A., Szczepanek, K., Meier, J., Derecka, M., Chen, Q., Hu, Y., Sisler, J., et al. (2013b). Mitochondrial localized Stat3 promotes breast cancer growth via phosphorylation of serine 727. Journal of Biological Chemistry *288*, 31280–31288.

Zhang, W., Ouyang, H., Dass, C.R., and Xu, J. (2016a). Current research on pharmacologic and regenerative therapies for osteoarthritis. Bone Research *4*, 15040.

Zhang, W., Zhu, Y., Li, J., Guo, Q., Peng, J., Liu, S., Yang, J., and Wang, Y. (2016b). Cell-derived extracellular matrix: basic characteristics and current applications in orthopedic tissue engineering. Tissue Engineering Part B: Reviews *22*, 193–207.

Zhen, G., Wen, C., Jia, X., Li, Y., Crane, J.L., Mears, S.C., Askin, F.B., Frassica, F.J., Chang, W., Yao, J., et al. (2013). Inhibition of TGF-β signaling in mesenchymal stem cells of subchondral bone attenuates osteoarthritis. Nature Medicine *19*, 704–712.

Zhong, L., Huang, X., Karperien, M., and Post, J. (2015). The regulatory role of signaling crosstalk in hypertrophy of MSCs and human articular chondrocytes. International Journal of Molecular Sciences *16*, 19225–19247.

Zimmermann, H., Zimmermann, D., Reuss, R., Feilen, P.J., Manz, B., Katsen, A., Weber, M., Ihmig, F.R., Ehrhart, F., Gessner, P., et al. (2005). Towards a medically approved technology for alginate-based microcapsules allowing long-term immunoisolated transplantation. J Mater Sci Mater Med *16*, 491–501.

Zouani, O.F., Chollet, C., Guillotin, B., and Durrieu, M.C. (2010). Differentiation of pre-osteoblast cells on poly(ethylene terephthalate) grafted with RGD and/or BMPs mimetic peptides. Biomaterials *31*, 8245–8253.

Appendix

List of publications

List of peer-reviewed publications

Publications related to Ph.D. project

Lolli A, Lambertini E, Penolazzi L, Angelozzi M, Morganti C, Franceschetti T, Pelucchi S, Gambari R, Piva R. "Pro-Chondrogenic Effect of miR-221 and Slug Depletion in Human MSCs." Stem Cell Rev. 2014 Dec; 10(6):841-55.

Lambertini E, Penolazzi L, Morganti C, Lisignoli G, Zini N, Angelozzi M, Bonora M, Ferroni L, Pinton P, Zavan B, Piva R. "Osteogenic differentiation of human MSCs: Specific occupancy of the mitochondrial DNA by NFATc1 transcription factor." Int J Biochem Cell Biol. 2015 Jul; 64:212-9.

Angelozzi M, Miotto M, Penolazzi L, Mazzitelli S, Keane T, Badylak SF, Piva R, Nastruzzi C. "Composite ECM–alginate microfibers produced by microfluidics as scaffolds with biomineralization potential." Mater Sci Eng C Mater Biol Appl. 2015 Nov; 1;56:141-53.

Penolazzi L, Lolli A, Sardelli L, Angelozzi M, Lambertini E, Trombelli L, Ciarpella F, RenataVecchiatini, Piva R. "Establishment of a 3D-dynamic osteoblasts-osteoclasts co-culture model to simulate the jawbone microenvironment in vitro." Life Sci. 2016 May, 1;152:82-93.

Lolli A, Narcisi R, Lambertini E, Penolazzi L, Angelozzi M, Kops N, Gasparini S, van Osch G.J.V.M, Piva R. "Silencing of anti-chondrogenic microRNA-221 in human mesenchymal stem cells promotes cartilage repair in vivo." Stem Cells. 2016 Jul, 34(7):1801-11.

Lisignoli G, Lambertini E, Manferdini C, Gabusi E, Penolazzi L, Paolella F, Angelozzi M, Casagranda V, Piva R. "Collagen type XV and the "osteogenic status". J Cell Mol Med. 2017 Mar, Epub ahead of print.

Angelozzi M, Penolazzi L, Miotto M, Mazzitelli S, Bottaro E, Lambertini E, Keane T, Badylak SF, Piva R, Nastruzzi C. "De-differentiated chondrocytes encapsulated in composite microfibers as tool for cartilage repair." Front Bioeng Biotechnol. 2017, submitted.

Other publications

Lisignoli G, Manferdini C, Lambertini E, Zini N, Angelozzi M, Gabusi E, Gambari L, Penolazzi L, Lolli A, Facchini A, Piva R. "Chondrogenic potential of Slug-depleted human mesenchymal stem cells." Tissue Eng Part A. 2014 Oct; 20(19-20):2795-805.

Piva R, Lambertini E, Manferdini C, Capanni C, Penolazzi L, Gabusi E, Paolella F, Lolli A, Angelozzi M, Lattanzi G, Lisignoli G. "Slug transcription factor and nuclear Lamin B1 are upregulated in osteoarthritic chondrocytes." Osteoarthritis Cartilage. 2015 Jul; 23(7):1226-30.

Vecchiatini R, Penolazzi L, Lambertini E, Angelozzi M, Morganti C, Mazzitelli S, Trombelli L, Nastruzzi C, Piva R. "Effect of dynamic three-dimensional culture on osteogenic potential of human periodontal ligament-derived mesenchymal stem cells entrapped in alginate microbeads." J Periodontal Res. 2015 Aug; 50(4):544-53.

Mandatori D, Penolazzi L, Pipino C, Di Tomo P, Di Silvestre S, Di Pietro N, Trevisani S, Angelozzi M, Ucci M, De Coppi P, Piva R, Pandolfi A. "Menaquinone-4 enhances osteogenic potential of human Amniotic Fluid Mesenchymal Stem Cells cultured in 2D and 3D dynamic culture system." J Tissue Eng Regen Med. 2016, submitted.

Communications for scientific conferences

Oral communications

Angelozzi M, Penolazzi L, Lambertini E, Trevisani S, Casagrandra V, Sardelli L, Lolli A, Vecchiatini R, Ferrari L, Nastruzzi C, Piva R. "Development of 3D stem cell culture systems: one

step closer to natural conditions." 7th Meeting Stem Cell Research Italy Society, 2016, Bologna, Italy.

Poster communications

Angelozzi M, Penolazzi L, Lambertini E, Lolli A, Miotto M, Vezzali F, Mazzitelli S, Pelucchi S, Pastore A, Nastruzzi C, Piva R. "Encapsulation of dedifferentiated nasal septal chondrocytes in alginate based scaffolds for cartilage tissue engineering." 5th Stem Cell Research Italy meeting, 2014 Salerno, Italy.

Angelozzi M, Lolli A, Lambertini E, Vezzali F, Di Ciano M, Penolazzi L, Piva R. "miR-221 and SLUG interplay in human mesenchymal stem cells and breast cancer cells." 56th Annual meeting of the Italian Cancer Society (SIC) "Dangerous Liaisons: translating cancer biology into better patients management", 2014 Ferrara, Italy.

Lolli A, Lambertini E, Penolazzi L, Narcisi R, Angelozzi M, Vezzali F, Miotto M, van Osch GJVM, Piva R. "Enhanced chondrogenic potential of Slug and miR-221 depleted human MSCs." 23rd Annual Meeting of the Netherlands Society for Biomaterials and Tissue Engineering (NBTE). 2015, Lunteren, The Netherlands.

Lolli A, Lambertini E, Penolazzi L, Narcisi R, Angelozzi M, Miotto M, van Osch GJVM, Piva R. "Enhanced chondrogenic potential of miR-221 and Slug depleted human MSCs." 4th Joint Meeting of European Calcified Tissue Society (ECTS) and the International Bone and Mineral Society (IBMS), 2015 Rotterdam.

Angelozzi M, Miotto M, Penolazzi L, Lolli A, Mazzitelli S, Badylak SF, Piva R, Nastruzzi C. "Composite ECM-alginate microfibers produced by microfludics as scaffolds with biomineralization potential" 4th Joint Meeting of European Calcified Tissue Society (ECTS) and the International Bone and Mineral Society (IBMS), 2015 Rotterdam.

Penolazzi L, Lolli A, Sardelli L, Angelozzi M, Ciarpella F, Vecchiatini R, Lambertini E, Piva R. "Establishment of a 3D-dynamic osteoblasts-osteoclasts co-culture model to simulate the jawbone microenvironment in vitro." 6th Meeting Stem Cell Research Italy Society. 2015, Bari, Italy.

Angelozzi M, Ciarpella F, Penolazzi L, Lambertini E, Lolli A, Lisignoli G, Pinton P, Piva R. "Osteogenic differentiation of human MSCs: specific occupancy of the mitochondrial DNA by NFATc1 transcription factor." 6th Meeting Stem Cell Research Italy Society, 2015, Bari, Italy.

Lisignoli G, Lambertini E, Manferdini C, Penolazzi L, Angelozzi M, Casagranda V, Paolella F, Gabusi E, Piva R. "The regulation of the expression of Collagen type XV and the osteogenic differentiation." 7th Meeting Stem Cell Research Italy Society, 2016, Bologna, Italy.

Mandatori D, Penolazzi L, Pipino C, Di Tomo P, Di Pietro N, Trevisani S, Angelozzi M, Ucci M, Piva R, Pandolfi A. "Vitamin K2 and bone: focus on osteogenesis." 7th Meeting Stem Cell Research Italy Society, 2016, Bologna, Italy.